WRC RESEARCH REPORT NO. 208

INCORPORATION OF UNCERTAINTIES IN REAL-TIME CATCHMENT FLOOD FORECASTING

by
Charles Steven Melching, Graduate Assistant
Ben Chie Yen, Professor
Harry G. Wenzel, Jr., Professor
Department of Civil Engineering
University of Illinois at Urbana-Champaign

Project Completion Report

Project No. G1223-04
Grant No. INT-14-08-0001-G1223

September 1987

The research on which this report is based was financed in part by the U.S. Department of the Interior, as authorized by the Water Research and Development Act of 1984 (PL-98-242).

University of Illinois
Water Resources Center
Urbana, IL 61801

ABSTRACT

INCORPORATION OF UNCERTAINTIES IN REAL-TIME CATCHMENT FLOOD FORECASTING

Floods have become the most prevalent and costly natural hazards in the U.S. When preparing real-time flood forecasts for a catchment flood warning and preparedness system, consideration must be given to four sources of uncertainty -- natural, data, model parameters, and model structure. A general procedure has been developed for applying reliability analysis to evaluate the effects of the various sources of uncertainty on hydrologic models used for forecasting and prediction of catchment floods. Three reliability analysis methods -- Monte Carlo simulation, mean value and advanced first-order second moment analyses (MVFOSM and AFOSM, respectively) -- were applied to the rainfall-runoff modeling reliability problem. Comparison of these methods indicates that the AFOSM method is probably best suited to the rainfall-runoff modeling reliability problem with the MVFOSM showing some promise. The feasibility and utility of the reliability analysis procedure are shown for a case study employing as an example the HEC-1 and RORB rainfall-runoff watershed models to forecast flood events on the Vermilion River watershed at Pontiac, Illinois. The utility of the reliability analysis approach is demonstrated for four important hydrologic problems: 1) determination of forecast (or prediction) reliability, 2) determination of the flood level exceedance probability due to a current storm and development of "rules of thumb" for flood warning decision making considering this probabilistic information, 3) determination of the key sources of uncertainty influencing model forecast reliability, 4) selection of hydrologic models based on comparison of model forecast reliability. Central to this demonstration is the reliability analysis methods' ability to estimate the exceedance probability for any hydrologic target level of interest and, hence, to produce forecast cumulative density functions and probability distribution functions. For typical hydrologic modeling cases, reduction of the underlying modeling uncertainties is the key to obtaining useful, reliable forecasts. Furthermore, determination of the rainfall excess is the primary source of uncertainty, especially in the estimation of the temporal and areal rainfall distributions.

Melching, Charles Steven, Ben Chie Yen and Harry G. Wenzel, Jr.
INCORPORATION OF UNCERTAINTIES IN REAL-TIME CATCHMENT FLOOD FORECASTING
University of Illinois Water Resources Center Research Report No. 208, September 1987, xiv + 194 pp.

KEYWORDS -- decision making/flood control/*flood forecasting/flood protection/flood warning/floods/hydrology/mathematical model/rainfall/real-time forecasting/reliability/risks/runoff/storms/watershed

ACKNOWLEDGMENTS

Presented in this report is one phase of a research program directed by Dr. B.C. Yen on reliability and risk analysis in hydraulic engineering. This report is essentially a rearrangement of the dissertation of the first author.

During the course of this research many people have contributed to its progress and success. Particularly, Professor Wilson H. Tang provided valuable suggestions and discussions simplifying the task considerably. Dr. Glenn E. Stout, Director of the Illinois Water Resources Center, provided timely encouragement and support. Support of computer time from the Research Board, Graduate College of the University of Illinois at Urbana-Champaign, is also appreciated.

Mr. David L. Sullivan, Superintendent of the Pontiac Wastewater Treatment Plant, provided information on the nature of flooding and flood warning in Pontiac. Mr. John L. Vogel and Ms. Michelle Pumphry of the Illinois State Water Survey provided the rainfall data and climatological information and advice for this research. Mr. Mike Bender of the Illinois State Water Survey provided insight and information regarding flood problems in the state of Illinois. Mr. Elmer Zuehls of the U.S. Geological Survey provided the hourly and bi-hourly streamflow records used in this research. Dr. Eric M. Laurenson of Monash University, Australia, provided the RORB Runoff Routing program and documentation which was used in this research. Their help is gratefully acknowledged.

TABLE OF CONTENTS

LIST OF TABLES

LIST OF FIGURES

1. INTRODUCTION

1.1 Severity of the Flooding Problem

Floods and flash floods have been the most prevalent and costly natural disaster in the United States over the last decade resulting in $1 billion in damages and 200 deaths annually (Mogil et al., 1978). This annual damage figure is expected to grow to around $4.3 billion annually (in 1975 dollars) by the year 2000 (Water Resources Council, 1977). White (1975) pointed out that flood events provoke far-reaching impacts in society that go beyond dollar and fatality numbers. Social disruption caused by floods includes social structures (i.e., families, communities, etc.) disruption, dislocation, unemployment, and deaths and injuries. Furthermore, this problem is national in scope since overflowing rivers and streams cause significant flooding in about half of the communities (representing approximately half of the nation's population) and over at least seven percent of the total land area of the United States (White, 1975). Finally, the flood problem is not restricted to the United States, floods and flash floods pose a severe threat to nearly every country around the globe. This is evidenced by the fact that the literature reviewed here describes flood warning schemes from countries all around the globe including Australia, Cambodia, India, Japan, Sweden, the United Kingdom, and the U.S.S.R.

The seriousness of flood hazards in the United States (and around the globe) has long been recognized and considerable effort has been expended to mitigate these hazards. For example, the 1980 fiscal year budgets of the Corps of Engineers and the National Weather Service included more than $1 billion for flood protection and control activities, while the budgets of the Federal Insurance Administration, the Office of Disaster Response and Recovery, and the Red Cross included nearly $1.2 billion for relief and assistance to flood victims (National Science Foundation, 1980). Pilgrim et al. (1982) reported even more startling figures for Australia where the annual capital investment in flood related works is approximately $30 per person. In the last decade non-structural flood control measures -- such as flood plain zoning, flood insurance, flood warning and preparedness systems, etc. -- have received a high priority in research and implementation due to Presidential directive (Executive Order 11988) and other statutes.

Flood warning and preparedness (FWP) systems are one of the most promising of the non-structural flood control measures. The goal of this study is to develop a methodology for evaluating the reliability of real-time flood forecasts produced by rainfall-runoff models which play a key role in the effectiveness of FWP systems. In the following sections the potential benefits and key characteristics of FWP systems will be discussed. The need for and benefits of proper evaluation of the uncertainty in real-time flood forecasts are also described in the following sections.

1.2 Basic Definitions: Flood Warning, Flood Watch, Flood Forecast

In order to properly understand the historical development and current "state-of-the-art" in FWP systems, basic definitions of flood warning, flood

watch, and flood forecast as typically given in the literature and as used in this study need to be discussed. Actually, in the National Weather Service (NWS) view of flood protection, these various concepts change definition depending on the size of the watershed and the type of flooding encountered.

For flash flood cases on small watersheds, flash flood watches are issued by NWS State Forecast Offices if meteorological and watershed conditions indicate the potential for flash floods (e.g., if heavy rains appear imminent on a fairly wet watershed). Flash flood warnings are issued if a NWS office determines a flash flood is occurring or flood producing rainfall is indicated by radar, automated gages, satellite data, or rainfall observers.

For larger watersheds, flood watches are not issued, only flood warnings based on hydrologic model predictions and observed flooding upstream are issued. Sittner (1977) noted that:

> The application of precipitation input to a hydrologic model yields a computed hydrograph, not a forecast. The forecast is produced by a human forecaster, based principally on the computed hydrograph, but using in addition observed stages and/or discharges from various river stations, including the one for which the forecast is being prepared.

Therefore, for larger watersheds, the flood forecast is itself the flood warning, i.e., a flood of certain magnitude is forecast to reach a town at a certain time and the residents of that town are encouraged to take appropriate mitigation measures.

In this study, the more traditional hydrologic definition of forecast is used. Chow (1972) defined a forecast as the transformation of one sequence of hydrologic events (the input to a hydrologic system -- rainfall, snowmelt, etc.) into another sequence that results due to the initial sequence (the output from the system -- the hydrograph). Hence, in this study, the computed hydrograph is the forecast hydrograph. A staged flood warning and preparedness system concept is then used to define the terms flood watch and flood warning. As for flash floods, flood watches are issued to activate and gear up the city's flood preparedness system, and they are issued when the forecast indicates that near flood discharges are expected. Flood warnings are issued to initiate the city's actual flood mitigation activities, and they are issued when peak discharges in excess of flood stage are forecast.

1.3 Potential Benefits of FWP Systems

FWP systems are one of the most promising non-structural means of reducing avoidable flood damages and fatalities. Day (1970) found that for the Susquehanna River basin as much as two-thirds of the avoidable flood damage could be realized as net benefits of a FWP system. Day and Lee (1976) estimated the potential benefit-cost (B/C) ratio (assuming full, timely community response to warnings) of a FWP system for the Connecticut River basin to be as high as 7.5, and they concluded that the actual B/C ratio from an FWP system should be at least 3. Heatherwick and Quinnell

(1976) concluded that the potential B/C ratios for total flood warning systems for urban areas in Australia, even when subject to rare flood events, are very high (e.g., for Brisbane B/C $\doteq$ 6.6). White (1975) noted that there is reasonable ground for thinking that warning systems might yield B/C ratios of 5 for most cases. Finally, Owen et al. (1983) concluded virtually any area with a significant flood problem can experience net benefits from the availability of adequate FWP systems either alone or in conjunction with other measures.

The benefits of FWP systems go far beyond the potential economic losses averted considered above. FWP systems also greatly reduce the social disruption, deaths, and injuries caused by floods. Indeed, Owen et al. (1983) reported that there are no known cases of avoidable flood deaths where well developed local flood warning programs are in operation.

1.4 Key Characteristics of FWP Systems

FWP systems require a unique combination of human and technical factors to ensure their efficient operation. In recent years, a fair amount of research has been devoted to develop methodologies for evaluating the performance of a specified flood warning system (e.g., Sniedovich and Davis, 1977; and Krzysztofowicz and Davis, 1983a-c). This research has resulted in several important insights regarding the efficiency of FWP systems, which are discussed below.

FWP systems can be idealized as two sequential systems: a forecasting system, which evaluates flood hazards and issues flood warnings, and a response system, which enacts protective measures upon receiving the warning. The forecasting system involves data collection, flood forecasting, and forecast dissemination steps, and so the proper functioning of this system can be controlled by engineering and/or technical factors. However, the response system involves decision making and action (i.e., protection) implementation steps, which are controlled by human factors. Krzysztofowicz and Davis (1983c) found that non-optimal response strategy does not allow the full forecast system potential to be realized. As a result, the actual value (effectiveness) of the FWP system is low, no matter what the quality of the forecasts. Thus, the human factors which control the response strategy of the flood plain dwellers are the key elements in the overall effectiveness of FWP systems.

Several researchers (White, 1975; Owen et al., 1983; and Krzysztofowicz and Davis, 1983c) have noted that one of the key factors which influences response to flood warnings is the public confidence in the warnings. If there are many "false alarms" people will tend to ignore warnings and so the FWP system becomes ineffective. Conversely, if floods occur without adequate warning (i.e., warning with a reasonable amount of preparation time) the forecasting system is ineffective, and this ineffectiveness also lowers public confidence.

Krzysztofowicz and Davis (1983c) found that the optimal response strategy tended to be anticipatory such that people begin to take some protective action even before it is expected the flood will reach their flood plain level. Such a strategy requires some understanding, usually

based on past experience, of the variable nature (i.e., uncertainty) of floods and their forecasts. However, they also noted that:

> "The ability of untrained people to think in probabilistic terms is generally very poor. As a result, people tend to ignore uncertainty and view future events as perfectly predictable, even if their past experience suggests to the contrary."

The officials in charge of issuing flood warnings should be capable of understanding the probabilistic nature of a flood resulting from a current storm, and given the proper information they can issue warnings which will solicit anticipatory responses from the public. An example of such flood warnings are those issued by "staged" flood warning arrangements (Owen et al., 1983). "Staged" flood warning provides for identifying several levels of flood threat and issuing appropriate warnings based on the anticipated magnitude of flooding and the certainty of its occurrence.

1.5 Uncertainty in Forecasts of the Rainfall-Runoff Process

Real-time flood forecasting models are the primary source of information regarding potential flooding due to a current storm event. In a typical FWP system, the expected flood hydrograph is estimated using the available rainfall data (and, possibly, precipitation forecasts), the best estimates of the model parameter values, and a hydrologic model the hydrologist feels comfortable with. When analyzing a hydrologic system (watershed) to determine the runoff (flood) hydrograph resulting from a storm event, a hydrologist is faced with four sources of uncertainty: (1) natural, (2) data, (3) model parameter, and (4) model structure uncertainties. Natural uncertainties refer to the random temporal and areal fluctuations inherent in natural processes. Plate (1986) noted the natural variability of the rainfall process and of the conversion of rainfall into runoff almost always enters a large amount of uncertainty into the physical process of runoff generation. The hydrologist, therefore, must deal with a large random residue even if a perfect model of the hydrologic cycle were available. Data uncertainties refer to: (a) measurement inaccuracy and errors; (b) the adequacy of the rain and/or stream gage network, soil data, vegetation data, etc.; and (c) data handling and transmission errors. Parameter uncertainty reflects variability in the determination of the proper parameter values to use in modeling a given storm event. Model structure uncertainty refers to the ability of the model to accurately reflect the watershed's true physical runoff process.

The National Science Foundation (1980) recommended that methods must be developed to quantify forecast uncertainty caused by the aforementioned sources of modeling uncertainty. Nevertheless, in current "state-of-the-art" real-time flood forecasting systems, these uncertainties are only partially considered either by updating schemes, which adjust the input data or model parameters such that the predicted discharge agrees with the available discharge measurements, or by adaptive filtering techniques which automatically update the forecasts. However, even for one of the most sophisticated of these techniques, Kitanidis and Bras (1980c) admitted that to truly enhance the accuracy of future forecasts, the correct structure of uncertainty, pertinent to the specific model and data must be hypothesized.

Reliability analysis methods, which were developed for structural safety analysis and have been successfully applied to hydraulic structure design problems, offer an innovative way to consider the various sources of uncertainty and their effects on the accuracy of the forecast hydrograph. Reliability analysis methods can provide an estimate of the probability of any level of flooding for the current storm event given information regarding the various sources of uncertainty. Hence, by applying reliability analysis to the real-time flood forecasting model the officials in charge of issuing flood warnings will be provided with not only an estimate of the expected flood hydrograph, but also with the probabilities that any critical flood level will be exceeded. Georgakakos (1986a) stated that such probability values are indispensible in the present day flood warning decision making process. Furthermore, such information can greatly aid flood warning decision making in two areas:

1. More definitive criteria can be established regarding when to issue a warning such that "false alarms" and unanticipated floods can be avoided,

2. The flood probabilities for different levels are key information for establishing a flood warning program which solicits anticipatory responses (e.g., a "staged" flood warning program).

Therefore, consideration of forecast uncertainties and reliability is very important to FWP system effectiveness since it can potentially improve both the information provided by the forecast and the response to the warning issued based on the forecast.

1.6 Research Objectives

To date, the research on the effects of the various sources of uncertainty on the reliability of rainfall-runoff modeling has been aimed at demonstrating the severity of these effects not at providing a simple, flexible means of estimating the reliability of a forecast or prediction made by a rainfall-runoff model. Therefore, the objective of this research is to develop a general procedure for using reliability analysis to consider the effects of rainfall-runoff model uncertainty on real-time flood forecasts to provide more complete information for flood warning decision making. The simplicity, flexibility, and utility of the general approach is demonstrated through a case study. The utility of the general procedure is demonstrated through the attainment of the potential benefits of considering uncertainties in rainfall-runoff modeling. These potential benefits include:

1. the enhancement of the forecast itself by providing a measure of its precision (this measure of precision may also be used to postulate on the reliability of hydrologic models used for design hydrograph estimation or synthetic series generation);

2. information which could allow flood warnings to be issued in such a way as to promote a more optimal response (i.e., an anticipatory response) from the flood plain dweller;

3. a reduction in "false alarms" and unanticipated floods due to more complete information on flood potential, leading to increased public confidence in the warning system and, hence, improved response to warnings;

4. determination of which hydrologic areas -- i.e., data, model parameters, and/or model structure -- will provide the greatest forecast improvement given future study;

5. a criterion for determining the optimal level of model complexity required for FWP systems to achieve a prescribed level of reliability;

A sixth potential benefit -- determination of the expected flood damage from actual or hypothetical (design) storms -- was not examined here due to the lack of adequate economic data on flood loss.

A secondary objective of this research is to assess the typical rainfall-runoff model forecast (or prediction) reliability considering the major sources of uncertainty.

1.7 Research Scope

The application of reliability analysis to real-time flood forecasting models is model and case dependent. Many factors influence the choice of the hydrologic model to be incorporated within a FWP system. Among the key factors influencing the model choice are watershed size and morphology. For large watersheds, where the flood peak reaches the area of interest (i.e., area to be warned) well after the significant runoff producing rainfall has ceased, the flood forecasts are usually made by physical or statistical routing models without considering the rainfall- runoff process. For medium sized watersheds, where the flood peak reaches the area of interest within a fairly short time (e.g., a day) after the significant runoff producing rainfall has ceased, rainfall-runoff models must be used for flood forecasting. Small watersheds or watersheds with steep slopes and/or large amounts of impervious area are subject to flash floods. The National Weather Service defines a flash flood as a flood that follows the causative event (usually heavy rainfall) within a few hours (Maddox and Chappell, 1979). Thus, precipitation forecasts must be incorporated with rainfall-runoff modeling to provide flood warnings with adequate lead times.

In this study, FWP systems for medium sized watersheds are considered. Flood forecasting for medium sized watersheds may make use of precipitation forecasts to improve warning lead time. However, in this research, the forecast hydrographs were based solely on the rainfall "on the ground" at the forecast time. Furthermore, no intermediate forecasts were studied, i.e., the verification event forecasts were made using all the significant runoff producing rainfall for the event. Consideration of precipitation forecasts and their uncertainties is left for future research. Thus, this research centers around using reliability analysis to consider the data, model parameter, and model structure uncertainties inherent in real-time hydrologic models of the rainfall-runoff process. Even though FWP systems for large and small watersheds are not specifically addressed, the principles described and developed here may be quite useful for analysis of

flood forecast uncertainties for such watersheds. For example, combining hydrologic model and precipitation forecast uncertainty analysis may greatly aid a flash flood warning program.

This study develops the basic concepts for dealing with uncertainties and applying reliability analysis so that one may apply the methodology to a wide range of models. The application of reliability analysis to selected real-time flood forecasting models is demonstrated for a medium sized Illinois watershed.

2. PROCEDURE FOR COMBINING RELIABILITY ANALYSIS AND HYDROLOGIC MODELING

2.1 General Framework

A review of some existing rainfall-runoff simulation models pertinent to the present study is given in Appendix A. A review of existing reliability analysis methods is presented in Appendix B. These existing tools and techniques can be used as the foundation of the procedure developed in this study. In this chapter the basic framework of the procedure which combines reliability analysis with hydrologic models to assess the reliability of these models and their forecasts or predictions is presented. Figure 2.1 presents a flow chart displaying the interrelationship between the reliability analysis procedure and the typical applicationof a hydrologic model for decision making. The double arrow between the reliability analysis method and the hydrologic model indicates the interplay between the two, wherein the reliability analysis method uses the hydrologic model to describe the performance of the system whose variability and/or uncertainty is being estimated.

The general framework is applicable to any hydrologic model except those which directly involve nonlinear partial differential equations (e.g., dynamic wave flow routing). Hence, the hydrologic models which fit into this framework include most of those used for real-time flood forecasting and design hydrograph estimation.

The key assumption in using the general procedure is that the hydrologic model and the uncertainties in its basic variables (input data, model parameters, and model structure correction factor) adequately describe the true variability in the natural rainfall-runoff process. This assumption must hold true if one wishes to estimate actual probabilities that specific hydrologic target levels will be exceeded by the event forecast or will be met by predicted design hydrograph. If one wishes to access the reliability of a model prediction or forecast or compare the relative reliability of models or design cases, the above assumption does not need to be closely approximated. In such cases, the description of the basic variable uncertainties must be accurate and consistently determined.

Figure 2.2 presents a flow chart of the general procedure for using reliability analysis to determine hydrologic target level exceedance probabilities. Each of the steps in this flow chart are described in detail in the following sections. Use of the hydrologic target level exceedance probabilities in decision making and in evaluating forecast or prediction reliability is also described in the following.

The first step in the approach is for hydrologists to select any model they "feel comfortable with" and which they feel is adequate for the problem being studied.

The second step is to formulate the system performance function, Z, (as defined in Appendix B.2) as

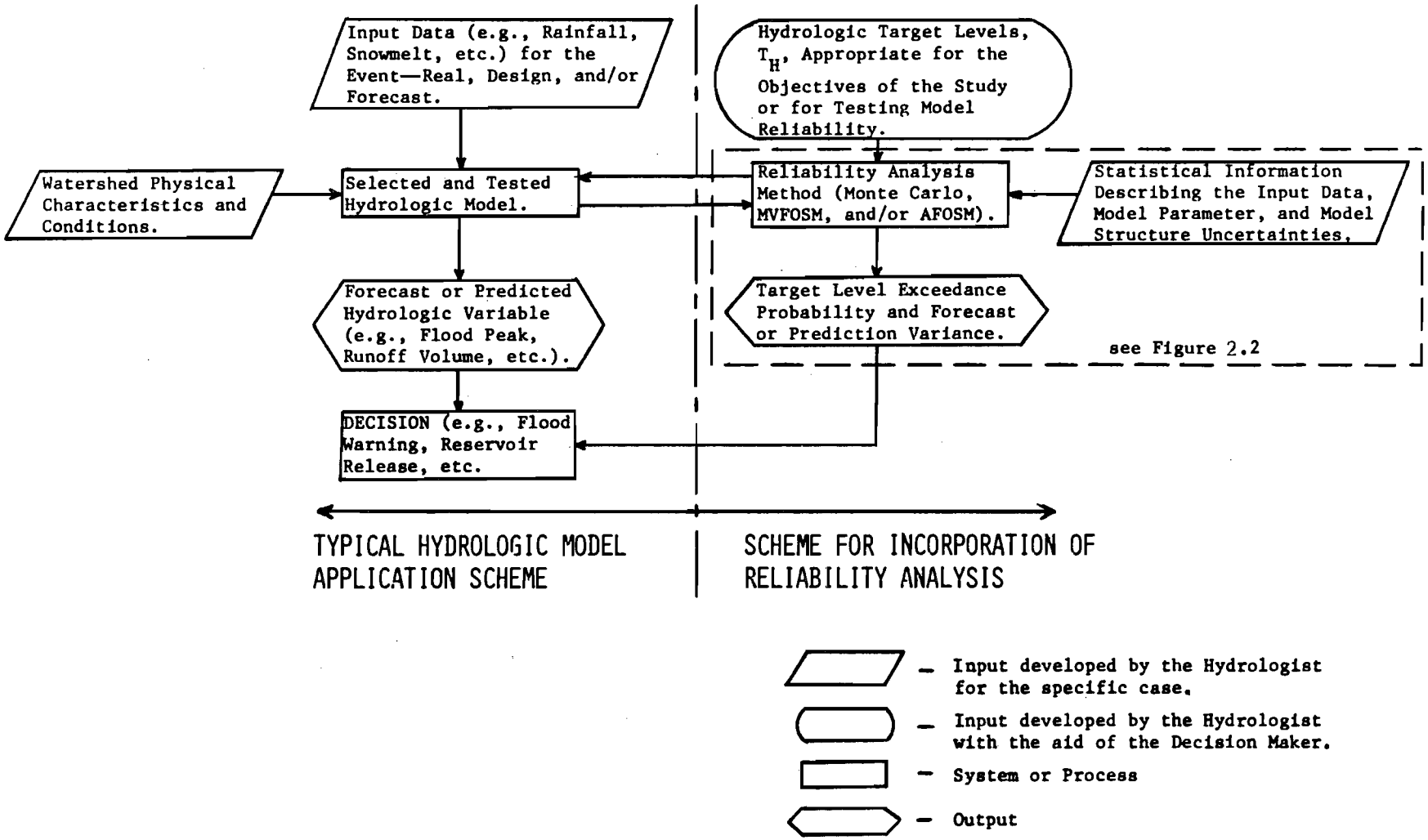

Figure 2.1. Flow chart of the incorporation of reliability analysis with hydrologic modeling for Decision making

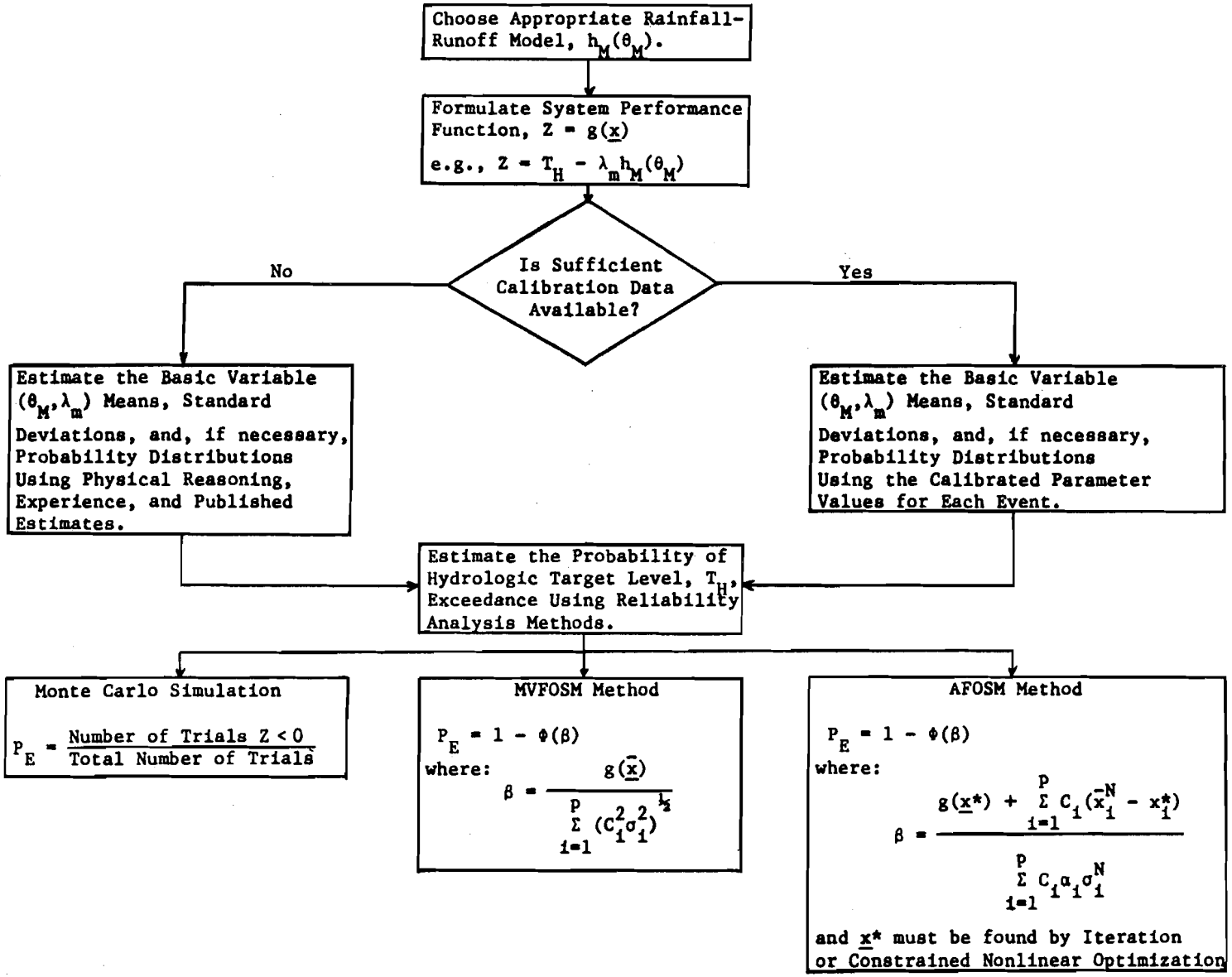

Figure 2.2. Flow chart of the general procedure for using reliability analysis to estimate hydrologic target level exceedance probabilities

$$Z = T_H - \lambda_m \, h_M(\theta_M) \tag{2.1a}$$

or

$$Z = \ell n[T_H/\lambda_m \, h_M(\theta_M)] \tag{2.1b}$$

where T_H = the hydrologic target level whose exceedance probability is sought,

λ_m = the model correction factor which expresses the relationship between the model's optimal performance and the true value of the hydrologic information estimated,

$h_M(\cdot)$ = a function which represents the model's estimate of the hydrologic information in question, and

θ_M = the vector of model basic variables minus the model structure correction factor, i.e., θ_M includes the input data and model parameters.

In this research, the hydrologic information estimated is the peak discharge resulting from a storm event (either real or design). Hence, the target level T_H is set equal to the measured peak discharge to check the model forecast and prediction reliability, and it is set equal to the critical flood stage to estimate the flood level exceedance probability. In evaluating forecast and prediction reliability, the measured peak exceedance probability is not the reliability measure. Instead, reliability is expressed as the difference between the measured and forecast peaks in terms of normalized forecast standard deviations, which may be determined from the exceedance probability. This approach is not limited to hydrograph peak estimates, it may be applied to check the reliability of model estimates of other hydrologic information of interest, e.g., runoff volumes, flood wave travel times, etc.

The third, and most important, step in the approach is to estimate measures which express the individual uncertainty in the basic variables of the model. In order to analyze the uncertainty in an engineering system, the MVFOSM method requires knowledge of the mean and standard deviation of the various factors (i.e., basic variables) which influence system response. The AFOSM also requires knowledge of the basic variable means and standard deviations, and it may use probability distribution data if it is available. Monte Carlo simulation requires assumptions regarding the basic variable distributions.

The following sections in this chapter present a general procedure for evaluating the uncertainties in data, model parameters, and model structure and then estimating the corresponding mean and standard deviation of the basic variables. Estimation of basic variable probability distributions is much more difficult. For calibrated models, if a representative, homogeneous calibration data set of sufficient size (each of these concepts is described in detail in section 2.3.1.1) is available, it is possible to statistically fit distributions to the calibrated parameter values. For non-calibrated physical simulation models, distributions must be assumed

based on personal experience and suggestions contained in the literature. For example, Rajendran et al. (1982) applied a lognormally distributed scaling factor to the average catchment hydraulic conductivity, K_H, to account for K_H's variation throughout the watershed; hence, hydraulic conductivity might be assumed as lognormally distributed.

The fourth step is the estimation of the exceedance probabilities for the selected hydrologic target levels. This estimation follows a procedure specific to the reliability analysis method utilized. The following subsections describe the probability estimation procedure for each of the reliability analysis methods.

2.1.1 Monte Carlo Simulation Probability Estimates

In Monte Carlo simulation, random basic variable values are generated in accordance with their corresponding probability distributions. A model simulation is performed using these basic variable values and the performance function is calculated. The hydrologic target level exceedance probability is estimated as the ratio of the number of exceedances ($Z < 0$) divided by the number of simulations. The risk estimated by Monte Carlo simulation is not unique, however, it may closely approximate the exact value if the number of trials is sufficiently large. Cheng (1982) compared Monte Carlo simulation results with direct integration for

$$Z = x_1 + x_2 - x_3 x_4$$

where x_1 and x_2 are uniformly distributed and x_3 and x_4 are lognormally distributed. Cheng found that a sample size of 1,000 produced near exact results for events with probabilities greater than 0.2 and a sample size of 8,000 produced near exact results for events with probabilities greater than 0.01. Thus, for relatively simple models (with four or five basic variables), sample sizes of 1,000 and 8,000 may be adequate for events with probabilities greater than 0.2 and 0.01, respectively. However, for more complex models or lower probability events, much larger sample sizes may be required.

2.1.2 MVFOSM Method Probability Estimates

In the MVFOSM method, the reliability index, β, is given by

$$\beta = \frac{E[Z]}{\sigma_z} = \frac{g(\bar{\underline{x}})}{\left[\sum_{i=1}^{p} c_i^2 \sigma_i^2\right]^{1/2}} \qquad (2.2)$$

As discussed in section B.5.1, for many cases of practical interest, β may

be assumed to follow a normal distribution, and the hydrologic target level exceedance probability, P_E, is approximately

$$P_E = 1 - \phi(\beta) \tag{2.3}$$

For simple algebraic models of the rainfall-runoff process, the partial derivatives, C_i, may be obtained analytically. For example, if the rational formula were used to estimate peak runoff, Q_p,

$$Q_p = C\ i_r\ A \tag{2.4}$$

where C = the runoff coefficient for the area,

i_r = the rainfall intensity in inches per hour, and

A = the drainage area in acres.

The system performance function would be

$$Z = T_H - \lambda_m\ C\ i_r\ A \tag{2.5a}$$

or

$$Z = \ell n[T_H/(\lambda_m\ C\ i_r\ A)] \tag{2.5b}$$

The resulting partial derivatives are

$$\begin{aligned} \partial Z/\partial \lambda_m &= -\ C\ i_r\ A \quad \text{for Eq. 2.5a} \\ &= -\ 1/\lambda_m \quad \text{for Eq. 2.5b} \end{aligned} \tag{2.6}$$

$$\begin{aligned} \partial Z/\partial C &= -\ \lambda_m\ i_r\ A \quad \text{for Eq. 2.5a} \\ &= -\ 1/C \quad \text{for Eq. 2.5b} \end{aligned}$$

and so on.

For hydrologic models which use more complex functional relations to estimate the hydrologic information of interest, the partial derivatives may not be obtained analytically (except for λ_m). The partial derivatives for

the input data and model parameters may be approximated by a forward difference at the mean

$$\left.\frac{\partial Z}{\partial x_i}\right|_{\underline{x}=\bar{\underline{x}}} = \frac{Z(\bar{\underline{x}}_j,\ \bar{x}_i + \Delta x_i) - Z(\bar{\underline{x}})}{\Delta x_i} \qquad (2.7)$$

where $\bar{\underline{x}}_j$ indicates that all the other basic variables are fixed at their mean values. The selection of appropriate Δx_is is a function of the particular model and performance function sensitivity to the basic variables.

2.1.3 AFOSM Method Probability Estimates

In the AFOSM method, the reliability index, β, for the case of transformed normal basic variables is given by

$$\beta = \frac{g(\underline{x}^*) + \sum_{i=1}^{p} C_i(\bar{x}_i^N - x_i^*)}{\sum_{i=1}^{p} C_i\ \alpha_i\ \sigma_i^N} \qquad (2.8)$$

Complete details on the transformation of the basic variables to equivalent normal variables are given in section B.6.2. It should be noted that not all basic variables must be transformed. In fact, β may be calculated without any distributional assumptions by using the basic variable means and standard deviations in place of x_i^N and σ_i^N in Eq. 2.8.

The partial derivatives may be estimated as for MVFOSM. For the case where forward differences must be used, $\underline{x}_w$, $\underline{x}_{jw}$, and x_{iw} should be substituted for $\bar{\underline{x}}w$, $\bar{\underline{x}}_j$, and x_i in Eq. 2.7 to signify that the partial is taken at point w which is a point in the iterations used to find $\underline{x}^*$.

The key problem in using the AFOSM method is locating the failure point $\underline{x}^*$. The failure point may be found by standard iteration approaches (e.g., Rackwitz' approach given in Fig. B.1) or by converting the hydrologic model to a subroutine for estimating Z and then using a standard GRG package (e.g., Lasdon et al., 1982) to minimize $|Z|$ as calculated by the hydrologic model subroutine. The GRG method is preferred for determining the failure point (see section B.6.1). However, if the hydrologic model used is a complex, established computer program, the difficulties associated with converting it to a subroutine may negate the advantages of the GRG approach from a practical viewpoint.

Whether using the standard iteration or the GRG approach, difficulties may be encountered in the estimation of β due to discontinuities in partial derivative approximations, especially for extreme $|\beta|$ values (> 2.5). For the ideal case, the iteration scheme terminates when the system performance

function approaches zero, the value of β converges to the second or third decimal place, and the basic variable values converge to within one or two percent of their values for the previous iteration. Cheng (1982) noted that the iteration approach frequently diverges when the value of β becomes large. The reason for this appears to be that as $|\beta|$ becomes large, the basic variable values are far removed from their mean values and in extreme cases ($|\beta| > 2.5$), the basic variable values often become somewhat unrealistic. As the iterations reach extreme basic variable values, the partial derivative values may change very rapidly (i.e., become discontinuous) in part due to the unrealistic variable values. Hence, the iterations approach the failure surface (Z=0) but have difficulty converging in both β and the basic variable values. In such cases, choosing the value of β to be that corresponding to the iteration wherein Z is closest to zero seems advisable. The β values so approximated are generally greater than 2.5 and the corresponding exceedance probabilities are less than 0.006. Therefore, from a practical viewpoint, the approximation errors are not serious.

For other cases, discontinuities in the effects of basic variables on the model output may lead to convergence problems at much smaller β values. Thus, when using either iteration or GRG to find the failure point, care must be taken to identify such discontinuities and to develop appropriate convergence criteria.

2.1.4 Evaluating Model Reliability

The previous sections describe how to use the reliability analysis to evaluate hydrologic target level exceedance probabilities. In this section, the use of the previously described probability estimates for model reliability evaluation is described.

If data is available for verification of the proposed reliability analysis approach, set the hydrologic target level equal to the measured peak. Determine the exceedance probability and reliability index corresponding to the measured peak, β_M, using Monte Carlo simulation, the MVFOSM method, or the AFOSM method. For Monte Carlo simulation, by assuming Z is normally distributed, β_M may be estimated as

$$\beta_M = \Phi^{-1}(1 - P_E) \tag{2.9}$$

In terms of the forecast variability, the β_M value is the standardized shortest distance between the forecast value and the measured value. If β_M is small, the forecast is quite reliable in a stochastic forecasting sense. However, if β_M is small and the absolute difference between the forecast and the measured value is large, the model is not very reliable in a practical sense because in such cases, the forecast variance is quite large. Alternatively, one may think of β_M as defining the forecast confidence interval which contains the measured value. In typical stochastic, time-series forecasting, a common "rule of thumb" for assessing the quality of the forecast is that the measured values fall within the 95 percent confidence

limits of the forecast. A $|\beta_M|$ value of 1.96 corresponds to the 95 percent confidence limit. Thus, all calculated $|\beta_M|$ values less than 1.96 indicate a "good" stochastic forecast. However, if the confidence interval (bounded by the confidence limits) is large, the utility of the forecasts is small. For cases wherein "good" stochastic forecasts of low utility are obtained, the model itself is probably capable of producing "good" forecasts from a practical viewpoint if the underlying uncertainties can be reduced.

By calculating β_M values for a large number of verification events, one can get an idea of the general reliability of the model and its forecasts.

For an individual forecast or prediction without knowledge of the measured peak, one estimate of the forecast or prediction reliability is the forecast standard deviation. For Monte Carlo simulation, the forecast statistics may be summed directly as the individual simulations are performed. For the MVFOSM method, the forecast standard deviation is approximated as

$$\sigma_z = \left[\sum_{i=1}^{p} (C_i^2 \, \sigma_i^2) \right]^{1/2} \tag{2.10}$$

For the AFOSM method, the forecast standard deviation is approximated as

$$\sigma_z = \sum_{i=1}^{p} C_i \, \alpha_i \, \sigma_i^N \tag{2.11}$$

with C_i and α_i evaluated when $\beta = 1$, which is the case where the standardized difference between the forecast and the target level equals the forecast standard deviation. Therefore, trial and error selection of the hydrologic target level is necessary to find the case where $Z = 0$ and $\beta = 1$.

The Monte Carlo simulation and the AFOSM methods can also evaluate the reliability of non-verifiable (at the time of their issuance) forecasts or predictions by estimating the CDF and PDF of the forecast. For the MVFOSM method, a normal distribution for Z is assumed; hence, this information is summarized in the mean and variance of the forecast. By varying the hydrologic target level and calculating the corresponding P_E, the forecast CDF is obtained which may be differentiated to produce the forecast PDF. Given the initial assumption that the hydrologic model and its uncertainty accurately reflect the variance of the true hydrologic system is valid, the reliability of the forecast is indicated by how closely the forecast CDF approximates a "step function" and the forecast PDF approximates a "spike." For reliable forecasts, the CDF will have a very steep slope and the PDF will be very sharp and distinct. For unreliable forecasts, the CDF will have a mild slope and the PDF will be broad and flat.

2.2 Model Choice and Uncertainty Analysis

As was discussed in Appendix A, the various types of hydrologic models which have been used for real-time flood forecasting are grouped into three types: abstract, physical-conceptual, and physical simulation. Generally, the choice of which type of model to incorporate in a FWP system is a function of the size of the watershed, the historical data available for the watershed, and the personal preference and experience of the hydrologist.

For any watershed size, the primary factor affecting the type of hydrologic model used is the amount of historical rainfall and runoff data available for the watershed. If a reasonable amount of historical data is available, the choice is generally an abstract model or one of the less complex physical-conceptual models (e.g., HEC-1 or RORB). These models take a greatly simplified view of the rainfall-runoff process and use calibration of the parameters to compensate for simplifications. Due to their simplified nature these models are generally less complex and more parsimonious than physical simulation or more complex physical-conceptual (e.g., Stanford model, SSARR, etc.) models. Hence, if data is available for calibration, use of either a stochastic, conceptual, or less complex physical-conceptual model is preferred. Generally, the choice between these is a function of the watershed conditions and personal preference. In cases where the amount of data available for calibration is perhaps a little less than is desirable, physical-conceptual models might be preferred because the hydrologist can supplement the calibration information with his knowledge and experience with such models on similar watersheds. For example, Muskingum flow routing coefficients may be estimated from physical considerations and various regionalization studies have been conducted for synthetic unit hydrograph parameters (e.g., Singh, 1981).

Physical simulation models are capable of generating reasonable hydrograph estimates using only a minimum amount of calibration. The parameters of the model may be estimated by considering the physical condition of the watershed (topography, geomorphology, vegetation, etc.) and by measuring physical properties of the watershed such as soil hydraulic conductivity, porosity, and capillary tension. Parameters derived from physical measurements, theoretical inferences, personal experience, or lumping of watershed conditions (e.g., average overland flow slope) are typically much more uncertain than those determined by calibration. Thus, physical simulation models should only be used as a last resort for cases with a dearth of calibration data, or where the watershed is continually changing (e.g., due to urbanization) and previous calibrated parameters are no longer valid.

The nature of modeling uncertainties is quite different for physical simulation models as opposed to calibrated models. Thus, two general procedures for evaluating data, model parameter, and model structure uncertainties are outlined in the following sections; one for physical simulation models, the other for calibrated abstract and physical-conceptual models (hereafter referred to as calibrated models). While techniques for evaluating the uncertainties in both calibrated and physical simulation models are presented in this chapter, the case study (detailed in Appendix C) only demonstrates the incorporation of reliability analysis with calibrated models. A case study considering only calibrated models is

sufficient to show the utility of reliability analysis of hydrologic modeling uncertainty. Hence, a detailed reliability analysis of the uncertainty encountered when using physical simulation rainfall-runoff models will be reserved for future research.

2.3 Evaluation of Data Uncertainties

Nearly all rainfall-runoff models require data from some combination of four sources: rainfall, streamflow, evapotranspiration, and watershed morphology. The basic sources of error and uncertainty in each of these types are discussed below, and methods to account for these uncertainties when using physical simulation or calibrated models are presented.

In this study, it is assumed that there are no problems with the data transmission network, and all data from the rain and stream gages will be available in real-time. Thus, the uncertainties introduced to real-time flood forecasting by missing data are not considered. From a practical viewpoint the assumption of no missing data is not necessarily good even with the most advanced telemetry systems. For example, the National Weather Service's 1981 report on the central Arizona floods of February, 1980, revealed the following interesting facts:

> "In Arizona . . . the density of real-time rain gage reports was very inadequate throughout the series of storms. The shortage of data was aggravated by the fact that some of the existing "real-time" rainfall and river gages malfunctioned, were late in reporting, or reported erroneous data at critical times."

The major problems encountered with the river gages were that they were plugged with debris or damaged on their mountings when rivers became swollen to near record levels or they mechanically or electrically malfunctioned. Outages in rainfall data were mainly due to telephone lines being down. Furthermore, Sargent (1984) reports that for the Haddington (U.K.) flood warning program radio telemetry was chosen to communicate real-time rain gage data because the telephone network was thought to be unreliable during periods of high rainfall. However, the telephone link to the base stream gage station has never yet failed, while the radio telemetry system has frequently failed. Thus, the question of whether the necessary rain and stream gage data will be available for forecasting is potentially a greater source of uncertainty than the uncertainty in the forecasts. Nevertheless, in this study only the uncertainty in the forecasts is considered.

2.3.1 Rainfall Data Uncertainty

There are eight primary sources of error or uncertainty involved in using point rainfall measurements to describe the true precipitation input for a watershed:

1) measurement error in the gage itself due to malfunction,

2) the gage data's representativeness of ground level precipitation at

the gaging point,

3) gage location, e.g., gages are in positions that consistently result in high or low readings relative to the watershed average,

4) gage network mean areal rainfall versus true mean areal rainfall,

5) effects of rainfall spatial variability,

6) effects of rainfall temporal variability,

7) lack of synchronization between time clocks for rain and stream gages,

8) lack of synchronization between time clocks for the various rain gages in the watershed.

Each of these sources of error or uncertainty require some further general discussion before the procedure for analyzing their total effects on calibrated models and on physical simulation models is described.

For rain gages, malfunctions include errors in reading, transmitting, and handling data and mechanical or electronic errors in the actual measurement of point rainfall. For modern telemetry systems such as those used in "state-of-the-art" real-time forecasting systems, the data communication errors are greatly reduced, except in cases of transmission failure. If there is no transmission failure, the rainfall data is fed directly into the computer data base, eliminating reading and handling errors while leaving transmission errors negligible. For example, Stalmann (1970) reported that signals from a radio-telemetry system of river level gages showed an almost faultless agreement with the water levels simultaneously transmitted by an automatic telephone telemetry system. The precision of transmission amounted to $\pm$ 2 cm water level at a total range of 9 m.

Thus, for real-time flood forecasting only the mechanical or electronic errors in the actual gage measurements need to be considered when using physical simulation models on previously ungaged watersheds. However, for calibrated models the nature of the gage network from which the calibration data was obtained must be considered. If the calibration data was not obtained from a telemetered system, data reading, transmission, and handling errors must be considered.

For real-time flood forecasting systems employing a modern telemetry system, synchronization of the various rain and stream gages is not a problem. For example, Sargent (1984) reports that for the Haddington (U.K.) flood warning system each gaging station has its own crystal clock which is synchronized with the base station clock when the base station issues a reset command during start up operations. Once again, for calibrated models the nature of the gage network from which the calibration data was obtained must be considered when dealing with time synchronization errors.

Errors due to the difference between gage data and the precipitation at ground level at the gaging point are primarily due to wind effects. A

generally accepted theory is that much of the total measurement error is the result of turbulence and increased wind speed in the vicinity of the gage orifice resulting from the obstacle of the gage itself to the wind stream. As the air rises to pass over the gage, precipitation that would have passed through the gage orifice is instead deflected and carried further downwind (Larson and Peck, 1974). Other sources of discrepancy between gage measurements and ground level precipitation are the so-called "wetting loss" due to water drops adhering to the walls of the gage funnel and the collector and sheltering of the rain gage by trees and buildings.

Gage location uncertainties refer primarily to cases where gages are located near the boundaries of the watershed. At such locations the gage measurements are less likely to reflect the true temporal and areal distribution of rainfall over the watershed. Troutman (1983) stated that given only a small amount of recorded rainfall at a single gage (or a few gages), it is not known whether the overall storm was indeed small or the storm was large with a center located at some distance from the gage(s). This could obviously result in considerable error in runoff prediction, especially if the gage is not located centrally in the basin. Furthermore, Troutman's (1983) numerical experiments found that for single gage networks, mean squared prediction bias generally increases as gage distance from the basin center increases. Hence, he concluded that the nonstationarity of rainfall imposes an additional form of bias when observed rainfall is from gages not centrally located within a basin. For previously ungaged watersheds where flood warning systems are to be established, intelligent network design can avoid this source of uncertainty. However, for watersheds where existing gages are adapted to work in a telemetry system consideration of gage location uncertainties may be necessary.

Even if the gages are located in spots where reasonably representative rainfall measurements can be made, there will still be considerable uncertainty regarding the quality of the estimated areal mean rainfall. Troutman (1982a and 1983) found that even if measured rainfall at a small number of gages is equal in expected value to the true areal average rainfall, the variance of basin average rainfall is always less than that for point rainfall. This difference in variability can result in serious biases in runoff prediction, e.g., for the models Troutman studied the bias was overprediction of large events and underprediction of small events. Thus, for models using lumped rainfall input data, variance of the network estimate of mean rainfall relative to the true mean rainfall must be considered.

Ideally, in order to obtain the best prediction of storm runoff knowledge of the rainfall intensity at each point in the basin and at each point in time is necessary. However, measurements of precipitation are always made at discrete intervals in time and at a limited number of points in space. Thus, there are uncertainties in the data due to unsampled temporal and areal variations in the true rainfall. Furthermore, Bras and Rodriguez-Iturbe (1976) demonstrated the natural "filter" characteristics of the watershed runoff process are insufficient to "damp out" the effects of these unaccounted for variations. Accounting for the data uncertainties due to spatial and temporal rainfall variability is not an easy task. Realistically, even if data from an extensive rain gage network with one minute readings are available, this fairly accurate reporting of spatial and

temporal variability could not be used by the hydrologic model. Almost all hydrologic models, even so-called distributed models, "lump", to some extent, the input data and hydrologic characteristics of watersheds in order to make hydrograph prediction practical. Furthermore, the temporal variations are also averaged for input to hydrologic models partly for computational practicality and partly because the model structure is insensitive to more detailed information. Therefore, the uncertainty related to the data's inability to account for the rainfall's true spatial and temporal variation is in part a function of the model structure uncertainties due to temporal and spatial "lumping" of the rainfall-runoff process.

2.3.1.1 Handling Rainfall Data Uncertainty in Calibrated Models

All eight of the possible errors in rainfall data listed earlier could have an effect on the reliability of the hydrograph predicted by a calibrated model.

Dawdy et al. (1972) reported that the bias (errors and uncertainty) in the recorded rainfall at each station is compensated by the curve-fitting ability of the model to adjust parameter values. Hence, bias in the amount of recorded rainfall affects the resulting fitted-parameter values, rather than the accuracy of the fit. Troutman (1982a and 1983) also found that errors and uncertainties in rainfall data were transferred to the parameters of the model as bias in the parameters (i.e., deviations from their true values). However, due to the curve-fitting properties of the calibration routine, the performance of the model using erroneous data and biased parameters is not greatly different from that using true data and parameter values. In fact, for a simple regression model of rainfall volume to runoff volume, Troutman (1982b) found two extremely interesting results. First, for cases where the rainfall input error is equivalent to a random process (11 of 13 subsets of the gage network considered), it was found that even though the erroneous rainfall values have more variability than the true values, runoff computed from the model evaluated with the erroneous rainfall and the adjusted parameters has less variability than that computed from the model evaluated with the true rainfall and parameters. Second, model predictions using erroneous rainfall measurements and the corresponding biased parameter values are unbiased estimates of mean runoff. Troutman (1982a and b) further pointed out for more realistic nonlinear models of runoff the curve-fitting never quite eliminates the bias in the mean runoff estimation. However, if more than one parameter is adjusted, there is a good chance that the bias will be fairly small over a wide range of rainfall input values.

Thus, if the common assumption that the calibration data is a representative sample of the range of flows to be predicted and of the range of data errors to be encountered is reasonably valid, the data uncertainties may be assumed to be included in the calibrated model parameters and their corresponding uncertainties. The sample must not only be representative but also homogeneous and of sufficient size to justify the statistical estimates. A homogeneous sample is one where all the events are a subset of the same event population and, hence, a product of a unique physical rainfall-runoff process. The primary causes for non-homogeneous samples are

changing watershed conditions due to human activity and seasonal variation in the rainfall-runoff process. With regard to the size of the sample, the U.S. Water Resources Council (1981) recommends that stream gaging records be at least ten years long before use of flood frequency analysis is warranted. Ang and Tang (1975, p. 236) stated that if sample size is large (for instance, greater than 20), the sample variance is a good estimator of the population variance.

Having decided to consider rainfall and runoff data uncertainties as included in model parameters by the calibration process, two issues still need to be addressed. First, how the calibration is to be performed, and how does the data uncertainty affect the physical interpretation of the calibrated parameters? These questions are addressed in the discussion of parameter uncertainties in section 2.4. Second, are there any errors in the calibration data that will not be present in the data for generating real-time forecasts, and if so, how do these errors affect the validity of the proposed reliability analysis?

If the data used for calibration was obtained from a telemetered gage network with data stored directly with a minimum amount of human handling, then the parameters will not contain any data uncertainty not present in the real-time forecasting data. However, if the existing gage network currently uses strip charts, punched strips, or even cassette recordings of the data, this data is subject to errors in interpretation (especially for strip charts) and in timing (i.e., synchronization of clocks). When developing a flood warning system the old clocks and chart recorders are replaced with new clocks and radio or telephone transmitters/receivers, eliminating timing and communication errors in the data. Thus, the calibrated parameters, which include these errors, are not truly representative of the uncertainty in data used for real-time flood forecasting.

The errors due to data reading, transmission, and handling are probably fairly small if the charts are read consistently and the readings are carefully checked for nonsensical values. The additional uncertainties these errors add to the parameters will not significantly affect the reliability analysis.

The timing errors, i.e., lack of synchronization between the rain gages and stream gages, have much greater effects on the calibrated parameters. Jackson and Aron (1971) found that timing errors due to clock malfunctions and lack of synchronization appear to be the most common cause of rain gage unreliability, and these errors take on major importance in parameter calibration. Laurenson and O'Donnell (1969) found that synchronization errors appear to result in the greatest errors in unit hydrograph derivation. Therefore, steps must be taken to account for the extra uncertainty in model parameters due to synchronization errors in the calibration data.

Unfortunately, about the only practical way to account for synchronization errors is to try to detect and eliminate (or at least reduce) them in the data. Poor calibration fits in the form of greatly underpredicted or overpredicted peak discharges or of extensive smoothing or flattening of the hydrograph may be caused by synchronization errors, which should be eliminated, or by rainfall temporal and spatial variability errors in data, which should be transferred to the parameters. Therefore, there is no

substitute for good quality calibration data checked carefully for synchronization errors. It is believed that the calibration and verification data used in this study (see Appendix C) is free from synchronization errors.

2.3.1.2 Handling Rainfall Data Uncertainty in Physical Simulation Models

Of the eight possible sources of error or uncertainty in rainfall data, only five need be considered in the data uncertainty for physically based models. Three other sources may be eliminated due to the design of the data network. Physical simulation models should only be used in cases where it is desired to establish a flood warning system on a previously ungaged (or poorly gaged) watershed or in cases where the watershed is changing (e.g., due to urbanization). Thus, a modern telemetry based rain and stream gage network should be designed and installed. The design of this network should be such that the gages are not in locations that result in consistently high or low readings. The telemetry system with its accurate clocks insures that timing errors due to clock malfunctions and synchronization problems are small. Also, since the telemetry system feeds the data directly into the computer for consistency checks and subsequent use in real-time forecasting, the data reading, transmission and handling errors are also small. Thus, only the gage measurement errors due to mechanical or electronic defects, gage measurement errors (e.g., due to wind effects), and the uncertainty regarding the quality of the gage network estimate of mean areal rainfall need to be considered for physically based models. The errors due to inaccurate representation of rainfall spatial and temporal variation are partially accounted for in the gage network estimate of mean areal rainfall uncertainty and in the model structure uncertainty.

Given below is an example of how the errors in rainfall measurements may be approximated. This example could serve as an initial approximation for reliability analysis. For accurate determination of hydrologic target level exceedance probabilities, a much more detailed analysis of the error sources is necessary.

Throughout the twentieth century, three types of rain gages have been used to provide a continuous record of rain depths and intensities: the tipping bucket, weighing-type, and float-type gages. The tipping bucket gage was quite popular in the early part of the century, but due to problems with jamming and underestimation of heavy rainfalls (see Parsons, 1941) the National Weather Service gradually began phasing them out. Float-type gages have been used extensively in Europe, while weighing-type gages have been used extensively in the United States. Each of these gages has its own mechanical problems which lead to inaccurate rainfall estimates. Frictional effects in the weighing mechanism of weighing-type gages and in float guides of float-type gages are the primary cause of inaccurate rainfall estimates. In self-emptying float-type gages the siphoning takes at least a few seconds, and hence rain falling into the receiver during siphoning period is recorded inaccurately. Furthermore, the rainfall amounts siphoned out are not always the same for all emptying cycles (Linsley et al., 1975).

For newly installed rain gages, as would be the case for watersheds using physical simulation models, frictional effects should be low and may

be kept that way with regular maintenance. Thus, the gage measurement errors due to mechanical defects may be considered insignificant relative to the wind effects uncertainty and limited rain gage network estimate of areal precipitation uncertainty. The above assumption is especially valid if modern electronic liquid level reading gages, such as the one described by Permut et al. (1979), are used for rain gage measurement. The gage developed by Permut et al. (1979) uses digital electronic elements to detect the highest liquid level sensing electrode in contact with the collected rainfall at any time. Changes in level must persist for a predetermined time period before the level sensing circuits recognize the change in level as incoming rainfall and report the corresponding intensity. Hence, short term level transient conditions caused by vibration, splashing, or wave motion do not influence measurements. With such gage equipment, reliable real-time measurements are virtually assured.

It is generally accepted that wind is the major cause of error in precipitation gage measurements. Sevruk (1975) reported that either a gage leveled with its orifice at the ground level and protected against in-splash and/or a carefully selected well-protected natural gage site can reduce the wind effects on precipitation measurement. However, Larson and Peck (1974) noted that no combination of gage location and shielding will entirely eliminate adverse effects of wind on gage catch. Furthermore, there is no guarantee that the gages may be located at ground level or naturally protected sites. Therefore, even for new and/or well designed gage networks wind effects play a significant role in rainfall measurement uncertainty.

The question of how to deal with this source of uncertainty is quite complicated. Larson and Peck (1974) developed Fig. 2.3 relating gage catch deficiencies and wind speed based on their own field studies in Danville, Vermont, and Laramie, Wyoming and the work of several other investigators. Morgan and Lourence (1969) compared the catch of a standard 8-inch rain gage mounted in the normal standing position, a USSR 3000-square-centimeter rain gage mounted at ground level, and a highly sensitive weighing lysimeter 20 feet in diameter for 24 storm events from two winter rainy seasons at Davis, California. For storms ranging in average wind speed from 2.5 to 14.3 miles per hour (mph) with the windiest hour speed twice the storm average, they found no apparent systematic relation between average wind speed for a particular storm and the difference in total storm precipitation caught by the rain gage and that measured by the lysimeter. Thus, relations of the type defined by Fig. 2.3 do not necessarily reflect the true wind effect on gage catch of rainfall.

A key factor which in addition to wind speed greatly influences the wind effect on gage catch accuracy is raindrop size. Mueller and Kidder (1972) used wind tunnel experiments with rain gage models to define velocity patterns, and then used computer simulation of these velocity patterns and drag on raindrops to estimate gage catch deficiencies due to wind speed and drop size. Their results are displayed in Fig. 2.4, and it should be noted that Mueller and Kidder estimated the maximum probable error of their results to be 15 percent. From Fig. 2.4 storms dominated by larger raindrops are less likely to be affected by wind. Laws and Parsons (1943) reported that high intensity (greater than 5 in./hr) storms have median drop diameters greater than 3 mm, while even medium intensity storms (0.5 to 5.0 in./hr) have median drop diameters between 2 and 3 mm. Therefore, it seems

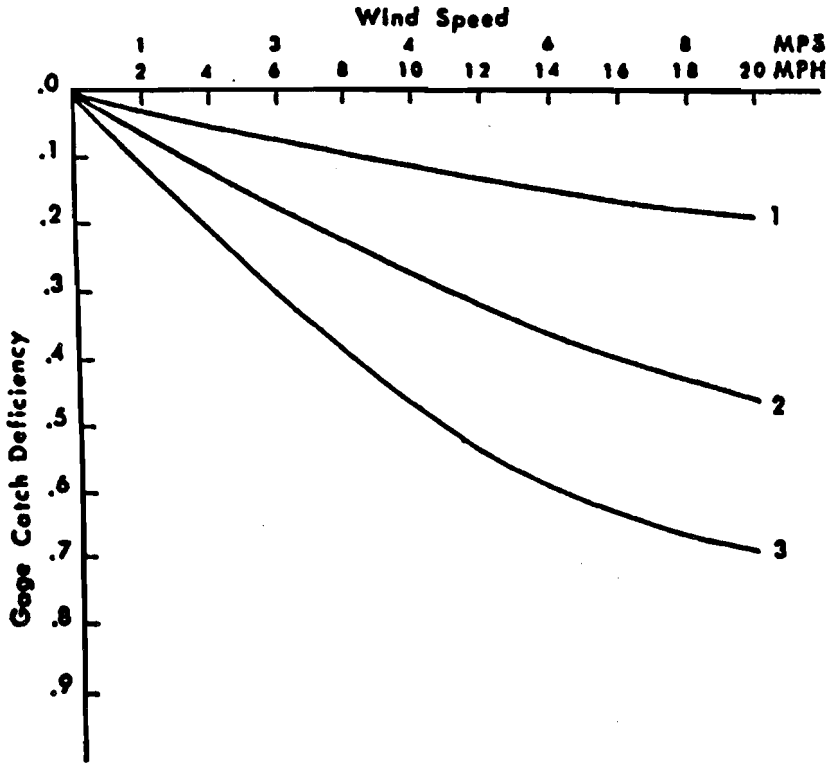

Figure 2.3. Gage catch deficiencies versus wind speed. Line 1 is for rain (shield makes little or no difference in deficiencies), line 2 is for snow with a shielded gage, and line 3 is for snow with an unshielded gage. (after Larson and Peck, 1974)

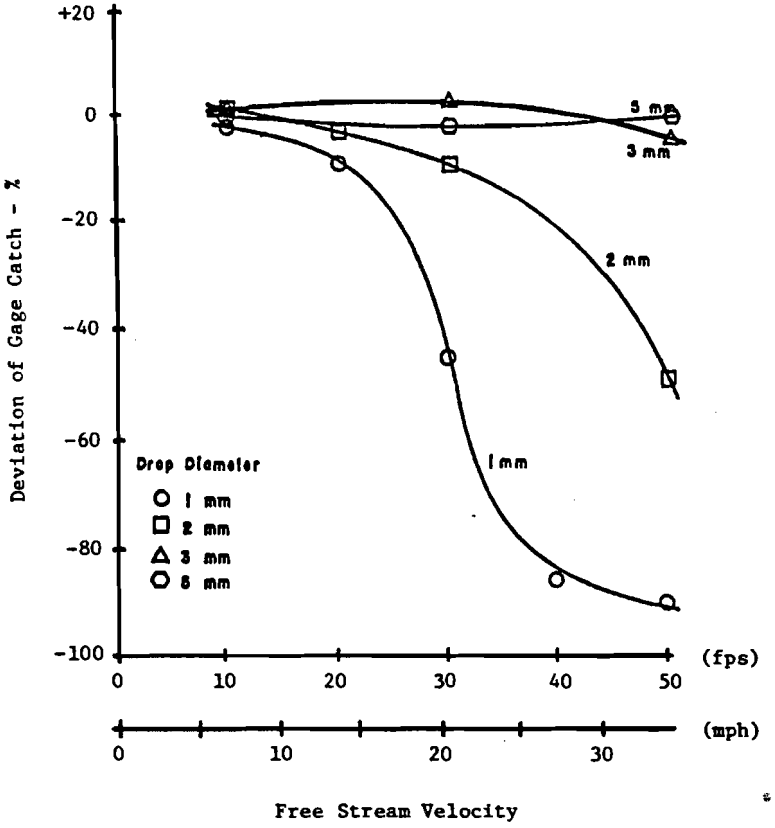

Figure 2.4. Percent deviation of gage catch relative to drop diameter and the free stream velocity. (after Muller and Kidder, 1972)

that Fig. 2.3 may have been obtained from data from lower intensity storms dominated by smaller drop sizes (the 1 to 2 mm range), while the work of Morgan and Lourence (1969) may be representative of higher intensity storms dominated by larger drop sizes (this assumption is reasonable for California winter rainy season storms).

Furthermore, it may be reasonable to assume that for the high intensity storms likely to cause floods in small and medium size watersheds, the wind effects may not be serious enough to require adjustment of the point precipitation measurement. This does not mean that rainfall data uncertainties due to wind are being ignored, but rather it means that the uncertainty can be accounted for in the variance of the measurement alone. That is, if the true catch, P_x, is considered to be

$$P_x = (\bar{a} + e_a)\, P_{xm} \tag{2.11}$$

where P_{xm} = the measured point precipitation;

$\bar{a}$ = the correction factor relating for the difference between the true and the measured rainfall at a point due to wind effects, obtained from Fig. 2.3 for example;

e_a = the uncertainty associated with using $\bar{a}$ (mean = 0, variance = σ_a^2);

all that is being assumed is that $\bar{a}$ equals unity. The uncertainty expressed in terms of variance in P_x due to wind effects is still considered and it is equal to $P_{xm}^2\, \sigma_a^2$. A reasonable assumption for the value of σ_a may be obtained by using a triangular distribution over $\bar{a}$ ranging between $\bar{a} \pm 0.15\, \bar{a}$ (recall 15 percent was the maximum probable error estimated by Mueller and Kidder). Actually, with $\bar{a}$ assumed to be unity, $\bar{a} - 0.15\, \bar{a}$ is unrealistic, fortunately within the first-order uncertainty analysis the variance due to wind effects can be constrained such that it is only considered when estimating the probability of a flood discharge greater than the expected flood discharge.

If a dense-rain-gage-network watershed exists which is subject to climatic and topographic conditions similar to those for the watershed being studied, then the uncertainty in estimating the mean areal precipitation from a small number of gages may be approximated by the following procedure. Assuming the "true" mean areal precipitation is obtained from the complete network information, by comparing the averages estimated by different subsets of the total gage network the uncertainty associated with mean areal rainfall estimates for various numbers of gages may be approximated. For this approximation to be reasonable, the wind effects uncertainty must be relatively constant for both the entire network and the various subsets. This approach has been used quite commonly and successfully in hydrology.

Horton (1923) compared the mean areal average yearly rainfall for various subsets of a 42 gage network for the River Derwent basin in England, to develop a criteria for the number of gages necessary to achieve an

estimate of annual rainfall on a basin within a specified accuracy. Light and Shands (1947) used this approach to derive a graph relating percent standard error in the estimate of mean areal rainfall volume as a function of watershed size and density of rain gages. Data from 38 relatively intense storms between 1937-1941 over the Muskingum watershed (8000 mi^2) in Ohio and from 1500 mi^2 and 375 mi^2 subareas of it were analyzed. Data from as many as 500 gages was available for the early part of the record; this number decreased to 250 by the end of the record. Linsley and Kohler (1951) sought to determine the relative reliability of the average areal storm rainfall computed from networks of different density. Hence, they computed the average precipitation for networks consisting of 1, 2, 3, 4, 10, 18, and 55 gages for each of 68 storms on the 220 square mile Army-Navy-NACA Weather Bureau network watershed near Wilmington, Ohio. In each case, the stations were selected on as nearly a uniform grid pattern as the network permitted. Hence, each sub-network approximated the ideal distribution of gages. Using this data, equations were developed which related the average absolute error in inches of areal storm rainfall, E, to the "true" precipitation depth, P_t in inches and the number of gages, N, for three different watershed sizes, 100, 160, and 220 square miles.

$$E_{220} = 0.186\ P_t^{0.47}\ N^{-0.60} \tag{2.12a}$$

$$E_{160} = 0.181\ P_t^{0.36}\ N^{-0.52} \tag{2.12b}$$

$$E_{100} = 0.176\ P_t^{0.44}\ N^{-0.78} \tag{2.12c}$$

While these equations vary with the area of watershed, there appears to be a certain general relation form which might be used for the purpose of this study.

McGuinness (1963) used a similar technique to derive an equation relating the average absolute error in inches of areal storm rainfall to the "true" precipitation and the gaging ratio, G, (i.e., the number of square miles per gage) for 81 storms on the 7.16 square mile Little Mill Creek watershed near Coshocton, Ohio.

$$E = 0.03\ P_t^{0.54}\ G^{0.24} \tag{2.13}$$

Huff (1970) also used this procedure to derive an equation relating the average absolute sampling error in inches of areal one-minute rainfall data, E_a, to the "true" one-minute average rate, R_a, in inches per minute and the gaging ratio for 29 storms on the 100 square mile Goose Creek watershed near Monticello, Illinois.

$$E_a = 0.03\ R_a^{0.87}\ G^{0.52} \tag{2.14}$$

If the 220 square mile watershed error equation is converted to be a function of gaging ratio,* one obtains

$$E = 0.0073\ P_t^{0.47}\ G^{0.60} \qquad (2.15)$$

It can be seen that the average errors in estimating mean areal rainfall for these three midwestern watersheds appear to be fairly consistent. Therefore, a general relationship may exist between errors in estimated areal precipitation, the "true" areal precipitation, and the gaging ratio for watersheds with similar topography in similar climates such as these three midwestern watersheds. The work of Huff and Schickedanz (1972) supports the above assertion. They developed a model for estimating the error in areal precipitation estimates from sparse gage networks based on climatological principles and a 4 gage network for the 400 square mile East Central Illinois network near Farmer City, Illinois. They found that the climatological estimates of the relative standard error of daily areal means were nearly the same as the dense network estimates. Hence, climate plays a significant role in the uncertainty of sparse gage network estimates of true areal precipitation. Therefore, a conglomeration of Eqs. 2.12, 2.13, and 2.14 could provide a reasonable estimate of variance due to this source of uncertainty.

McGuinness (1963) performed just such a conglomeration. Using his own results for Coshocton, Ohio as representative of small midwestern watersheds; Huff and Neill's (1957) results for the Panther Creek, Goose Creek, El Paso, and east central Illinois networks (see Table 2.1) as representative of medium size (25 to 400 mi^2) midwestern watersheds; and Light and Shands' (1947) results for the Muskingum, Ohio network as representative of large midwestern watersheds he prepared a nomogram (Fig. 2.5) relating average error in mean areal rainfall estimates to rainfall depth, gaging ratio, and a climatic/geographic factor (the 5-year 24-hour rainfall from Hershfield, 1961). Error estimates from Fig. 2.5 compare well with Linsley and Kohler's (1951) results which were not used in deriving the nomogram. Therefore, Fig. 2.5 may be used to estimate the average error in mean areal total rainfall estimates for midwestern watersheds.

To obtain error estimates for shorter time periods within a storm, Eq. 2.14 may be useful for midwestern watersheds. Equation 2.14 was derived for one-minute data, however, Huff (1970) found the spatial correlations of rainfall rate are not changed significantly by averaging over intervals of 5 to 10 minutes as opposed to using the one minute rates. Hence, applying Eq. 2.14 to longer time period data should provide reasonable estimates of the uncertainty.

---

*Since the independent variable in this equation has been changed from N to G, this equation no longer represents a true least squares fit, however, the coefficient values are probably still fairly reasonable for comparison with the other equations.

TABLE 2.1. A Partial Listing of Dense Rain Gage Networks in the United States

Network	Nearest City	Area (mi^2)	Number of Gages	Gaging Ratio (mi^2/gage)	Reference
ARMY-NAVY-NACA-Weather Bureau	Wilmington, OH	220	55	4.00	Linsley & Kohler, 1951
Boneyard Creek	Champaign, IL	10	11	0.91	Huff & Schickendanz, 1972
Central Illinois	Bloomington, IL	2317	260	8.9	Vogel & Changnon, 1981
Chicago Area	Chicago, IL	4015	320	12.5	Vogel & Changnon, 1981
Chickasha, OK	Chickasha, OK	900	36	25.00	Hershfield & Engman, 1981
East Central Illinois	Farmer City, IL	400	49	8.16	Huff & Schickendanz, 1972
El Paso	El Paso, IL	290	48	5.83	Huff & Neill, 1957
Goose Creek	Monticello, IL	100	50	2.00	Huff & Schickendanz, 1972
Little Egypt	Marion, IL	550	49	11.22	Huff & Schickendanz, 1972
Little Mill Creek	Coshocton, OH	7.16	64	0.11	McGuinness, 1963
Metromex	St. Louis, MO	2010	225	8.9	Vogel & Changnon, 1981
Muskingum Basin	Zanesville, OH	8000	250-500	16.0-32.0	Light & Shands, 1947
Panther Creek	Bloomington, IL	100	9	11.11	Huff & Schickendanz, 1972
San Dimas Experimental Forest	San Dimas, CA	25.6	318	0.08	Phanartzis & Kisiel, 1972
Shawnee	Cairo, IL	386	44	8.8	Vogel & Changnon, 1981
Walnut Gulch	Tombstone, AZ	57.7	93	0.62	Renard, 1970

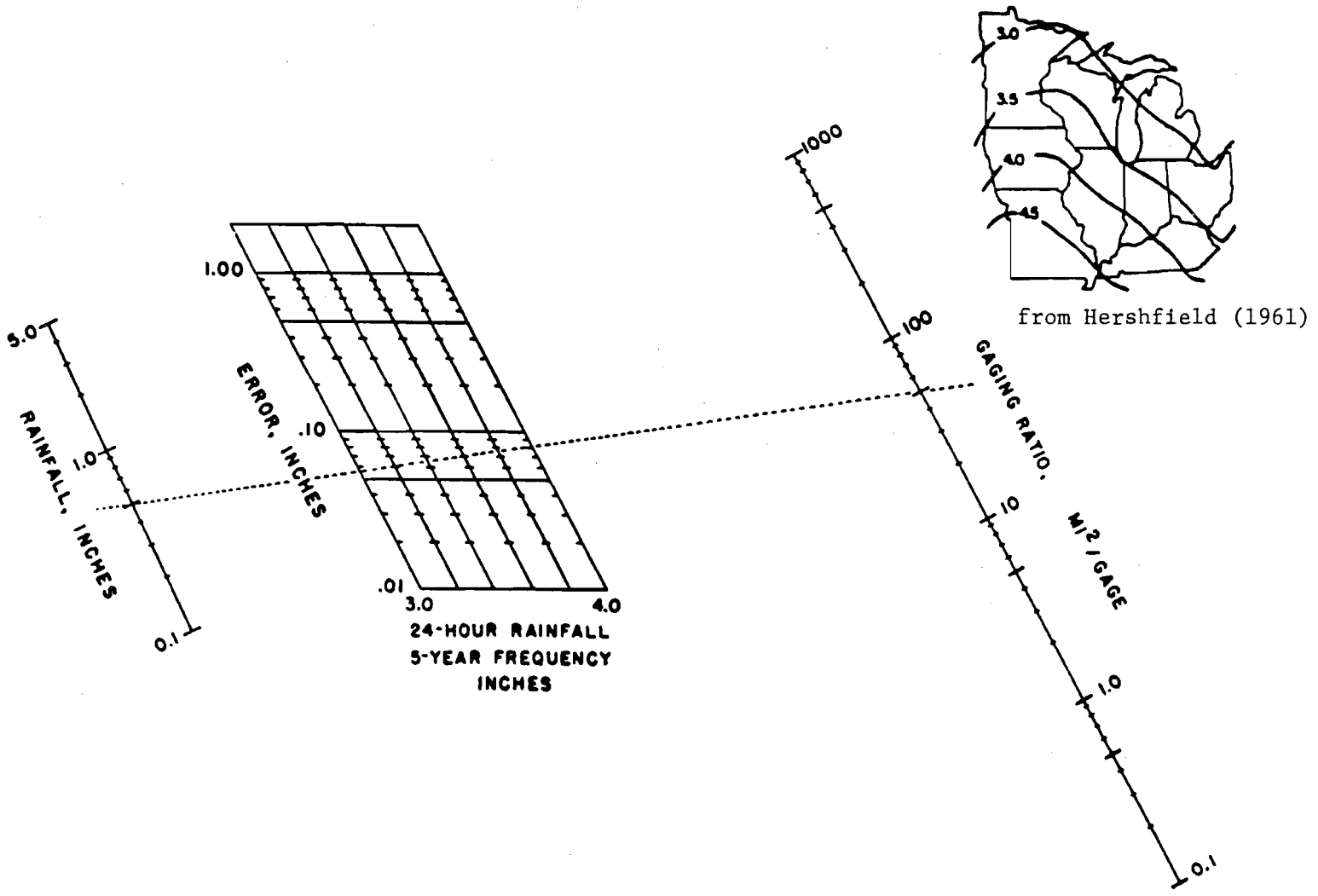

Figure 2.5. Nomogram for estimating average error in mean watershed rainfall determination (after McGuinness, 1963)

Unfortunately, in real-time flood forecasting the values of the true areal storm, P_t, or one-minute precipitation, R_a, data are not known, but rather only the erroneous values P_e and R_{ae}, respectively. If P_e or R_{ae} are used in Fig. 2.5 or Eq. 2.14 to estimate the average absolute error, these estimates may be greatly over- or under-predicted due to the nature of the error in P_e or R_{ae}. A reasonable way to estimate the true error in P_e or R_{ae}, would be to calculate E for R_{ae} and P_e and then for $P_e \pm E$ and $R_{ae} \pm E_a$ and take a weighted average of the calculated E values as an approximation of the true error. For the purpose of FOSM analyses, the standard error (i.e., standard deviation of the sample) of the mean areal rainfall estimate is needed rather than the average absolute error. Light and Shands (1947) note that for normally distributed variables the average error equals 0.8 of the standard error. This relation may be used to convert the weighted average error to an estimated standard error.

Similar equations and nomograms may be derived for other regions of the country using dense rain gage network information available in these regions. Table 2.1 displays a partial listing of dense rain gage networks in the United States. Data for additional dense rain gage networks (as well as some listed in Table 2.1) may be found in Thurman and Roberts (1986) and the references therein.

Many other factors influence the validity of Fig. 2.5 and Eq. 2.14 including: (1) rain type, (2) storm type, (3) total storm rainfall (Eq. 2.14 only), (4) storm duration, (5) storm mean intensity, (6) location of the storm center with respect to the center of the sampling area, (7) the direction of movement and orientation of the major axis of the storm, (8) the number and distribution of individual storm cells at any given time in the sampling area. Huff (1970) attempted to access the first five of these factors, however, his 29 storm sample size was too small to detect any trends in the data due to these factors. Nevertheless, the fact that he frequently found relatively large differences in the sampling errors between storms of apparently similar characteristics, led him to believe that these factors are quite important. The consistency in the form of Eqs. 2.12, 2.13, and 2.14 indicates that they will perform well, for the purpose of this study, despite these other factors. However, when developing similar equations for other areas of the country, attention should be paid to the eight factors listed above. Especially for mountainous eastern and western watersheds where topography, rain type (i.e., orographic precipitation), and storm type (e.g., heavy thunderstorms in the west) greatly influence these error relations.

For the first-order second moment analysis, the mean value of the precipitation input is simply the areal mean precipitation estimate from the gage network measurements, P_e. If the wind velocities across the watershed are fairly uniform, the wind effects errors at each gage will be similar percentage-wise. Therefore, the areal mean precipitation estimate may be used with the coefficient of variation of the error in rainfall measurements due to wind effects, σ_a, to determine the associated variance. Furthermore, the wind effects and inadequate gage network uncertainties may be considered independent. Hence, the variance of the precipitation input, σ_p^2, is the sum of variance in the point measurements due to wind effects (only affects the case where the target level is overpredicted) and the variance in the gage network estimate of the areal rainfall.

$$\sigma_p^2 = \sigma_a^2 P_e^2 + \sigma_A^2 \qquad \text{for } \hat{Q}_p > T_H \tag{2.16a}$$

$$\sigma_p^2 = \sigma_A^2 \qquad \text{for } \hat{Q}_p \leq T_H \tag{2.16b}$$

where σ_A^2 = the variance in the difference between "true" areal average rainfall and that estimated from the rain gage network,

$\hat{Q}_p$ = the peak discharge estimated by the flood forecasting model using the expected values (best estimates) of the parameters and input data.

The question of how to apply first-order second moment analysis to multi-period storms still requires further examination.

Finally, many of the existing physical simulation rainfall-runoff models are so-called distributed models which subdivide the watershed into subwatersheds, planes, finite elements, etc. For each of these subdivisions, the governing physically based equations and procedures for handling abstractions and runoff time distribution are applied to the precipitation input for that subdivision. The resulting runoff from each of the subdivisions is then numerically routed either overland, through the channel system, or both to obtain the hydrograph at the channel outlet. The use of such subdivisions allows more accurate accounting for the details of the physical runoff process by breaking down the watershed into areas of similar soil conditions, topography, and geomorphology. Hence, the uncertainties due to spatial lumping are reduced.

Separate rainfall inputs are made to each of the watershed subdivisions, and the uncertainty for each of these inputs may be estimated as described above. However, there may arise occasions when one (or more) of the subdivisions does not have a rain gage in it. In these cases the uncertainty in the areal rainfall estimates is increased as isohyetal maps are extrapolated, data from rain gages outside the subdivisions are used (Troutman, 1982a, discusses just how great the errors of this can be), etc. It seems ill-advised to use distributed models which subdivide the watershed to levels smaller than the resolution of the rain gage data network unless topographic conditions require it. As pointed out by Packer (1972), no mathematical calculation, however sophisticated, can be better than the validity, reliability, adequacy, and completeness of the data used in the analysis. Therefore, if new gage networks are being set up for previously ungaged watersheds to be incorporated with distributed physical simulation models for real-time flood forecasting, these networks should be designed considering the model's subdivision of the watershed so that adequate data is available to make use of the main advantage of such hydrologic models.

2.3.2 Streamflow Data Uncertainty

The uncertainties in streamflow measurement and their effects on hydrologic modeling reliability are generally considerably smaller than those for uncertainty in rainfall measurement. This is due to the fact that streamflow data represents the integration of the watershed system's complicated rainfall-runoff process, while rainfall data merely provide point measurements from the complicated rainfall process over the watershed system. Nevertheless, considerable uncertainty exists in streamflow data, and this can be considered as coming from primarily three sources:

1) uncertainty in the gage measurement,

2) uncertainty regarding the validity of the derived stage-discharge relation,

3) uncertainty regarding the quality of discharge measurements used to derive the stage-discharge relation.

It is generally conceded that using modern techniques the stage can easily be determined with relatively high accuracy (International Organization for Standardization, 1983). Therefore, the last two sources of uncertainty should be concentrated on.

The stage-discharge relation is defined by the complex interaction of channel characteristics, including cross-sectional area, shape, slope, and roughness. The primary sources of the uncertainty in stage-discharge relations are changing stream cross-sectional controls due to the effects of a changing (meandering) channel, scour and fill in an alluvial channel, backwater, variable channel storage (i.e., hysteresis in the stage-discharge relation due to unsteady flow effects), and aquatic vegetation (Boyer, 1964). Furthermore, there is always uncertainty regarding the fitting of the stage-discharge relation to the data.

The most commonly used method of obtaining actual stream discharge measurements is the velocity-area method. This method breaks the stream cross section down into a number of verticals. The mean velocity for these verticals is determined from one or two point velocity measurements (depending on the flow depth with two point measurements preferred) and a velocity distribution based on theoretical and empirical evidence. The mean velocity is multiplied by the average area represented by the vertical to determine the discharge for that vertical, and the overall discharge is the sum of the vertical discharges. There are many sources of uncertainty in discharge measurements including uncertainties in widths and depths represented by a vertical, in determination of mean velocity for the vertical, and in determining the number of verticals to use. Furthermore, uncertainties in the mean velocity estimate arise from errors in point velocity measurements due to instrumentation and turbulence and from errors in the assumed velocity distribution.

2.3.2.1 Handling Streamflow Uncertainties in Calibrated Models

As was the case with rainfall data, the uncertainties in streamflow data are incorporated in the parameters (and their uncertainty) in calibrated models.

Generally, a flood is defined as the occurrence of flows whose depth is greater than some critical stage (e.g., bankfull stage). In order to determine whether a flood is imminent, either the critical stage must be converted to a critical discharge or the model predicted peak flow must be converted into a peak stage. Both of these conversions require the use of a stage-discharge relation, and hence the uncertainties associated with stage-discharge relations also affect the estimation of whether the critical stage will be exceeded. When using calibrated models the uncertainties in the stage-discharge relation are already incorporated in the model parameters and their uncertainties. Therefore, the conversion of the critical stage to the critical discharge can be considered error free with the actual uncertainties accounted for in the model peak discharge uncertainty analysis.

2.3.2.2 Handling Streamflow Uncertainties in Physical Simulation Models

When using physical simulation models, the uncertainty in the conversion of critical stage to critical discharge must be considered based on physical reasoning. The sources of uncertainty in the stage-discharge relation have been discussed previously. By choosing a stable channel control section and performing periodic maintenance on it, several of the sources of uncertainty in stage-discharge relations including changing channel effects, scour and fill in an alluvial channel, and aquatic vegetation may be reduced.

Even with well selected channel control sections for discharge measurement, the effects of backwater and variable channel storage (hysteresis) may still greatly effect the stage-discharge relation. In fact, Fread (1975) found that the dynamic (unsteady flow) effect may be significant if the channel bottom slope is less than 0.001 when the rate of change of stage is greater than about 0.10 ft/hr. Boyer (1964) offers insight into the nature of these effects and describes some of the procedures proposed to correct for them. Nevertheless, the key point is that even under the best conditions, the stage discharge relation is non-unique and looped. Thus, the analysis of the uncertainties in the stage discharge is quite complex and beyond the scope of this study.

Carter and Anderson (1963) performed an extensive study of the sources of error and subsequent total error in discharge measurements using the velocity-area method. They used hundreds of laboratory and field measurements to determine the errors due to current meters, time sampling of velocity (i.e., turbulence effects), approximation of the assumed velocity distribution in the vertical, point sampling of depth and horizontal velocity distribution, and the number of verticals (stations) used. Figure 2.6 shows the standard deviation of the total error in discharge measurements, S_T, as a function of the number of verticals (stations) and the approximation of mean velocity (equal to velocity at 0.6 of the depth or

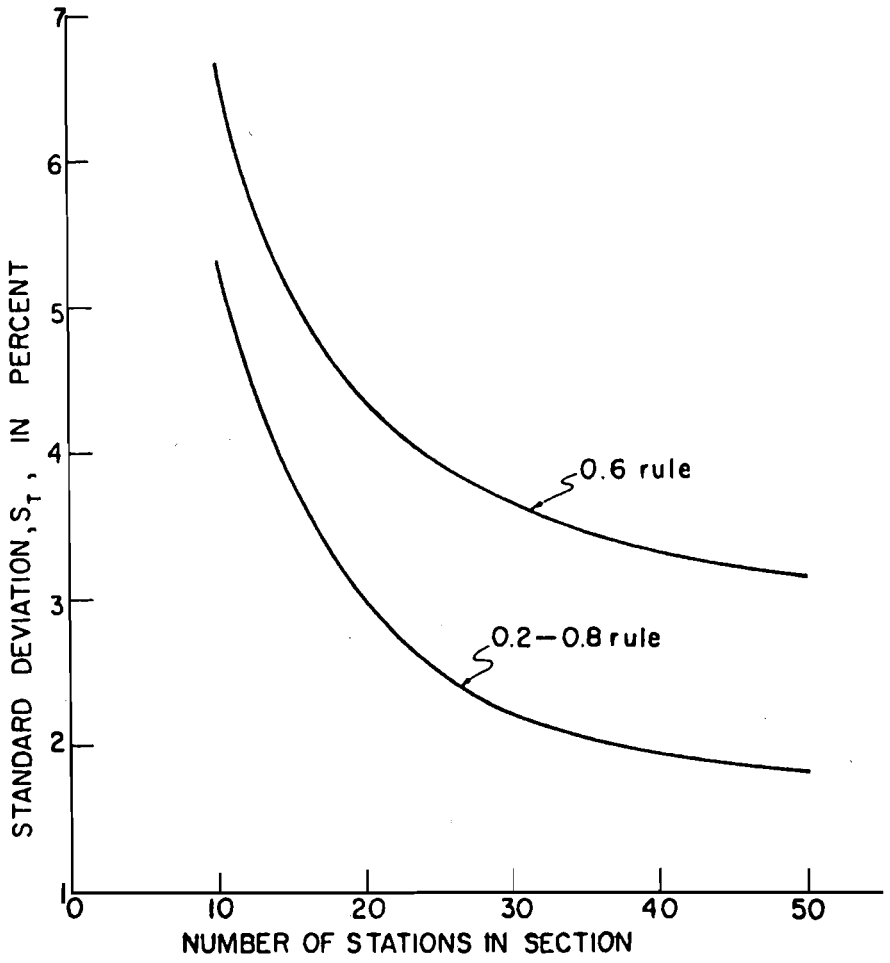

Figure 2.6. Standard deviation of total error of discharge measurement.(after Carter and Anderson, 1964)

the average of the velocity 0.2 ad 0.8 of the depth) used. The World Meteorological Organization (1984) performed its own assessment of the uncertainty in discharge measurements using the velocity-area method. For a measurement using 25 verticals, a one minute averaging of point velocity, and the 2-point method of mean velocity estimation, the total uncertainty was estimated to be $\pm$ 5.7 percent at the 95 percent confidence level (i.e., standard deviation $\simeq$ 2.9 percent). This agrees fairly well with the results of Carter and Anderson shown in Fig. 2.6; hence, this figure may be used to estimate uncertainty in discharge measurements.

The overall variance in stage-discharge relations is a function of the uncertainty in deriving the stage-discharge relation and in the discharge measurements.

2.3.3 Evapotranspiration and Soil Moisture Data Uncertainty

Generally, the effects of the evapotranspiration are considered to be negligible for short term hydrologic events such as floods. Hence, most of the hydrologic models proposed for real-time flood forecasting do not consider evapotranspiration. However, some physical-conceptual models and every physical simulation model require the use of an estimate of the soil moisture. For most watersheds, very little data is available on the soil moisture and so it is typically estimated using some kind of antecedent precipitation index which relates evapotranspiration, antecedent precipitation, and soil capillary storage. Previous experience has shown these indices to be very rough approximations, at best, especially if the time since the last storm is fairly long. Therefore, it is recommended that in addition to rain and stream gages, the watershed should be monitored by devices which can provide estimates of the actual soil moisture at the beginning of the storm. Estimates of soil moisture may be obtained from a number of sources including tensiometer data, neutron probes, and remote sensing (Jackson and Schmugge, 1986). The uncertainty in these measurements may be handled indirectly as described below.

Generally, in the physical simulation and physical-conceptual models which use soil moisture estimates, the estimates are combined with other parameters, such as soil porosity, hydraulic conductivity, etc., in order to estimate infiltration and, possibly, prompt subsurface flow. If it is assumed that the soil moisture is known with certainty, the uncertainty in infiltration may be considered as due to uncertainties in the other parameters which influence infiltration. The uncertainty in the other parameters is generally large enough that it may be assumed to encompass soil moisture uncertainties also, especially when consideration is given to the fact that the variations in hydraulic conductivity are a function of soil moisture.

2.3.4 Watershed Morphology Uncertainty

Many of the hydrological models, especially physical simulation and physical-conceptual models, used for real-time flood forecasting require knowledge of various aspects of watershed morphology, such as total area; fractions of ground cover, canopy cover, and impervious area; overland flow

slope and length; channel slope and length; etc. There is some uncertainty or error involved in determining any of these parameters. For example, Yen et al. (1976) asked 34 engineering students to inspect a three square mile drainage basin at Urbana, Illinois, and then determine the area from a USGS 7.5 minute map. The average error measured in terms of the coefficient of variation was found to be 0.045. Hence, they assumed that the coefficient of variation describing the estimation uncertainty associated with N_p persons each making one independent prediction is approximately $0.050/\sqrt{N_p}$. The relationship may be applied to any of the areal estimates: total, impervious, ground cover, canopy cover, etc.

It is unlikely that the expected errors in determining channel length will greatly influence the predicted hydrograph. However, local variations in channel slope relative to the lengthwise channel average could possibly influence the timing of the predicted hydrograph. These local variations can partially be accounted for by subdivision of the watershed as done in distributed and quasi-distributed physical-conceptual and physical simulation models. However, even this will not eliminate problems with local variations. Hence, it is probably best to consider uncertainties due to the use of a lengthwise channel average slope as part of the model structure uncertainty due to "lumping."

The average overland flow slope is generally computed as the weighted average of the overland flow slopes of overland flow paths determined at regular intervals along the channel. Hence, data on the variation of overland flow slope is readily available for the watershed and may be used to estimate the corresponding coefficient of variation. The overland flow slope greatly influences the timing of the predicted hydrograph. Thus, it is best to consider the overland flow slope uncertainty directly rather than as part of the model structure uncertainty, which will be accounted for with a magnitude correction factor (see section 2.5).

For many physical simulation models, the overland flow length is, by definition, calculated as the width of a plane which when multiplied by the channel length equals the "true" plane area. Hence, it is best to consider uncertainty in the overland flow length as a portion of model structure uncertainty. Furthermore, the overland flow slope and length work together to determine the timing of overland flow, and the weighted average used to estimate the average overland slope partially accounts for this. Therefore, it is reasonable to account for the uncertainty in the timing of the overland flow using the uncertainty in the overland flow slope alone.

There may be many more watershed morphologic factors used in the various real-time flood forecasting models. It is hoped that the above discussion presents the basic guidelines on how to deal with uncertainties in watershed morphologic parameters, and that these guidelines be applied to other morphologic factors.

2.4 Evaluation of Model Parameter Uncertainties

Wood (1976) observed that there seemed to be two types of unknown parameters, those that are fixed but unknown and those that vary from rainfall event to rainfall event. Watershed morphologic characteristics,

such as area, overland flow slope and length, etc., are examples of fixed but unknown parameters. While those which vary from rainfall event to rainfall event are studied in this section. Generally, these may have values within a known, specified range, but their true values may be greatly different for consecutive storms. When using a rainfall-runoff model in current "state-of-the-art" flood forecasting, a "best estimate" of each parameter value is determined from the corresponding range and is used throughout the forecasting procedure. By assuming the "best estimate" of the parameter value is equivalent to its expected value and by knowing the range over which the true parameter value is likely to exist, model parameter uncertainties may easily be accounted for in reliability analysis methods as described below.

2.4.1 Handling Model Parameter Uncertainties in Calibrated Models

For calibrated models, the parameter uncertainty reflects not only the uncertainty in estimating the true parameter value for a particular event, but it also contains a measure of the data uncertainty which is transferred to the parameters by the calibration process. Fortunately, the calibration process also provides a significant amount of information regarding the range of values over which each of the true values of the parameters is likely to exist. Hence, the expected value (mean) and the standard deviation of the model parameter values may be estimated as follows. First, calibrate each of the storm events separately. Second, determine the overall mean value for each of the parameters by:

1) Simultaneous calibration of all the storm events, if practical; if this method is used it may be advisable to use some sort of transformation of the objective function in order to make the error of estimation more commensurable for the large and small events;

2) If (1) is not practical, use some sort of weighted average of the calibrated values for the events.

The standard deviation may then be estimated from the variance of the calibrated parameter values for each storm about the overall mean. For nonlinear rainfall-runoff models, there is no reason for the mathematical mean of the individual event calibration results to be equal to the overall best estimate parameter value (however, the two values should be fairly close if a good, homogeneous calibration data set is used). Therefore, the variance about the overall best estimate is larger than that about the mathematical mean, but it is still a reasonable expression of the parameter variance for the MVFOSM method. For the AFOSM method, distributions will be fit to the basic variables based on the individual event calibration results. In such cases, the transformed normal means and standard deviations rather than the actual means and standard deviations are of key importance (see Eqs. B.37 to B.39).

An independent check of the estimate of the parameter standard deviation may be made by using the method proposed by Mein and Brown (1978). For the case of models calibrated based on an ordinary least squares (i.e., sum of squares difference between measured and calculated discharges) objective function, they developed a method to estimate the one standard deviation

confidence intervals for the calibrated parameters. This method makes use of a first-order Taylor series expansion of the model's hydrograph prediction and the central limit theorem to derive an approximate multivariate normal distribution for the optimal parameter values.

The key assumptions of Mein and Brown's method are that the parameter calibration is done using an ordinary least squares objective function and that the response surface surrounding the optimum is fairly linear such that the first-order Taylor series approximation is reasonable. The parameter variance calculated by Mein and Brown's method primarily considers uncertainty in the parameters due to errors transferred to the parameters from the data and, to lesser extent, due to model structure inadequacy effects on the parameters. Thus, the variance estimates obtained by Mein and Brown's method provide a very interesting comparison with the parameter variance estimated from the calibration results, which includes a measure of both the parameter and data uncertainty. Unfortunately, Mein and Brown's method was not employed in this study due to the fact that the models chosen as examples were not easily adapted to a form compatible with Mein and Brown's approach (i.e., HEC-1 has a built-in calibration scheme while RORB required the use of an "ad-hoc" optimization approach, see Appendix C).

The most important factor in the determination of model parameters and their uncertainties as outlined above is the calibration procedure used, and the key to calibration is the form of the objective function to be minimized. The calibrated parameter value may vary greatly depending on the criteria chosen to define the "best fit," i.e., a weighted sum of peak discharge difference, total runoff volume difference, and sum of squares difference between measured and predicted hydrographs. The selection of the calibration criteria is a function of what the model is to be used for. For real-time flood forecasting, the primary interest is in the magnitude of the peak, and if the peak is likely to exceed the critical level, the timing of the peak is of great importance. Hence, a criteria which emphasizes matching the peak discharge is important for real-time flood forecasting. In this study, a weighted sum of squares difference between the measured and predicted hydrographs is minimized, as explained in Appendix C.

When calibrating a physical simulation model, the fitting process should be constrained such that the physically determinable parameters remain within their reasonable ranges. These constraints may reduce the quality of fit obtainable, however, the model structure uncertainty estimate (see section 2.5) will be much more reasonable.

Given that minimization of a weighted sum of squares difference between measured and predicted hydrographs has been chosen as the calibration criterion, two important causes for poor parameter fitting must be discussed.

First, the use of this criterion presupposes that any errors present in the data are uncorrelated, have a constant variance, and zero mean. Considering the discussion of data uncertainties in section 2.3 it is clear that these assumptions are quite often violated. Hence, Sorooshian et al. (1982) developed a maximum likelihood parameter estimation procedure which accounts for the autocorrelation and heteroscedasticity (i.e., changing variance) of data errors in the fitting process. They showed for a

simple example that the maximum likelihood criterion provided improved parameter values for forecasting relative to those provided by a least squares criterion. However, when using reliability analysis, the examination of the forecasting uncertainty considers data error autocorrelation and heteroscedasticity either directly or as part of the parameter uncertainty. Thus, it is likely that while the maximum likelihood parameter estimates will have a smaller variance, the flood probabilities estimated by reliability analysis may not be significantly different. This is a subject for further research outside the scope of the this study. Furthermore, by considering the uncertainty in parameters obtained by a simple weighted least squares criterion, this research provides an uncertainty analysis for standard hydrologic practice.

Second, when calibrating a model using any fit criterion, the question of the non-uniqueness of the calibrated parameters must be considered. That is, because various parameters tend to have similar effects on the predicted hydrograph, it is quite possible that many greatly different combinations of parameter values may result in nearly identical hydrographs. Thus, the variation in calibrated parameter values may be a function of this non-uniqueness property rather than the true parameter variation from storm to storm. By using multiple starting points for the least squares calibration, it may be possible to identify the true storm to storm variation. However, this may not be necessary for hydrologic models with a relatively small number of parameters because non-uniqueness becomes more prevalent as parameters are added to improve the fit.

2.4.2 Handling Parameter Uncertainties in Physical Simulation Models

For physical simulation models, the parameters are directly related to the physical characteristics, e.g., soil types, vegetal cover, channel morphology, etc., of the watershed, allowing them to be determined without using calibration or at most a small amount of calibration. For previously ungaged watersheds, parameter information may be obtained from physical measurements at various locations, tables prepared from study of similar conditions (e.g., USDA soil surveys), and other relations developed to express physical characteristics in terms of commonly used hydrologic/hydraulic parameters (e.g., the pictures relating channel conditions to Manning's n in Ramser, 1929; Scobey, 1939; and Barnes, 1967). Using the available information, the physically reasonable range for each of the parameters may be determined. The best estimate (mean value) of the parameter may then be determined by: (1) field measurements at various sites in the watershed, or (2) if (1) is not practical, personal judgment and experience. Personal experience of using the model on other watersheds may also greatly aid in determining the parameter's mean value. For example, Melching and Wenzel (1985) found that in calibrating a simple five parameter physical simulation model for 17 storm events of five small mid-western watersheds, each calibrated parameter tended to stay within a certain region of its physically reasonable range. The standard deviation may then be estimated by assuming the parameter follows a triangular distribution over its range with the apex at the mean value. This procedure has worked quite well for determining the coefficient of variation for Manning's n in sewer pipes (Yen et al., 1976).

Also, additional information on physical parameter best estimates and standard deviations or coefficients of variation may be found in the literature. For example, Rawls et al. (1983) reported mean values and standard deviations of Green and Ampt infiltration equation parameters as they relate to USDA soil textural classes based on measurements for 1200 soils in 34 states. McBean et al. (1984) analyzed McLean and Anderson's (1980) measurements of Manning's n on the Peace River in northern Alberta, Canada, and found that a coefficient of variation of 12 to 18 percent is realistic when field measurements have been undertaken.

For watersheds which are changing in time, e.g., due to urbanization, and hence require a physical simulation model for flood forecasting, the mean values of the parameters must be evaluated based on current watershed conditions. However, the parameter variance may be estimated based on previous calibration results. The validity of this estimation of parameter variance is based on the reasonable assumption that despite the changing watershed morphology, the relative variance of the physical parameters about the watershed and the relative uncertainty in determining them remains constant.

2.4.3 Forecast Updating

The advantages and disadvantages of forecast updating schemes are discussed in Appendix A. The primary disadvantage of updating for flood events is that a minimum amount of data must be collected before updating will yield valid data and/or parameter adjustments. The time necessary to gather such data leads to a reduction in the forecast lead time, which is very important for flood warning and preparedness systems.

The goal of this study is to demonstrate the utility and suitability of reliability analysis as a means of evaluating the reliability of forecasts produced by rainfall-runoff models in real-time and as a means of estimating the flood level exceedance probabilities corresponding to these forecasts. For forecasts made immediately after the end of the significant rainfall, sufficient runoff data for data and parameter updating will not be available for typical events on medium sized watersheds. Therefore, forecast updating need not be considered in meeting the objectives of this study and it is not included. However, reliability analysis may be combined with forecast updating schemes to provide supplemental information for flood watch/warning decision making. In the following paragraphs, some suggestions are made which provide insight on the future combination of reliability analysis with forecast updating.

As described in Appendix A, many technologically advanced methods (e.g., adaptive filtering) have been developed to continuously update forecasts. Nevertheless, the primary means of updating is still simply adjusting the input data or parameters until the predicted hydrograph agrees with the available measured hydrograph data. Generally, the input data is adjusted because it does not require recalibration of the parameter values. However, for calibrated models adjusting the input data violates the assumption that the data uncertainty has been transferred to the model parameters. Hence, in future research on the combination of reliability analysis and forecast updating, updating should involve adjusting the

parameters so that the available measurements are matched by the predicted hydrograph.

When performing the reliability analysis, the updated parameter value is considered the mean value, while the standard deviation remains the same as computed earlier. For calibrated models, the standard deviation remains unchanged because the parameters are still subject to the same data uncertainty transfer. For physical simulation models, the parameter values may change with time due to the nature of the runoff process, and so the updated value is still quite uncertain. Hence, a constant standard deviation seems reasonable.

Combination of reliability analysis with the more advanced adaptive filtering automatic updating schemes is not necessary. Georgakakos (1986a) pointed out that the updated error covariance matrix may be used to estimate the flood level exceedance probability. Nevertheless, the information on errors and uncertainties contained in this chapter may be of use for these advanced automatic updating schemes. For example, Kitanidis and Bras (1980a) developed a scheme for automatic updating wherein the data and parameters are adjusted only if the errors found exceed specified tolerances. The information summarized in this chapter may aid in selecting these tolerances. Also, Kitanidis and Bras (1980c) noted that for longer term forecasts, selection of the appropriate error variances is important. The information summarized in this chapter may also aid in estimating these error variances.

2.5 Evaluation of Model Structure Uncertainty

Model structure uncertainty stems from the model's inability to truly represent the watershed's physical runoff processes. For stochastic hydrologic models, the approximation assumes that the runoff process may be adequately described by the correlation between rainfall and streamflow, between upstream and downstream flows, and the autocorrelation in downstream flow. For conceptual hydrologic models, the approximation assumes a specified deterministic function represents the rainfall-runoff process. For physical simulation and physical-conceptual models, the approximation assumes many simplifications of the natural runoff process, such as spatial and temporal lumping of watershed characteristics and input, kinematic flow routing, etc., in order to make calculations practical.

The uncertainties introduced by each of these approximations affect the shape, volume, and magnitude and timing of the peak of the predicted hydrograph. Hence, it is difficult to consider and account for the total effect of model structure uncertainty on the predicted hydrograph. For the purpose of this study, the primary interest is the model's ability to estimate the magnitude of the peak discharge. Sittner (1977) noted that when a stage above flood level is predicted to occur at a certain time, a flood plain dweller may be expected to take precautions as soon and as fast as is prudently possible. The flood plain dweller does not normally delay the start of his protective measures because the predicted interval is somewhat greater than the time required to complete these measures. Consequently, Sittner reasoned a timing error in an otherwise good forecast is not of great importance. Thus, a correction factor, λ_m, is used to

account for the model structure's inability to accurately estimate the true peak discharge magnitude. The following sections will discuss the determination of λ_m for calibrated models and then for physical simulation models.

2.5.1 Handling Model Structure Uncertainties in Calibrated Models

Garen and Burges (1981) pointed out that if a historical flow record representative of a wide range of watershed responses and of sufficient length to constitute a statistically significant sample is available, comparison of simulated and recorded flows to measure uncertainty might be extrapolated to estimate uncertainty in subsequent model predictions. Troutman (1982b) pointed out the variance between the measured discharge and the estimated discharge using the true input and model parameters is due entirely to model structure inadequacies. For calibrated models, the variance between the measured discharge and the estimated discharge is not truly due to the model structure inadequacy alone, however, the bias in the estimate due to error laden data and parameters is minimized by the calibration process. Therefore, the expected value and standard deviation of the difference between the measured and calibrated peak discharges taken over a wide range of storm events provides a reasonable estimate of λ_m and its uncertainty.

2.5.2 Handling Model Structure Uncertainties in Physical Simulation Models

Generally, for physical simulation models, calibration data are not available to allow approximation of model structure uncertainty via comparison of estimated and measured peak discharges for the watershed in question. However, by calibrating* the model for data on another watershed the model structure uncertainty may be approximated. This transfer of model structure uncertainty also applies to the case where a physical simulation model is used for real-time flood forecasting for a watershed which is changing, e.g., due to urbanization. Calibration of previous data for this watershed may be used to determine model structure uncertainty effects, i.e., λ_m and its variance.

If calibration data is not readily available for the watershed in question or other watersheds, the model structure uncertainty may be roughly approximated by assuming that the physical approximations made in the model are at least as good as the conceptual or stochastic approximations made by various other models. Thus, model structure uncertainty estimates gained from experience with other models may be applied to the current problem. Although this assumption seems quite reasonable, it does lump physical simulation models of various levels of complexity at the same uncertainty level. Hence, comparison among physical simulation models is not possible and the probabilities determined may be somewhat conservative (i.e., overestimated).

---

*When calibrating a physical simulation model, physically reasonable bounds must be placed on the parameters in order to identify the effects of model structure inadequacies.

A typical example of the model structure uncertainty on the predicted peak discharge is provided by Melching and Wenzel (1985). They calibrated the predicted hydrographs from a physical simulation model, which uses Wooding's open book approximation of watershed geometry, kinematic wave flow routing, and a modified Green and Ampt infiltration equation to estimate the runoff hydrograph, for 17 storm events on five small midwestern watersheds. They found the expected value of the peak discharge was within 2 percent of the true peak discharge, the standard deviation was approximately 16 percent, and values were normally distributed about the mean. Hence, the expected value and coefficient of variation of λ_m may be approximated as 1 and 0.16, respectively. This provides a rough approximation of the typical magnitude of the effects of model structure uncertainties.

CHAPTER 3. PRESENTATION OF RESULTS

3.1 Introduction

In this chapter, the utility of the proposed procedure for employing reliability analysis to consider the uncertainties in hydrologic modeling is demonstrated for the case of real-time flood forecasting using two simple physical-conceptual rainfall-runoff simulation models, HEC-1 and RORB. A brief description of these models is given in Appendix C.3. The procedure is applied to an Illinois watershed as an example. The description of the watershed, calibration of the two models, and statistical analysis of the calibration results are presented in Appendix C. It should be noted that the case study using the selected models is for demonstration purposes, and similar reliability analyses could be carried out for any hydrologic model (as described in section 2.1) and for any watershed. Initially, standard model verification results are discussed. Subsequently, these verification results are reexamined considering the stochastic nature of the forecasts as estimated by reliability analysis. Reliability analysis is used to:

1. determine the key basic variables influencing model forecast (or prediction) reliability,

2. select hydrologic models based on a comparison of model forecast (or prediction) reliability, and

3. develop "rules of thumb" regarding the likelihood of flood occurrence to aid in flood warning decision making.

Finally, the various reliability analysis methods are compared for this case study.

3.2 Real-Time Flood Forecasting Scheme Verification

Table 3.1 displays the measured Q_p and t_p values for each of the verification storms and the respective percent errors in the HEC-1 and RORB forecasts of these values. In general, both models do a reasonable job forecasting the peak discharge timing with 10 of the peak times estimated within ten percent and another 5 between ten and twenty percent for HEC-1, while for RORB these numbers are 7 and 6, respectively. Even for events whose peak discharge magnitude is greatly overestimated, the forecast peak times are quite reasonable. Only for the May 10, 1962 storm are the t_p values forecast by HEC-1 and RORB greatly erroneous.

The forecasts of the peak discharge magnitude display much less reliability. For non-summer, non-convective storm events, excluding the April 16, 1957 and May 12, 1970 (which is suspect due to incomplete data) storms, the average absolute error in the peak discharge magnitude forecast is 18 percent for HEC-1 and 19.3 percent for RORB. However, the forecast peak magnitudes are more than fifty percent greater than the measured magnitudes for six storms for HEC-1 and for eight storms for RORB. With the exception of the April 16, 1957 and May 12, 1970 storms, all the extremely

Table 3.1. Comparison of Measured and Predicted Peaks for the Verification Events

Date	Measured		HEC-1		RORB	
			Percent Error		Percent Error	
	Q_p (cfs)	t_p (hr)	Q_p	t_p	Q_p	t_p
6/21/56	2956.	50.	82.65	-28.00	95.77	8.00
4/16/57	4448.	52.	90.57	7.69	107.22	0.00
4/24/57	9020.	100.	-27.68	-12.00	-18.72	-12.00
7/13/57	3334.	30.	62.98	13.33	55.76	20.00
7/22/57	3055.	30.	180.55	6.67	238.63	-13.33
6/09/58	5558.	46.	43.02	-4.35	60.18	7.14
6/12/58	6630.	34.	-4.60	-6.25	23.24	0.00
7/14/58	8480.	36.	77.68	-5.56	97.56	-22.22
4/26/59	5545.	40.	3.23	-5.00	5.04	15.00
9/23/61	3500.	66.	-34.90	3.03	-23.41	12.12
5/10/62	5580.	26.	-26.76	38.46	-29.53	61.54
4/05/65	4622.	36.	-29.04	16.67	-27.81	27.78
4/08/65	3440.	34.	-7.68	0.00	-6.50	5.88
4/23/65	4552.	44.	8.95	4.55	21.25	27.27
5/04/65	7700.	32.	4.32	18.75	10.91	18.75
6/16/73	6685.	30.	40.28	13.33	56.92	-6.67
5/12/70	9790.	46.	74.74	-21.74	96.03	-26.09
12/02/82	12300.	34.	19.30	5.88	30.73	0.00

erroneous forecasts are for summer, convective storms. The July 22, 1957 storm is tremendously overpredicted by both HEC-1 (180 percent) and RORB (240 percent).

Such results are as expected when the seasonal variation of model parameters is recalled (see Tables C.10 and C.11). The seasonal variation indicates that the expected values of the hydrograph parameters, TC and S_R in HEC-1 and C_1 and m in RORB, remain fairly constant throughout the year.

Hence, the generally good results in the peak time forecasts were expected. The expected value of the continuing loss rate is significantly larger for summer storms than for those in the remainder of the year. Thus, using the overall average continuing loss rate, which is biased toward the lower non-summer values, leads to overestimation of the precipitation excess and subsequently the peak discharge magnitude. However, these arguments do not explain the large error for the April 16, 1957 event or the low error for the June 12, 1958 event.

In general, it appears that the real-time flood forecasting schemes perform quite well for non-summer, non-convective storm events. Furthermore, it seems that if applied properly, either of the real-time flood forecasting schemes will provide reasonably reliable and useful forecasts for such events. For summer convective storm events, neither model appears useful when using the overall mean parameters.

3.3 Verification of the AFOSM Method

The AFOSM method has not previously been applied to hydrologic modeling cases where the output from a complex nonlinear mathematical model is necessary to define the system performance function. Hence, verification of the accuracy of the AFOSM method for this problem must be performed before comments regarding the reliability of the real-time flood forecasting schemes may be made based on the AFOSM method results.

Assessment of the exact forecast reliability for the real-time flood forecasting schemes via direct integration is not possible due to the multiple variable, complex, nonlinear mathematical model description of the hydrologic loading (forecast peak discharge). Hence, Monte Carlo simulation was used to check the accuracy of the AFOSM method. In this study, three sets of 1,000 simulations were used to estimate the measured peak and flood level exceedance probabilities for events for which these exceedance probabilities were estimated as greater than 0.2 by the AFOSM method (the April 24, 1957 event is a slight exception to this rule). For events with AFOSM method exceedance probability estimates between 0.01 and 0.2, a single set of 10,000 simulations was used to estimate the exceedance probabilities for both the measured peak and the flood level. The selection of the appropriate number of simulations was based on Cheng's (1982) work reported in section 2.1.1. No Monte Carlo simulation was performed for the five events with flood level exceedance probabilities estimated by the AFOSM method to be less than 0.01 due to the prohibitively large number of simulations required to obtain a near exact exceedance probability. In fact, the major disadvantage of Monte Carlo simulation is the often prohibitive time required to generate a sufficient number of simulations. In this study, using an IBM PC-AT with math co-processor chip, 1,000 simulations took nearly 6.5 hours for HEC-1 and 10.5 hours for RORB.

Tables 3.2 and 3.3 display the comparison between Monte Carlo simulation and the AFOSM method for HEC-1 and RORB, respectively. As pointed out by Wood (1976), $E[f(\underline{x})]$ (estimated by Monte Carlo simulation) is not equal to $f(E[\underline{x}])$ (given by the AFOSM method). However, for this case, the difference between the two is acceptably small with the AFOSM approximation generally displaying less than five percent errors.

The comparison between the standard deviation of the simulated Q_p values and the first-order approximation about the mean basic variable values displays greater discrepancy. The forecast standard deviation as estimated by the AFOSM method is not truly shown in Tables 3.2 and 3.3;. instead, the MVFOSM method estimate is shown because the variance about the mean is of greater hydrologic significance. The discrepancy was expected because one of the key assumptions of the MVFOSM method, and hence, the estimate of the variance at $\underline{\hat{x}}$ is that the basic variable coefficients of variation are small (this is less important for the AFOSM method due to the distributional transformations and the analysis at the failure surface). For example, Garen and Burges (1981) found that for the first-order approximation of the variance at $\underline{\hat{x}}$ to be reasonable for the Stanford watershed model the coefficients of variation of the sensitive basic variables should be no greater than about 0.25. For HEC-1, the respective coefficients of variation for TC, S_R, and CL are 0.24, 0.15, and 0.70, while the coefficient of variation values range from 0.29 to 2.51 for IL and from 0.043 to 0.065 for λ_{mh}. For RORB, the respective coefficients of variation for C_1 and CLR are 0.18 and 0.67, while the coefficient of variation values range from 0.29 to 2.52 for ILR and from 0.057 to 0.086 for λ_{mh}. It should be noted that the events for which the agreement in $SD(Q_p)$ is good are not the events with the smallest IL coefficients of variation. Nevertheless, the large coefficients of variation partially explain the disparity between the Monte Carlo and first-order estimates of $SD(Q_p)$.

The most important comparison between the two approaches is for the exceedance probabilities. The AFOSM method consistently overpredicts the exceedance probabilities relative to Monte Carlo simulation. The AFOSM method assumes Z is continuous over all the basic variables. However, as noted in section C.8.2, Z no longer is continuous in IL when IL and CL are related to the accumulated precipitation up to and including period i, P_i, such that

$$P_i - b\ CL < IL < P_i \tag{3.1}$$

where b = 2 for RORB and is related to the difference between IL and P_i for HEC-1.

Hence, the assumed continuity causes the AFOSM to overestimate the exceedance probability relative to Monte Carlo simulation, which accounts for the discontinuity. This overestimate results from the fact that by ignoring the discontinuity, the partial derivative is overestimated and, hence, the AFOSM method perceives the forecast to have greater variability than it truly does (recall $VAR(Z) = f(C_i^2)$). Therefore, β is underestimated and a higher target level exceedance probability is estimated.

Events with at least one period of very high rainfall relative to E[IL] are affected less by the discontinuity, and thus the Monte Carlo simulation and AFOSM methods should be quite close for the measured peak. The April 17, 1957, July 13, 1957, July 22, 1957, July 14, 1958, and June 16, 1973 events have such high rainfall periods and, as expected, very close agreement between the Monte Carlo simulation and AFOSM methods was found.

Table 3.2. Comparison of Monte Carlo Simulation and the AFOSM Method for HEC-1

Date	Expected Peak Discharge, $E[Q_p]$ (cfs)		$SD(Q_p)$, cfs[1]		P_M[2]		P_F[3]	
	AFOSM	Monte Carlo	AFOSM	Monte Carlo	AFOSM	Monte Carlo	AFOSM	Monte Carlo
4/17/57	8476.	8587.	2428.	2310.	0.976	0.952	0.239	0.192
4/24/57	6523.	6928.	2390.	2583.	0.243	0.217	0.125	0.108
7/13/57	5434.	5074.	2229.	3339.	0.686	0.687	0.034	0.023
7/22/57	8571.	8089.	2603.	2957.	0.946	0.929	0.251	0.191
6/09/58	7949.	7914.	3163.	2752.	0.834	0.811	0.214	0.164
6/12/58	6325.	6536.	2778.	1690.	0.549	0.492	0.036	0.023
7/14/58	15067.	14850.	2434.	2883.	0.983	0.981	0.954	0.933
4/26/59	5724.	5494.	2497.	2736.	0.628	0.517	0.035	0.019
4/23/65	4960.	4988.	3199.	2370.	0.682	0.577	0.0094	0.0046
5/04/65	8033.	7972.	2804.	2404.	0.656	0.583	0.222	0.160
6/16/73	9377.	9006.	1954.	2399.	0.900	0.869	0.335	0.260

[1]Standard deviation of Q_p. For the AFOSM method taken as $(\Sigma C_i^2 \sigma_i^2)^{1/2}$ with C_i evaluated at $\bar{x}$.

[2]Exceedance probability for the measured peak discharge.

[3]Exceedance probability for the flood level.

Table 3.3. Comparison of Monte Carlo Simulation and the AFOSM Method for RORB

Date	Expected Peak Discharge, $E[Q_p]$ (cfs)		$SD(Q_p)$, cfs[1]		P_M[2]		P_F[3]	
	AFOSM	Monte Carlo	AFOSM	Monte Carlo	AFOSM	Monte Carlo	AFOSM	Monte Carlo
4/17/57	9662.	9747.	2433.	2539.	0.979	0.977	0.425	0.363
4/24/57	7331.	7611.	2836.	2439.	0.299	0.303	0.170	0.162
7/13/57	5193.	4966.	2497.	3745.	0.650	0.631	0.078	0.057
7/22/57	10345.	10152.	2621.	3143.	0.982	0.980	0.504	0.438
6/09/58	8903.	8958.	3073.	2976.	0.908	0.885	0.340	0.278
6/12/58	8171.	8308.	2980.	2340.	0.818	0.777	0.290	0.228
7/14/58	16753.	16638.	3659.	4123.	0.984	0.978	0.960	0.944
4/26/59	5824.	5556.	3108.	2715.	0.601	0.525	0.044	0.026
4/23/65	5519.	5411.	2419.	2467.	0.750	0.636	0.040	0.026
5/04/65	8540.	8620.	3585.	2839.	0.712	0.636	0.314	0.254
6/16/73	10490.	10353.	2819.	3224.	0.911	0.894	0.552	0.485

[1]Standard deviation of Q_p. For the AFOSM method taken as $(\Sigma C_i^2 \sigma_i^2)^{1/2}$ with C_i evaluated at $\bar{x}$.

[2]Exceedance probability for the measured peak discharge.

[3]Exceedance probability for the flood level.

In general, the comparison over all the events indicates the AFOSM and Monte Carlo simulation methods provide quite reasonable and consistent estimates of the measured peak and flood level exceedance probabilities. However, it is interesting to speculate which method gives the value which is closer to the truth. The basic assumption in this reliability analysis is that HEC-1 and RORB and their model parameter and model correction factor (i.e., model structure) uncertainties approximate the true rainfall-runoff process for the Vermilion River watershed. The calibration results reported in Appendix C demonstrate that for a wide variety of storms both HEC-1 and RORB can accurately model the true Vermilion River watershed rainfall-runoff process given the proper parameter values for that storm. These proper parameter values are essentially independent and describable by simple normal and lognormal distributions, the estimation of which utilizes calibration and distribution fitting procedures assuming continuous relationships. Furthermore, the true physical rainfall-runoff process is continuous for rainfalls in excess of the infiltration capacity. Therefore, the AFOSM method, which disregards the discontinuity in the initial loss-continuing loss rate scheme, is in better agreement with the true physical process and with the underlying assumptions used to derive the basic variable uncertainties than is the Monte Carlo simulation method. Hence, the somewhat conservative AFOSM method estimates of the hydrologic target level exceedance probabilities may be more realistic than the Monte Carlo simulation estimates.

The discontinuity effects also contribute to the difference between the Monte Carlo and first-order estimates of the mean and variance of the forecast peak discharge.

3.4 Reliability of the Real-Time Flood Forecasting Schemes

3.4.1 Forecast Reliability

The forecasts produced by the HEC-1 and RORB based real-time flood forecasting schemes are actually stochastic forecasts. In stochastic, time-series forecasting a common "rule of thumb" for assessing the quality of the forecasting model is that the measured values fall within the 95 percent confidence limits of the forecast. Table 3.4 displays the AFOSM method β values corresponding to the measured peak, β_M, and the flood level, β_F, for both HEC-1 and RORB. A β value of $\pm$ 1.96 corresponds to the 95 percent confidence limits. Hence, all $|\beta_M|$ values less than 1.96 indicate a "good" stochastic forecast with the measured peak within the forecast's 95 percent confidence limits. Discounting the May 12, 1970 event for which theinput data is questionable, HEC-1 forecasts violate this rule of thumb for 2 of 17 events, while RORB forecasts violate it for 3 of 17 events. Furthermore, all five of the violations are very small with the worst corresponding to 96.6 percent confidence limits. Hence, from a stochastic forecasting viewpoint, both HEC-1 and RORB provide "good" forecasts for all the verification events.

From a practical viewpoint, however, the "good" stochastic forecasts with more than 50 percent overpredictions of the peak discharge are not particularly useful. For these cases, the forecast variance is very large such that large differences between forecast and measured peaks fall into

the reasonable "stochastic" range when standardized. This high forecast variance does not mean that HEC-1 and/or RORB should or should not be used for real-time flood forecasting in general. Reliability analysis indicates that each model is quite capable of providing adequate forecasts given an accounting of the model's stochastic nature. Therefore, to increase the reliability of the forecasts, more complex models are not required; instead, the high forecast variance must be decreased by reducing the underlying uncertainties in modeling. If the underlying basic variable uncertainties cannot be appreciably reduced, then the model is not adequate for the task at hand and another, possibly more complex, model should be selected.

Table 3.4. Comparison of AFOSM β Values Between Models and Discharge Levels

Date	Q_{pm} (cfs)	HEC-1 $\hat{Q}_p^*$ (cfs)	HEC-1 β_M	HEC-1 β_F	RORB $\hat{Q}_p^*$ (cfs)	RORB β_M	RORB β_F
6/21/56	2956.	5399.	-0.856	2.800[2]	5787.	-1.600	1.903
4/16/57	4448.	8476.	-1.980	0.710	9662.	-2.031	0.189[1]
4/24/57	9020.	6523.	0.696	1.151	7331.	0.527	0.953
7/13/57	3334.	5434.	-0.484	1.820	5193.	-0.385	1.421
7/22/57	3055.	8571.	-1.607	0.672	10345.	-2.105	-0.011
6/09/58	5558.	7949.	-0.974[1]	0.794	8903.	-1.330[1]	0.413
6/12/58	6630.	6325.	-0.124	1.805[2]	8171.	-0.918	0.553
7/14/58	8480.	15067.	-2.119	-1.680	16753.	-2.136	-1.756
4/26/59	5545.	5724.	-0.326	1.806	5824.	-0.256	1.702
9/23/61	3500.	2278.	0.344	4.400[2]	2681.	0.217	3.410[3]
5/10/62	5580.	4087.	0.593	3.470[2]	3932.	0.720	2.783[2]
4/05/65	4622.	3280.	0.453	3.750[2]	3337.	0.496	3.070[2]
4/08/65	3440.	3176.	-0.168	4.070[2]	3216.	-0.091	3.185[2]
4/23/65	4552.	4960.	-0.472	2.350	5519.	-0.676	1.748
5/04/65	7700.	8033.	-0.401	0.767	8540.	-0.560	0.484
6/16/73	6685.	9377.	-1.281	0.427	10490.	-1.345	0.130
5/12/70	9790.	17107.	-2.941	-2.810	19192.	-3.320	-3.163
12/02/82	12300.	14674.	-0.987	-1.617	16080.	-1.158	-1.689

[1]Iteration scheme has difficulty converging in the basic variables due to discontinuity in $\partial g/\partial IL$.
[2]Iteration scheme has difficulty converging in the basic variables due to the extreme probability of the event.
[3]Iteration scheme has difficulty converging in the basic variables due to both 1 and 2.

Another means to examine the reliability of the forecasts is to prepare the cumulative density function, CDF, for the forecast. The closer the CDF curve is to a step function, the more reliable the forecast. By varying the hydrologic target level and estimating the exceedance probability, P_E, the CDF may be obtained by

$$CDF = 1 - P_E = \phi(\beta) \tag{3.2}$$

Figures 3.1 and 3.2 display the exceedance probabilities (which are the complements of the CDF) as a function of the discharge level for three spring events of various peak discharge magnitudes (April 8, 1965, April 26, 1959, and May 4, 1965) and one small summer event (July 13, 1957) for forecasts using HEC-1 and RORB, respectively. The April 8, 1965 event is the most reliably forecast of the four events, and, in general, the curves display the consistently high reliability of spring event forecasts. The July 13, 1957 event curve displays the high forecast variance and low reliability generally encountered for the summer event forecasts.

The dashed portions of the April 26, 1959 and July 13, 1957 event curves at the lower discharge values are due to the discontinuity in the initial loss-continuing loss rate abstraction scheme. For discharges greater than the break, the failure point is a function of both IL and CL. However, for discharges less than the break, the failure point is only a function of CL. Hence, this change in problem dimensionality causes CL and the other basic variables to move to more extreme values, greatly increasing β and P_E.

The forecast probability distribution function, PDF, is the derivative of the CDF, and it provides an interesting picture of the forecast variance and reliability. Figure 3.3 displays the PDFs for the HEC-1 and RORB forecasts of the May 4, 1965 event. The scatter of the points about these curves is a function of the method (making the area under the PDF up to a point equal to the CDF at that point) and the interval (1000 cfs) used to derive the PDF. Nevertheless, the approximate PDF curves shown in Fig. 3.3 display the reasonable reliability of the HEC-1 and RORB forecasts with the measured peak discharge nicely with the peak region of the PDFs.

3.4.2 Sources of Modeling Uncertainty

One of the strengths of the first-order second moment techniques is that they allow the assessment of the relative contributions of the individual basic variable uncertainties to the overall system uncertainty. Recall that in the first-order second moment techniques, the variance of Z is approximated as

$$VAR(Z) = \sum_{i=1}^{m} C_i^2 \, \sigma_i^2 \tag{3.3}$$

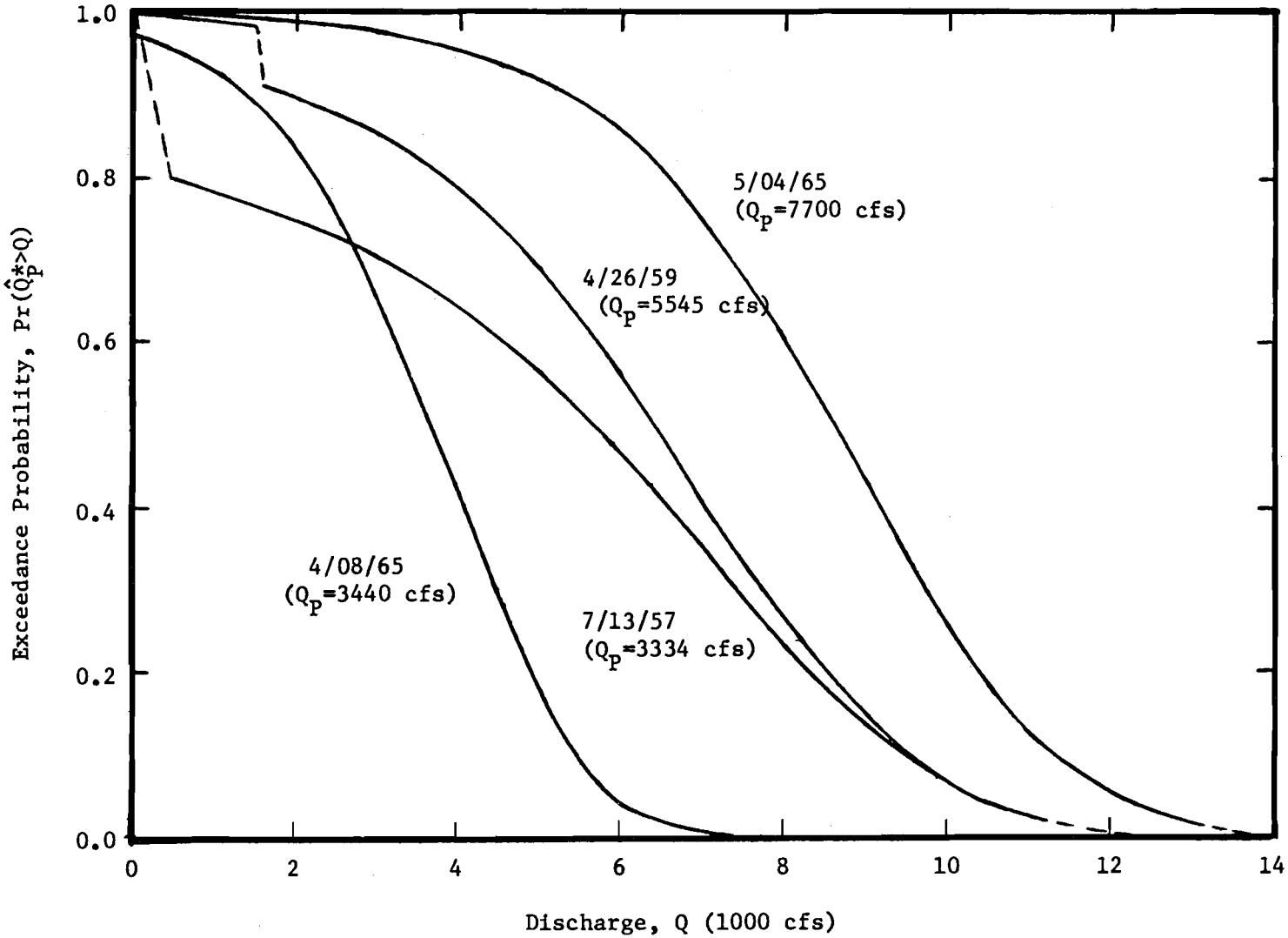

Figure 3.1. Exceedance probability as a function of discharge for HEC-1 forecasts

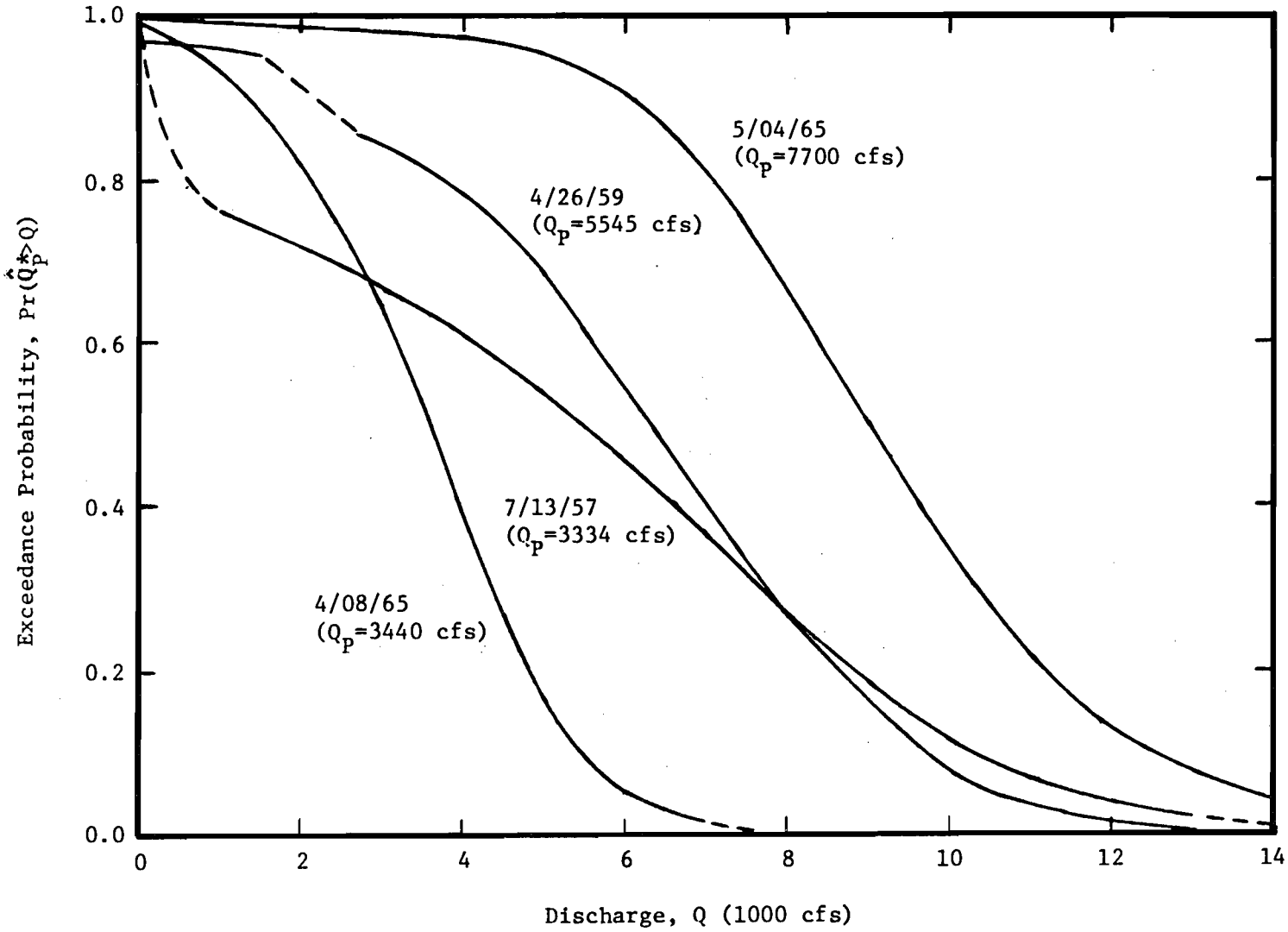

Figure 3.2. Exceedance Probability as a function of discharge for RORB forecasts

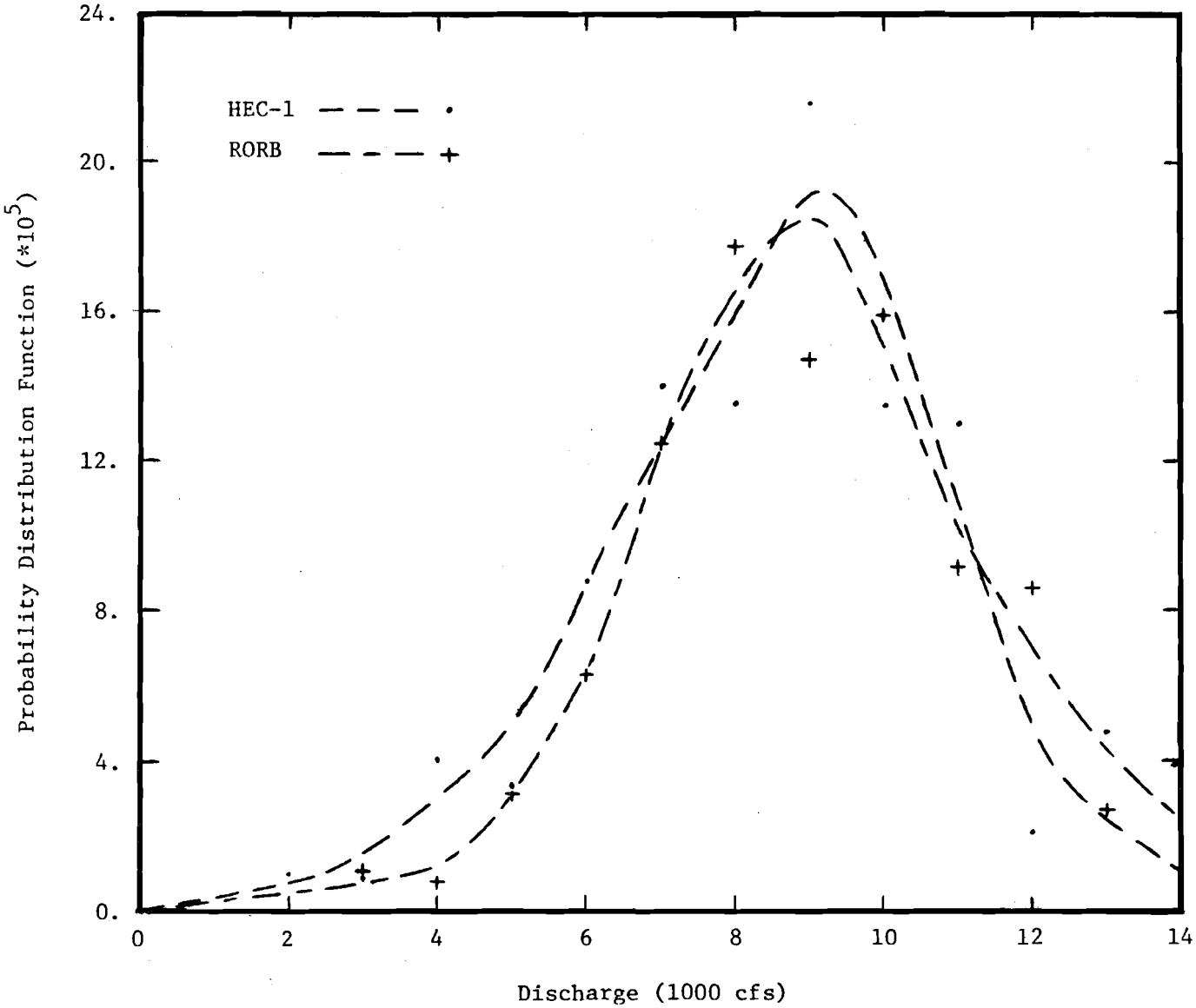

Figure 3.3. Forecast probability distribution functions for the May 4, 1965 event estimated by the AFOSM method

where $C_i = \partial g(\underline{x})/\partial x_i$ evaluated at a point of interest in x_i, and

σ_i = the variance of x_i.

The contribution of each basic variable to the forecast variance is $C_i^2 \sigma_i^2$ with C_i evaluated at $\bar{\underline{x}}$. Comparison with Monte Carlo simulation (discussed in section 3.3) reveals that the variance estimated by Eq. 3.3 is not always a good approximation of the "true" variance. Nevertheless, it is reasonable to assume that the relative contributions of the basic variables to the true forecast variance is similar to that for the approximate variance.

Tables 3.5 and 3.6 display the average contribution of each of the basic variables to the forecast variance and the relative rankings for each

Table 3.5. Contribution of the Basic Variables to the HEC-1 Forecast Variance

Basic Variable	Ave. Percent Contribution	Number of Times Contribution Ranked 1st	2nd	3rd	4th	5th
IL	25.5	3	11	1	0	3
CL	58.4	14	3	0	0	1
TC	7.4	1	4	11	2	0
S_R	4.9	0	0	5	12	1
λ_{mh}	3.8	0	0	1	4	13

Table 3.6. Contribution of the Basic Variables to the RORB Forecast Variance

Basic Variable	Ave. Percent Contribution	Number of Times Contribution Ranked 1st	2nd	3rd	4th
ILR	31.4	5	9	3	1
CLR	44.5	9	6	2	1
C_1	19.2	4	3	10	1
λ_{mr}	4.9	0	0	3	15

basic variable summed over 18 verification events for HEC-1 and RORB, respectively. These tables show that the vast majority of the forecast variance is contributed by the initial loss-continuing loss rate abstraction scheme used by both models to determine rainfall excess. On the average, nearly 84 percent of the HEC-1 forecast variance is due to IL and CL with these basic variables being the largest contributor to forecast variance for 17 of 18 events and the second largest for 14 of 18 events. While for RORB,

these values are 76 percent, 14 of 18 events, and 15 of 18 events, respectively. These number are so dominant that it is unlikely the errors in the first-order approximation of the variance will bias the following conclusions.

The relative contribution of the hydrograph parameters and the model correction factor to the forecast variance is generally quite small for both models. Therefore, each model's conversion of rainfall excess into the runoff hydrograph is reasonably accurate (i.e., has relatively small uncertainty) given average hydrograph parameters derived from careful calibration of the model over a wide range of events. This conclusion is supported by the generally reasonable forecasts of the hydrograph peak times.

It is important to stress that the high forecast variance due to IL and CL is not simply due to the uncertainty in these basic variables. Rather, the high forecast variance is due to the uncertainties in the rainfall excess estimated by the initial loss-continuing loss rate abstraction scheme, and hence, rainfall data uncertainties play a major role. Therefore, in order to improve forecast and prediction reliability, steps must be taken to reduce the rainfall data uncertainty and research should be conducted to develop improved methods of modeling abstractions. Actually, it is likely that the majority of the uncertainty comes from the rainfall data. For example, McGuinness' (1963) nomogram (see Fig. 2.4) estimates the average absolute error for a 3 in. rainstorm on the Vermilion River watershed to be 0.6 in. Such an error is much larger than one would expect to come from the initial loss-continuing loss rate approximation of the true abstraction process uninfluenced by data uncertainties. Nevertheless, further study of the abstraction approximation uncertainties is also merited.

The primary sources of rainfall data uncertainties are the descriptions of the areal and temporal rainfall distributions. Actually, these descriptions are not totally separate. The areal description has two facets: accurate estimation of the areal average rainfall (of importance for lumped models such as HEC-1) and accounting for the actual rainfall spatial variability (of importance to distributed and quasi-distributed models such as RORB). Furthermore, ignorance of spatial variability may add increased uncertainty to lumped model predictions.

Laurenson and Mein (1985) noted that a time increment of around one-fifth the time of hydrograph rise is often satisfactory for RORB. Shorter time increments increase the processor time and the computer memory requirements for the computation but often give no significant increase in modeling accuracy. Thus, the temporal distribution of the rainfall data is adequately described in this study, and so the description of the areal rainfall distribution is the main source of rainfall data uncertainty and forecast uncertainty. This conclusion agrees with the work of Schilling and Fuchs (1986) who performed a sensitivity analysis considering the major factors affecting forecast reliability for urban stormwater models and concluded that the spatial resolution of rainfall has a dominant influence on the reliability of computed runoff for small urban basins. Furthermore, this conclusion was expected in light of the large errors in assessing the average areal rainfall from a limited number of gages, e.g., as reported by

McGuinness (1963). Also, as discussed in Appendix A, many researchers including Bras and Rodriguez-Iturbe (1976), Wilson et al. (1979), Troutman (1982a and b, 1983), and Schilling (1984), warned of the severe effects of rainfall spatial variability on runoff predictions from small watersheds, especially for peak discharge predictions. Interestingly, all of the above work on the effects rainfall spatial variability has been for small watersheds (areas less than 82 square miles) both real and hypothetical, far smaller than the Vermilion River watershed at Pontiac (579 square miles). It could be that even for a watershed of this size with a fairly long time of concentration (38 hrs as defined for HEC-1), the natural runoff process does not filter out the effects of rainfall spatial variability. However, the data used in this study is not sufficient to separate out the effects of inaccurate areal average precipitation versus rainfall spatial variability and to then draw general conclusions.

In summary, accurate and reliable runoff forecasts require detailed information on the areal distribution of rainfall for any watershed utilizing rainfall-runoff modeling. Furthermore, the reliability of forecasts and predictions currently being made by hydrologic models using data from just a few rain gages is questionable at best.

3.4.3 Forecast Reliability as Guide for Comparing the Selecting Models

In hydrologic modeling, there is a trade-off between a simple model's lesser data requirements and parsimonious and more accurately estimated parameters versus the greater potential output accuracy from a complex model. This trade-off obviously affects the accuracy and reliability of the model forecasts and predictions. Reliability analysis offers a possible means of evaluating the trade-off. If the forecasts from a simple model and a complex model are equally reliable, the simple model should be used.

In truth, both HEC-1 and RORB are about equally complex. Each model uses approximately the same initial loss-continuing loss rate scheme of determining abstractions. Each model uses conceptual modeling principles to convert the rainfall excess into runoff: HEC-1 uses Clark's (1945) time-area method, while RORB uses a sequential series of nonlinear reservoirs. Finally, HEC-1 forecasts are a function of five basic variables while RORB's are a function of four basic variables (the variance from a fifth basic variable has been buried in that of another basic variable).

Despite these similarities, there are two important differences between HEC-1 and RORB. HEC-1 models the watershed as a single, linear lumped system, while RORB is a quasi-distributed model visualizing the watershed output as a nonlinear sum of the outputs from conceptually identical lumped system subwatersheds. In truth, many "distributed" models discussed in hydrologic literature are actually just a conglomeration of lumped system models and are correctly described as quasi-distributed. Therefore, the reliability comparison between HEC-1 and RORB provides an interesting example of the relative utility of linear lumped system and nonlinear quasi-distributed models.

Table 3.4 displays the β values for the measured peak, β_M, and flood level β_F, estimated by the AFOSM method for both HEC-1 and RORB. If the

concept of considering β_M as a confidence limit on the forecast is utilized, the RORB β_M value would lie outside the corresponding HEC-1 forecast confidence limits for 13 of 18 events. For four of these events, the difference between the β_M values for HEC-1 and RORB is quite small. Hence, it appears that the HEC-1 forecasts are generally a bit more reliable than the RORB forecasts. One reason for HEC-1's slightly better reliability may be that HEC-1's conversion of rainfall excess to runoff is purely conceptual, while RORB's is limited by physical constraints (i.e., the subdivision of the watershed and stream network). These constraints may hinder RORB's performance for cases with inadequate data.

Comparison of the forecast CDFs and PDFs also provides information on the relative reliability of models. Comparison of Figs. 3.1 and 3.2 reveals that the reliabilities of the HEC-1 and RORB are nearly equivalent with the HEC-1 and RORB CDFs for the April 26, 1959 and April 8, 1965 events nearly identical. Figure 3.3 also shows good agreement between the HEC-1 and RORB forecast PDFs for the May 4, 1965. Hence, this more complete check of forecast reliability indicates that HEC-1 and RORB produce forecasts of equal reliability for the Vermilion River watershed at Pontiac.

Each model is being used for real-time forecasting of potential flood events. A comparison of the flood level exceedance probability estimated based on each model's forecast and the AFOSM reliability analysis method provides interesting information on the relative reliability and utility ofthe two models. A comparison of the β_F values in Table 3.4 shows the RORB β_F values to be consistently less than the HEC-1 β_F values and often the difference between the two is quite large. Cornell (1972) pointed out that the utility of FOSM methods should not be judged solely on the exactness of the estimated probabilities but rather in terms of whether the errors in the approximated probabilities significantly change the final decision or design parameters. Thus, for the assessment of model utility relative to flood forecast performance, the estimated flood level exceedance probabilities and their effects on flood watch and warning decisions must be considered. Table 3.7 displays the flood level exceedance probabilities estimated by incorporation of the AFOSM method with HEC-1 and RORB. In general, the probabilities compare quite well and in only four cases -- April 16, 1957, July 22, 1957, June 12, 1958, and June 16, 1973 events -- would the difference in P_F values be likely to alter the flood warning decision.

The application of the AFOSM reliability analysis method to the uncertainties in the RORB and HEC-1 modeling schemes has shown that these models produce forecasts of nearly equal reliability, especially on a flood warning decision making level. Therefore, relative to each other, both HEC-1 and RORB will "suffice" for real-time flood forecasting on the Vermilion River watershed. However, to more stringently test whether these models truly "suffice" for real-time flood forecasting as an aid to flood warning decision making, reliability analysis examinations of other models with better input data must be carried out to determine what reliability levels can be achieved.

For this case, a simple linear lumped system model performs as well as a more complex nonlinear quasi-distributed model. This result is not surprising in light of the work of Singh (1977) who noted that errors in estimating rainfall excess often overpower the nonlinearity effects in the

Table 3.7. Flood Level Exceedance Probabilities for the Given Events Estimated by HEC-1 and RORB Incorporating the AFOSM Method

Date	P_F	
	HEC-1	RORB
6/21/56	0.0026	0.029
4/16/57	0.239	0.425
4/24/57	0.125	0.170
7/13/57	0.034	0.078
7/22/57	0.251	0.504
6/09/58	0.214	0.340
6/12/58	0.036	0.290
7/14/58	0.954	0.960
4/26/59	0.035	0.044
9/23/61	0.000005	0.00033
5/10/62	0.00026	0.0027
4/05/65	0.000088	0.0011
4/08/65	0.000024	0.00072
4/23/65	0.0094	0.040
5/04/65	0.222	0.314
6/16/73	0.335	0.552
5/12/70	0.998	0.999
12/02/82	0.947	0.954

runoff process making linear models preferable to nonlinear models for some truly nonlinear rainfall-runoff processes. This conclusion also supports the observation of Packer (1972) that no mathematical calculation, however sophisticated, can be better than the validity, reliability, adequacy, and completeness of the data used in the analysis. Thus, the common assumption that distributed and quasi-distributed models provide greater accuracy and reliability is only justified when the input data is also sufficiently distributed. For cases where the available input data is sparse, simple lumped system models will "suffice" and are preferred.

3.5 Use of the Probability of Flooding for Flood Warning Decision Making

The December 12, 1982 event is an example of the hoped for result of the incorporation of reliability analysis with real-time flood forecasting models to produce an estimate of the probability of flooding for the given event to aid flood warning decision making. If the people of Pontiac had known 20 hours before the peak reach town that there was 95 percent chance that the most damaging flood level would be exceeded, Pontiac's flood warning and preparedness program would have greatly reduced the $2.3 million damages. Unfortunately, as discussed below, the real-time flood forecasting models -- HEC-1 and RORB -- are not sufficiently accurate or reliable representations of the true rainfall-runoff process to permit direct use of the flood level probability estimated by the AFOSM method.

In statistical testing, confidence limits are often used to define the confidence with which one can reject a hypothesis that a certain data set is a subset of the overall population. If the β_F value were considered a confidence limit on the forecast peak, for 5 of 17 events (excluding the May 12, 1970 event) for HEC-1 and for 7 of 17 events for RORB, the actual measured peak value could be rejected with greater confidence than the flood level (i.e., $|\beta_M| > |\beta_F|$) even though the flood level was much greater than the measured peak for 16 of these events. This demonstrates that the two models are not sufficiently reliable to permit direct use of the flood level probability estimates in flood warning decision making.

However, by considering the typical, standardized forecast error (i.e., the average absolute value of β_M) some "rules of thumb" for flood warning decision making may be derived which consider the forecast and its reliability. These "rules of thumb" are as follows:

1) For cases where the likelihood of flooding indicated by the value of β_F is within the bounds of the average $|\beta_M|$ for that type of event (summer or non-summer), the occurrence of a flood has a likelihood equivalent to that for the typical measured peak. Therefore, a flood watch should be issued.

2) For cases where the likelihood of flooding is greater than that due to the typical error in the forecasts (i.e., $\beta_F < -|\beta_M|$), a flood warning should be issued.

Tables 3.8 and 3.9 display the average magnitudes of $|\beta_M|$ from the various FOSM methods for HEC-1 and RORB, respectively. Using these average magnitudes "rules of thumb" for flood warning decision makingwere established for non-summer and summer events as described above.

Table 3.8. Average Magnitudes of $|\beta_M|$ from the Various First-Order Second Moment Methods for HEC-1

Event Type	Event Number	MVFOSM Z=R-L	MVFOSM Z=ℓn(R/L)	AFOSM
Non-Summer	10	0.599	0.611	0.642
Summer	7	1.339	1.798	1.060
Overall	17	0.904	1.010	0.816

Table 3.9. Average Magnitudes of $|\beta_M|$ from the Various First-Order Second Moment Methods for RORB

Event Type	Event Number	MVFOSM Z=R-L	MVFOSM Z=ℓn(R/L)	AFOSM
Non-Summer	10	0.601	0.679	0.673
Summer	7	1.458	2.069	1.400
Overall	17	0.954	1.250	0.974

Tables 3.10 and 3.11 display the decisions made based on these "rules of thumb" for HEC-1 and RORB, respectively. Also shown in these tables is the actual result of the event and the flood warning decision made based on the forecasts alone (flood watch = expected total runoff peak discharge exceeds 90 in. above the water supply dam or 7270 cfs, flood warning = expected total runoff peak discharge exceeds flood stage 130 in. above the dam or 10880 cfs).

Table 3.10. Comparison of Flood Warning Decisions Using Reliability Analysis Based "Rules of Thumb" Versus Standard Real-Time Forecasts for HEC-1

Date	AFOSM	MVFOSM Z=R-L	MVFOSM Z=ℓn(R/L)	Forecast Alone	Actual Result
6/21/56	No	No	No	No	No
4/16/57	No	No	No	Watch	No
4/24/57	No	No	No	Watch	Flood**
7/13/57	No	No	Watch	No	No
7/22/57	Watch	Watch	Watch	Watch	No
6/09/58	Watch	Watch	Watch	Watch	No
6/12/58	No	Watch	Watch	Watch	Watch
7/14/58	Warning	Warning	Warning	Warning	Evac.*
4/26/59	No	No	No	No	No
9/23/61	No	No	No	No	No
5/10/62	No	No	No	No	No
4/05/65	No	No	No	No	No
4/08/65	No	No	No	No	No
4/23/65	No	No	No	No	No
5/04/65	No	No	No	Watch	Watch
6/16/73	Watch	Watch	Watch	Watch	No
5/12/70	Warning	Warning	Warning	Warning	Flood
12/02/82	Warning	Warning	Warning	Warning	Flood

*For this event, the Evacuation Center in Pontiac would be opened.
**This event does not exceed the worst flood level, but it is one of the five serious floods listed in Table C.2.

Table 3.11. Comparison of Flood Warning Decisions Using Reliability Analysis Based "Rules of Thumb" Versus Standard Real-Time Forecasts for RORB

Date	AFOSM	MVFOSM		Forecast Alone	Actual Result
		Z=R-L	Z=ℓn(R/L)		
6/21/56	No	No	No	No	No
4/16/57	Watch	Watch	Watch	Watch	No
4/24/57	No	No	No	Watch	Flood**
7/13/57	No	No	Watch	No	No
7/22/57	Watch	Watch	Watch	Watch	No
6/09/58	Watch	Watch	Watch	Watch	No
6/12/58	Watch	Watch	Watch	Watch	Watch
7/14/58	Warning	Warning	Warning	Warning	Evac.*
4/26/59	No	No	No	No	No
9/23/61	No	No	No	No	No
5/10/62	No	No	No	No	No
4/05/65	No	No	No	No	No
4/08/65	No	No	No	No	No
4/23/65	No	No	No	No	No
5/04/65	Watch	Watch	Watch	Watch	Watch
6/16/73	Watch	Watch	Watch	Warning	No
5/12/70	Warning	Warning	Warning	Warning	Flood
12/02/82	Warning	Warning	Warning	Warning	Flood

*For this event, the Evacuation Center in Pontiac would be opened.
**This event does not exceed the worst flood level, but it is one of the five serious floods listed in Table C.2.

In general, the real-time forecast based flood warning decisions perform well relative to actual outcome of the event. The advantage of the real-time forecasting schemes relative to the existing FWP system in Pontiac is that the forecasts provide civil defense authorities much more time (> 10 hours) to prepare for the flood. The real-time forecasts alone tend to overestimate the flood potential relative to the forecasts considering probabilistic information. For HEC-1, the forecast alone indicates watches where none are needed for the April 16, 1957 and May 4, 1965 events, and for RORB the forecast alone indicates a warning for the June 16, 1973 while the probabilistic "rules of thumb" indicate only a watch. However, this tendency is not always bad because the forecast alone approach is the only one which indicated even a watch for the severe flood caused by the April 24, 1957 event. Nevertheless, it is felt that the probabilistic "rules of thumb" generally provide improved decision making, if for no other reason than the improvement in the forecast gained from knowing its relative accuracy.

For the summer events, the performance of the forecast based decisions is somewhat less desirable with flood watches indicated for the July 22, 1957, June 9, 1958, and June 16, 1973 events where none are really necessary. To establish a FWP system for Pontiac based on real-time forecasting, it would be best to establish seasonal modeling schemes using different parameters for summer and non-summer events. However, the establishment of such schemes is beyond the scope of this research.

For future incorporation of reliability analysis with real-time flood forecasting, if large verification data sets are not available, a possible set of preliminary "rules of thumb" would be:

Flood watch: absolute value of β_F less than 1,
Flood warning: β_F value less than -1.

These correspond to the typical results found in this study over all events for two different hydrologic models. If it is felt that the real-time flood forecasting scheme being used is more reliable than those studied here (e.g., better input data is available), the "rules of thumb" found here for non-summer events may be appropriate.

The accuracy and reliability of the real-time flood forecasting scheme plays a key role in the utility of the "rules of thumb" as a screening tool for flood warning decision making. Hence, the utility to flood warning decision makers of incorporation of reliability analysis with real-time flood forecasting schemes is a function of the reliability of the schemes. Nevertheless, it appears that reliability analysis can provide useful information for flood warning decision making even for real-time flood forecasting schemes of questionable reliability. An examination of the proposed procedure for cases with better input data is needed and should further demonstrate the utility of reliability analysis.

3.6 Comparison of First-Order Second Moment Methods

Tables 3.12 and 3.13 compare the β_M values estimated by the two MVFOSM method formulations to the AFOSM method β_M estimate and to the relative errors these β_Ms represent for HEC-1 and RORB, respectively. Examination of the β_M values shows that the difference in β_M values between events is quitesimilar for all three methods, but that the actual values estimated by the MVFOSM methods are, in general, significantly different from the AFOSM method values.

It is important to remember that these methods are to be used as decision tools for the assessment of real-time flood forecasting scheme reliability and of flood level exceedance probabilities. Hence, the utility of the simplified approaches should be judged on the decisions made and not the absolute accuracy of the probabilities estimated. In terms of the reliability of the real-time flood forecasting schemes, the MVFOSM method with Z=R-L indicates the measured value is outside the forecast 95 percent confidence limits for 2 of 17 events for HEC-1 and 3 of 17 events for RORB, while the MVFOSM method with $Z=\ell n(R/L)$ indicates this for 3 of 17 events for HEC-1 and 4 of 17 events for RORB. Thus, the conclusion that each modeling scheme provides good forecasts in a stochastic sense would also be reached

by the MVFOSM methods. In terms of flood warning decision making, the probabilistic "rules of thumb" for the MVFOSM methods are quite similar to those for the AFOSM method, and perform equally well, see Tables 3.10 and 3.11.

Tables 3.14 and 3.15 compare the β_F values estimated by the two MVFOSM method formulations to the AFOSM method β_F estimate and to the relations between the measured, predicted, and flood level discharges for HEC-1 andRORB, respectively. In general, the various β_F values compare quite well for all three methods with the exception of the values from MVFOSM method with $Z=\ell n(R/L)$ for the very low probability events. Tables 3.16 and 3.17 compare the flood level exceedance probabilities corresponding to these β_F values and to Monte Carlo simulation for HEC-1 and RORB, respectively. These probabilities compare very favorably for all events and all estimation methods, especially if compared in terms of their use in flood warning decision making.

Table 3.12. HEC-1 β Values Corresponding to the Measured Peak

Date	Q_{pm} (cfs)	$\hat{Q}_p^*$ (cfs)	Percent Error	β_M AFOSM	β_M MVFOSM Z=R-L	β_M MVFOSM Z=ℓn(R/L)
6/21/56	2956.	5399.	82.65	-0.856	-1.356	-1.805
4/16/57	4448.	8476.	90.57	-1.980	-1.657	-2.251
4/24/57	9020.	6523.	-27.68	0.696	1.045	0.884
7/13/57	3334.	5434.	62.98	-0.484	-0.942	-1.191
7/22/57	3055.	8571.	180.55	-1.607	-2.119	-3.396
6/09/58	5558.	7949.	43.02	-0.974[1]	-0.756	-0.899
6/12/58	6630.	6325.	-4.60	-0.124	0.112	0.109
7/14/58	8480.	15067.	77.68	-2.119	-2.707	-3.559
4/26/59	5545.	5724.	3.23	-0.326	-0.072	-0.074
9/23/61	3500.	2278.	-34.90	0.344	0.648	0.519
5/10/62	5580.	4087.	-26.76	0.593	0.782	0.666
4/05/65	4622.	3280.	-29.04	0.453	0.810	0.679
4/08/65	3440.	3176.	-7.68	-0.168	0.115	0.111
4/23/65	4552.	4960.	8.95	-0.472	-0.127	-0.133
5/04/65	7700.	8033.	4.32	-0.401	-0.118	-0.121
6/16/73	6685.	9377.	40.28	-1.281	-1.378	-1.624
5/12/70	9790.	17107.	74.74	-2.941	-2.646	-3.452
12/02/82	12300.	14674.	19.30	-0.987	-0.618	-0.674

[1]Iteration scheme has difficulty converging due to discontinuity in $\partial g/\partial IL$.

Table 3.13. RORB β Values Corresponding to the Measured Peak

Date	Q_{pm} (cfs)	$\hat{Q}_p^*$ (cfs)	Percent Error	β_M AFOSM	β_M MVFOSM Z=R-L	β_M MVFOSM Z=ℓn(R/L)
6/21/56	2956.	5787.	95.77	-1.600	-1.466	-2.104
4/16/57	4448.	9622.	107.22	-2.031	-2.142	-3.080
4/24/57	9020.	7331.	-18.72	0.527	0.595	0.536
7/13/57	3334.	5193.	55.76	-0.385	-0.745	-0.922
7/22/57	3055.	10345.	238.63	-2.105	-2.782	-4.815
6/09/58	5558.	8903.	60.18	-1.330[1]	-1.088	-1.365
6/12/58	6630.	8171.	23.24	-0.919	0.517	0.573
7/14/58	8480.	16753.	97.56	-2.136	-2.261	-3.118
4/26/59	5545.	5824.	5.04	-0.256	-0.090	-0.092
9/23/61	3500.	2681.	-23.41	0.217	0.340	0.294
5/10/62	5580.	3932.	-29.53	0.720	0.765	0.639
4/05/65	4622.	3337.	-27.81	0.496	0.600	0.508
4/08/65	3440.	3216.	-6.50	-0.091	0.084	0.073
4/23/65	4552.	5519.	21.25	-0.676	-0.400	-0.440
5/04/65	7700.	8540.	10.91	-0.560	-0.234	-0.247
6/16/73	6685.	10490.	56.92	-1.345	-1.350	-1.677
5/12/70	9790.	19192.	96.03	-3.320[2]	-2.206	-3.031
12/02/82	12300.	16080.	30.73	-1.158	-0.760	-0.866

[1]Iteration scheme has difficulty converging due to discontinuity in $\partial g/\partial IL$.
[2]Iteration scheme has difficulty converging due to the extreme probability of the event.

In general, the MVFOSM method with Z=R-L performs much better than with Z=ℓn(R/L) for the extreme cases (low probability floods and greatly overpredicted measured peaks). Initially, one might think that because the two greatest sources of forecast uncertainty -- the initial loss and the continuing loss rate -- are lognormally distributed, the MVFOSM method with Z=ℓn(R/L) might offer better estimates than with Z=R-L. However, the dominating factor appears to be the near linearity in the actual system performance not the basic variable distributions. When Z is defined as ℓn(R/L), overprediction errors yield larger (in absolute value) β values than equal underprediction errors. In the actual system performance, however, overprediction and underprediction errors of equal magnitude indicate roughly equal forecast uncertainty. Hence, for summer events with generally large overpredictions of the measured peak, the MVFOSM method with Z=ℓn(R/L) greatly overpredicts the magnitude of β_M relative to the AFOSM method. Conversely, for the events with low flood level exceedance probabilities (greatly underpredicted flood levels), the MVFOSM method with Z=ℓn(R/L) greatly underpredicts the magnitude of β_F relative to the AFOSM method. The linear system performance experienced here seems likely for typical cases of real-time flood forecasting using hydrologic models. Therefore, the nonlinearity assumptions of the MVFOSM method with Z=ℓn(R/L) are not valid for the analysis of uncertainties in the real-time flood

forecasting schemes using rainfall-runoff models or for the analysis of rainfall-runoff modeling uncertainties in general.

The MVFOSM method with Z=R-L gives quite reasonable estimates of model reliability and flood level exceedance probabilities relative to AFOSM method and Monte Carlo simulation results. The good agreement between methods could, in part, be due to the general inaccuracy and unreliability of the real-time flood forecasting schemes. That is, the unreliability in the schemes themselves could be so great that the difference between the reliability analysis methods are relatively insignificant. The real-time flood forecasting schemes perform quite well for the non-summer events, and for these events the MVFOSM method with Z=R-L compares quite well (in a decision sense) with the AFOSM method. Therefore, it seems the differences between the methods may be insignificant even for cases where the forecasts are reasonably reliable. Further investigation of the MVFOSM method with Z=R-L is merited to verify its utility for rainfall-runoff modeling uncertainty analysis. At this time, the AFOSM method appears to be the best method to assess the reliability of rainfall-runoff models and real-time flood forecasting schemes.

Table 3.14. HEC-1 β Values Corresponding to the Flood Level

Date	Q_{pm} (cfs)	$\hat{Q}_p^*$ (cfs)	Q_F (cfs)	β_F AFOSM	β_F MVFOSM Z=R-L	β_F MVFOSM Z=ℓn(R/L)
6/21/56	2956.	5399.	10646.	2.800[1]	2.911	2.034
4/16/57	4448.	8476.	10418.	0.710	0.800	0.720
4/24/57	9020.	6523.	9930.	1.151	1.425	1.147
7/13/57	3334.	5434.	10774.	1.820	2.396	1.669
7/22/57	3055.	8571.	10565.	0.672	0.766	0.689
6/09/58	5558.	7949.	10548.	0.794	0.822	0.711
6/12/58	6630.	6325.	9800.	1.805[1]	1.251	1.015
7/14/58	8480.	15067.	10690.	-1.680	-1.782	-2.126
4/26/59	5545.	5724.	10605.	1.806	1.954	1.425
9/23/61	3500.	2278.	10800.	4.400[1]	4.523	1.882
5/10/62	5580.	4087.	10220.	3.470[1]	3.209	1.960
4/05/65	4622.	3280.	10102.	3.750[1]	4.119	2.228
4/08/65	3440.	3176.	9680.	4.070[1]	2.837	1.554
4/23/65	4552.	4960.	10312.	2.350[2]	1.673	1.135
5/04/65	7700.	8033.	10240.	0.767	0.787	0.696
6/16/73	6685.	9377.	10412.	0.427	0.529	0.502
5/12/70	9790.	17107.	10420.	-2.810	-2.418	-3.067
12/02/82	12300.	14674.	10080.	-1.617	-1.196	-1.435

[1]Iteration scheme has difficulty converging due to the extreme probability of the event.
[2]Iteration scheme has difficulty converging due to discontinuity in $\partial g/\partial IL$.

Table 3.15. RORB β Values Corresponding to the Flood Level

Date	Q_{pm} (cfs)	$\hat{Q}_p^*$ (cfs)	Q_F (cfs)	β_F AFOSM	β_F MVFOSM Z=R-L	β_F MVFOSM Z=ℓn(R/L)
6/21/56	2956.	5787.	10646.	1.903[1]	2.516	1.827
4/16/57	4448.	9662.	10418.	0.189	0.310	0.108
4/24/57	9020.	7331.	9930.	0.953	1.091	0.784
7/13/57	3334.	5193.	10774.	1.421	2.235	1.518
7/22/57	3055.	10345.	10565.	-0.011	0.084	0.083
6/09/58	5558.	8903.	10548.	0.413	0.535	0.382
6/12/58	6630.	8171.	9800.	0.553	0.547	0.498
7/14/58	8480.	16753.	10690.	-1.756	-1.657	-2.057
4/26/59	5545.	5824.	10605.	1.702	1.538	1.123
9/23/61	3500.	2681.	10800.	3.410[3]	3.188	1.459
5/10/62	5580.	3932.	10220.	2.783[2]	2.920	1.744
4/05/65	4622.	3337.	10102.	3.070[2]	3.158	1.725
4/08/65	3440.	3216.	9680.	3.185[2]	2.186	1.120
4/23/65	4552.	5519.	10312.	1.748	1.981	1.426
5/04/65	7700.	8540.	10240.	0.484	0.474	0.432
6/16/73	6685.	10490.	10412.	-0.130	-0.028	-0.028
5/12/70	9790.	19192.	10420.	-3.163	-2.058	-2.751
12/02/82	12300.	16080.	10080.	-1.689	-1.206	-1.510

[1]Iteration scheme has difficulty converging due to discontinuity in $\partial g/\partial IL$.
[2]Iteration scheme has difficulty converging due to the extreme probability of the event.
[3]Iteration scheme has difficulty converging due to both 1 and 2.

Table 3.16. Probabilities of Flood Level Exceedance Estimated for HEC-1 Using Monte Carlo, AFOSM, and the MVFOSM Methods

Date	Monte Carlo	AFOSM	MVFOSM	
			Z=R-L	Z=ℓn(R/L)
6/21/56	---	0.0026	0.0018	0.021
4/16/57	0.192	0.239	0.212	0.236
4/24/57	0.108	0.125	0.077	0.126
7/13/57	0.023	0.034	0.0083	0.048
7/22/57	0.191	0.251	0.222	0.245
6/09/58	0.164	0.214	0.206	0.239
6/12/58	0.023	0.036	0.105	0.155
7/14/58	0.933	0.954	0.962	0.983
4/26/59	0.019	0.035	0.025	0.077
9/23/61	---	0.000005	0.000003	0.030
5/10/62	---	0.00026	0.00067	0.025
4/05/65	---	0.000088	0.000020	0.013
4/08/65	---	0.000024	0.0023	0.061
4/23/65	0.0046	0.0094	0.047	0.128
5/04/65	0.160	0.222	0.216	0.243
6/16/73	0.260	0.335	0.298	0.308
5/12/70	---	0.998	0.992	0.999
12/02/82	---	0.947	0.884	0.924

Table 3.17. Probabilities of Flood Level Exceedance Estimated for RORB Using Monte Carlo, AFOSM, and the MVFOSM Methods

Date	Monte Carlo	AFOSM	MVFOSM	
			Z=R-L	Z=ℓn(R/L)
6/21/56	---	0.029	0.0059	0.034
4/16/57	0.363	0.425	0.378	0.457
4/24/57	0.162	0.170	0.138	0.217
7/13/57	0.057	0.078	0.013	0.065
7/22/57	0.438	0.504	0.467	0.467
6/09/58	0.278	0.340	0.296	0.351
6/12/58	0.228	0.290	0.292	0.309
7/14/58	0.944	0.960	0.951	0.980
4/26/59	0.026	0.044	0.062	0.131
9/23/61	---	0.00033	0.00091	0.072
5/10/62	---	0.0027	0.0018	0.041
4/05/65	---	0.0011	0.00079	0.042
4/08/65	---	0.00072	0.014	0.131
4/23/65	0.026	0.040	0.024	0.077
5/04/65	0.254	0.314	0.318	0.333
6/16/73	0.485	0.552	0.511	0.511
5/12/70	---	0.999	0.980	0.997
12/02/82	---	0.954	0.886	0.934

4. CONCLUSIONS AND RECOMMENDATIONS

4.1 Conclusions

A general procedure was developed for applying reliability analysis to consider the uncertainties in hydrologic models used in forecasting and prediction. The reliability analysis approach is capable of considering all sources of modeling uncertainty -- data, model parameters, and model structure -- to produce estimates of the probability that specific hydrologic target levels will be exceeded due to actual, design, or simulated rainstorms. Proper selection of these target levels allows estimation of interesting hydrologic information including assessment of model reliability, supplementation of real-time flood forecasts with flood level exceedance probabilities, etc.

The general procedure describes how reliability analysis may be incorporated with calibrated or physical simulation (non-calibrated) models. However, in this study, the approach was demonstrated only for the case of two calibrated models applied to real-time flood forecasting. In such cases, the data and model parameter uncertainties are assumed to be represented by the variation of the individual event calibration results about the parameter best estimates. The model structure uncertainty is accounted for by a multiplicative correction factor, which is the ratio between the measured peak discharge and peak discharge of the best fit hydrograph. Statistics are estimated and distributions fit for each of the basic variables (the model parameters and the model correction factor). The various reliability analysis methods (Monte Carlo simulation, mean value first-order second moment, and advanced first-order second moment) are then employed to evaluate the reliability of the real-time forecasting schemes utilizing the estimated statistics and distributions.

A case study demonstrated the utility and potential benefits of the general procedure. Based on the case study, the following conclusions are made regarding the performance of the various reliability analysis methods; the reliability of the specific hydrologic models used and hydrologic modeling, in general; and the sources of modeling uncertainty.

1. A comparison of system reliability analysis methods indicates:

    a. Monte Carlo simulation may be used to analyze hydrologic model uncertainty and flood likelihood, but its high computer time requirements make it impractical for real-time forecasting at this time. As computer capabilities increase, the 1,000 to 10,000 simulations necessary for the Monte-Carlo method may be obtained inexpensively and efficiently (in about 30 min.).

    b. The AFOSM method provides estimates of model uncertainty and flood likelihood comparable to those from Monte Carlo simulation at a considerable savings in computer time.

c. The MVFOSM method with Z=R-L provides reasonable estimates of model uncertainty and flood likelihood at the decision (accuracy) level.

d. The nonlinearity assumptions of the MVFOSM with Z=ℓn(R/L) are not valid for the analysis of uncertainties in rainfall-runoff models.

e. At this time, the AFOSM method appears to be the best method to assess the reliability of rainfall-runoff models and real-time flood forecasting schemes.

2. Often forecasts of low practical usefulness are "good" stochastic forecasts. In such cases, the forecast variance (uncertainty) is high, indicating reduction of this forecast variance via decreasing the modeling uncertainties is the key to obtaining forecasts with high practical usefulness.

3. "Rules of thumb" may be developed by considering typical forecast reliability to detect likely flood events and aid in flood warning decision making. These "rules of thumb" work fairly well even for the case of somewhat unreliable real-time flood forecasting schemes.

4. The bulk of the forecast uncertainty is due to the uncertainties in the estimation of the rainfall excess via the initial loss-continuing loss rate abstraction scheme. The rainfall data inadequacies apparently make up the majority of these uncertainties.

5. The reliability of forecasts and predictions currently produced by hydrologic models using data from just a few rain gages is questionable at best.

6. The hydrograph parameters and model (structure) correction factor contribute relatively little to the forecast uncertainty.

7. The common assumption that distributed and quasi-distributed models provide greater accuracy and reliability relative to simpler linear, lumped system models is only justified when the input data is sufficiently distributed. For cases where the available input data is sparse, simple linear, lumped system models will "suffice" and are preferred.

4.2 Recommendations for Future Research

Based on the results of this study and the conclusions made in the previous section, a number of recommendations for future research can be made.

1. An examination of the general procedure for combining reliability analysis with real-time rainfall-runoff models should be performed for cases with better input data to demonstrate the ultimate

utility of reliability analysis for flood warning decision making.

2. In order to improve forecast and prediction reliability, steps must be taken to reduce the uncertainties in the abstraction model, and especially, in the rainfall data.

3. Further investigation of the MVFOSM method with Z=R-L is merited, especially for cases of recommendation 1, to verify its utility for rainfall-runoff modeling uncertainty analysis.

Based on the results of this study, several other future research topics should be valuable and feasible.

1. A reliability analysis of the uncertainty in physical simulation models should be performed utilizing the basic procedure outlined in this study. Analysis of the reliability of predictions from physical simulation models used on ungaged watersheds would be of great interest in the development of design hydrographs for these watersheds and in evaluating the usefulness of generating synthetic series via such models for these watersheds.

2. Reliability analysis is capable of considering uncertain information from a wide variety of sources. The potential usefulness and reliability of forecasts made using radar rainfall measurements or remotely sensed soil moisture or snow cover data can be assessed and compared to the reliability of forecasts made with conventionally obtained data. The uncertainties in quantitative precipitation forecasts may be analyzed and combined with rainfall-runoff modeling uncertainties to improve forecast lead time and perhaps be useful for flash flood watch/warning decision making.

3. Combination of reliability analysis methods with the simple, currently employed forecast updating techniques may doubly improve flood warning decision making by improving the forecast and increasing the information available for decision making.

4. Collection of the necessary economic data on avoidable (and other) flood damage versus stage and estimation of expected flood damage via reliability analysis for specific events may greatly aid flood warning decision making by allowing an expected net economic benefit criterion to be developed. Such economic considerations might also be of interest in determining design hydrographs for ungaged catchments.

5. Further case studies should be performed over the wide range of watershed conditions (and sizes) and the wide variety of models commonly used in hydrology. Such studies will undoubtedly increase knowledge of modeling uncertainty and improve designs and decisions made based on uncertain information.

Reliability analysis methods have been shown to easily and efficiently account for the various sources of modeling uncertainty providing important supplementary information for designers, forecasters, and decision makers. It is hoped and recommended that in the future, hydrologists will commonly employ these simple techniques to deal with the uncertainty over the wide range of problems faced in hydrology and in the even wider range of methods used to solve these problems.

APPENDIX A. REVIEW OF RAINFALL-RUNOFF MODELS AND THEIR UNCERTAINTY SOURCES

In the first section of Appendix A some of the rainfall-runoff models which have been proposed for or applied to the task of real-time flood forecasting within FWP systems are reviewed. Section A.2 describes the reason for the uncertainty in the supposedly deterministic forecasts provided by these models. Section A.3 reviews research studying the effects of errors and/or uncertainties in the data or model parameters on the output from the hydrologic model. Consideration of these areas illustrates the need for the study of the application of reliability analysis methods to real-time flood forecasting models used in FWP systems. The last part of Appendix A describes the potential usefulness of such reliability analysis applications in the highly important selection of the hydrologic model for use in real-time flood forecasting.

A.1 Real-Time Flood Forecasting Models

Any hydrologic model, which has been proposed for simulation of the rainfall-runoff process, could be used for real-time flood forecasting. However, since a comprehensive review of all hydrologic models is beyond the scope of this research, a review of a cross section of the hydrologic models which have been used or specifically proposed for real-time flood forecasting on an event basis is presented. This cross section will illustrate the wide variety of models which have been proposed, including models from each of the major classifications (Chow, 1972): abstract (includes stochastic and conceptual models) and physical simulation models, as well as physical-conceptual models (which combine aspects of abstract and physical simulation models). Furthermore, several types of hybrid models combining properties of conceptual, physical-conceptual, or physical simulation models with stochastic models have been developed. These models and their advantages and shortcomings are also reviewed in this section. This review of real-time flood forecasting models begins with a brief history of real-time forecasting for flood warning leading to an assessment of the current "state-of-the-art."

A.1.1 Historical Development of the Current "State-of-the-Art" of Real-Time Flood Forecasting for Flood Warning

Prior to the development of high speed digital computers, the primary means of obtaining flood information for the purpose of issuing flood warnings were:

1) empirical graphical or tabular relations between upstream and downstream flows developed from the historical record,

2) flood indices which relate rainfall and soil moisture conditions to flood potential, i.e., when the measured rainfall exceeds the flood index for the given soil moisture conditions, a flood warning is issued,

3) flood alarm systems which set off an alarm in a key public place (fire station, police station, etc.) when the upstream stage exceeds a critical level.

These methods remain the primary source of information for flood warnings in the majority of smaller communities in the U.S. Flood forecasting models of some sort were developed only for cases where flood warnings were likely to have very high benefits.

Japanese watersheds are characterized by relatively short river reaches, remarkably steep river slopes, and tremendously heavy rainfall intensities due to typhoons. Hence, in 1963 an electric analog model was developed for flood forecasting on the River Kitakami (Iwasaki, 1967). This model solved the Laplace transform of the convolution integral for discharge from sub-basins and lateral inflow to the river using the output from a cascade delay circuit whose resistance and capacitance were calibrated to produce the unit hydrograph for the sub-basin. This model performed quite well in forecasting the September, 1964, and the July and September, 1965, floods.

The streams along the northern coast of California were subjected to severe flooding in 1964. Hence, a program was initiated to establish a flood warning system incorporating real-time flood forecasting. The runoff hydrograph was generated using unit hydrograph theory with the effective rainfall estimated from charts relating it to the basin Antecedent Index, which results from a combination of a modified Antecedent Precipitation Index and the Integrated Temperature Index (Burnash and Ferral, 1968). Likewise, up to 1967 real-time flood forecasting in Australia was performed using unit hydrographs derived for three hour rainfall duration over the watershed of interest (Heatherwick, 1969).

In the early days of digital computer use in India, the unit hydrograph, synthetic unit hydrograph, instantaneous unit hydrograph, and system models of network of linear filter models were considered for real-time flood forecasting use for the rivers in peninsular India between 7°N and 17°N (Kumaraswamy, 1973). The results of these mathematical models were compared and contrasted with the forecasts from a 1:10000 physical scale model of this portion of peninsular India. The flood forecasting and warning system worked as described below. As soon as the telemetered data are received at the computer center, the computer analyzes it utilizing the mathematical model already developed and derives all the parameters and constraints in a dynamic sense. The predicted flow values are computed for each river cross section and after they are confirmed by the physical model, they are transmitted to the various field engineers in charge of regulation and control of the respective river basins. The main advantage of this approach is that both the physical model and the mathematical model can be used to calibrate each other in the absence of a truly good hydrologic record.

The shortcomings of unit hydrograph theory and electric analogs are well known, and hence their use in the pre-digital computer era was out of necessity. These early approaches generally can deal adequately with average situations but they lack the flexibility to handle unusual

situations (e.g., large floods) with the same accuracy (Heatherwick, 1969). With the advent of digital computers much more flexible and general mathematical models of the rainfall-runoff process were developed and implemented, and the quality of real-time flood forecasts greatly improved.

In the U.S. the effort to establish a large scale real-time forecasting program on the nation's rivers began in 1971 (National Weather Service, 1972). In 1971, a decision was made that the NWS Hydrologic Research Laboratory should develop a river forecast system based on hydrologic models and to present the digital computer programs needed for its implementation. They tested the SSARR (Streamflow Synthesis and Reservoir Regulation) model, the Sacramento model, and a modified Stanford IV model by applying each to six river basins representing various climatic and hydrologic regimes throughout the contiguous U.S. Based on the results of the statistical analyses of the tests completed as of August 1971, the modified Stanford IV model was selected for use in the NWS River Forecast System package. In 1976, a major revision was made in the soil moisture accounting for the NWS system (Peck, 1976). The components for soil moisture accounting of the Sacramento model replaced those of the modified Stanford IV model. Also, dynamic (implicit) routing techniques (Fread, 1974) were incorporated into the system for use on major rivers where serious backwater problems are encountered due to interconnected river systems or tidal effects.

The NWS River Forecast System package provides continuous simulation and forecasting of streamflow given soil moisture and rainfall data and quantitative precipitation forecasts. The standard routing interval is 6 hours, hence, the package forecasts flood discharges at 6 hour intervals over the expected duration of the flood. The package has a built-in updating routine which attempts to determine the cause of the error so that the adjustment applied will correct the error and will minimize future deviations between the measured and forecast hydrographs. Thus, the NWS River Forecast System package is quite sophisticated and its use has been quite successful. However, its 6 hour routing and forecast interval (which may be adjusted downward, but generally is not) has led to its being used primarily for larger watersheds, leaving smaller watersheds (and smaller communities) generally relying on the pre-computer methods.

Several innovations have been proposed to try to improve the accuracy of real-time flood forecasts. The use of radar to measure rainfall intensity has long been thought to be potentially useful to hydrologists preparing real-time flood forecasts. Hughes and Longsdorf (1978) recommended that radar measurements of rainfall intensity be combined with flood indices and/or flood advisory tables for flash flood warning where insufficient time is available for real-time flood forecasting. Barge et al. (1979) recommended the combined use of radar and rain gage measurements to determine a better estimate of the true areal rainfall with the gage improving the measurement accuracy of the radar and the radar providing areal distribution information not available from rain gages. Nnaji et al. (1983) combined automated rain gage data and radar measurement of rainfall intensity to determine the temporal and areal rainfall distribution over a watershed in South Carolina. A simple soil moisture relation was applied to this rainfall data to determine the precipitation excess which in turn was converted into the runoff hydrograph by convoluting

an impulse response function derived for the watershed. Similar uses have been proposed for satellite measurements of areal rainfall.

Nevertheless, despite the advances proposed above, the current "state-of-the-art" involves using the available rainfall data, the best estimates of the model parameter values, a hydrologic model the hydrologist feels "comfortable" with, and some sort of updating. In the following sections the various models that some hydrologists have "felt comfortable with" and have applied to real-time (operational) flood forecasting mostly for larger watersheds are presented. It is interesting to note that in all the papers reviewed only Bergstrom (1981) recommended using alternative simulations (sensitivity analysis based on different meteorological forecasts) to estimate the risk of flooding.

A.1.2 Abstract Models

Chow (1972) describes abstract models as models which attempt to represent the prototype theoretically in a mathematical form. In abstract modeling, hydrologic phenomena are treated as systems which convert input to output via a mathematical transfer function which does not require information on the actual physical rainfall-runoff process. Examples of abstract models include the regression and time series models, commonly thought of when the term "stochastic modeling" is mentioned, and conceptual "black box" models.

A.1.2.1 Stochastic Models

In this section, the conventional definition of stochastic models as models which approximate the relation between random input (rainfall or streamflow measurements) and the random output (streamflow at the area of interest). Later, in section A.2, a more general view of stochastic processes, models, and forecasts is discussed. For real-time flood forecasting, the stochastic models used are generally regression models which utilize autocorrelation in the downstream flows and the correlation between downstream flows and the upstream flows, basin precipitation, and their time series.

The most common of these regression models are the simple single stream cases where upstream and downstream flows may be related by simple graphical, equation, or tabular relations. Such graphical or tabular relations are generally not as reliable as is desired for community flood warning, but they may be of sufficient reliability for other uses. For example, Mimikou (1984) used such relations to protect site workers and engineering equipment from floods during the construction of diversion works for the Pournari dam on the Aracthos river in western Greece. In this case, high reliability in forecasts is not necessary because the response system is known with certainty.

Bidwell (1979) used multiple linear regression and autoregression to forecast flood levels on the Klang river at Kuala Lumpur, Malaysia. The watershed upstream of Kuala Lumpur was subdivided into three sub-basins

representing the Klang river and its two main tributaries. Regression equations were prepared for gages on each of these rivers just before their confluence. A fourth regression equation was prepared relating the stage at these three gages and at Kuala Lumpur. The resulting equations provide 4 hour lead time forecasts which do not possess a high degree of forecast accuracy, but do serve the purpose of the local authorities.

The most innovative use of stochastic methods in real-time flood forecasting has been applying filtering techniques to the output from conceptual or physical simulation models to obtain adaptive (i.e., continually updated) real-time forecasts. These techniques are described in detail in section A.1.5.

A.1.2.2 Conceptual Models

Conceptual or "black box" hydrologic models are mathematical transfer functions which convert the effective rainfall input to the hydrologic system into the runoff hydrograph. These transfer functions are "best fit" mathematical formulations which do not consider the physics of the runoff process within the watershed system. The unit hydrograph and its relatives (i.e., synthetic and instantaneous unit hydrographs) are the most common examples of conceptual models. For the purest form of conceptual models, the rainfall excess is determined by calibrated runoff coefficients, while models which determine rainfall excess via physical relations and then convert this to runoff via conceptual means are physical-conceptual models (see section A.1.3).

As noted in section A.1.1.2, unit hydrographs were the "state-of-the-art" in real-time flood forecasting before the advent of digital computers. Since the development of digital computers, several conceptual models have been proposed and used for real-time flood forecasting.

Kumaraswamy (1973) used unit hydrographs, synthetic unit hydrographs, instantaneous unit hydrographs, and system models of network of linear filter models for real-time flood forecasting for rivers in peninsular India between latitudes 7°N and 17°N.

Bel'chikov (1975) used linear reservoir type models to estimate the surface runoff and storm seepage from a watershed and a linear model of transformation to covert these flows into the runoff hydrograph at the outlet. He applied this model to real-time flood forecasting for the Rioni River upstream of Sakochakidze (U.S.S.R). Later in 1977, Bel'chikov applied this model to estimate runoff from the mountainous upper half of the Ingoda River basin upstream of Chita (U.S.S.R.).

The inflow-storage-outflow (ISO) model used by Lambert (1981) for operational forecasting on the River Dee (Wales) is similar to a unit hydrograph approach. The method assumes that a natural catchment area may be represented by a single unified natural storage. By integrating the storage/outflow relation derived for each subcatchment and using standard channel routing techniques, the total outflow hydrograph is obtained.

Nnaji et al. (1983) used an impulse-response function to convert the effective rainfall determined from a combined rain gage and radar rainfall measurement system into discharge for a South Carolina watershed.

Goring (1984) used the fast Fourier transform method to find the transfer function between upstream and downstream gages on the Grey River in New Zealand. For the Grey River, only 57 percent of the outlet discharge is accounted for by the upstream gages, and so regression methods were deemed unwise.

The CLS (Constrained Linear System) model developed by Natale and Todini (1976a and b) uses a rather interesting hybrid approach by combining the instantaneous unit hydrograph with physical principles. They imposed a set of constraints that can be deduced from the physics of the hydrologic system on the instantaneous unit hydrograph in order to reduce the high sensitivity of the classical parameter estimation techniques to errors in the available data. Using Monte Carlo tests, they found that in the field of "small samples" (<100 rainfall-runoff records), which is the usual hydrologic range, constrained estimation is much better than classical unconstrained estimation. Askew (1981) applied the CLS model to real-time flood forecasting for Central American watersheds with mixed results.

The Isolated Event Model is a very simple conceptual model, and yet it has been used quite successfully for real-time flood forecasting within a FWP system. Eyre and Crees (1984) used this model to simulate runoff from the Yeading West catchment (northwest of London), and Sargent (1984) used this model for the River Tyne at Haddington (Scotland). The Isolated Event Model is a simple four parameter rainfall-runoff model which uses a rainfall-runoff ratio based on soil moisture, nonlinear reservoir routing, and a pure time delay in the routing to estimate the outflow hydrograph.

A.1.3 Physical-Conceptual Models

A large group of models has been developed which combine physical principles with the "black box" idealizations of conceptual models. Such models are often referred to a "conceptual models" in the literature because they are based in part on physical "concepts." However, the term conceptual models is probably best reserved for the "black box," input-output type models described in section A.1.2.2, while the term physical-conceptual models better describes those which combine physical and conceptual principles.

Physical-conceptual models mimic the rainfall-runoff process via a combination of physically based and conceptual approximations whose parameters are chosen such that they may often be directly obtained from physical measurements or inferred from the physical characteristics of the watershed. However, the nature of how to infer the parameters from physical characteristics and measurements is not always known. Furthermore, often "curve fitting" parameters are added to these models which have no physical meaning, but do improve the quality of the models' hydrologic fit. Therefore, in most cases, calibration is required for physical-conceptual models. For some physical-conceptual models, if the

hydrologist has considerable (a) experience with the model and/or (b) knowledge of the watershed's physical characteristics, the model may be applied to watersheds without sufficient calibration data (e.g., ungaged watersheds). For example, hydrologists have devoted considerable time to estimating the initial values of many of the Stanford Watershed model parameters on the basis of observable basin characteristics. However, Nordenson (1967) noted that even though this effort has met with some success it is doubtful whether this approach can ever provide more than reasonable estimates for further refinement. Therefore, when using physical-conceptual models for ungaged watersheds, care must be exercised in selecting parameter values, and calibration data should be collected and utilized as soon as possible.

There are two main types of physical-conceptual models. Type I combines a physically based representation of abstractions with a conceptual conversion of the resulting rainfall excess to the runoff hydrograph.

The HEC-1, Flood Hydrograph Package of the U.S. Army Corps of Engineers (1985) is perhaps the most well known physical-conceptual model of Type I. In its most commonly used form, HEC-1 determines the rainfall excess using one of four abstraction approaches (initial loss and continuing loss rate, exponential loss rate, SCS curve number, or Holtan loss rate), and then the rainfall excess is converted to the runoff hydrograph via a synthetic unit hydrograph. For more complex watersheds, hydrographs from subareas are synthesized as detailed above and then routed through the channel network using any one of a number of routing methods (Muskingum, modified Puls, working R&D, level pool reservoir routing, or average-lag routing). Recently, kinematic routing methods have been incorporated into HEC-1 both for overland flow generation and channel routing. Nevertheless, the conceptual options remain most commonly used for areal hydrograph generation employing HEC-1. Ford et al. (1980) report the application of HEC-1 for forecasting inflows to the W. Kerr Scott Reservoir on the Yalkin River in North Carolina. The results of this application will be discussed in section A.1.5.

The RORB (Runoff Routing, the B refers to a version) program is another physical-conceptual model of Type I which is gaining popularity. RORB breaks the watershed down into a number of subareas each of which may have separate rainfall input which is converted to rainfall excess using a single initial loss-continuing loss rate scheme. The rainfall excess is then routed through the channel network which is modeled as a series of nonlinear reservoirs. RORB has become extremely popular for a wide variety of hydrologic studies in Australia and Malaysia. In fact, in Australia it was used by all water authorities and consultants working in the water business (Laurenson, 1986).

In the second type of physical-conceptual models, the runoff process within sub-basins is modeled as a series of interconnected (generally linear) reservoirs. Each of the reservoirs represents a portion of the hydrologic flow path taken by the rainfall input, i.e., a surface storage reservoir, an unsaturated subsurface reservoir (vadose zone), and saturated subsurface reservoirs (groundwater). The interrelations between these reservoirs are modeled using physical and/or empirical considerations. The

combined output from each of these reservoirs for each of the sub-basins is then routed through the watershed's channel network using standard flood routing techniques, e.g., the Muskingum-Cunge method, multi-phase lake routing, kinematic wave routing, etc.

The Stanford Watershed model (Crawford and Linsley, 1966) is perhaps the most famous and most complex of the physical-conceptual models of Type II; and, as noted earlier, a modified version of this model was initially adopted for use in the NWS River Forecast System (NWS, 1972). The Sacramento model (Burnash et al., 1973) is a somewhat simpler physical-conceptual model of Type II which has replaced the modified Stanford model in the NWS River Forecast System (Peck, 1976). The SSARR model (Schermerhorn and Kuehl, 1968) is another well known physical-conceptual model of Type II. The SSARR model was originally developed for operational forecasting along the Columbia River, and it has also been used for real-time flood forecasting on a number of other watersheds around the world including the lower Mekong Basin in Cambodia (Rockwood, 1968, and Sangsit, 1973). A fourth well known physical-conceptual model of Type II is the USGS flood hydrograph simulation model (Dawdy and O'Donnell, 1965).

Several other simpler physical-conceptual models of Type II have been used by various researchers for real-time flood forecasting applications. Kadoya and Hayase (1973) applied such a model to the Shino River in Japan, and obtained good forecasts of both long term and short term runoff. Bailey and Dobson (1981) applied such a model to the River Teme basin upstream of Tenbury (England) with good results. Finally, the Swedish Meteorological and Hydrological Institute has developed a model of this type for operational forecasting in Sweden (Bergstrom, 1981).

A.1.4 Physical Simulation Models

Chow (1972) states that a simulation retains the essence of the prototype without actually attaining reality itself. A simulation model reproduces the behavior of a hydrologic phenomenon in every important detail but does not reproduce the phenomenon itself. Physical simulation models attempt to mimic the land phase of the hydrologic cycle in a watershed on a digital computer. The key advantage of physical simulation models is that all their parameters may be determined from physical measurements and/or relations developed in the literature. Hence, these models are suitable for ungaged watersheds as long as the parameters are selected carefully based on physical measurements and experience with the model on watersheds where calibration is available.

The most common type of physical simulation models divides the watershed into subcatchments. For each subcatchment, the rainfall excess is determined via simple infiltration relations (e.g., Green-Ampt, Holtan, etc.) and coefficients for the other abstractions. Kinematic wave flow routing is then used to convert the rainfall excess to a runoff hydrograph at the subcatchment outlet. The subcatchment hydrographs are then routed through the channel system using kinematic flow routing. As noted earlier, such an approach has recently been added as an option in the standard HEC-1 Flood Hydrograph Package (U.S. Army Corps of Engineers, 1985). Chowdhury and Bell (1980) have also developed such a model and their verification

results in simulating floods from the Eastern Creek and South Creek Experimental Catchments, Sydney, Australia are quite encouraging. More complicated flow routing schemes have also been examined. For example, a watershed model using full dynamic wave or kinematic wave overland flow routing and dynamic wave channel model has been developed at the University of Illinois (Yen, 1984).

A.1.5 Updating and Hybrid Models

In real-time flood forecasting the typical means of updating (i.e., getting the forecast to agree with the available flow data) is adjusting the rainfall input until the forecast hydrograph and available measurements agree. However, in recent years several hybrid models combining conceptual or physical simulation models with stochastic models have been developed with the stochastic part designed to automatically account for the discrepancy between the measured and forecast flows.

Jamieson et al. (1972) proposed a two-stage approach to real-time forecasting. The first stage comprises a simple rainfall-runoff model such as described in the previous sections. Inspection of the first-stage residuals show that they are seldom purely random (Dawdy et al., 1972; and Clarke, 1973) which suggests that there is a residue of information that has not been accounted for by the simple model. Rather than resort to restructuring the model, Jamieson et al. proposed modeling the residuals using time-series analysis as a second stage of the model. Thus, rather than using an updating procedure, the time series analysis model simply prorates the effects of the known differences between forecast and measurements to the future time periods. This method was applied to the Brenig experimental catchment in Wales with a modified version of the Stanford Watershed model as the first stage and a first-order autoregressive model as the second. They concluded that forecast errors can be significantly reduced by the use of a simple second-stage mathematical model.

Kitanidis and Bras (1980a-c) developed an innovative means to continually update the forecasts from a rainfall-runoff model. They defined the state of the real-time flood forecasting system as a set of variables which summarize all past inputs into the system. In their method, every time an observation becomes available Bayes' theorem is utilized to update (via adaptive filtering) the distribution of the states, given available information. Filtering is used to update the forecasts because the structure of the filter can partially account for the various sources of forecast uncertainty. Hence, the model error covariance matrix is the critical filter parameter; and in adaptive filtering it is an unknown parameter to be estimated, on-line, as part of the filtering objectives. In order to apply adaptive filtering to a real-time flood forecasting model, each of the individual interactions in the model must be quasi-linearized and then combined in a linearized form representing the complete hydrologic system.

Kitanidis and Bras (1980c) applied this methodology to the NWS River Forecast System model, and compared forecast results from this model and a simple abstract model for the Cohocton River at Campbell, New York. They found that for the shortest lead time (six hours), the simple abstract model

performed as well as the stochastic-physical simulation model. However, for longer forecast lead times, the stochastic-physical simulation model gives significantly better results than the abstract model. The stochastic-physical simulation model was also found to be more reliable than the abstract model in forecasting the most important features of the hydrograph such as the beginning of the rising limb, the time and height of the peak, and the total water volume. Hence, they concluded the use of feedback via adaptive filtering significantly improves the overall forecasting capability of the model even when the model and input error statistics are not perfectly known.

Georgakakos and Bras (1982) developed an improved quasi-linearization method for linearization of a nonlinear kinematic routing scheme. This routing procedure was combined with the adaptive filtering scheme for simultaneous stage and parameter estimation developed by Kitanidis and Bras (1980a-c). The effectiveness of this adaptive routing procedure was demonstrated for flood data from Bird Creek, Oklahoma, using the NWS River Forecast System model to obtain the channel inflow hydrographs to be routed.

Georgakakos (1986a and b) further expanded the application of adaptive filtering for automatic updating to consider the uncertainties in a combined hydrologic/meteorologic model of the rainfall-runoff process. The meteorological model employs the surface temperature, surface pressure, and surface dew-point (either measured or interpolated from nearby stations) to produce forecasts of areal average precipitation over the basin. The precipitation forecasting technique also compensates for orographic effects within the watershed and between stations if needed. The precipitation forecasts and available precipitation measurements (if any) are input to the rainfall-runoff model to produce real-time forecasts of the hydrograph. The states of the various sub-models (meteorologic, rainfall-runoff, and routing) are recursively updated via adaptive filtering to improve the agreement between measured and forecast hydrographs.

Wood (1981) noted that one drawback of using adaptive filtering techniques, like those described previously, is a restriction, related to the size of the state vector due to computation and computer limitations, which constrains hydrological applications to small headwater catchments. He proposed a methodology that allows forecasting of large systems by partitioning the system into subsystems, where the filtering of subsystems is performed in parallel or sequentially (depending on the situation). The interactions between the partitioned subsystems are accounted for by supplementing the noise processes. He compared the performance of this partitioned filter methodology and the full system filter approach for the use of the CLS model on the River Dee watershed in Wales, and found that the partitioned method worked equally well at a considerable savings in computer time.

The results of all the adaptive filtering updating reported above display excellent one-time step ahead forecasts (30 minutes for Wood, 1981; 6 hours for all others). However, in real-time flood forecasting, the efficiency of the flood warning scheme is a function of the forecast lead time (i.e., time between the issuance of the forecast and occurrence of the expected peak). For longer term forecasts (on the order of the watershed

response time, say 24 to 48 hours for medium sized watersheds), the results of updating are less encouraging.

The U.S. Army Corps of Engineers tested updating schemes for real-time forecasts of inflows to the W. Kerr Scott reservoir on the Yadkin River in North Carolina (Ford et al., 1980). They found that for 23 of 25 updated forecasts (over four events) predictions made using the average parameter values (determined from calibration of seven events) produced lower total error for the event than did forecasts using optimal parameter values from the previous forecast. Kitanidis and Bras (1980c) also noted difficulties in making forecasts with lead times of practical interest. For forecast lead times of three to six time steps (18 to 36 hours), the standard error of the real-time forecasts from adaptive filter models was nearly identical for three different estimations of the model error statistics: 1) fixed based on an educated guess; 2) fixed based on final statistics for an optimal adaptive filtering of the entire flow period; and 3) variable estimated by adaptive filtering for rainfall-runoff events where errors in data exceed a threshold level, or taken as fixed values otherwise (note: this is methodology advocated by Kitanidis and Bras, 1980a). Therefore, it seems for forecast lead times of practical interest (e.g., the watershed response time) the forecasts are somewhat insensitive to the updating procedure and assumed error statistics.

Ford et al. (1980) suggest a possible reason for the poor performance of updating for longer term forecasts. Due to the appreciable lag time between the measurement of rainfall on the basin and its occurrence at the stream gage, when a forecast is issued early in the flood event, only a small portion of the recorded precipitation contributes to the simulated (and measured) discharge prior to the time of forecast. In such cases, it is possible that the updating scheme may cause substantial changes in the model's parameters which do not truly reflect the model parameters for the entire event. Kitanidis and Bras (1980a) recognized these facts in designing transient error identification approach for adaptive filter updating. They noted that in real-time forecasting with hydrologic models, a common problem is the incorrect estimation of the time when the rising limb begins. They attributed this problem to either model inadequacy, especially due to the fact that the spatial distribution of the storm is not accounted for, or to the system nonlinearity. Under such conditions, they advised that a minimum number of measurements should be collected before the presence of an error in the input is inferred. The necessity of making a minimum number of measurements before the updating becomes efficient obviously limits the utility of such schemes for longer term forecasts of the flood hydrograph. Kitanidis and Bras (1980c) note that feedback (through adaptive filtering) becomes valuable only after the hydrograph starts moving steeply, leaving little time before the peak arrives to adjust and correct timing and other errors.

In summary, despite the fine results obtained via automatic updating for short term forecasts, it appears long term (three or more time steps ahead) forecasts are still best made with measured input and "best estimates" of the parameters. Hence, assessment of forecast reliability has high priority.

A.2 Deterministic Versus Stochastic Models and Forecasts

A key element in hydrologic modeling is understanding the nature of the physical process being modeled. Hydrologic systems (e.g., watersheds) may be represented by a series of variables and parameters. Clarke (1973) defined a variable as a characteristic of a system which may be measured, and which assumes different values when measured at different times (e.g., precipitation, streamflow, soil moisture, etc.). He defined a parameter as a quantity characterizing a hydrological system, and which remains constant in time (e.g., watershed area, channel length and slope, overland flow slope, etc.). Hydrologic processes may be classified based on assumptions regarding the nature of the variables and modeled based on assumptions regarding the nature of both the variables and parameters. Chow (1964) stated that if the chance of occurrence of the variables involved in a hydrologic process is ignored and the model is considered to follow a definite law of certainty but not any law of probability, the process and its model are described as deterministic. Conversely, if the chance of occurrence of the variables is taken into consideration and the concept of probability is introduced in formulating the model, the process and its model are described as stochastic or probabilistic.

When modeling the rainfall-runoff phenomena, there are actually two processes which may be considered as either stochastic or deterministic. Only if the rainfall process and its conversion to runoff can be properly modeled as deterministic will the forecast or prediction made by the model be deterministic. If either the rainfall process or its conversion to runoff are stochastic, the resulting forecast or prediction will be stochastic and uncertain.

In truth, the actual process converting rainfall to runoff is deterministic. However, as pointed out by Plate (1986), even if a perfect model of this process were available, a large random residue would exist in forecasts made with this model due to the natural variability inherent in the pertinent soil, plant, and atmospheric conditions, as well as, in the rainfall process. Nevertheless, most rainfall-runoff models used for real-time flood forecasting are viewed as deterministic. Even the real-time flood forecasts made with stochastic, time-series type models are made in a deterministic sense ignoring a portion of the randomness accounted for in the model. A deterministic forecast assumes certainty in the outcome of an event wherein no matter how many times a hydrologic phenomenon is processed under a given set of invariant conditions the same outcome results (Chow, 1972). Such a result occurs only when both the rainfall process (input data) and its conversion to runoff (model) are truly deterministic. In practice, generally, both the input data and the model are stochastic due to imperfect information (regarding watershed conditions and the data) and to model simplifications.

When using abstract models such as conceptual rainfall-runoff models or stochastic, time-series models for deterministic forecasting, the watershed is viewed as "black box" for which a given input yields a specific output. However, the inability to properly describe the true temporal and areal distribution of rainfall (stochastic input) can lead to two very different storms being considered the same hydrologic phenomenon as far as the input data is able to discern them. Hence, even under invariant

conditions, the true results cannot be forecast with certainty. Furthermore, truly invariant conditions are difficult to attain in the "real-world" and model parameters which are affected by varying conditions are rarely adjusted to account for the variations, primarily because such adjustments are difficult and poorly understood.

Physical simulation and physical-conceptual models are subject to all the foibles of abstract models given above to some degree. Such physical models also often describe physical processes such as infiltration with parameters when in truth these processes are better described by variables. For example, the resaturated hydraulic conductivity commonly used in the infiltration routine of physical models is typically viewed as single lumped parameter over an entire subarea. In truth, the resaturated hydraulic conductivity varies both spatially over the subarea and temporally through the storm event modeled.

A.3 Studies of the Effects of Uncertainties on Hydrologic Model Predictions

For most practical real-time flood forecasting cases, the resulting forecast is stochastic and uncertain. The various methods developed for updating forecasts have been the main attempts to date at considering the uncertainty involved in real-time hydrologic modeling within FWP systems. When using updating procedures, the various sources of uncertainty are lumped together as the procedure seeks to match the predicted discharges with the measured discharges up to the current time. While such procedures may lead to better estimates of the expected flood hydrograph, the basic underlying uncertainties remain, and their analysis is necessary to provide better information for the purpose of flood warning. One of the most sophisticated and successful updating procedures is the adaptive Kalman filter method proposed by Kitanidis and Bras (1980c), and their conclusions reinforce this reasoning:

> "This work has suggested that the problem of real-time forecasting of river flows is considerably more difficult than has often been implied in the literature . . . Feedback information can only provide better "initial conditions" for the forecasting. Even in utilizing feedback information, the problem of taking correct compensating actions is not simple. In order to make the right corrections in the state of the system and thus enhance the accuracy of future forecasts, the correct structure of uncertainty, pertinent to the specific model and data, must be hypothesized. This is especially important in improving the accuracy of the magnitude and timing estimate of the hydrograph peak."

To date, the sources of hydrologic modeling uncertainty have yet to be studied in detail in conjunction with current real-time flood forecasting models to provide estimates of the reliability of these forecasts. However, the basic uncertainty and variability in hydrologic modeling have not been ignored. Hydrologists have long been aware that hydrology was a blend of science and art, often more the latter than the former, and hence they have realized the shortcomings of their assumptions and the uncertainty

associated with the art of hydrologic modeling. For example, Horton (1932) discussed the physical significance and usefulness of various factors (parameters) which had been developed to describe watershed morphology (i.e., geometry, slope, shape, overland flow length, etc.) and related to the runoff characteristics of the watershed. Before the advent of the digital computer, sensitivity analysis was impractical because all hydrologic calculations were made by hand. Thus, while early hydrologists were aware of the inadequacies of their assumptions, they could do little more than acknowledge these inadequacies and qualitatively evaluate the corresponding uncertainty based on physical reasoning as Horton had done. With the development of the digital computer, hydrologists could perform hydrograph calculations in a fraction of the time previously required, and this allowed them to perform numerical experiments to quantitatively examine the effects of uncertainty on the predicted hydrograph. The results of these numerical experiments are discussed in the following sections.

A.3.1 Studies of the Effects of Rainfall Data Uncertainties on Runoff Prediction

The studies of the effects of rainfall data uncertainties fall mainly into two categories: (1) perturbation of an assumed error free rainfall trace and (2) comparison of runoff prediction made using different levels of the existing (or hypothetical) rain gage network.

In the perturbation approach, a recorded (or hypothetical) rainfall trace is assumed to be error free and is routed through the hydrologic model with a set of parameters, which are also assumed to be correct, thus obtaining a "true" hydrograph. Then a random error with mean zero and standard deviation, σ_r, is applied to all rainfall values. These "erroneous" rainfall values are then routed through the "true" model and the resulting standard error of the simulated hydrograph is computed.

Laurenson and O'Donnell (1969) used the perturbation approach to examine the effects of the six most likely types of errors in unit hydrograph derivation. Combinations of three hyetograph shapes and two unit hydrograph shapes were used to detect the effect of data errors on estimated unit hydrograph shape and the ability of four common methods of unit hydrograph derivation to deal with these errors. They found reasonable errors in the estimation of total rainfall, discharge rating curve, and base flow separation resulted in surprisingly low unit hydrograph errors. However, errors in the assumption of uniform loss rate and in rainfall synchronization between rain gages and between rain and stream gages resulted in significant unit hydrograph errors.

Ibbitt (1972) used the perturbation approach to examine the effects of random errors in the rainfall, runoff, and evapotranspiration data sets. The standard deviation of these random errors was taken as ten percent of the error-free value. Various combinations of erroneous and true data sets were then calibrated and the resulting optimal parameters were compared. He found that the random errors caused no significant change in parameter values. Hence, he concluded that since the random errors in the data had been deliberately set on the large size to aggravate any effects, the random errors of the size normally encountered in hydrologic records would have

negligible effects on estimates of the true parameter values and on flood hydrographs. However, these results are somewhat misleading because the dominant data errors in hydrologic modeling are systematic (e.g., inability to deal with rainfall spatial variability) not random. Furthermore, while random errors alone do not cause significant prediction errors, they cannot be ignored in the overall analysis because, when combined with the systematic errors, their contribution to prediction and forecast uncertainty may be significant.

Singh (1978) assumed the results from the Converging Overland Flow Model (CONV), which is a kinematic wave flow routing model that nonlinearly transforms rainfall excess over a watershed to runoff at its outlet, were the true watershed outflows. He then fit a nonlinear kinematic plane model, similar to that used by Chowdhury and Bell (1980), and three linear conceptual models, including the Clark unit hydrograph, to the "true" watershed outflows. Using the perturbation approach, he found that if rainfall excess errors are sufficiently large, a perfectly identified nonlinear model does not always perform as well as an optimally identified linear model in predicting peak runoff. He concluded that under certain circumstances, a linear model may be preferable to a nonlinear one although the watershed system is truly nonlinear. These circumstances arise when the input errors overpower the nonlinearity of the runoff process.

Dawdy (1969) proposed an extension of the perturbation approach which estimates a hydrologic model's standard error of prediction. Upon obtaining the hydrograph resulting from the "erroneous" data and the "true" model, a calibration run is made to adjust the parameters such that the "erroneous" hydrograph is reproduced. The "true" rainfall is then routed through the "calibrated" parameters, and the corresponding standard error is computed. Assuming independence of the two sources of error, one in the input data and the other in the model parameters, the error of prediction should be approximately equal to the square root of the sum of squares of the two separate estimates. Similarly, such errors may be introduced into the streamflow or other data and the standard error of prediction due to errors in these data sources may be estimated. By using this approach and by varying σ_r, Dawdy (1969) and Dawdy et al. (1972) were able to study how errors in data are transmitted to the model and obtain an empirical measure of the effect of data errors on the accuracy of prediction in simulation.

Dawdy et al. (1972) reasoned that the variance, U, in the model predictions relative to the true streamflow could be approximated as

$$Q + M + P + V + T - F = U \qquad (A.1)$$

where Q = the variance in discharge computation that results from stream gage measurement error, from error in the rating curve, and from undefined rating changes;

M = the variance resulting from the approximations used in the model in order to simplify known physical laws or to reflect physical laws which are not exactly known;

P = the bias error resulting from the use of incorrect mean annual rainfall values for the basin when determining rain gage weights;

V = the error introduced by the fact that a point measurement of volume for a given storm differs from the mean basin volume for that storm;

T = the error introduced by the fact that point measurements of time variability of intensity during a storm differ, and any point measurement differs from an "effective time distribution" which best represents average conditions over the basin for simulation purposes;

F = the curve-fitting error introduced into the model parameters by the fitting process; the negative sign is because this error acts to minimize U for a specific calibration event; however, for use of the model in prediction, F adds to the modeling error.

Equation A.1 presents more of a qualitative picture of the sources of hydrologic model uncertainty than an estimate of the actual model prediction uncertainty. In truth, the model prediction uncertainty is a weighted sum of the variance contributions from each of these sources with the weights being, in part, functions of how these sources interact leading to the data, model parameter, and model structure uncertainties. Nevertheless, Eq. A.1 is adequate for initial studies of the effects of uncertainties on model predictions.

Dawdy et al. (1972) applied the approach of Dawdy (1969) to examine the effects of the error sources in Eq. A.1 on prediction accuracy when modeling three small watersheds: Santa Anita Creek, California; Beetree Creek, North Carolina; and Little Beaver Creek, Missouri. For these three basins the standard error of prediction considering all errors was generally found to be about 30 to 35 percent. The use of a single rain gage to estimate rainfall variability over the watershed seems to introduce an error of about 20 to 25 percent into the simulation. Time variability errors alone can introduce 20 to 25 percent errors in peak-discharge estimates. Storm volume errors can introduce as great as 20 percent errors to the overall predicted hydrograph.

The varying levels of rain gage network complexity approach assumes that the predicted runoff based on rainfall data from a "large" number of rain gages (real or hypothetical) is the "true" runoff against which various predictions based on simpler rain gage networks are compared.

Dawdy and Bergman (1969) used the rain gage network approach to examine precipitation spatial and temporal distribution effects on USGS flood hydrograph simulation model runoff prediction for the Santa Anita Creek basin in southern California. They found that runoff prediction was enhanced by considering the rainfall spatial distribution using all three gages as opposed to any single gage.

Bras and Rodriguez-Iturbe (1976) used the rain gage network approach to study the accuracy of the discharge estimated by a nonlinear, spatially distributed, runoff model as a function of the spatial variability of the

rainfall process and the number, location, and inherent measurement error of the rain gages in a hypothetical watershed. A multivariate state-space stochastic rainfall model, which accounts for the nonstationarity and spatial correlation exhibited by actual rainfall, was used. Infiltration over the watershed was also modeled as a random process, and hence effective rainfall was calculated as the difference between two random variables. The effective rainfall was then input to a nonlinear, spatially distributed runoff model which estimated the outflow hydrograph based on the solution to the kinematic wave equations for overland and channel flow. Furthermore, the storm hyetograph varied as a random process about a mean hyetograph and the reference hydrograph was generated using the mean hyetograph.

Bras and Rodriguez-Iturbe (1976) found two important conclusions which influence real-time flood forecasting. First, many investigators have suspected that the "filter" characteristics of the basin are such that the spatial variability of rainfall does not greatly influence discharge, and so only a small number of rain gages is needed for discharge forecasting. However, Bras and Rodriguez-Iturbe found that the rising limb of the hydrograph was greatly influenced by rainfall near the watershed outlet, while the magnitude and timing of the peak are influenced by rainfall in upstream areas. They also found that there is a large decrease in the mean square error of the predicted hydrograph when the all eight rain gages are used. Hence, the spatial variability of rainfall is not filtered out by the natural runoff process and must be accounted for by either a more extensive rain gage network or reliability analysis measures. Second, it was found that for most of the rain gage network alternatives, the bulk of the uncertainty is in the peak and rising limb of the hydrograph. These are the most important hydrograph characteristics for real- time flood forecasting. Hence, even for watersheds with very good rain gage networks, reliability analysis should be incorporated with real-time flood forecasting schemes.

Wilson et al. (1979) confirmed the results found by Bras and Rodriguez-Iturbe (1976) for an example considering a real watershed. They used Bras and Rodriguez-Iturbe's (1976) nonstationary, spatially varying multi-dimensional rainfall generation model to produce realistic rainfall input for a physical simulation rainfall-runoff model of the Rio Fajardo basin in Puerto Rico. Their experiments found that spatial distribution of rainfall has a marked influence on the predicted runoff hydrograph, especially in terms of peak discharge.

Schilling (1984) used the rain gage network approach to examine the effects of rainfall spatial variability on runoff predictions from small urban watersheds. A two square kilometer urban watershed with 1,000 inlets and data available from five rain gages within or close to the watershed was modeled. His experiments indicated that damping of rainfall depth measurement errors almost never occurs. In fact, errors caused by disregarding the rainfall spatial distribution were amplified rather than damped by the rainfall-runoff transformation. These findings add emphasis to those of Bras and Rodriguez-Iturbe (1976) and Wilson et al. (1979). Finally, Schilling concluded that even for small urban catchments, areal averaging of rainfall measurements means a significant loss of information and, hence, it is preferable to use a distributed runoff model with multiple input.

Troutman (1982a and b) used the rain gage network approach to examine the effects of rainfall spatial variability on runoff prediction and on bias in model parameters calibrated for inferior rain gage networks. He fitted both a simple regression model of rainfall volume to runoff volume and the USGS flood hydrograph simulation model to data from nine rain gages for Turtle Creek near Dallas, Texas. Troutman (1983) refined his previous work by using a fairly simple stochastic rainfall generation model, similar to that of Bras and Rodriguez-Iturbe (1976) except that the storm center remained stationary, to produce a more accurate "true" rainfall over a hypothetical watershed. By doing this he also had more control and knowledge regarding the storm spatial distribution and storm center relative to the watershed center. Hence, he was able to derive more general information on the bias in model parameters and runoff prediction caused by inaccurate rainfall data.

All of Troutman's studies also support the premise that the effects of rainfall spatial variability cannot be ignored in hydrologic modeling of actual events. He concluded that even if measured rainfall at a small number of gages is equal to the areal average rainfall in an expected value sense, the variance of basin average precipitation is always less than that of point rainfall; this difference in variability can result in serious biases in runoff prediction. For the models he studied, this bias resulted in overprediction of large events and underprediction of small events. Such a bias could lead to an abundance of "false alarms" and, hence, poor FWP system performance. This provides yet another reason to incorporate reliability analysis with real time flood forecasting.

The research reviewed in this section demonstrates that errors and uncertainties in input data (especially rainfall data) for hydrologic models greatly affect the reliability of predictions and forecasts made by these models. Hence, these uncertainties need to be explicitly considered when using hydrologic models for real-time forecasting, hydraulic structure design, synthetic data generation, etc. The research reviewed was designed to study and demonstrate the effects of data uncertainties on model output, as such the methods developed do not truly have the capacity to provide simple, straight-forward estimates of forecast or prediction reliability for cases of practical interest. Furthermore, the research reviewed only considers as single source (data uncertainty) of the overall modeling uncertainty, and it considers assumed error magnitudes as opposed to actual error magnitudes.

A.3.2 Sensitivity and Error Analysis for Model Parameters

Sensitivity analysis is a common technique in operations research. Basically, numerical sensitivity analysis involves slightly perturbing the model parameters, generally one at a time, from the values which best represent the system modeled to see what changes in system output correspond to small modifications of (errors in) model parameters.

The basic objective of sensitivity analysis is to identify particularly sensitive model parameters, so that special care may be taken in estimating them more closely and in selecting a solution which performs well for most of their likely values (Hillier and Lieberman, 1980, p. 196).

The basic objective of reliability analysis is to evaluate the model output accuracy considering the uncertainty (errors) in the data, model parameters, and model structure. Hence, an ad hoc reliability analysis may be performed using the principles of sensitivity analysis, i.e., assuming various errors in the data, model parameters, etc. and observing the changes in the model output to get an idea of its reliability. Therefore, the sensitivity analysis of hydrologic model parameters reported below provides some useful information regarding the effect of model parameter errors on model output reliability.

Dawdy and O'Donnell (1965) were among the first to consider sensitivity analysis in hydrologic modeling. They varied each of the eight parameters in the USGS flood hydrograph simulation model by 1, 5, and 10 percent, and examined the changes in the sum of squares of the difference between the true and predicted discharges. Their purpose was to identify the most sensitive model parameters so that a more efficient and physically reasonable parameter optimization procedure could be developed. Hence, their conclusions are not directly applicable to the reliability problem at hand.

Salomonson et al. (1975) demonstrated that watershed model sensitivity analyses offer an effective means of obtaining accuracy requirements that can be used in developing instrumentation and associated accuracy and precision factors for remote sensing programs to improve watershed management. They applied a modified version of the Stanford Watershed Model to the Town Creek, Alabama, watershed. Six of the model's parameters may be determined by remote sensing. Using sensitivity analysis to determine the maximum variation in each of these parameters which will keep the output within a specified tolerance of the "true" value, they were able to determine the required accuracy of estimating each of these parameters by remote sensing.

Yeh et al. (1978) performed a sensitivity analysis of the input to (precipitation and snowmelt) and the embedded parameters of the Sacramento model. The purpose of this sensitivity analysis was to examine the value of more accurate hydrologic forecasts for hydropower operations considering the flows for an entire month. Folsom Lake on the American River and Folsom Power Plant of the California Central Valley project were used as a case study. The input and watershed parameters were individually varied from -50 to +50 percent of their expected values, and the resulting volumes were compared to the expected volume. They found that the major error sources in runoff estimation using the selected model arise from deficiencies in the temporal and spatial sampling of the parameters embedded in the model, from a lack of predictability of weather and other climatic factors, and from the exclusion of other elements that vary with time but are difficult to sense on a frequent basis.

As noted earlier, sensitivity analysis is not the only means with which the effects of parameter uncertainty have been examined. The following relates some of the other methods used to examine parameter uncertainty.

Wood (1976) considered the uncertainty in an infiltration parameter of a simple rainfall-runoff model. By assuming that the other parameters of

the model were known with certainty and taking advantage of the simple form of the model, he was able to analytically solve for the influence of infiltration parameter uncertainty on the predicted output in terms of a probability distribution. While it is doubtful that such analytical solutions would be possible when considering several uncertain parameters, more complex models, or both, this work provides considerable insight into the effect that even relatively small parameter variations can have on flood simulation and especially flood frequency estimates based on a rainfall-runoff model generated flood series.

Mein and Brown (1979) developed a procedure by which the variance of each fitted parameter of a watershed model can be determined. This information can be used to determine the degree to which the model parameters can be related to physical watershed characteristics. That is, if the model parameters are insensitive (i.e., have coefficient of variation > 0.25), then this model may be useful for ungaged watersheds but not useful for simulation of flow changes due to physical changes in the watershed (e.g., urbanization). Furthermore, this procedure may be quite useful when analyzing parameter uncertainty within the reliability analysis framework.

Garen and Burges (1981) offer perhaps the most similar work to that proposed here except that they consider only parameter uncertainty. They use both first-order second moment uncertainty analysis (which will be discussed further in Appendix B) and Monte Carlo simulation to evaluate the effects of parameter variability for a simplified version of the Stanford Watershed model. The end result of their research is the generation of the error bounds (i.e., $\pm$ one standard deviation) due to parameter uncertainty (coefficient of variation values were assumed equal for all parameters) for the predicted hydrograph. This type of information could be used to determine the probability of different flood magnitudes. Examples of the confidence limits they found due to parameter uncertainty alone are shown in Fig. A.1. Based on the figure, it is clear that parameter uncertainty can have a great effect on forecast reliability even when coefficient of variation values are assumed to be small and equal for all parameters. Furthermore, their Monte Carlo simulations found that uncertainty in hourly flows increased with increasing precipitation intensity and duration (with parameter uncertainty held constant).

The research reviewed in this section demonstrates that errors and uncertainties in determining the proper model parameter values for a given modeling purpose (forecast, design, etc.) can greatly effect the reliability of the model result in relation to its purpose. As was the case for the studies of input data uncertainty, these studies of model parameter uncertainty do not provide a comprehensive picture of overall modeling uncertainty, nor do they consider the true magnitude of the model parameter uncertainties instead use is made of assumed errors.

A.3.3 Studies of Model Structure Uncertainties

Very little research has been performed to examine the influence of model structure uncertainties on runoff prediction. The primary reason for this lack of research is the difficulty in separating out the effects of

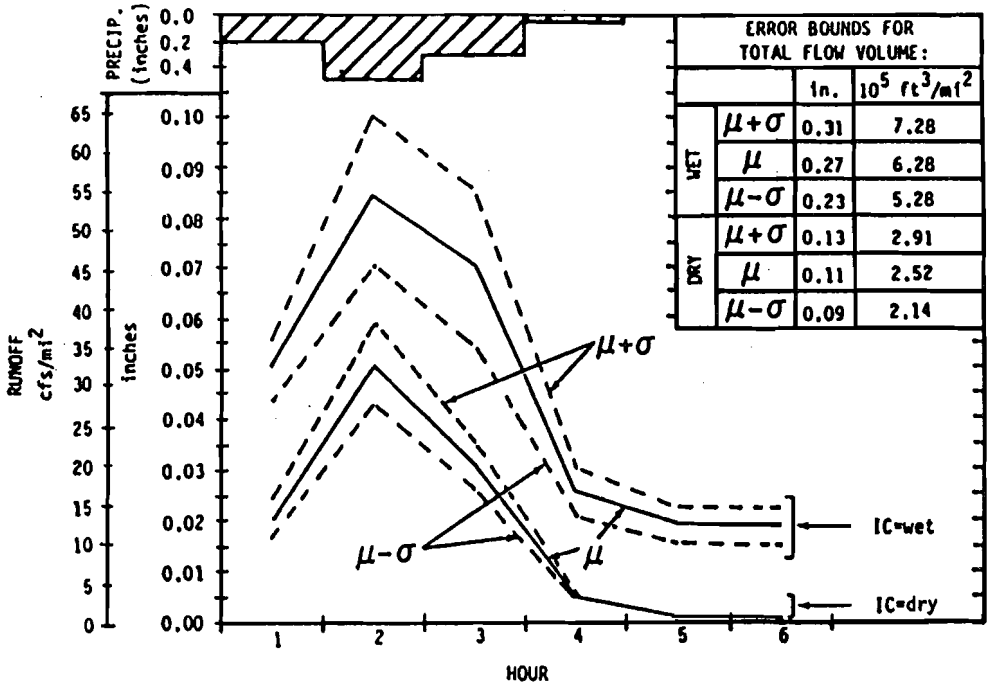

(a)

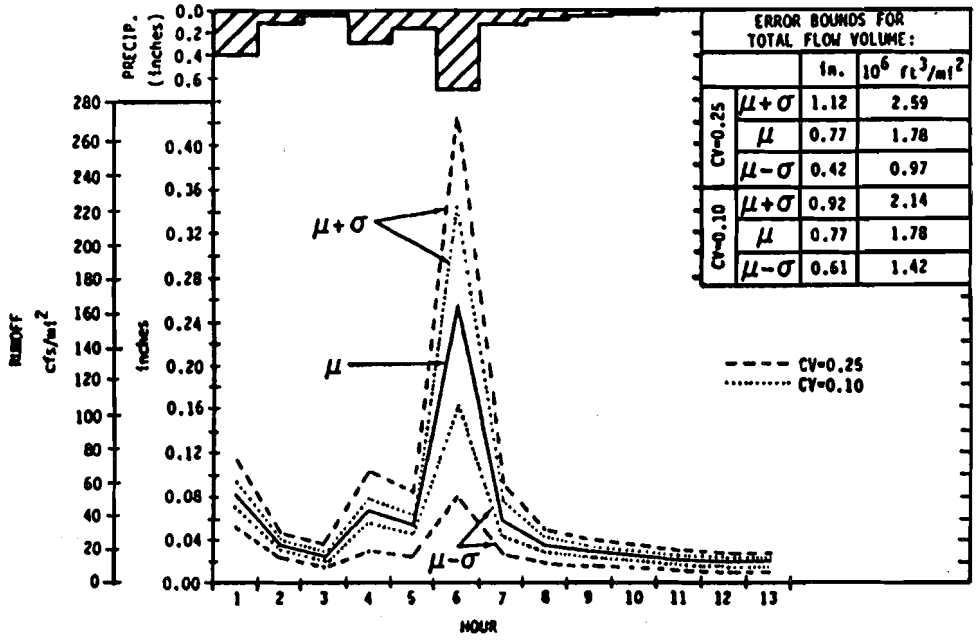

(b)

Figure A.1. Channel inflow hydrographs showing the mean, μ, and one standard deviation, σ, error bounds for: (a) storm D, wet and dry initial conditions, coefficient of variation, CV, of all parameters = 0.10, (b) storm H, wet initial conditions, CV of all parameters = 0.10 and 0.25. (after Garen and Burges, 1981)

model structure uncertainties from those in the input data and the model parameters. Also, a perfect model of the rainfall runoff process does not exist, and so simplified models cannot be compared to the results of a perfect model to determine the model structure uncertainties. As pointed out by Garen and Burges (1981), if the historical record is representative of a wide range of watershed responses and is of sufficient length to constitute a statistically significant sample, comparison of simulated and recorded flows to measure uncertainty might be extrapolated to estimate model structure uncertainties. Hence, in order to study model structure uncertainty, a sufficient amount of runoff data must be available so that the effects of the other sources of uncertainty may be separated out. Another reason for the lack of study is that the results are model dependent and cannot be generalized.

A.3.4 Studies of Overall Modeling Uncertainties

As discussed in section A.3.1, Dawdy et al (1972) presented a simplified, somewhat idealized approach to estimating overall model prediction error. However, their study concentrated more on data effects than a clear view of overall errors.

Schilling and Fuchs (1986) compared the results from a complicated urban rainfall runoff model with distributed rainfall input to the results from several simplified models to determine the modeling uncertainty caused by the simplifications. The "complex" model used distributed rainfall data based on radar measurements as input to the 81 subcatchments in the basin, a time varying increasing fraction of paved area to model abstractions, and dynamic wave routing of the runoff through the sewer network. The "common practice" model assumed one rain gage at the center of the watershed as input for all 81 subcatchments, used constant proportional losses to model abstractions, and used dynamic wave routing. The "simple" model assumed one rain gage at the center of the watershed as input for all 81 subcatchments, used constant proportional losses to model abstractions, and used time offset routing.

Schilling and Fuchs (1986) found that errors in rainfall input are amplified by the rainfall-runoff transformation. For example, on the average, a rainfall depth error of 30 percent results in a runoff volume error of 60 percent and a peak flow error of 80 percent. A better routing procedure was also found to improve the accuracy of computed runoff. Nevertheless, it was concluded that the spatial resolution of rainfall has a dominant influence on the reliability of computed runoff. They recommended that it is inappropriate to use a sophisticated runoff model to achieve a desired level of modeling accuracy if the spatial resolution of rainfall input is low. Instead, increased spatial resolution of rainfall data and use of a fast and simple runoff model gives results accurate enough to be used for real-time operation.

As discussed previously, adaptive filtering schemes are able to combine the various sources of modeling uncertainty and lump them together in the forecast error covariance matrix. Georgakakos (1986a) suggested that based on the predicted mean state vector and the predicted covariance matrix, the mean and variance of the predicted observation variables can be

obtained. Then assuming a normal distribution for the prediction errors, and given a critical flood level, the probability of flood level exceedance can be computed. However, Kitanidis and Bras (1980a-c) pointed out that proper determination of the error covariance matrix is the "art" in adaptive filter updating. For flood events, Kitanidis and Bras (1980a and c) suggested that adaptive filtering should be used to determine the model parameters only after a minimum number of measurements are available on the rising limb of the hydrograph. Therefore, the approach suggested by Georgakakos (1986a) is only useful for longer lead time estimates of flood level exceedance for cases where good estimates of the component errors are known a priori.

The majority of research which has been conducted to determine the nature and/or magnitude of uncertainties in hydrologic model forecasts or predictions has concentrated on the effects of one source of modeling uncertainty (generally either data or model parameters). The few attempts to consider the combined effects of data, model parameter, and model structure uncertainties have been marred by the need for complex and time consuming sensitivity calculations of simplified "ad-hoc" interrelations between the sources (Dawdy et al., 1972; and Schilling and Fuchs, 1986). The adaptive filter considerations for overall modeling uncertainty are also very complex mathematically and are of limited use for long term (three or more time steps ahead) forecasts and design hydrograph prediction. Finally, all of these studies are marred by the assumption of error magnitudes rather than some formal determination of truly representative error magnitudes in hydrograph forecasting (long term) or prediction. Therefore, a simple, systematic, unbiased, and consistent approach needs to be developed for considering overall hydrologic modeling uncertainty and, subsequently, providing simple and useful information on the reliability of forecasts and predictions made by hydrologic models. The approach developed in this study, which uses reliability analysis (see Appendix B) to analyze the combined effects of data, model parameter, and model structure uncertainties on hydrologic model reliability, meets the above criteria.

A.4 Model Choice Considerations

When developing an on-line (i.e., real-time) flood forecasting system, the correct choice of model is the most important single investment decision from which all other investment decisions naturally follow (Lambert, 1981). The primary practical problems with the use of complex hydrologic models is that their extensive data and computer requirements often cancel out their model structure accuracy advantage. Sangsit (1973) reported the use of the SSARR model for flood forecasting in the lower Mekong Basin, Cambodia, produced mixed results. That is, the model produced fairly good forecasts, but its data and computer requirements made it difficult to run in an area with limited data and computer facilities. Askew (1981) reported similar results for the application of the Sacramento model (as operated by the NWS) and the CLS model to flood forecasting in Central America. Given this problem and other considerations, Lambert (1981) noted that operational experience has shown that it is advantageous to use relatively simple hydrologic models for on-line forecasting, the choice of models being specifically geared to the simulation problems requiring solution. Dawdy (1969) agreed with this principle stating 'if a simple model will suffice,

none more complex is necessary. Chow (1972) pointed out this rule fails in practice unless "suffice" is better defined. Linsley (1986) advocated accuracy as the prime definition of "suffice" stating 'until equivalent accuracy is demonstrated, simplicity should be a second-order criterion in model selection.' Clarke (1973) pointed out choosing a model sufficiently simple for the purpose at hand is the art of model-building.

For the purpose of flood warning, the key characteristics of the forecasting model are the accuracy, reliability, and timeliness of the forecasts. Hence, the tendency has been to use more and more complex hydrologic models because of their potentially greater accuracy. However, Dawdy (1969) pointed out:

> "A desire for completeness in a model tends to lead toward inclusion of all (hydrologic) components which intuitively are known to exist. However, the desire for completeness may lead to the inclusion of many parameters which are merely curve fitting factors rather than physical parameters describing the process they supposedly are modeling."

Furthermore, Larimore and Mehra (1985) noted that the purpose of modeling is to obtain a model of the predictable behavior of the process but to avoid incorporating the random characteristics of the particular data set. Beyond a certain complexity, the model ends up fitting to the noise in the data trying to explain every wiggle in the data. These considerations have lead several researchers (Wood, 1976; Garen and Burges, 1981; Yeh, 1982) to conclude that as hydrologic models become larger and more complex, the information about parameter values often decreases. As the number of parameters increases, the model structure uncertainty (as represented by a least-squares criterion) will generally decrease, but in order to estimate this increasing amount of parameters more and more data is necessary, and the quality and availability of the data generally decreases as more is needed. Hence, for more complex models the data and model parameter uncertainties may be greater than for simpler models. Therefore, in comparing models an optimum exists that "trades off" the greater potential output accuracy from a complex model with a simple model's parsimony and greater accuracy of parameters and input data (Garen and Burges, 1981).

Reliability analysis methods consider all the sources of uncertainty-- data, model parameter, and model structure -- and so they may be quite useful in determining the nature of the "trade off" between simple and complex models. By applying reliability analysis to real-time flood forecasting models of differing complexity, comparison of the flood probabilities may reveal the models provide comparable estimates of flood potential even if the estimated hydrographs are greatly different. If simpler models provide comparable information regarding flood probabilities, they are "sufficient for the purpose at hand" and should be used.

The question of which hydrologic area -- data, model parameters, or model structure -- should receive the most future attention is similar to the model complexity question. By applying reliability analysis to the sources of uncertainty, those which contribute most to the overall uncertainty in forecasts can be identified. By identifying the hydrologic

factors which have significant effects on overall forecast uncertainty and whose individual uncertainties can be significantly improved through further study, reliability analysis methods can find those hydrologic areas whose future study offers the greatest gains in hydrologic modeling reliability. These gains are not restricted to forecasting, but rather they lead to more reliable hydrograph simulation and synthetic data generation as well.

APPENDIX B. RELIABILITY ANALYSIS METHODS

B.1 Introduction

The results of studies of data, model parameter, model structure, and overall modeling uncertainty effects on predicted hydrographs discussed in Appendix A, show that the value of any kind of real-time forecast (for flood warning, reservoir operations, etc.) is enhanced if some measure of its precision can be derived. Dawdy et al. (1972) pointed out that the standard error of estimate is a measure of error in reproduction of the fitted data, while the standard error of prediction is somewhat greater than the standard error of estimate because it includes both the measure of lack of fit of the data used to calibrate the model and the measure of error in the fitted parameters. Dawdy et al. (1972) and Clarke (1973) further pointed out that if the residuals of the calibrated model (i.e., the differences between the measured and simulated hydrographs) are uncorrelated, normally distributed, and homoscedastic (i.e., have constant variance), the standard error of prediction could be computed from the standard error of estimate, the deviations of the independent variables (input data) from their means, and the error in the model parameters. Unfortunately, the nonlinear nature hydrologic processes precludes any theoretical description of the mechanism by which errors in data are transferred to model parameters and, in turn, are combined with input errors in the period studied to produce errors in the streamflow forecast (Dawdy et al., 1972). Furthermore, for practical cases, the model residuals very rarely correspond to the above conditions (Clarke, 1973). Therefore, it is doubtful a theoretically correct measure of forecast precision can be derived, despite its potential usefulness.

Dawdy et al. (1972) approximated the standard error of prediction via the method described in section A.3.1. In their study the errors in the streamflow estimates were found to be approximately related linearly to the errors in the rainfall input data. They concluded that the linearity of errors indicates that there may be some hope for the derivation of a theory of errors for streamflow simulation.

For calibrated models, an estimate of the forecast precision (standard error of prediction) must consider the data uncertainty which has been transferred to the model parameters, the uncertainty in the estimate of the model parameters for a given event, and the model structure uncertainty. Similarly, for non-calibrated (i.e., physical simulation) models, an estimate of the forecast precision must consider the data, model parameter, and model structure uncertainty as specific entities with special interrelations. In either case, the forecast precision estimate may take advantage of the apparent linearity of errors between the rainfall data and predicted streamflow. Such an estimate may be obtained using modern reliability analysis methods.

Over the past 30 years, reliability analysis methods have been developed by structural engineers seeking a scientific base for structural safety codes. In the past 15 years, hydraulic engineers have adapted these methods to evaluate the safety of hydraulic structures. Yen (1987) presented a "state-of-the-art" review of the reliability analysis methods which have been applied to hydraulic structures. Four of these methods

appear to be potentially useful for evaluating the uncertainties involved in hydrologic modeling, and hence, for providing estimates of the probability of flood occurrence given the available real-time storm data and an estimate of the model parameter and structure uncertainties. These methods are direct integration, Monte Carlo simulation, the mean value first-order second moment method, and the advanced first-order second moment method. A thorough review of all these methods for engineering systems in general is given by Ang and Tang (1984), while one for hydraulic systems is given by both Cheng (1982) and Yen (1987). Hence, only brief reviews of the first two methods and more extensive reviews of the first-order methods, especially their strengths and weaknesses, are given here.

B.2 Definition of System Risk and Reliability

The risk associated with an engineering system is the probability that the system will fail to perform the function for which it was designed. For engineering systems, the concept of the system failure is generally defined as the load, L, placed on the system exceeding the system's capacity to resist, R. For a flood warning system, the resistance may be considered as the critical flood stage (e.g., bankfull) whose exceedance leads to flooding of low lying areas where damages could be reduced via flood warning. The load is the peak discharge estimated by the real-time flood forecasting model. From the previous chapter, it is clear that the peak discharge estimate (load) is highly uncertain. Furthermore, since the critical flood stage (resistance) must be converted to an equivalent critical flood discharge for comparison to the estimated peak discharge, it too may be uncertain due to errors in the stage-discharge relation. Thus, the flood risk (system risk), R_s, may then be defined as

$$R_s = 1 - R_\ell = P_r(L > R) \tag{B.1}$$

where $P_r(X)$ is the probability of event X occurring and R_ℓ is the system reliability.

A convenient way to evaluate system failure risk is to use a system performance function, Z, which relates the basic variables (i.e., the data, model parameters, and model correction factors which describe the system) of the system to the load and the resistance. The performance function may take on several equivalent mathematical forms where a negative value indicates system failure, e.g., R-L, (R/L)-1, and $\ell n(R/L)$. Thus, the system risk can be defined as

$$R_s = P_r(Z < 0) \tag{B.2}$$

where $Z = g(x_1, x_2, \ldots, x_p) = g(\underline{x})$

$\underline{x}$ = the vector of the basic variables of the system, and

p = the number of basic variables for the system.

B.3. Direct Integration Method

The probability of failure, i.e., the system risk, can be expressed as

$$R_s = \int_o^{\infty} \int_o^{\ell} f_{R,L}(r,\ell)\, dr\, d\ell \qquad (B.3)$$

in which $f_{R,L}(r,\ell)$ is the joint probability density function of R and L. If the resistance, R, is statistically independent of the load, L, then Eq. B.3 can be simplified as

$$R_s = \int_o^{\infty} f_L(\ell) \left[\int_o^{\ell} f_R(r)\, dr \right] d\ell \qquad (B.4)$$

If the appropriate distribution functions can be found which describe the load and resistance correctly, then the risk evaluated by this method is exact. However, there are several practical problems with this method.

The greatest difficulty with this method is the selection of the proper distribution functions. The estimated risk is greatly sensitive to the distribution functions selected, and, in fact, improper assumption of distribution functions may negate the accuracy merits of direct integration. Determination of the probability density functions for load and resistance is further complicated by their dependence upon the probability functions of the individual basic variables and the nature of the functions relating the basic variables to the load and resistance (CIRIA, 1977). Additionally, in many practical cases (although not for the flood warning case), load and resistance will be related to some of the same basic variables and will therefore be subject to some degree of correlation (CIRIA, 1977). Hence, the more complicated form of Eq. B.3 must be used. Finally, Shinozuka (1983) pointed out that practically for all cases of engineering interest, the multidimensional integration over the generally irregular domain is impossible to carry out analytically and quite costly to perform numerically, if not impossible. Given the nature and severity of these practical problems in applying the direct integration method, its use is generally limited to very simple systems or analysis of a portion of the total system reliability.

Wood (1976) used direct integration to analyze the effects of the uncertainty of a single parameter of a very simple hydrologic model on a flood frequency relation generated from rainfall data and the hydrologic model.

Davis and Nnaji (1982) performed a simplified study of flood forecast reliability for a 33 square kilometer drainage basin called the Airport Wash near Tucson, Arizona. They determined the conditional probability of streamflow given measured rainfall near the outlet of the Wash based on a bell shaped model of convective storms and a modification of the Purdue

rainfall-runoff model. This probability distribution was integrated to determine the probability of a critical flood stage being exceeded given the measured rainfall. This study did not consider the uncertainties in the data or the parameters of the rainfall or runoff models.

Kooman et al. (1978) developed a reliability-analysis-based design for the foundation of the Oosterschelde storm surge barrier in The Netherlands by combining direct integration of the load (wave and static forces) and a partial safety factor analysis of the resistance. The results of this design method were checked by the advanced first-order second moment method and were found to be quite reasonable for practical design applications.

Tung and Mays (1980 and 1981) proposed perhaps the most innovative means of using direct integration. They handled the problems with basic variable distributions and their relations to load and resistance by using first-order approximations to determine the parameters of the distribution functions for the load and resistance. This innovative approach is still faced with the problem of selecting appropriate distributions for load and resistance and possible numerical integration problems. However, with reasonable selections of the distributions fairly good approximations of the system risk may be obtained as demonstrated by Tung and Mays for culverts (1980) and levees (1981).

Despite these relative successes for hydraulic systems and others for structural systems, the general consensus of several researchers (Cornell, 1972; Rackwitz, 1976; CIRIA, 1977; and Cheng, 1982) is that direct integration methods are not suitable for normal design purposes because of their theoretical and numerical difficulties. For system design, direct integration methods are useful for simple systems, checking the validity and accuracy of simplified reliability methods for specific cases, and for systems which require highly accurate risk determination. For uncertainty analysis of hydrologic models applied to real-time flood forecasting, similar conclusions may be made. Direct integration can only be used for very simple hydrologic models such as the one used by Wood (1976). Thus, for realistic flood warning cases, direct integration methods are not practical.

B.4 Monte Carlo Simulation Method

Monte Carlo simulation is a process using, in each simulation, a particular set of values of random variables generated in accordance with the corresponding basic variable probability distributions. For each simulation, the performance function is calculated using the appropriate basic variable values, and the risk is estimated as the ratio of the number of failures versus the number of simulations.

The Monte Carlo simulation method is an extremely flexible method (i.e., it can be used to solve a great variety of problems); and as such, it is a very useful method. In fact it may be the only method which can estimate risk for cases with highly nonlinear and/or complex system relationships. Despite its flexibility, Monte Carlo simulation is not a highly recommended way to analyze system risk. The risk estimated by using this method is not unique, i.e., it depends on the size of the samples and

the number of trials. To combat this flaw, large numbers of trials must be performed and thus the computer time required can become prohibitive. These high computation costs tend to cancel out the flexibility of Monte Carlo simulation methods. Furthermore, Monte Carlo simulation methods are also quite sensitive to the assumed distributions for the basic variables. Hence, Monte Carlo simulation methods are generally used as a last resort.

The conclusions reached above are supported for the case of analyzing the uncertainty in real-time hydrologic forecasts by the work of Garen and Burges (1981). They used Monte Carlo simulation of model parameter variability to estimate error bounds for the hydrograph predicted by a simplified version of the Stanford Watershed model. The error bounds estimated by Monte Carlo simulation were used to check those estimated using the mean value first-order second moment reliability analysis method. The first-order method's results compared favorably with the Monte Carlo simulation's results. Hence, they recommended the first-order method be used to avoid the high computation cost of Monte Carlo simulation.

B.5 Mean Value First-Order Second Moment (MVFOSM) Method

The concept behind the first-order second moment reliability analysis methods was initially proposed long ago. Mayer (1926) suggested use of the mean and variance of the random variables in the analysis of structural safety. However, Mayer's suggestion went unheeded for more than thirty years, perhaps because engineers were still trying to obtain better formulations of the physical side of engineering design problems. In 1959, Su proclaimed that the physical side of many structural problems is now well explored, but the conventional method of structural design is still far from satisfactory. He developed a MVFOSM formulation based on the normal distribution and recommended its use for more rational determination of structural safety factors. But it was not until Cornell (1967) elaborated on a formulation very similar to Su's that the MVFOSM method established a foothold in structural engineering. The MVFOSM method was first adopted for hydraulic system risk evaluation by Tang and Yen (1972).

In the first-order methods, a Taylor series expansion of the performance function is truncated after the first-order term

$$Z = g(\underline{x}) + \sum_{i=1}^{p} (x_i - \bar{x}_i) \frac{\partial g}{\partial x_i} \qquad (B.5)$$

where $\bar{x}_i$ are the mean values of the basic variables. In the MVFOSM method, the expansion point is at the mean values of the basic variables. Thus, the performance function's expected value and variance are

$$E[Z] \approx g(\bar{\underline{x}}) \qquad (B.6)$$

$$VAR(Z) \approx \sum_{i=1}^{p} C_i^2 \, VAR(x_i) + \sum_{\substack{i=1 \\ i \neq j}}^{p} \sum_{j=1}^{p} C_i \, C_j \, COV(x_i, x_j) \qquad (B.7)$$

where C_i and C_j are the values of the partial derivatives $\partial g/\partial x_i$ and $\partial g/\partial x_j$, respectively, evaluated at $\bar{x}_1, \bar{x}_2, \ldots, \bar{x}_p$. If the variables are statistically independent, the covariance terms will vanish and Eq. B.7 becomes

$$VAR(Z) = \sigma_z^2 \approx \sum_{i=1}^{p} C_i^2 \, VAR(x_i) \qquad (B.8)$$

This is a reasonable approximation if the coefficients of variation of the basic variables are not large and the system performance function, Z, is approximately linear.

For many practical engineering problems, the partial derivatives, C_i, cannot be determined explicitly. For such cases, C_i can be approximated numerically by a forward difference at point w.

$$C_i = \frac{\partial g}{\partial x_i}\bigg|_{\underline{x}=\underline{x}_w} = \frac{g(\underline{x}_{jw}, x_{iw} + \Delta x_i) - g(\underline{x}_w)}{\Delta x_i} \qquad (B.9)$$

where Δx_i = a small change in the value of x_i, and $\underline{x}_{jw}$ indicates all other basic variables are fixed at point w. This method was successfully used by Garen and Burges (1981) in their determination of error bounds on predictions made by a modified version of the Stanford Watershed model. The forward difference method was employed in this study as described in Appendix C.

B.5.1 Probability Estimates Based on the MVFOSM Method

Risk is measured in terms of a reliability index, β, which is defined as

$$\beta = \frac{E[Z]}{\sigma_z} \qquad (B.10)$$

which is the reciprocal of the coefficient of variation of Z. In many cases of engineering system design, the value of β alone is used to compare the reliability of various alternatives. In other instances (such as flood forecast uncertainty analysis), an estimate of the system risk is required. In these cases a probability distribution is assumed for the performance function, Z, and β is visualized as a normalized measure of the departure

from the system's mean state to the system failure level. Thus, the probability corresponding to the value of β is taken as the system reliability.

In the MVFOSM method, no distributional assumptions are made regarding the basic variables. Hence, the distribution of Z remains undefined, and the probability information contained in β is poor. Typically, it is assumed that Z is normally distributed, and thus the system risk is

$$R_s = 1 - \Phi(\beta) \tag{B.11}$$

where $\Phi(\cdot)$ is the standard normal integral (e.g., see Ang and Tang, 1975). This assumption has several practical advantages. If the system performance function is linear (i.e., Z=R-L) and the load and resistance are normally distributed, Eq. B.11 yields the exact risk. If the system performance function is nonlinear such that $Z=\ell n(R/L)$ is appropriate and the load and resistance are lognormally distributed, Eq. B.11 yields a very close approximation of the exact risk as long as the coefficients of variation of L and R are relatively small. Therefore, the selection of the normal distribution for Z is quite reasonable and efficacious because many natural systems and/or variables can be shown to be normally or lognormally distributed.

Yen et al. (1986) noted that usually some information on the nature of the basic variable distributions is available. Though imperfect and imprecise, such limited information provides great help in obtaining risk evaluation with acceptable accuracy. For example, they reasoned that if the basic variable distributions are uni-modal with the mode near the beginning of the range, setting $Z=\ell n(R/L)$ and assuming Z is normally distributed will provide reasonable estimates of risk. If the basic variable distributions are uni-modal with small skewness, setting Z=R-L and assuming Z is normally distributed will provide reasonable risk estimates. Furthermore, Cheng (1982) found that even for the case of

$$Z = x_1 + x_2 - x_3x_4 \tag{B.12}$$

where x_1 and x_2 are uniformly distributed and x_3 and x_4 are lognormally distributed, the MVFOSM method with Z=R-L ($R=x_1+x_2$, $L=x_3x_4$) and Z assumed normal gave acceptable estimates of risk relative to the exact solution when the risk is high, e.g., $R_s > 0.01$. In summary, very reasonable estimates of system risk can be made with the MVFOSM method despite the necessity of assuming a distribution for Z.

B.5.2 Practical Advantage of the MVFOSM Method

The greatest advantage of the MVFOSM method is its simplicity; no higher order moments or distributional information on the system's basic variables are necessary, only the mean and variance of the variables are needed to obtain a reasonable estimate of the system risk. While many may

argue that first-order methods are oversimplified and too inaccurate to be useful, Cornell (1972) made a strong defense of them from a practical standpoint. He stated:

> "An approach based on means and variances may be all that is justified when one appreciates: (1) that data and physical arguments are often insufficient to establish the full probability law of a variable; (2) that most engineering analyses include an important component of real, but difficult to measure, professional uncertainty; and (3) that the final output, namely the decision or design parameters, is often not sensitive to moments higher than the mean and variance."

Furthermore, Cornell (1972) pointed out the most important consideration in any reliability analysis:

> "It is important to engineering applications that we avoid the tendency to model only those probabilistic aspects that we think we know how to analyze. It is far better to have an approximate model of the whole problem than an exact model of only a portion of it."

B.5.3 Applications of the MVFOSM Method in Hydraulic Engineering

The simplicity and practicality of the MVFOSM method has made it popular for a variety of water resources systems uncertainty analyses. The MVFOSM method has been directly applied to hydraulic structure reliability analysis for storm sewers (Tang and Yen, 1972) and culverts (Yen et al., 1980), and indirectly applied to such analysis by Tung and Mays (1980 and 1981) as described previously. Burges (1979) applied the MVFOSM method to the analysis of flood plain mapping uncertainty due to errors in the estimation of the design discharge and in the routing procedures used to determine the flood plain. However, Burges' work erroneously equated the design discharge uncertainty to the channel capacity uncertainty. McBean et al. (1984) and Oegema and McBean (1986) corrected Burges' error and determined the one standard deviation error bounds for flood plain width combining the design discharge and channel capacity uncertainties. Tung (1987) used the MVFOSM to estimate confidence bounds for the precipitation depths in the National Weather Service rainfall frequency atlas -- U.S. Weather Bureau Technical Paper Number 40 (Hershfield, 1961). Finally,Garen and Burges (1981) used Eq. B.8 to approximate the error bounds fora simulation of total flow volume produced by a modified version of the Stanford Watershed model.

Yen and Tang (1977) applied MVFOSM analysis to flood routing model uncertainties for the purpose of evaluating the reliability of real-time flood forecasts provided by such models. They separated out the various sources of uncertainties as correction factors and then applied the MVFOSM analysis. This work marks the first attempt to consider the uncertainties involved in real-time flood forecasts, however, the correction factor approach reduces the utility of the analysis. The simplification of using correction factors allows the MVFOSM method to be used, but it also takes away validity from the overall analysis because it is unclear how known

available information on model parameter and data uncertainties equate to correction factors. Thus, some of the knowledge of these sources of uncertainty may be lost in the assumptions of the correction factor approach. A better approach would be one which can directly make use of available information on model parameter and data uncertainties and their direct effects on model predictions.

B.5.4 MVFOSM Method Summary

When applied to engineering design problems, the MVFOSM method does, however, have several theoretical and/or conceptual problems as pointed out by Rackwitz (1976) and Cheng (1982). These problems are listed below with 1 to 3 being the most serious:

1) the relative accuracy of the first-order Taylor series approximation;

2) for engineering systems the events of failure generally happen at extreme values rather than near the mean load and resistance;

3) most real world engineering systems exhibit nonlinear behavior;

4) the results of this method vary depending on the particular mathematical formulation of Z and on the dimension (i.e., number of variables) of the reliability problem;

5) the reliability index, β, gives only weak information on the probability of failure and thus the appropriate system probability distribution must be assumed;

6) this method provides no logical way to include available information on basic variable probability distributions.

However, for evaluating the uncertainties in real-time flood forecasts, the system failure (i.e., flood peak exceeding critical stage) generally will not be at extreme values. Furthermore, the flood risk levels considered are high enough such that it is reasonable to assume β is normally distributed. Therefore, the MVFOSM method might be quite useful for real-time flood forecast uncertainty analysis. Finally, both Cheng (1982) and Yen et al. (1986) found that $Z=(R/L)-1$ gave consistently poorer estimates of risk than either $Z=R-L$ or $Z=\ell n(R/L)$. Hence, in this study, the MVFOSM method with $Z=R-L$ and $Z=\ell n(R/L)$ is examined for real-time flood forecast uncertainty analysis.

B.6 Advanced First-Order Second Moment (AFOSM) Method

Recent research has sought to maintain some of the simplicity of the MVFOSM method and yet reduce its flaws. The result is the advanced first-order second moment method. The basic concept behind the AFOSM method was first proposed by Hasofer and Lind (1974), but Rackwitz (1976) was the first to tie the entire AFOSM method together. Rackwitz's version of the AFOSM method will be outlined in the following paragraphs.

The essence of this method is to linearize the performance function via Taylor series expansion at a likely failure point (x_1^*, x_2^*, . . ., x_p^*) on the failure surface, i.e., when the performance function, $g(\underline{x}^*)$, equals zero. The expected value and variance of the performance function as approximated by a first-order Taylor series at this point for the case of statistically independent basic variables are

$$E[Z] \approx g(\underline{x}^*) + \sum_{i=1}^{p} C_i(\bar{x}_i - x_i^*) \tag{B.13}$$

$$VAR(Z) = \sigma_z^2 \approx \sum_{i=1}^{p} C_i^2 \, VAR(x_i) \tag{B.14}$$

$$\sigma_z \approx \left[\sum_{i=1}^{p} (C_i \, \sigma_i)^2\right]^{1/2} \tag{B.15}$$

where C_i, in this case, is $\partial g/\partial x_i$ evaluated at (x_1^*, x_2^*, . . ., x_p^*). The expression for σ_z may be rewritten in a linearized form

$$\sigma_z \approx \sum_{i=1}^{p} \alpha_i \, C_i \, \sigma_i \tag{B.16}$$

in which the α_i's are sensitivity factors and are evaluated from

$$\alpha_i = \frac{C_i \, \sigma_i}{\left[\sum_{j=1}^{p} (C_j \, \sigma_j)^2\right]^{1/2}} \tag{B.17}$$

Substituting Eqs. B.13 and B.16 into Eq. B.9, the reliability index for the AFOSM method is

$$\beta = \frac{g(\underline{x}^*) + \sum_{i=1}^{m} C_i(\bar{x}_i - x_i^*)}{\sum_{i=1}^{p} \alpha_i \, C_i \, \sigma_i} \tag{B.18}$$

B.6.1 Methods for Finding the Failure Point

The formulations in the previous paragraph appear to be fairly simple and straightforward; however, it must be pointed out that determination of the failure point is generally not a simple task. Several iteration methods have been proposed for determining the failure point (e.g., Rackwitz, 1976; and CIRIA, 1977). The Rackwitz approach has become the "standard" iteration approach as evidenced by its inclusion in the text book summary of the AFOSM method presented by Ang and Tang (1984, p. 361). A flow chart of the Rackwitz iteration scheme is given in Fig. B.1. Recently, the use of constrained nonlinear optimization has shown great promise as an alternative to the iteration schemes. The constrained nonlinear optimization schemes of Shinozuka (1983) and Cheng (1982) are described below.

If the basic variables are standardized, i.e.,

$$y_i = (x_i - \bar{x}_i) / \sigma_i \tag{B.19}$$

The standardized basic variables, y_i, have a mean of zero and a standard deviation of one. Shinozuka (1983) solved the following optimization problem:

$$\text{Minimize:} \quad \gamma_0 = (\underline{y}^T \underline{y})^{1/2} \tag{B.20}$$

$$\text{Subject to:} \quad g_1(\underline{y}) = 0 \tag{B.21}$$

where $\underline{y}^T$ = the transpose of the standardized basic variable matrix.

Using the Lagrange multiplier method to solve this problem, the Lagrangian is

$$L_g = (\underline{y}^T \underline{y})^{1/2} + \lambda \, g_1(\underline{y}) \tag{B.22}$$

where λ = the Lagrange multiplier.

Setting $\partial L_g/\partial y = \partial L_g/\partial \lambda = 0$, the solution for $\underline{y}^*$ and λ^* is obtained from

$$\underline{y}^* = -\lambda^* \gamma \, \underline{G}_* \tag{B.23}$$

where γ = the minimum of γ_0, and

$\underline{G}_*$ = the vector of $\partial g_1/\partial_{yi}$ evaluated at $\underline{y}^*$.

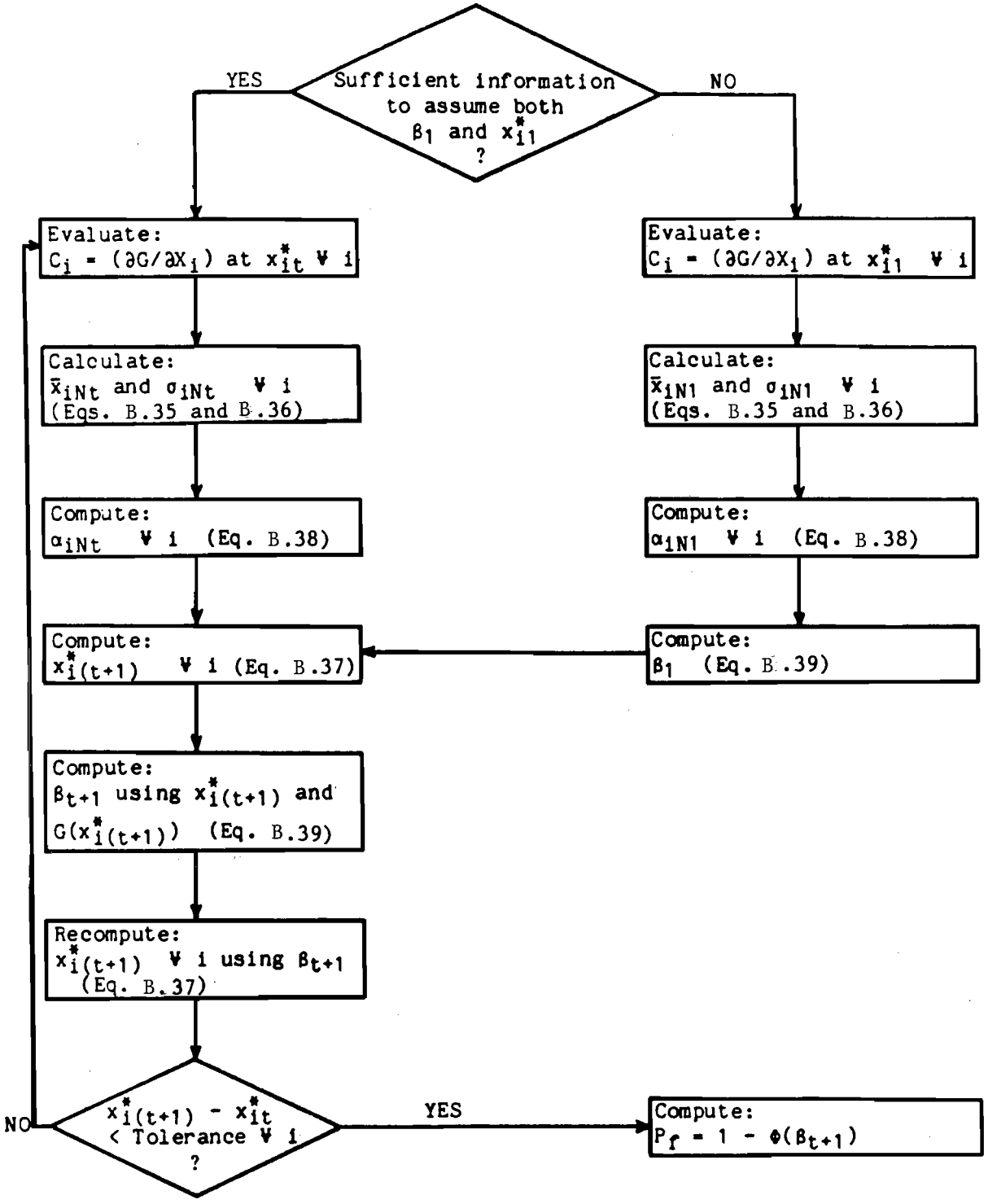

Figure B.1. Flow chart of Rackwitz's iterative algorithm (note: the subscipts 1, t, t+1 denote trials in the iterative algorithm)

Solving for γ yields

$$\gamma = \pm \frac{\underline{y}^{*T}\ \underline{G}_*}{(\underline{G}_*^T\ \underline{G}_*)^{1/2}} \geq 0 \qquad \text{(B.24)}$$

The system performance function, Z, may also be expressed in terms of the standardized basic variables, y_i, i.e., $Z=g_2(\underline{y})$. Taking a first-order Taylor series expansion at the failure surface

$$E[Z] \cong g_2(\underline{y}^*) - \sum_{i=1}^{p} G_{2i}\ y_i^* \qquad \text{(B.25)}$$

$$\text{Var}[Z] = \sigma_z^{\ 2} = \sum_{i=1}^{p} G_{2i} \qquad \text{(B.26)}$$

where $G_{zi} = \partial g_2/\partial y_i$ evaluated at $\underline{y}^*$.
At the failure surface, $g_2(\underline{y}^*)=0$, therefore, the reliability index, β, is

$$\beta = - \frac{\sum_{i=1}^{p} G_{2i}\ y_i^*}{\left[\sum_{i=1}^{p} G_{2i}^{\ 2}\right]^{1/2}} \qquad \text{(B.27)}$$

Rewriting Eq. B.26 in vector form,

$$\beta = - \frac{\underline{G}_2\ \underline{y}^*}{(\underline{G}_2^T\ \underline{G}_2)^{1/2}} \qquad \text{(B.28)}$$

Shinozuka (1983) stated the comparison between Eqs. B.24 and B.28 indicates that if $g_1(\underline{y})$ is set as $g_2(\underline{y})$, the reliability index (or its absolute value) is the shortest distance in standardized space between the system mean state (i.e., where all basic variables are at their mean values) and the failure surface. Hence, optimization algorithms currently available for nonlinear programming methods, including the Lagrange multiplier method, can be used for determination of the failure point.

For example, Wang et al. (1983) used the a Lagrange multiplier approach incorporating an iterative "redesign travel" formula to solve for the failure point. They found that for the problems they studied, the "redesign travel" optimality criterion algorithm is highly efficient with convergence generally obtained in 5 to 8 iterations. Furthermore, they found the speed

generally obtained in 5 to 8 iterations. Furthermore, they found the speed of convergence appeared to be almost independent of problem size.

Cheng's (1982) constrained linear programming approach takes a different view of the problem. Cheng noted that for points on the failure surface $g(\underline{x}^*) = 0$, so Eq. B.18 may be rearranged as

$$\sum_{i=1}^{p} C_i(\bar{x}_i - x_i^* - \alpha_i \beta \sigma_i) = 0 \qquad \text{(B.29)}$$

Solving this equation gives

$$\bar{x}_i - x_i^* - \alpha_i \beta \sigma_i = 0 \; ; \qquad \text{for all } i \qquad \text{(B.30)}$$

Hence, Eq. B.30 defines the failure point $\underline{x}^*$ and it may be thought of as a series of equality constraints. By selecting an objective function of

$$\text{Min} \; | \; g(\underline{x}^*) | \qquad \text{(B.31)}$$

subject to Eq. B.30 and the definitions of α_i and β as given by Eqs. B.17 and B.18, respectively, the failure surface may be found. It should be noted that while this problem has an equal number of constraints and variables, it defies straightforward solution because β and the α_i are different at each point. Hence, at each point, a new optimization problem must be solved. Cheng (1982) proposed to find the failure point and β by using the generalized reduced gradient algorithm, GRG, (Abadie and Carpentier, 1969). Like all nonlinear programming algorithms, GRG cannot guarantee to find the global optimum, and so a number of different starting points for the algorithm may be necessary. Fortunately, Cheng (1982) found that if the minimum of $|g(\underline{x})|$ approaches zero, the solutions of β and $\underline{x}^*$ usually are the global ones. Thus, if the objective function is sufficiently close to zero, one may conclude that the appropriate valueof β has been found.

The strength of Cheng's GRG method is the robustness of the GRG algorithm. Sandgren and Ragsdell (1980a and b) performed an extensive review and comparison of the existing computer codes for nonlinear optimization, and they found that the GRG based codes were far more efficient than the other methods, and GRG based codes were capable of solving a wide variety of problems. Therefore, the AFOSM method using Cheng's GRG method should be useful for any system where a concise, orderly mathematical description of the problem can be made. Hence, considering the efficiency of the GRG algorithm and the possible problems in determining the Lagrange multipliers for real-time flood forecasting cases, the GRG method for finding the failure point is preferred.

B.6.2 Probability Estimates Based on the AFOSM Method

Just as with the MVFOSM method, the reliability information in terms of a probability statement contained in β remains poor and is of the Tchebychev-inequality type (Rackwitz and Fiessler, 1978). Unlike the MVFOSM method, however, for the AFOSM method more precise probability statements can be made if distributional assumptions for the basic variables are adopted. For linear failure surfaces where all the basic variables are normally distributed, the probability of failure (risk) is exactly given by Eq. B.11.

For convex failure surfaces where all the basic variables are normally distributed, the probability of failure (risk) is bounded as

$$1 - \Phi(\beta) \leq R_s \leq 1 - \chi_p^2(\beta^2) \tag{B.32}$$

where $\chi_p^2(\cdot)$ is a chi-squared distribution with p degrees of freedom (Hasofer, 1974). Rackwitz' (1976) experience with structural problems indicated that if β (i.e., the distance function from the system mean to the failure surface) shows a unique minimum, then the lower bound will generally serve as a relatively good probability estimate within the accuracy of the first-order approximation. Based on a limited amount of experience with storm sewer reliability, it would appear that hydraulic problems have a unique minimum of the distance function, and thus the lower bound is a good risk estimate for hydraulic systems just as it is for structural problems.

Unfortunately, for most real systems not all the basic variables are normally distributed. Thus, it is desirable to transform the non-normal variables into equivalent normally distributed variables. Rackwitz (1976) proposed a transformation where the values of the cumulative distribution function, CDF, and the probability density function, PDF, of the non-normal distributions are the same as those of the equivalent normal distributions at the failure point; i.e.,

$$F_{x_i}(x_i^*) = \Phi\left(\frac{x_i^* - \bar{x}_i^N}{\sigma_i^N}\right) \tag{B.33}$$

$$f_{x_i}(x_i^*) = f^N\left(\frac{x_i^* - \bar{x}_i^N}{\sigma_i^N}\right) / \sigma_i^N \tag{B.34}$$

in which $F_{x_i}(x_i^*)$ and $f_{x_i}(x_i^*)$ are the CDF and PDF of x_i at x_i^*, and $\Phi(\cdot)$ and $f^N(\cdot)$ are the CDF and PDF of the standard normal distribution, respectively. In order to do this, Rackwitz (1976) approximated the non-normal distribution function by a first-order Taylor series expansion. Thus, the mean, $\bar{x}_i^N$, and the standard deviation, σ_i^N, of the equivalent normal distributions become

$$\bar{x}_i^N = x_{i_N}^* - \Phi^{-1}(F_{x_i}(x_i^*))\ \sigma_i^N \tag{B.35}$$

$$\sigma_i^N = \frac{f\ (\Phi^{-1}(F_{x_i}(x_i^*)))}{f_{x_i}(x_i^*)} \tag{B.36}$$

The constraints for the nonlinear optimization problem are then

$$\bar{x}_i^N - x_i^* - \alpha_i\ \beta\ \sigma_i^N = 0 \quad ; \qquad \text{for all } i \tag{B.37}$$

where

$$\alpha_i = \frac{C_i\ \sigma_i^N}{\left[\sum_{j=1}^{p} (C_j\ \sigma_j^N)^2\right]^{1/2}} \tag{B.38}$$

and

$$\beta = \frac{g(\underline{x}^*) + \sum_{i=1}^{p} C_i(\bar{x}_i^N - x_i^*)}{\sum_{i=1}^{p} C_i\ \alpha_i\ \sigma_i^N} \tag{B.39}$$

Rackwitz and Fiessler (1978) pointed out that this normal transformation of non-normal variables is exact within the accuracy of the first-order theory under consideration. Furthermore, Yen et al. (1986) and Cheng (1982) compared the AFOSM using transformed normal variables and risk taken as the lower bound of Eq. B.32 with exact solutions for a number of simple examples. They found the AFOSM method yields risk values very close to the exact values even for low risk cases (i.e., $R_s < 0.001$). Ang and Tang (1984, p. 383) noted that AFOSM method risk estimates have been found to be quite accurate for a variety of problems with nonlinear performance functions which are typical of those found in practical engineering problems. Therefore, estimating risk as the lower bound in Eq. B.31 appears to be fairly exact within the accuracy of the first-order approximation for systems with convex failure surfaces where all the basic variables are either normally distributed or transformed normal.

B.6.3 Applications of AFOSM Method to Hydraulic Engineering Problems

The AFOSM method has been used quite successfully in assessing the risk for several types of hydraulic structures. Kooman et al. (1978) and Vrijling (1982) used the AFOSM method to check the reliability of the components of the Oosterschelde storm surge barrier in The Netherlands, including the main sections of the concrete components, the steel gate, the sill, and the foundation. Mol et al. (1983) used the AFOSM method for the design of rubble mound breakwaters. Melching and Yen (1986) used the AFOSM method to analyze the effects of construction errors (as they affect the design slope) on storm sewer reliability. Melching et al. (1986) demonstrated the potential usefulness of the AFOSM method for hydrologic problems by studying the uncertainties in a rainfall-runoff flood frequency model and comparing the AFOSM results with the analytical results obtained by Wood (1976). Cheng (1982) used the AFOSM method to evaluate dam overtopping risk. Cheng (1982) also compared the various risk evaluation methods for a simple example. He concluded considering accuracy, consistency, and computational cost, the AFOSM method with the GRG optimization technique is highly recommended for dam safety evaluation or for any other system where risk levels less than 10^{-3} are important.

B.6.4 AFOSM Method Summary

Considering the successful uses of the AFOSM method for hydraulic structure uncertainty evaluation and the general characteristics of this method, the AFOSM method is probably the reliability analysis method best suited to engineering system design problems due to its relative simplicity, accuracy, and robustness. This sentiment is echoed by researchers in structural engineering who have strongly supported the use of the AFOSM method as a scientific base for structural safety codes, e.g., Rackwitz (1976) and CIRIA (1977). Given the strong support the AFOSM method receives for design problems, it will undoubtedly be of use for real-time flood forecast uncertainty analysis. The primary strength of the AFOSM method for flood forecasting problems is its robustness which allows it to work with many different model formulations of the rainfall-runoff process.

It should be noted that the presentation of the AFOSM method given here assumes that the basic variables are uncorrelated. Methods exist for dealing with correlation of the basic variables of the AFOSM method (e.g., see Ang and Tang, 1984), but from a practical simplicity viewpoint, it would be best if these could be avoided. Garen and Burges (1981) found that their Monte Carlo simulation results considering parameter correlation differed insignificantly from the results ignoring the correlation. Hence, the assumption that small correlations between basic variables do not significantly affect the AFOSM risk estimates may be justified. In this study, for the example hydrologic models, only a few of the basic variable interrelations have correlations significantly different from zero, and it is reasonable to assume that the nonzero correlations would have small effects on the risk estimates (see Appendix C).

APPENDIX C. EXAMPLE WATERSHED FOR CASE APPLICATION

C.1 Introduction

In this study, two well-known and well-tested rainfall-runoff simulation models are adapted for real-time flood forecasting on a flood prone Illinois watershed. This watershed, its flood history, and the data available to fit hydrologic models to it are described in this appendix. Brief descriptions are given of the two hydrologic models utilized. The calibration results for each model are presented. The use of these results to establish real-time flood forecasting schemes is discussed. Also, the use of the calibration results to determine the model parameter and model structure uncertainty measures necessary for incorporation of reliability analysis into the real-time flood forecasting schemes is described.

C.2 Example Watershed

C.2.1 Watershed Selection Criteria

To adequately meet the objectives of this study, the chosen example watershed must satisfy the following requirements:

1. It has a history of causing significant flood damages at a city near its outlet such that a flood warning and preparedness system would be beneficial, and

2. It is of medium size (say 100-700 square miles) so that rainfall-runoff modeling is a necessary and efficient tool for flood warning. If the watershed is large, flood forecasts may be efficiently achieved using stream routing techniques alone without rainfall-runoff modeling; or if the watershed is small, forecast lead times may not be sufficient for the flood warning system to be effective.

Furthermore, for this study it was decided to demonstrate the incorporation of reliability analysis with rainfall-runoff models for the calibrated model case only. Therefore, sufficient rainfall and runoff data must be available to properly identify the "best estimates" of the model parameters and the corresponding parameter and model structure uncertainties. Data must also be available to verify the real-time flood forecasting schemes developed.

The Vermilion River watershed at Pontiac, Illinois, meets the criteria given above. In the following sections, a general description of its physical properties, flood history, and data inventory are given.

C.2.2 Watershed Description

The Vermilion River watershed at Pontiac comprises 579 square miles in east central Illinois, primarily in Livingston and Ford counties. Figure C.1 displays the Vermilion River watershed and its soil types.

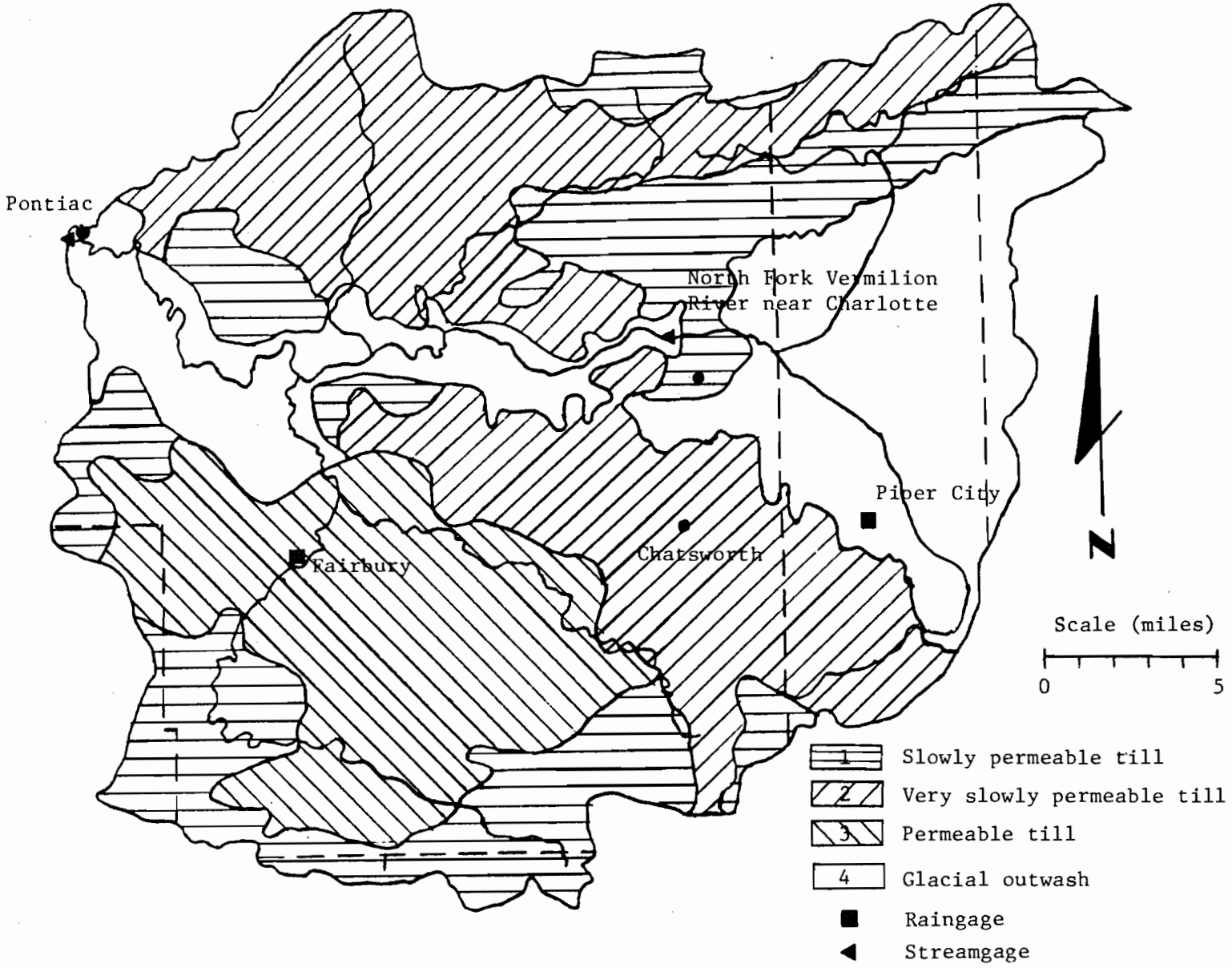

Figure C.1. Soil types for the Vermilion River watershed upstream of Pontiac

The Vermilion River watershed outline is formed from morainal ridges left behind by glacial action occurring during the Wisconsin Period, beginning about 15,000 to 20,000 years ago. With the exception of these morainal ridges, the watershed is a nearly level plain which ranges in elevation from 600 to 650 ft, while the ridges range in elevation from 750 to 780 ft. Consequently, the slope of the Vermilion River is quite mild, 0.064 percent (3.36 ft/mile) over the 50.75 mile length of the Vermilion River and its North Fork, and ranging from 0.136 percent (7.20 ft/mile) in the upland 21.11 mile reach of the North Fork above Charlotte to 0.012 percent (0.63 ft/mile) for the 29.64 mile reach from Charlotte to Pontiac. The tributary streams and overland flow paths have similarly mild slopes ranging from 0.017-0.229 percent (0.9-12.1 ft/mile) for the streams and 0.03-0.65 percent (1.6-34.3 ft/mile) for overland flow.

The Vermilion River watershed consists of extremely rich agricultural soils and hence the land use in the basin is dominated by cropland. Zebrun (1969) reported the land use in Livingston county, which includes the majority of the basin, to be 86 percent cropland, 5 percent pasture, 2 percent woodland, and 3 percent other uses. Visual inspection and comparison to earlier USGS maps of the watershed reveals the land use remains approximately the same in the 1980s. Agricultural drainage systems play a major role in the rainfall-runoff process for this watershed as expected given the mild slope of the land, the low permeability of the soils (described in the following section), and the watershed land use. The most significant impact of agricultural drainage on the watershed rainfall-runoff process occurred in 1954. The Vermilion River Outlet Drainage District initiated a major channelization project involving the Vermilion River, its North Fork, and North Fork tributaries. This project was completed in the summer of 1955 and resulted in changing the natural 35 ft wide North Fork channel to a trapezoidal channel 100 ft in width and the natural 75 ft wide Vermilion River channel to a trapezoidal channel 166 ft in width. Each channel was also deepened 1 to 6 ft (U.S. Army Corps of Engineers, 1986). This channelization greatly altered the Charlotte to Pontiac average flood wave travel time from 24.9 hours prior to 1955 to 17.6 hours after 1955.

The Vermilion River Outlet Drainage District dredged the channel system again in 1982 to restore it to its 1955 dimensions. Cross sections prepared for the 1982 channel dredging indicated only a moderate amount of sediment removal was necessary (U.S. Army Corps of Engineers, 1986). Therefore, it is reasonable to assume that since the completion of the 1955 channelization the watershed's physical characteristics have remained nearly constant and are likely to remain so for the next 20 to 30 years.

C.2.3 Watershed Soil Conditions

The soils in the Vermilion River watershed upstream of Pontiac are predominantly silt loams, silty clay loams, and clay loams which are nearly level to moderately sloping with very slow to moderate permeabilities. Figure C.1, compiled from Wascher et al. (1949) and Smith et al. (1933), displays the major soil groups in the basin and their location. Table C.1 lists the soil types which dominate each of the soil groups, the percentages of Ford and Livingston county areas occupied by each of these soil types, and the saturated hydraulic conductivity (permeability) and available water

Table C.1. Vermilion River Watershed Major Soil Types and Their Characteristics

Soil Group	Soil Type and Number	Percent of Livingston County	Percent of Ford County	K_H Top Layer (in./hr)	K_H Deep Layers (in./hr)	Available Water Capacity Top Layer (in./in.)	Available Water Capacity Deep Layers (in./in.)
1	(146) Elliott Silt Loam	11.79	37.68	0.6-2.0	0.2-0.6	0.21-0.24	0.14-0.20
1	(232) Ashkum Silty Clay Loam	20.56	---	0.2-0.6	0.2-0.6	0.12-0.23	0.18-0.20
2	(91) Swygert Silty Clay Loam	9.95	---	0.2-0.6	0.06-2.0	0.21-0.23	0.10-0.19
2	(147) Clarence Silt Loam	3.57	17.28	0.2-0.6	>0.63	0.21-0.23	0.08-0.10
2	(235) Bryce Silt Clay	17.33	---	0.2-0.6	0.06-0.2	0.12-0.23	0.09-0.13
3	(145) Saybrook Silt Loam	3.05	3.13	0.6-2.0	0.2-2.0	0.22-0.24	0.17-0.19
3&4	(152) Drummer Clay Loam	16.02	28.17	0.6-2.0	0.6-2.0	0.21-0.23	0.19-0.21
4	(149) Brenton Silt Loam	3.50	3.21	0.63-2.0	0.63-2.0	0.20-0.25	0.16-0.18
4	(153) Pella Clay Loam	---	1.14	0.63-2.0	0.63-2.0	0.20-0.25	0.14-0.18
4	(156) Ridgeville Sandy Loam	0.26	1.69	0.6-2.0	0.6-2.0	0.16-0.18	0.16-0.18

capacity* for both the top layer and deep (underlying) layers for each of these soils as given by USDA Soil Surveys. A brief description of each of the soil types listed in Table C.1 is given below (based on Wascher et al., 1949, and Smith et al., 1933).

Ashkum series soils are poorly drained, nearly level to very gently sloping, dark brown to black silty clay loams with moderately slow permeability and high to very high available water capacity. Surface drainage is slow to ponded, hence, for agricultural use measures should be taken that will drain the surplus water off promptly. Tile draw is not as free as in many other soils. Thus, the tile should be laid fairly close together and as shallow as is safe, open ditches or furrows may be used to advantage to supplement the tile in places where the lay of land permits.

Brenton series soils are somewhat poorly drained, nearly level to very gently sloping, brown to dark brown silt loams with moderate permeability and high available water capacity. Surface drainage is moderate to slow. The soil profile is permeable to water throughout, and tile draw satisfactorily.

Bryce series soils are poorly drained, nearly level to very gently sloping, very dark colored silty clays with slow permeability and high available water capacity. Surface drainage is slow to ponded. Hence, underdrainage is quite important for agricultural use of this soil. Tile are only moderately effective because water moves so slowly through the subsoil and underlying glacial till. If a tiling system is installed, surface inlets might well supplement underdrainage with surface drainage.

Clarence series soils are somewhat poorly drained, very gently sloping to gently sloping, brown to grayish brown silt loams with very slow permeability and moderate available water capacity. Surface drainage is moderate to rapid. Due to poor underdrainage, tile are not effective in this soil and ponded areas should be surface drained.

Drummer series soils are poorly drained, nearly level black clay loams with moderate permeability and very high available water capacity. Surface drainage is slow to ponded. Tile draw adequately in this soil, however, without proper crop management, the good underdrainage can be adversely affected.

Elliott series soils are somewhat poorly drained, nearly level to gently sloping, dark colored silt loams with moderately slow permeability and high available water capacity. Surface drainage is medium. Tile draw well with no serious problems reported.

Pella series soils are poorly drained, nearly level to level, black clay loams with moderate permeability and very high available water capacity. Surface drainage is slow to ponded. Tile draw readily, but

---

*Available water capacity is the capacity of the soil to hold water that can be used by plants, which is defined as water held between the wilting point (15 atmospheres of tension) and the field capacity (1/3 atmosphere).

because of lack of adequate slope they require very careful leveling when installed.

Ridgeville series soils are somewhat poorly drained, nearly level to gently sloping, brown to dark brown sandy loams with moderate to moderately rapid permeability and moderate to high available water capacity. Surface drainage is slow. Tile drainage may be necessary in a few areas to take care of low wet spots.

Saybrook series soils are moderately well to well drained, very gently sloping to gently sloping, dark colored silt loams with moderate permeability and high available water capacity. Surface drainage is medium. Because this soil is moderately well to well drained, tile are not generally necessary.

Swygert series soils are somewhat poorly drained, nearly level to sloping, brown to dark-brown silt loams with slow permeability and moderate available water capacity. Surface drainage is slow to rapid. Underdrainage for this soil is very slow, hence, tile should be installed to aid this drainage.

The Vermilion River watershed upstream of Pontiac is a highly productive agricultural area. In order to maintain this high productivity, farmers in the basin have generally followed the drainage guidelines for each soil described above. Hence, the basin is dominated by a complex tile and surface drainage (i.e., drainage ditch) network which greatly influences the hydrologic response of the watershed. Consideration of the effects of this drainage network may be necessary when modeling the basin.

C.2.4 Flood History and Flood Stage

The city of Pontiac has a population of 11,227 (1980 census) and it has suffered five significant flood events in the last 30 years. The U.S. Army Corps of Engineers (1984) documented these events, and Table C.2 presents a summary of their findings. It should be noted that the dates given in Table C.2 correspond to the day the flood peak reached Pontiac, while for subsequent tables listing the calibration and verification events, the date corresponds to the beginning of the rainfall event. Furthermore, Fig. C.2 displays the flood inundation pattern over the city of Pontiac as estimated by the U.S. Army Corps of Engineers (1984) using the HEC-2 flood routing package. The extent of the flood severity in Pontiac is well displayed by this figure.

The definition of the flood stage at Pontiac varies considerably. The Flood Insurance Study (Federal Insurance Administration, 1979) and the U.S. Army Corps of Engineers River Basin Study (1986) report the bankfull stage to be 12.5 ft with a corresponding discharge of 5800 cfs. U.S. Army Corps of Engineers Section 205 Report (1984) indicates the flood stage at Pontiac starts at 14 ft (6800 cfs) which agrees with the NWS flood stage commonly listed in the Weather Section the Chicago Tribune. The 205 Report also notes that the channel will pass flows of approximately 8000 cfs at bankfull stage, which makes the bankfull stage approximately 15.4 ft.

Table C.2. Significant Flood Events at Pontiac and Their Effects

Date	Stage (ft)	Discharge (cfs)	Damages
July 10, 1951	17.90	11000	500 homes were damaged and 150 persons evacuated. Approximately three-fourths of Pontiac residents had water in their homes, basements, or front yards. Gas and electric services were disconnected from 1400 homes. Persons were advised to boil water because there were 15 in. of water in the water treatment plant. Hospital services were affected.
April 28, 1957	17.20	9970	No details available.
May 14, 1970	17.46	10300	No details available.
June 3, 1980	18.12	11300	250 homes affected.
December 4, 1982	19.16	13100	Livingston County declared a Federal disaster area by President Reagan on December 15, 1982. 689 homes, 10 businesses, and 1 public facility were affected with 125 of these reporting structural damage. 350 persons were evacuated and gas was disconnected for many residences. Total cost of flood damages estimated to be $2,300,000.

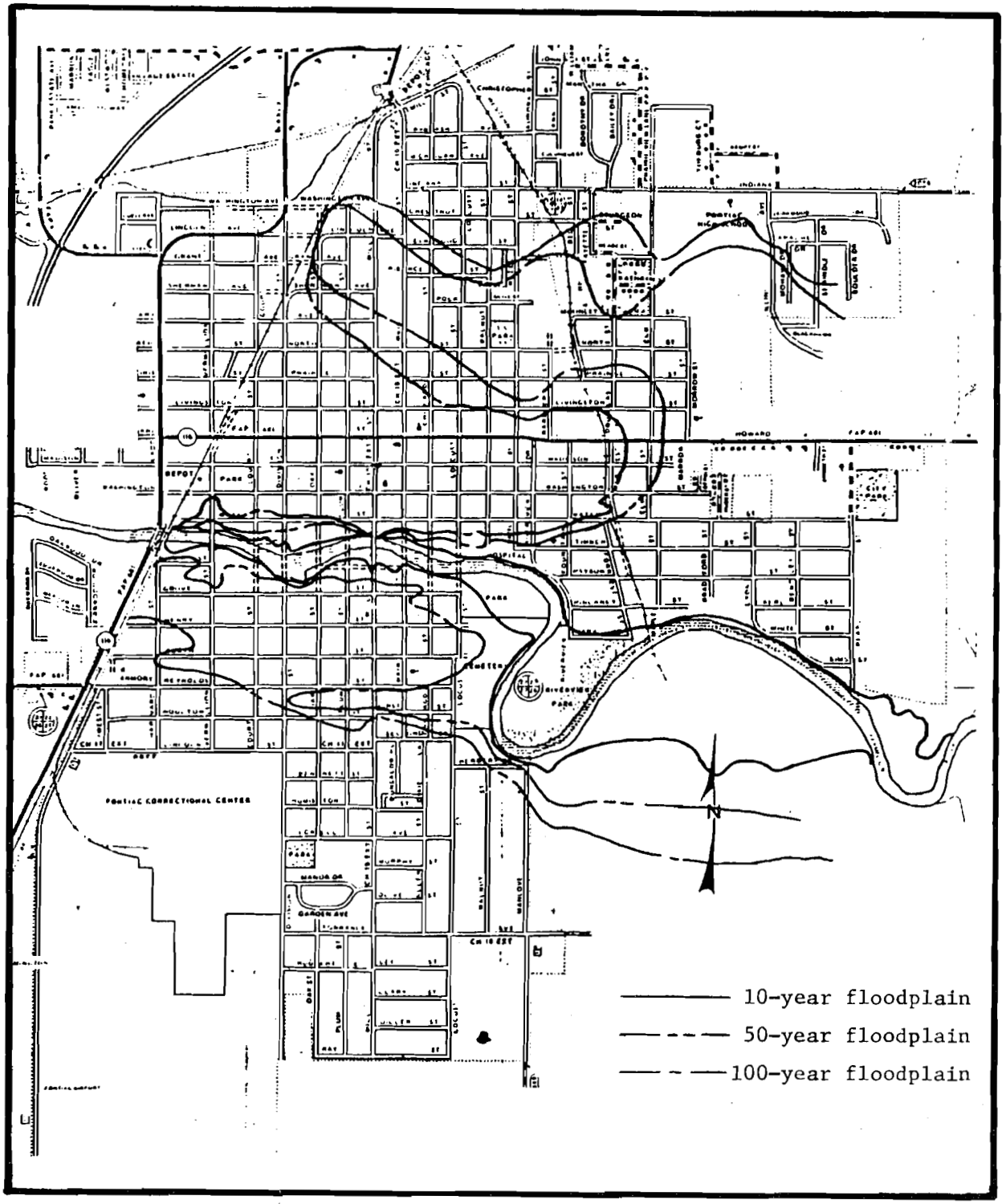

Figure C.2. Flood inundation patern over the city of Pontiac, Illinois (after U.S. Army Corps of Engineers, 1984)

In order to clear up this confusion regarding flood stage, David L. Sullivan, Superintendent of the Pontiac Wastewater Treatment Plant, was consulted. According to Mr. Sullivan (1986), the current flood warning procedure and significant flood stages at Pontiac are as follows:

1. When the river stage reaches 90 in. above the water supply dam just upstream from Mill Street, the fire department monitors the stage at two-hour intervals.

2. When the river stage reaches 100 in. above the dam, street flooding begins.

3. When the river stage reaches 105 in. above the dam, the evacuation center in Pontiac is opened.

4. When the river stage reaches 120-130 in. above the dam, damaging flooding occurs.

The U.S. Army Corps of Engineers (1984) performed a detailed flood routing of the Vermilion River through Pontiac using HEC-2, and Harza Engineering performed the same task using WSP-2 for the Flood Insurance Study (Federal Insurance Administration, 1979). Using their published flood profiles, the stages above the dam can be translated to gage heights at Vermilion Street and then to the corresponding significant flood discharges via the rating table. Table C.3 shows the significant flood stages above the dam and their corresponding gage heights and discharges.

Table C.3. Significant Flood Stages and Their Corresponding Gage Heights and Discharges

Stage Above Dam (in.)	Gage Height (ft)	Discharge (cfs)
90	14.55	7270
105	15.80	8460
120	17.00	9700
130	17.85*	10880

*Note: Harza's analysis using WSP-2 yielded 18.05 ft while the U.S. Army Corps of Engineers' analysis using HEC-2 yielded 17.85 ft. Since the July 10, 1951 flood had a crest of 17.90 ft and led to considerable damage, the lower value was chosen even though the channel is significantly different now.

A comparison of the flood levels given in Table C.3 and the flood history given in Table C.2 validates the flood stage guidelines presented by Mr. Sullivan. Therefore, in this study the flood level of interest was chosen to correspond to the worst flooding level, stage equal to 17.85 ft (discharge 10880 cfs).

C.2.5 Hydrometric Data Available

C.2.5.1 Rainfall Data

Three rainfall gages, one daily gage and two hourly recording gages, are currently in operation on the Vermilion River at Pontiac watershed. NWS hourly gage 11292300 was established at the Fairbury water works on July 1, 1948. NWS hourly gage 11681900 was established in Piper City on February 1, 1949. The locations of these rain gages are shown in Fig. C.1, and they are used to define the temporal and areal rainfall distribution over the watershed for the real-time flood forecasting schemes. NWS daily precipitation gage 116910 was established in Pontiac on January 1, 1903. Before July 1952, it was read once daily at 6 p.m. and since that time it has been read once daily at 7 a.m. The daily values from this gage have been used to check the consistency of the daily totals at Piper City and Fairbury for the calibration and verification events. In general, the agreement between the daily totals at the three gages is quite good. The Pontiac gage record also contains snowfall data which was used to detect snowmelt influenced events and to remove them from the list of possible calibration or verification events.

At the start of this research, data from each of these gages had only been processed up to 1983. Thus, the records from each of these gages were obtained from their beginnings to 1983.

C.2.5.2 Streamflow Data

A wire weight gage was placed on the Vermilion Street Bridge in Pontiac on September 24, 1942, and continuous records have been maintained from October 1, 1942 to date. On November 8, 1965, a digital water stage recorder was installed. Prior to this time, the gage was read twice daily providing daily average flows and flood peaks. From November 8, 1965 to February 4, 1974, bi-hourly streamflows are available, and hourly streamflows from February 5, 1974 to date. This streamflow data availability makes selection of the calibration and verification data sets quite easy. From November 8, 1965 to the present, complete hydrograph information is available for model calibration, hence, this period provides the calibration data set. The flood peaks in the data from 1955 (after channelization) to 1965 provide an adequate verification data set given that flood peaks are of prime importance for FWP systems.

On the North Fork of the Vermilion River near Charlotte at Foreman Highway Bridge (see Fig. C.1) a temporary wire weight gage was installed on October 1, 1942 and this was replaced on January 14, 1943 by a water stage recorder. On October 1, 1962, the gate was converted to crest gage. For this gage's period of record, continuous strip charts of stage are available.

C.2.5.3 Evapotranspiration Data

The closest daily evaporation pan to the Vermilion River watershed at Pontiac is located in Urbana approximately 50 miles south of the center of

the watershed. However, John L. Vogel (1986), Head of the Climate Information Unit of the Illinois State Water Survey, recommends against using the Urbana data due to some inconsistencies in the record in the 1970s. Also, the pan operates from mid-March or early April to October; hence, for many Spring events, insufficient evaporation data would be available for proper soil moisture accounting. Vogel (1986) recommended instead the use of Hamon's (1960 and 1961) simple equation for estimating potential evapotranspiration, which Jones (1966) found to give reasonable results for Illinois.

Hamon's equation requires only the mean daily temperature to estimate the potential evapotranspiration. Daily minimum and maximum temperature data are available at Pontiac from January 1, 1903 to date.

C.3 Rainfall-Runoff Models

The U.S. Army Corps of Engineers (1985) HEC-1, Flood Hydrograph Package, and the Australian RORB, Runoff Routing Program (Laurenson and Mein, 1985), were chosen as example models to demonstrate the utility and feasibility of employing reliability analysis to consider the uncertainties in real-time flood forecasting. It should be remembered that the reliability analysis approach is not limited to these particular models. These models were chosen because each has been well-tested for a variety of hydrologic modeling uses, including real-time flood forecasting, under many different conditions around the world. Furthermore, HEC-1 has become one of the most commonly used rainfall-runoff simulation models in the United States; while in Australia, RORB is used by all water authorities and all consultants working in the water business (Laurenson, 1986). Brief descriptions of each of these models are given below.

C.3.1 HEC-1 Flood Hydrograph Package

The HEC-1, Flood Hydrograph Package, computer program was originally developed in 1967. Since that time, it has been extensively tested and used with satisfactory results for a wide range of watersheds across the United States and the world. Also since 1967, the program has frequently been revised, updated, and/or appended. In the current version of the program (U.S. Army Corps of Engineers, 1985), the computational capabilities of the dam-break (HEC-1DB), project optimization (HEC-1GS), and kinematic wave (HEC-1KW) special versions of HEC-1 have been combined with standard hydrologic and hydraulic computation portion of HEC-1. A microcomputer version (PC version) developed in 1984 is also available. The PC version contains all the hydrologic and hydraulic computation capabilities of the mainframe HEC-1; however, the flood damage and ogee spillway capabilities were omitted due to PC memory and compiler limitations.

For this study, only the hydrograph simulation portion of HEC-1 is used. Within the hydrograph simulation portion of HEC-1, there are several options for calculating abstractions, converting rainfall excess to the runoff hydrograph, and routing streamflow. The options used in this study are described below.

For the calibration data set (1965-1983), runoff data is only available at Pontiac (the watershed outlet). Therefore, the watershed was modeled as a lumped system. Thus, no streamflow routing will be required, and rainfall, abstractions, and hence, rainfall excess are viewed as spatially uniform over the watershed. The areal average rainfall is estimated by applying the Thiessen weights 0.543 and 0.457 to the rain gages at Fairbury and Piper City, respectively.

Abstractions were modeled via the initial loss-continuing loss rate option in HEC-1. This simple approach was chosen over the more sophisticated exponential loss rate function, SCS curve number, and Holtan loss rate options for several reasons. Ford et al. (1980) pointed out that if the temporal and spatial distribution of precipitation is not well defined (as is the case for the Vermilion River watershed), an initial loss, followed by a uniform loss rate may be most appropriate. Furthermore, the above fact has led the initial loss-continuing loss rate option to become the most commonly used abstraction option for typical hydrologic analyses employing HEC-1. Finally, RORB also utilizes an initial loss-continuing loss approach, which facilitates a comparison of model results.

The Clark unit hydrograph option was chosen to convert the rainfall excess hyetograph to the runoff hydrograph. This option was chosen because it has been the basis of HEC-1 runoff generation since the model's development, and as such it has been well tested.

The Clark method (1945) is based on the principle that the runoff time distribution is defined by a time-area curve, which characterizes the cumulative area of the watershed contributing runoff to the watershed outlet as a function of time. HEC-1 contains a dimensionless time-area curve based on a generalized watershed shape. This curve was utilized, and it is given as

$$AI = 1.414\ T^{1.5} \qquad \text{for } 0 \leq T \leq 0.5 \qquad \text{(C.1.a)}$$

$$1 - AI = 1.414(1 - T)^{1.5} \qquad \text{for } 0.5 < T < 1 \qquad \text{(C.1.b)}$$

where AI = the cumulative area contributing runoff as a function of total watershed area, and

T = the fraction of the watershed time of concentration (TC, a model parameter).

Ford et al. (1980) noted that experience by the HEC has indicated the use of a detailed time-area relationship is usually not warranted and that the time-area curve contained in HEC-1 is satisfactory in most instances. The high quality calibration results obtained in this case study (see section C.4) support Ford et al.'s argument.

The ordinates of the time-area curve are converted to volume of runoff per second for unit rainfall excess and interpolated to the given time interval for the translation hydrograph. To simulate the watershed storage

effects, the translation hydrograph is routed through the linear reservoir:

$$Q(2) = CA * I + CB * Q(1) \qquad (C.2)$$

where $CA = \Delta t/(S_R + 0.5 * \Delta t)$,

$CB = 1 - CA$,

$Q(2)$ = the instantaneous flow at the end of the period,

$Q(1)$ = the instantaneous flow at the beginning of the period,

I = the ordinate of the translation hydrograph,

Δt = the computation time interval in hours (two hours was chosen corresponding with finest runoff time interval available throughout the calibration data set), and

S_R = the watershed storage factor in hours (a model parameter).

The resulting unit hydrograph for instantaneous rainfall excess is then averaged to produce the hydrograph for unit rainfall excess occurring in the given time interval.

In this study, only the direct runoff hydrograph is modeled, and hence, the baseflow routines in HEC-1 were not used. Therefore, the direct runoff hydrograph is a function of four parameters: the initial loss in inches, IL; the continuing loss rate in inches per hour, CL; the watershed time of concentration in hours, TC; and the watershed storage factor in hours, S_R. Rough estimates of each of these parameters may be obtained by considering the physical conditions of the watershed, but the best way to determine the proper parameter values is by calibrating the model to observed rainfall-runoff data. Details of the calibration procedure are given in section C.4.

C.3.2 RORB Runoff Routing Program

The RORB model has been under development at Monash University in Australia since the early 1970s. Mein et al. (1974) first described the general principles behind RORB, and since that time it has been further refined and tested extensively in Australia.

In RORB, the watershed is divided into subcatchments that are based on the major tributaries with drainage areas of the same order of magnitude. Nodes are drawn on the map of the watershed so that there is a node on the main stream in each subcatchment at the point nearest its centroid, at each confluence where subcatchment flows combine, and at each gaging station. Figure C.3 shows how the Vermilion River watershed is divided into 21 subcatchments and their respective nodes, while Fig. C.4 shows a schematic diagram of the stream network and nodes.

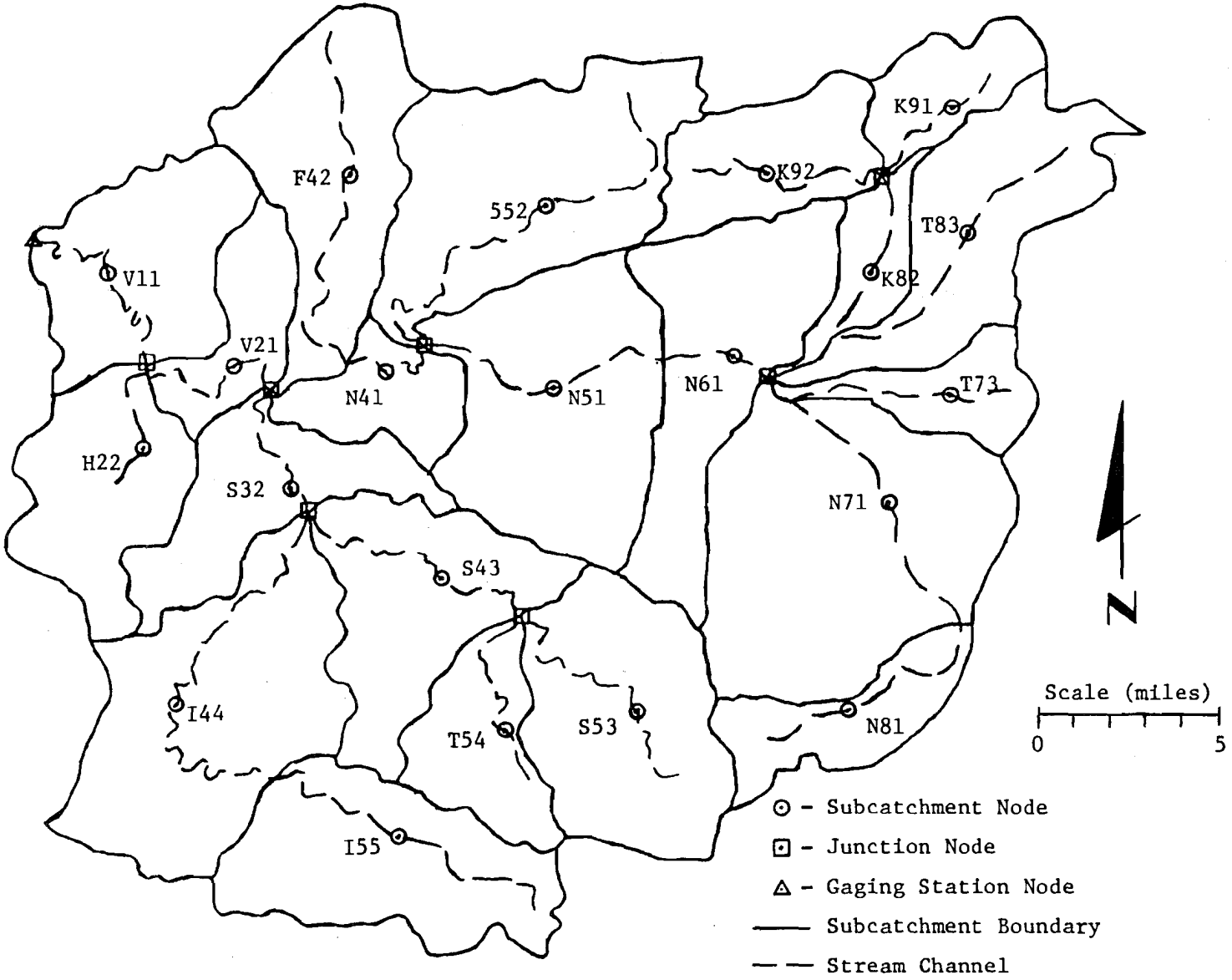

Figure C.3. Vermilion River watershed subdivided for RORB

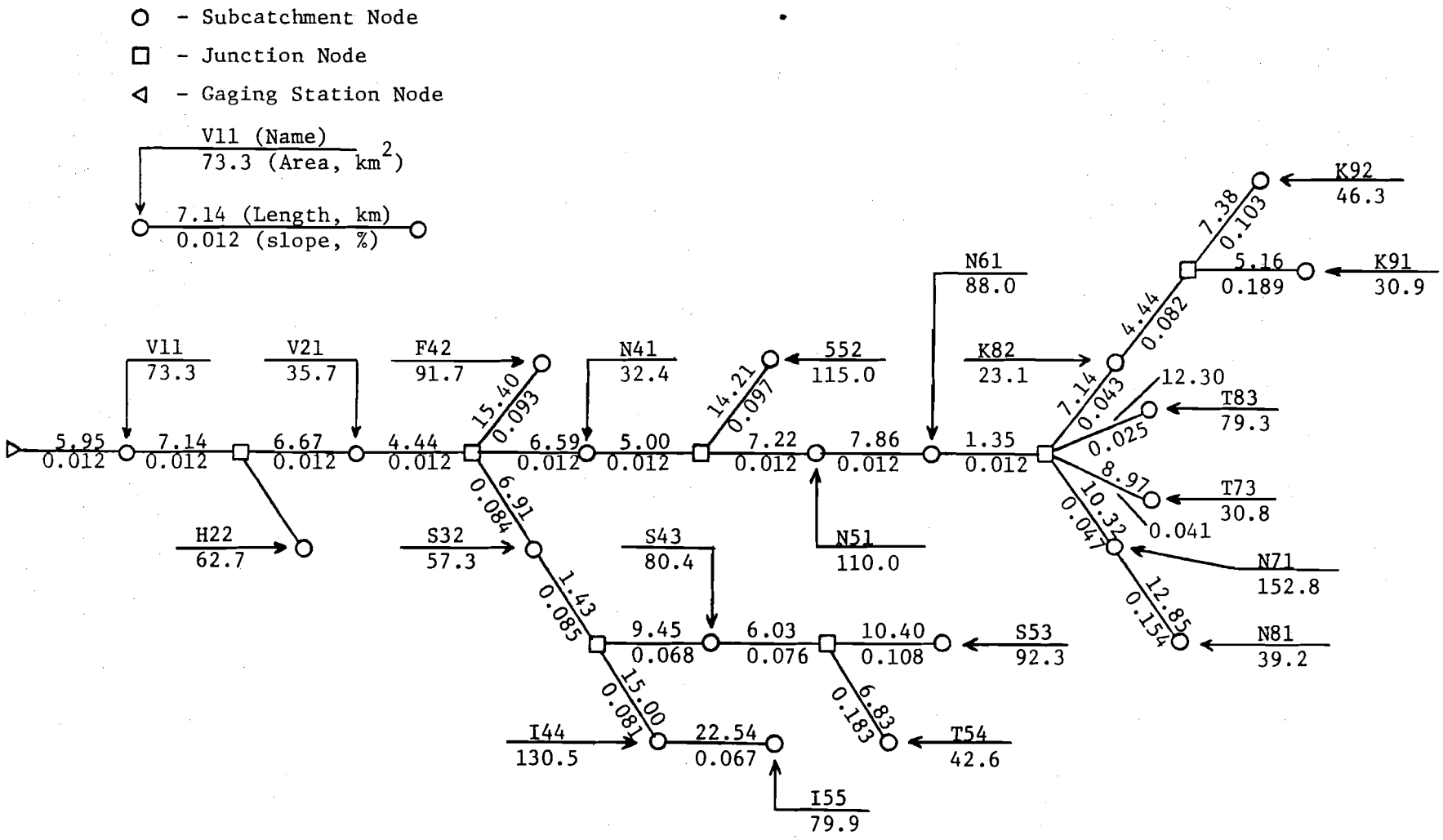

Figure C.4. Schematic diagram of Vermilion River channel network for RORB modeling

The rainfall input to each subcatchment is determined by two factors. Each subcatchment is assigned to the rain gage which best represents it. The rainfall depth for each subwatershed is determined from an isohyetal map and this depth is distributed in time proportionally as for the representative rain gage. For this study, however, the data needed to define such an isohyetal map is not available, and hence, both the depth and temporal distribution at the representative rain gage is input to the subcatchment. The rainfall excess is determined via an initial loss-continuing loss rate scheme similar to that used by HEC-1. The initial loss, ILR, and continuing loss rate, CLR, are uniform for each subcatchment upstream from a single stream gage. Therefore, RORB is a "quasi-distributed" model which allows for varying areal and temporal input but then operates on this input uniformly over the watershed. For this study, only one stream gage is available, therefore, ILR and CLR are uniform over the entire watershed.

Each of the subcatchments is modeled as a single point in space represented by the node. At this point (node), the rainfall excess for the subcatchment enters the stream network. The rainfall excess and streamflow are then routed from node to node through the stream network using the continuity equation:

$$\frac{I_t + I_{t+1}}{2} - \frac{Q_t + Q_{t+1}}{2} = \frac{S_{t+1} - S_t}{\Delta t} \qquad (C.3)$$

where I_t = inflow to the channel reach between nodes at time t,

Q_t = outflow from the channel reach at time t,

S_t = storage in the channel reach at time t, and

Δt = the time step.

The relationship between reach storage and outflow is described by a nonlinear reservoir of the form

$$S_t = K\, Q^m \qquad (C.4)$$

where K = a parameter related to the travel time in the reach, and

m = the nonlinearity exponent.

Based on Manning's equation, Mein et al. (1974) estimated the theoretical values of m for several common channel shapes including wide rectangular channels (m=0.60), triangular channels (m=0.75), wide parabolic channels (m=0.69), and trapezoidal channels (m=0.74). Laurenson and Mein (1985) reported that the typical value of m for catchment studies ranges between 0.6 and 1.0 with a value of 0.8 recommended as a first trial value for "fit runs." Considering the fact that the majority of the stream

reaches in the Vermilion River watershed are trapezoidal or approximately wide rectangular channels, one might suspect lower values of m to be appropriate. However, the appropriate m value is best determined by calibration.

The parameter K is considered to consist of two parts, such that

$$K = C_l \, k_l \qquad (C.5)$$

where k_l = a parameter determined from physical characteristics of the stream channel between adjacent nodes and intended to be proportional to the delay time of a given reach storage, and

C_l = a constant for a watershed determined by calibration of the model to observed rainfall-runoff data.

For the simple case of a wide rectangular channel, k_l is a function of the reach width, roughness, length (L), and bed slope (S_c). Laurenson and Mein (1985) report that use of the reach length alone to represent k_l has proved adequate for many watersheds. However, they also note that $k_l = L/S_c^{1/2}$ may be desirable for cases involving extreme slope variations and including very low slopes, say less than 0.05 percent. Therefore, k_l is taken as $L/S_c^{1/2}$.

In this study, the direct runoff hydrograph is a function of four parameters: the initial loss in mm, ILR; the continuing loss rate in mm per hour, CLR; the nonlinearity exponent, m; and the watershed delay time factor, C_l. Each of these parameters is best determined by calibrating the model to observed rainfall-runoff data as described in section C.4.

C.4 Calibration Procedure

C.4.1 Objective Function

The choice of the calibration objective function depends greatly on the proposed use for the model. In this study, the models are to be used for real-time flood forecasting within a flood warning and preparedness system. Hence, accurately predicting the magnitude and, to a lesser extent, the timing of the peak discharge is the goal of modeling. Therefore, an objective function which emphasizes the hydrograph peak is appropriate.

An automatic calibration scheme is built into HEC-1. This scheme minimizes a weighted sum of the squared deviations between the measured, Q_{m_i}, and predicted Q_{c_i}, flows

$$\text{Min} \left[\sum_{i=1}^{n} (Q_{m_i} - Q_{c_i})^2 * WT_i / n \right]^{1/2} \qquad (C.6)$$

where n is the total number of hydrograph ordinates and the weights, WT_i, emphasize the peak flows:

$$WT_i = (Q_{m_i} + \bar{Q}_m) / (2 * \bar{Q}_m) \qquad (C.7)$$

where $\bar{Q}_m$ = the average measured discharge.

This objective function was chosen for use in this study because while it places emphasis on the peak discharge, it also considers matching the entire hydrograph. Hence, the parameters obtained are likely to be quite representative of the general rainfall-runoff process of the watershed system.

C.4.2 HEC-1 Calibration Methodology

As noted above, HEC-1 has a built-in calibration scheme. The constrained nonlinear optimization scheme employed by HEC-1 is a univariate search technique that uses Newton's method. Complete details on this scheme are presented by Ford et al. (1980). As for all nonlinear optimization schemes, this calibration approach cannot guarantee that a "global" optimum will be found for each of the model parameters. Nevertheless, if the "fit" quality is acceptable, the calibrated parameters are adequate, representative values for consideration of parameter uncertainty.

C.4.3 RORB Calibration Methodology

Unlike HEC-1, RORB does not have a built-in automatic calibration scheme. Instead, the "fit runs" of RORB proceed as follows. For a given value of initial loss, RORB automatically computes the continuing loss rate which matches the calculated rainfall excess and the measured runoff volume. The user then iterates on m and C_1 until a reasonable match between the measured and calculated hydrographs is obtained. Therefore, for this study, it was necessary to develop a formal calibration procedure for RORB.

Both HEC-1 and RORB are physical-conceptual models based on hydrograph principles (i.e., the time-area curve for HEC-1 and a network of cascading nonlinear reservoirs for RORB). Therefore, one might expect the "optimal" rainfall excess for both models to be similar. Thus, the optimal initial loss found for HEC-1 was also assumed to be optimal for RORB. This assumption is slightly erroneous due to the somewhat different initial losscontinuing loss schemes used by the two models. In HEC-1, the initial loss is assumed to occur only in the initial fraction of the time step with the continuing loss rate beginning only after the initial loss is satisfied as shown in Fig. C.5a. In RORB, however, both the initial loss and the continuing loss are assumed to occur over the entire time step as shown in Fig. C.5b. Also, the two models differ somewhat in the weights applied to the two rain gages.

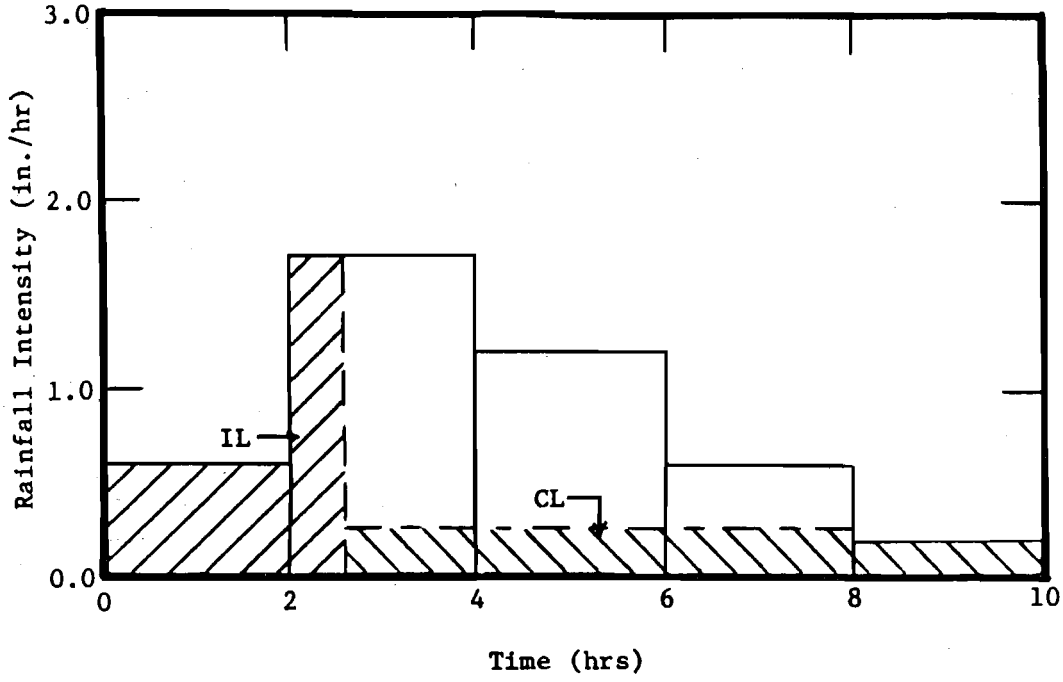

(a)

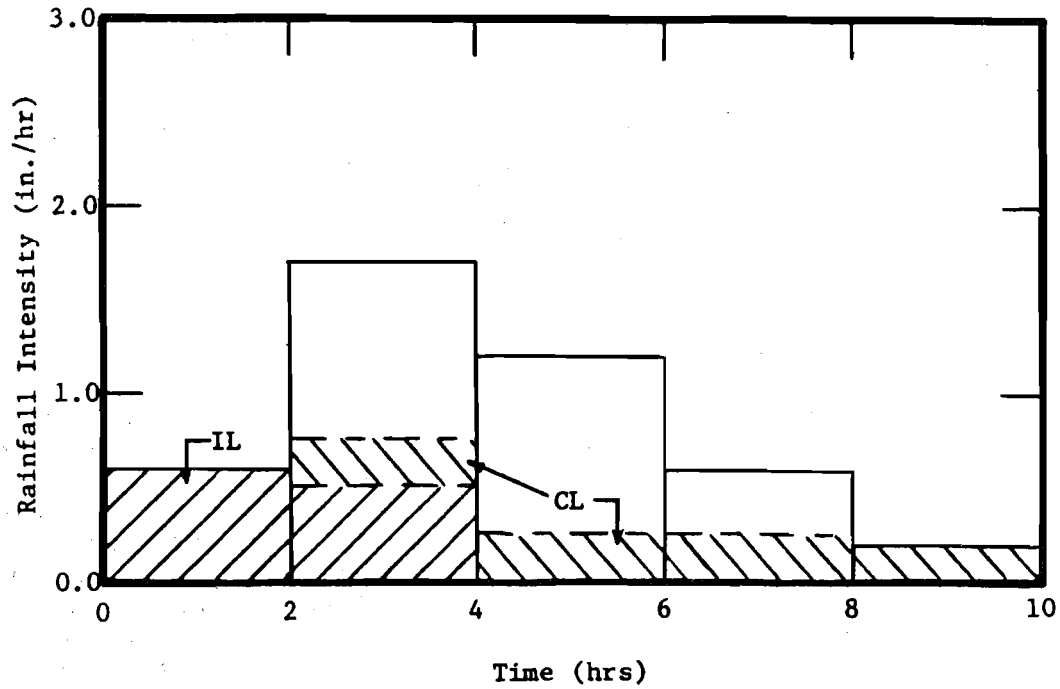

(b)

Figure C.5. Comparison of initial loss-continuing loss rate abstractions schemes for (a) HEC-1 and (b) RORB

RORB then automatically determines the optimal continuing loss rate which matches the measured and calculated runoff volumes. These will differ slightly from their HEC-1 counterparts for the reasons given above.

Laurenson and Mein (1985) noted that C_1 is the principal parameter of the model and is the main means of achieving a fit. The effects of m are sometimes useful in improving a fit, but are less important than those of C_1. Therefore, it was decided to vary the value of m in increments of 0.01 over its reasonable range for this catchment (found to be, generally, 0.83-0.96) and optimize Eq. C.6 over C_1 for each m via quadratic interpolation (Rao, 1979, p. 226). Quadratic interpolation is an efficient univariate nonlinear optimization technique wherein three values of the true objective function are used to define a quadratic function. The minimum of the quadratic function can be calculated directly. If the difference between the quadratic approximation and the true objective function is small at the quadratic minimum point, the true minimum has been reached. Otherwise, a new quadratic approximation should be established with the previous quadratic minimum and its adjacent points, and this new quadratic checked for convergence. If the three initial points are chosen properly, the method converges quite rapidly.

C.4.4 Storms for Calibration

Selection of events for calibration from November 1965 to December 1983 was based on several criteria:

1. The events must be the product of a single separable rainstorm with no snowmelt in the direct runoff,

2. Complete information from each rain gage and the stream gage must be available, or the missing data must be easily estimated (e.g., a few missing points on the rising or recession limbs of the hydrograph which may be easily interpolated),

3. The event must be of sufficient magnitude such that it is representative of the storms for which a flood warning official may wish to know the predicted peak discharge.

The third criterion given above was developed in a somewhat "ad-hoc" way. The events considered must include flood events and near flood events, which are difficult to differentiate from true flood events at the time a forecast is made. Therefore, events with a total runoff peak in excess of 6800 cfs, the discharge corresponding to the National Weather Service flood stage, should be included. However, if the set of calibrated events contained only flood or near flood events, the forecasts made based on the calibration results may be biased toward predicting such flood or near flood events. A more unbiased set of calibrated events should include other large events which lead to runoff sometimes considerably less than flood stage.

The cutoff point for these events was chosen somewhat arbitrarily to be those events whose direct runoff peaks are greater than 3000 cfs. In the USGS official yearly records for a stream gage, there is a section entitled "Extremes for Current Year" which separately lists the peak discharges

occurring during the year that exceed a prescribed target level. For the Vermilion River at Pontiac, this level is 2500 cfs. Hence, the events with direct runoff peaks in excess of 3000 cfs are significant events for this watershed. A second cutoff criterion was chosen for the volume of direct runoff. Laurenson and Mein (1985) pointed out that small events, containing less than about 10 mm (0.4 in.) of direct runoff, should be avoided in calibration data sets because they are often difficult to fit due to extreme areal variability of runoff, partial area runoff, and large differences in the time distribution of rainfall excess caused by small errors in the adopted loss model.

In summary, the calibration events must have snowmelt free direct runoff hydrographs with peak discharges in excess of 3000 cfs and volumes in excess of 0.4 in. These direct runoff hydrographs are determined as follows. For events not immediately preceded by another storm or a snowmelt period, the baseflow remains fairly constant. Therefore, the baseflow for the rising limb of the hydrograph up to the peak is assumed to be constant at this initial value. In the recession limb of the hydrograph, the slope eventually reaches a nearly constant, straight line recession (on linear graph paper with a slope of 10 to 15 cfs per two hours for this watershed). This straight line is extended backward to the inflection point on the recession limb to represent the baseflow at the end of the event. The baseflow at the peak is then connected to that at the inflection point to complete the baseflow separation. This approach is illustrated in Fig. C.6a. For cases where two runoff events must be separated, it is assumed the recession properties of the first event are essentially the same as for the second event. Thus, the recession of the first event is extended approximately parallel to that for the second event. This recession also serves as the initial baseflow for the second event. The baseflow separation for the recession limbs of each of these events is handled as described previously. The event separation and subsequent baseflow separation techniques are illustrated in Fig. C.6b.

For the period November 1965 to December 1983, 60 events had total runoff peak discharges greater than 3000 cfs after checking them versus the criteria given above, 31 events were selected for calibration (11 events were eliminated due to snowmelt effects, 10 due to missing data, 5 due to inadequate direct runoff volume, and 3 due to separation problems). It is unfortunate that two of the most serious flood producing storms -- May 12, 1970 and December 2, 1982 -- were eliminated due to missing data, but they may possibly be used for verification. The significant storm and direct runoff characteristics (including the baseflow at the beginning of the event, Q_B, the measured peak discharge, Q_p, and time to peak, t_p) for each of 31 events is given in Table C.4. The July 12, 1978 storm falls slightly under the direct runoff peak and volume requirements. Nevertheless, it was included in the calibration set because it is representative of large summer convective storms, and the set of calibrated events should include several storms of this type.

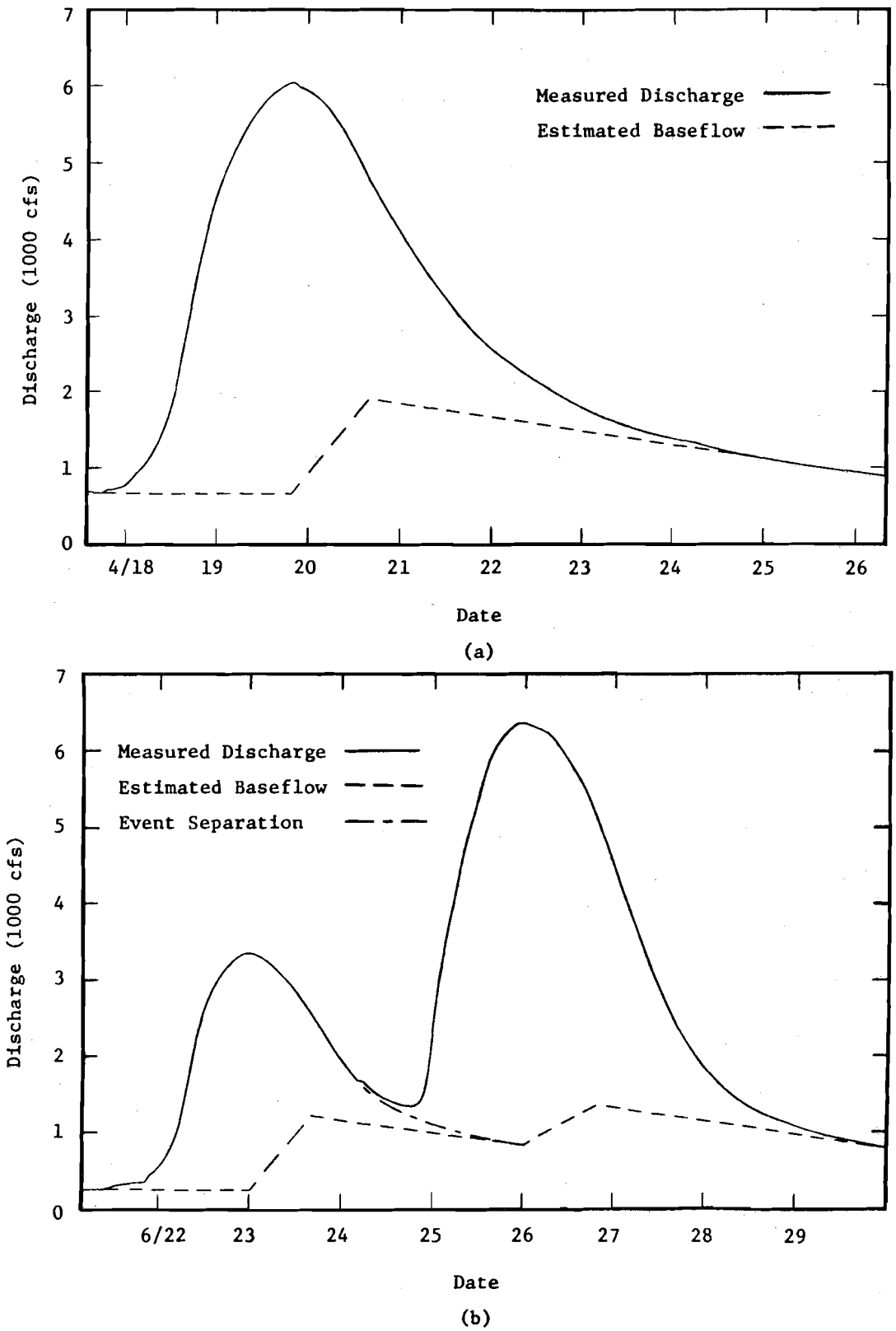

Figure C.6. Baseflow separation examples without (a: April 18, 1970) and with (b: June 21, 1981) event separation

Table C.4. Storms for Calibration

Date	Precipitation Fairbury (in.)	Precipitation Piper City (in.)	Q_B (cfs)	Q_p (cfs)	t_p (hr.)	Volume (in.)
12/24/65	3.90	3.15	43.	5068.	50.	0.727
12/11/67	1.02	0.99	2020.*	3207.	36.	0.439
2/01/68	1.60	1.99	1108.	6656.	48.	1.116
6/24/68	4.27	2.75	335.	7836.	40.	1.388
4/18/70	2.49	2.49	683.	5345.	54.	0.788
9/21/70	2.64	1.67	264.	4269.	60.	0.757
11/12/72	1.12	1.40	630.	3450.	56.	0.484
3/09/73	1.56	1.10	853.	3604.	68.	0.414
3/31/73	0.65	0.80	2060.*	3127.	50.	0.468
4/20/73	2.50	2.90	592.	6702.	68.	1.238
6/03/73	0.75	1.30	715.	3365.	64.	0.441
5/21/74	0.70	1.90	2670.*	3600.	28.	0.458
6/05/74	1.77	0.70	462.	4385.	56.	0.468
6/21/74	2.60	2.30	776.	6220.	58.	1.260
2/16/76	1.37	2.30	306.	4924.	46.	0.629
2/20/76	1.92	1.30	1500.*	4391.	40.	0.623
3/03/76	1.52	1.70	1640.*	5670.	56.	0.911
4/23/76	3.01	1.30	193.	3145.	64.	0.432
9/22/77	1.45	1.40	473.	4224.	44.	0.566
7/12/78	3.04	2.90	73.	2943.	32.	0.326
4/11/79	2.75	2.00	709.	7050.	52.	1.150
8/18/79	4.80	3.20	23.	3566.	82.	0.524
6/01/80	5.51	5.60	347.	10523.	62.	2.510
6/07/80	0.90	0.80	2640.*	3867.	34.	0.462
4/13/81	1.00	1.80	2120.*	4510.	32.	0.594
5/09/81	2.10	1.70	437.	3820.	60.	0.465
5/13/81	2.10	1.80	2360.*	5676.	52.	0.906
6/24/81	2.90	1.20	1590.*	5539.	44.	0.710
8/14/81	2.70	1.70	264.	5631.	42.	0.760
4/01/83	1.50	1.60	744.	4707.	54.	0.627
4/12/83	1.40	1.50	1210.*	4271.	50.	0.563
5/01/83	1.60	1.00	2300.*	5268.	28.	0.598

*Flow at the beginning of this storm is in recession from a previous event (storm or snowmelt).

C.5 Calibration Results

C.5.1 HEC-1 Calibration Results

HEC-1 was fit to each of the 32 storm events listed in Table C.4. As shown in Figs. C.7 and C.8, the typical quality of the HEC-1 and RORB calibrated hydrographs relative to the measured hydrograph is quite good.

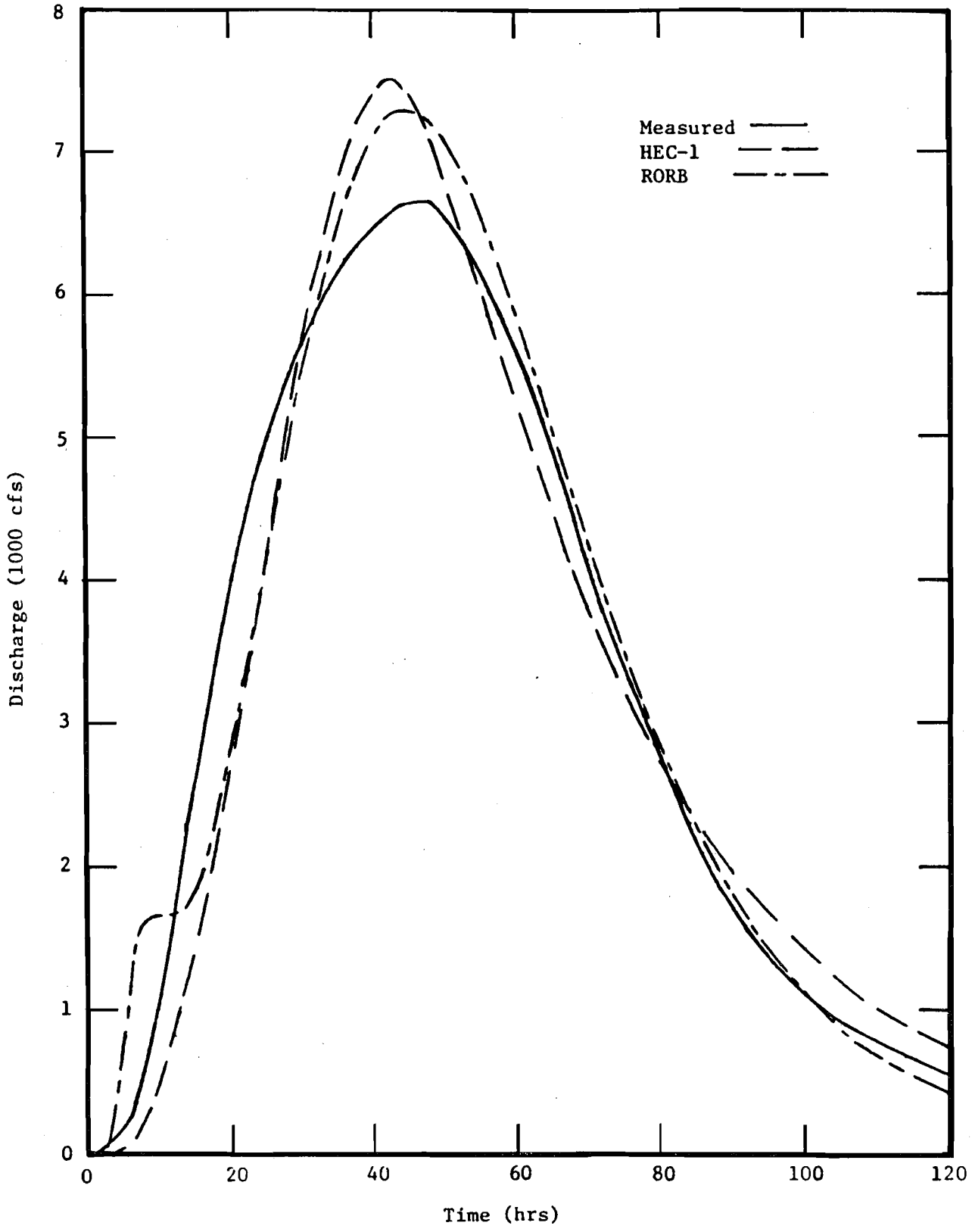

Figure C.7. Comparison of measured and best fit hydrographs for the February 1, 1968 event

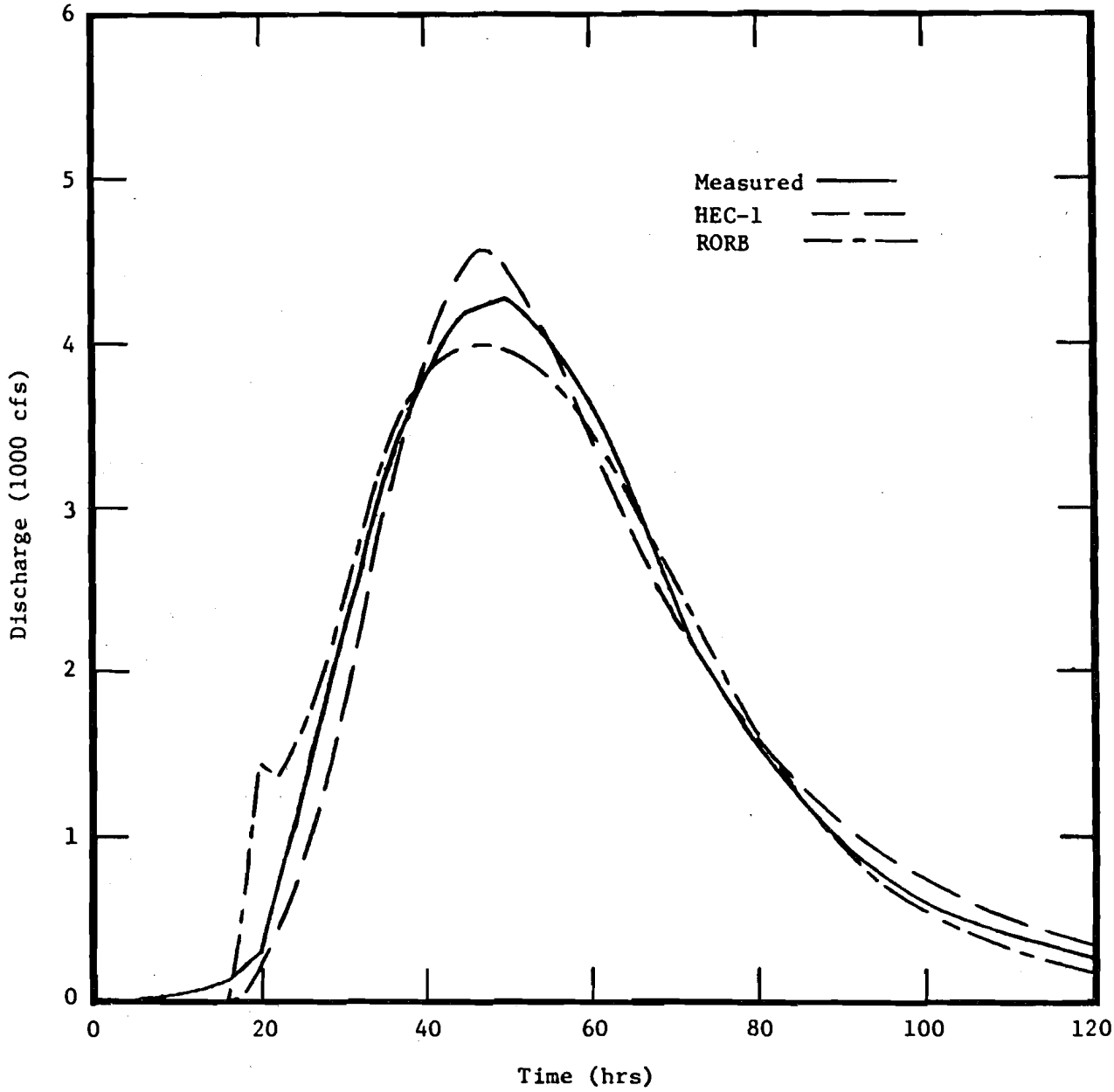

Figure C.8. Comparison of measured and best fit hydrographs for the April 12, 1983 event

The high quality of the fits obtained for each event is further illustrated in Table C.5 where the percent errors in both magnitude and timing of the calibrated peaks are displayed. Also shown in Table C.5 is the coefficient of model fit efficiency, EFF (in percent) defined on an event basis as:

$$EFF = \frac{\sum_{i=1}^{n} (Q_{m_i} - \bar{Q}_m)^2 - \sum_{i=1}^{n} (Q_{m_i} - Q_{c_i})^2}{\sum_{i=1}^{n} (Q_{m_i} - \bar{Q}_m)^2} \qquad (C.8)$$

Table C.5. Quality of Hydrologic Fit

Date	HEC-1			RORB		
	Percent Error		EFF	Percent Error		EFF
	Q_p	t_p	(%)	Q_p	t_p	(%)
12/24/65	3.53	0.	99.6	-1.46	-8.00	97.0
12/11/67	0.65	5.56	98.8	0.70	0.	97.4
2/01/68	12.52	12.50	98.6	9.39	-8.33	97.4
6/24/68	10.17	-5.00	96.1	9.33	5.00	96.2
4/18/70	-1.23	-3.70	99.7	-2.05	-14.81	98.5
9/21/70	1.73	-3.33	99.7	-8.35	-10.00	94.7
11/12/72	-5.54	-3.57	99.2	-8.11	-3.57	97.3
3/09/73	1.02	0.	99.6	-2.55	0.	96.1
3/31/73	-2.78	-4.00	99.4	-4.82	-8.00	97.9
4/20/73	4.12	-20.59	97.4	4.27	-8.82	98.3
6/03/73	-9.24	-3.13	97.3	-6.02	-6.25	97.5
5/21/74	9.11	7.14	96.8	--	--	--
6/05/74	-0.59	-3.57	99.0	-2.90	-3.57	96.3
6/21/74	1.67	-6.90	99.0	-10.62	0.	95.9
2/16/76	-5.87	-4.35	99.2	7.60	-4.35	98.0
2/20/76	3.19	0.	99.7	-2.65	-5.00	95.7
3/03/76	9.07	-3.57	97.0	11.39	-7.14	95.1
4/23/76	-8.17	-3.13	99.1	-3.84	-6.25	96.5
9/30/77	-1.61	0.	98.9	-1.92	-4.55	98.4
7/12/78	5.40	0.	98.7	3.72	-6.25	98.5
4/11/79	14.71	-3.85	95.9	4.41	-7.69	91.4
8/18/79	3.87	-2.44	98.5	-4.16	-4.88	96.3
6/01/80	22.44	-9.68	81.0	--	--	--
6/07/80	1.47	5.88	98.6	15.80	11.76	91.7
4/13/81	11.77	0.	97.0	28.66	6.25	80.0
5/09/81	-10.99	0.	96.4	-12.20	-6.67	93.7
5/13/81	9.57	0.	98.6	6.72	0.	98.8
6/24/81	8.92	0.	96.6	1.59	0.	95.3
8/14/81	17.88	-4.76	92.2	6.90	0.	97.7
4/01/83	4.80	0.	99.6	1.28	-3.70	98.6
4/12/83	6.39	-4.00	98.7	-6.70	-4.00	98.1
5/01/83	6.13	0.	98.2	3.95	0.	98.4

Nash and Sutcliff (1970) suggested this coefficient is analogous to the fraction of variance explained statistic commonly used in regression andstochastic analyses. Also, EFF gives an indication of the agreement between the measured and calibrated hydrograph shapes.

Generally, the HEC-1 calibrated hydrograph peak is within ten percent of the measured hydrograph peak magnitude and timing. This good calibration fit in terms of peak time is further amplified when one considers that for 28 of the 32 events the calibrated peak time is within two hours (one time step) of the measured peak time, and that the hydrograph peaks for this watershed are typically flat and broad as shown in Figs. C.7 and C.8. The coefficient of model fit efficiency is also quite acceptable, indicating in almost all cases that more than 95 percent of the data variance has been explained.

The calibrated parameter values corresponding to these fine fits are shown in Table C.6. Also shown in Table C.6 are the optimal parameters TP and CP for the Synder (1938) unit hydrograph option of HEC-1, which aredetermined by HEC-1 in addition to the Clark unit hydrograph parameters,and the model correction factor λ_{mh}. The model correction factor, λ_{mh}, is the ratio between the measured, Q_p, and calibrated, Q_{pc}, peak discharges

$$\lambda_{mh} = Q_p/Q_{pc} \qquad (C.9)$$

C.5.2 RORB Calibration Results

RORB was fit to 30 of the 32 storm events listed in Table C.4. The May 21, 1974 event and the June 1, 1980 event each had such a large variation in rainfall measured at Fairbury and Piper City that RORB could not properly reproduce the measured hydrograph. For the May 21, 1974 event, the rainfall at Piper City was so large that the optimal continuing loss rate leads to zero rainfall excess at Fairbury, and subsequently, the rainfall excess areal distribution and the runoff timing are highly erroneous. A typical RORB "fit" (m=0.90) for this event is shown in Fig. C.9. For the June 1, 1980 event, the 3.10 in. rainfall at Piper City in the storm's last two hours leads to difficulties in properly defining the rainfall temporal distribution. A typical RORB "fit" (m=0.90) for this event is shown in Fig. C.10. These problems do not have the same effects in HEC-1 because it does not try to explicitly account for the spatial distribution of rainfall over the watershed, instead it takes an areal average-lumped system approach. For these two events, the lumped system approach is superior to the quasi-distributed system approach given the limited data.

For the 30 events, which were calibrated, RORB provides excellent results as evidenced by Figs. C.7 and C.8 and Table C.5. The initial sharp rise in the RORB hydrograph is due to the prompt response from the downstream subcatchments, which does not get smoothed by multiple nonlinear routing. This effect could be compensated for in RORB, but the high fit quality makes this unnecessary. Generally, the RORB calibrated hydrograph peak is within ten percent of the measured hydrograph peak magnitude and timing (within two hours in 17 of 30 events). The coefficient of model fit efficiency is also quite acceptable indicating in almost all cases that more than 95 percent of the data variance has been explained. In summary, both

RORB and HEC-1 provide excellent calibration fits of comparable quality for a wide variety direct runoff events for the Vermilion River watershed, and each is potentially useful for real-time flood forecasting on this watershed.

The calibrated parameter values corresponding to the fine RORB fits are shown in Table C.7. Also shown in Table C.7 are the model correction factor, λ_{mr}, and the optimal C_l and λ_{mr} values for m fixed at 0.90 (the reason for including these values in the table is described subsequently).

Table C.6 Calibrated Parameters for HEC-1

Date	TC (hr)	S_R (hr)	IL (in.)	CL (in./hr)	λ_{mh}	TP (hr)	CP
12/24/65	37.61	30.60	1.566	0.134	0.966	34.25	0.64
12/11/67	38.20	30.15	0.192	0.053	0.994	34.74	0.65
2/01/68	39.65	30.49	0.181	0.028	0.889	35.57	0.65
6/24/68	30.28	40.85	0.893	0.119	0.908	28.95	0.49
4/18/70	50.65	26.07	0.378	0.097	1.009	42.73	0.75
9/21/70	59.51	30.56	0.281	0.058	0.983	49.99	0.74
11/12/72	47.89	27.70	0.169	0.040	1.059	41.30	0.72
3/09/73	33.64	22.52	0.319	0.065	0.982	29.36	0.68
3/31/73	52.62	26.79	0.102	0.015	1.029	44.01	0.74
4/20/73	39.42	32.69	0.460	0.065	0.960	35.79	0.63
6/03/73	53.49	22.55	0.162	0.040	1.102	43.28	0.78
5/21/74	30.99	26.37	0.487	0.108	0.917	28.39	0.63
6/05/74	28.63	21.42	0.159	0.050	1.006	25.36	0.66
6/21/74	53.22	32.72	0.466	0.042	0.984	46.22	0.71
2/16/76	45.06	23.85	0.421	0.101	1.062	37.93	0.74
2/20/76	36.41	31.76	0.278	0.105	0.969	33.24	0.62
3/03/76	33.72	31.41	0.097	0.037	0.917	31.04	0.60
4/23/76	36.14	26.33	0.835	0.051	1.089	32.41	0.67
9/30/77	38.39	29.93	0.475	0.063	1.016	34.83	0.65
7/12/78	34.96	19.71	2.451	0.166	0.949	29.69	0.72
4/11/79	44.84	23.66	0.090	0.101	0.872	37.67	0.74
8/18/79	43.78	28.62	2.825	0.208	0.963	38.62	0.70
6/01/80	25.31	59.37	0.165	0.222	0.817	24.98	0.33
6/07/80	23.76	28.98	0.041	0.035	0.986	22.42	0.52
4/13/81	29.26	28.15	0.340	0.159	0.895	26.89	0.59
5/09/81	35.49	26.21	0.708	0.049	1.124	31.56	0.66
5/13/81	32.35	32.32	0.071	0.044	0.913	30.08	0.58
6/24/81	34.66	24.72	1.039	0.270	0.918	30.87	0.67
8/14/81	31.86	25.03	1.079	0.108	0.848	28.77	0.65
4/01/83	35.95	26.15	0.352	0.044	0.954	32.14	0.67
4/12/83	31.65	26.12	0.354	0.058	0.940	28.78	0.63
5/01/83	27.22	24.56	0.287	0.068	0.942	24.77	0.60

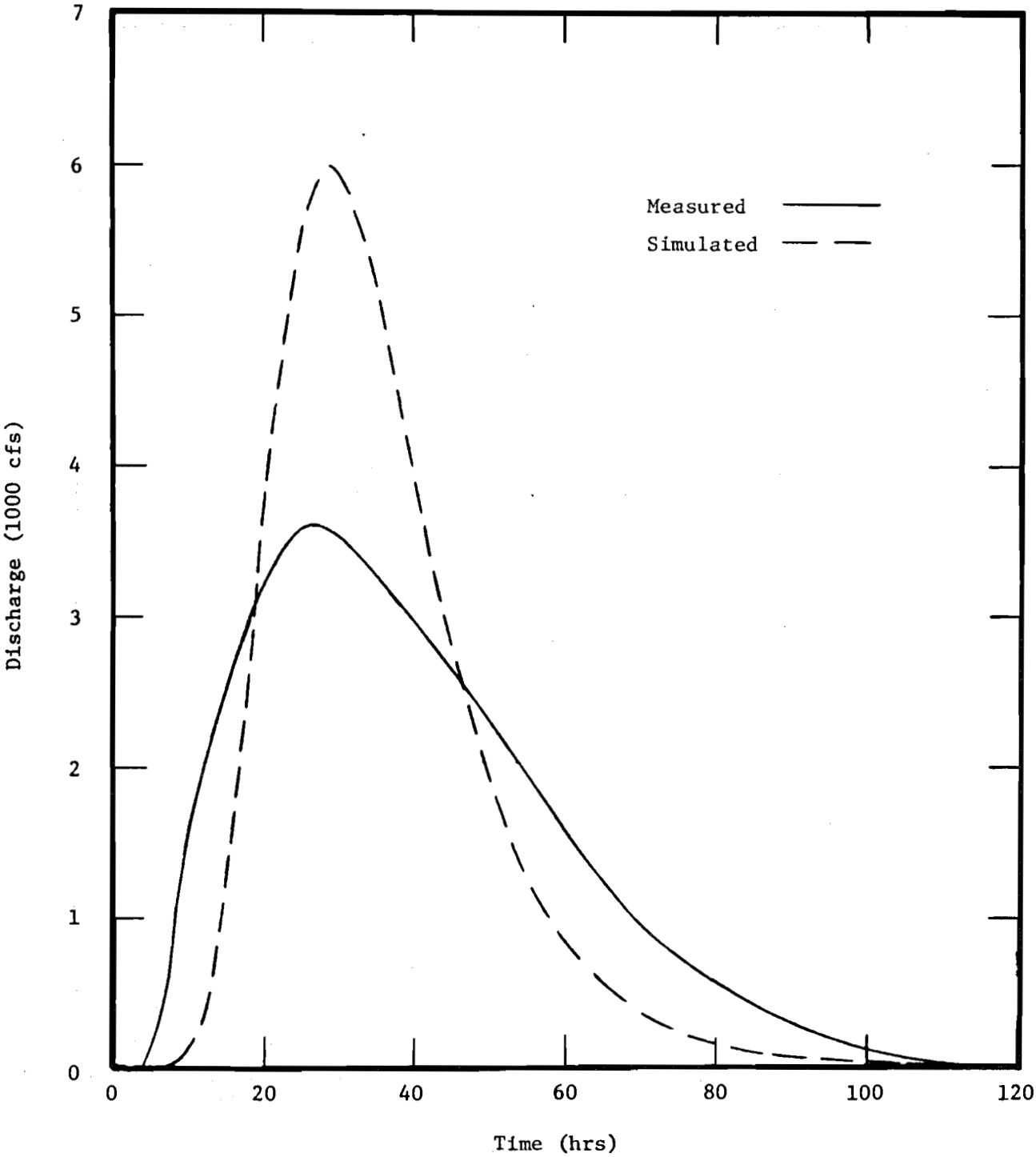

Figure C.9. Typical RORB fit (m=0.90) of the May 21, 1974 event

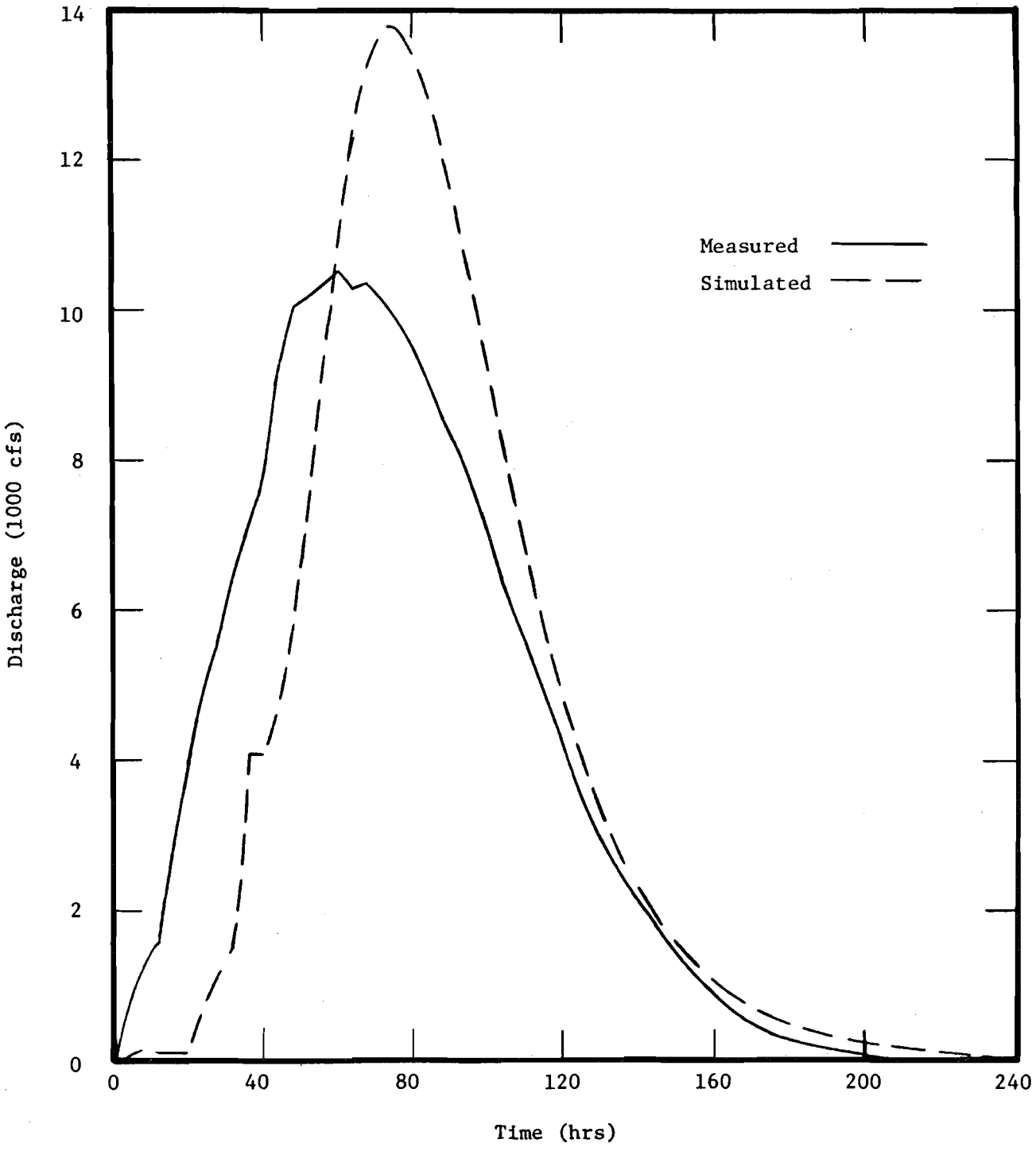

Figure C.10. Typical RORB fit (m=0.90) of the June 1, 1980 event

Table C.7. Calibrated Parameters for RORB

Date	m	C_1	C_1 (m=0.90)	ILR* (mm)	CLR (mm/hr)	λ_{mr}	λ_{mr} (m=0.90)
12/24/65	0.83	94.85	68.48	39.78	3.15	1.015	1.000
12/11/67	0.87	69.94	61.57	4.88	1.25	0.993	0.992
2/01/68	0.90	65.70	65.70	4.60	0.71	0.914	0.914
6/24/68	0.87	96.68	83.17	22.68	3.24	0.915	0.916
4/18/70	0.90	66.40	66.40	9.60	2.37	1.021	1.021
9/21/70	1.04	48.78	92.20	7.14	1.63	1.091	1.124
11/12/72	0.90	65.00	65.00	4.29	1.08	1.088	1.088
3/09/73	0.91	60.51	63.14	8.10	1.47	1.026	1.026
3/31/73	0.96	52.29	67.35	2.59	0.48	1.051	1.053
4/20/73	0.96	50.64	68.00	11.68	1.72	0.959	0.957
6/03/73	0.95	48.75	60.86	4.11	1.13	1.064	1.065
6/05/74	0.83	84.98	60.87	4.04	1.46	1.030	1.018
6/21/74	1.09	35.02	86.25	11.84	1.31	1.117	1.149
2/16/76	0.88	60.59	55.14	10.69	2.26	0.929	0.929
2/20/76	0.88	79.64	72.33	7.06	2.56	1.027	1.018
3/03/76	1.01	38.30	65.61	2.46	1.13	0.898	0.885
4/23/76	0.88	80.19	73.50	21.21	1.67	1.040	1.042
9/30/77	0.88	64.95	59.42	12.07	1.90	1.020	1.020
7/12/78	0.95	39.31	48.56	62.26	1.60	0.964	0.972
4/11/79	0.99	45.85	71.89	2.29	2.73	0.958	0.955
8/18/79	0.94	72.61	86.75	71.76	5.94	1.043	1.049
6/07/80	0.74	86.84	41.75	1.04	1.45	0.864	0.919
4/13/81	0.79	85.19	49.99	8.64	3.73	0.777	0.792
5/09/81	0.81	85.23	57.46	17.98	1.26	1.139	1.125
5/13/81	0.77	119.14	64.21	1.80	1.15	0.937	0.934
6/24/81	0.95	58.51	75.07	26.39	6.75	0.984	0.991
8/14/81	0.94	56.09	68.15	27.41	1.96	0.936	0.942
4/01/83	0.85	73.72	58.65	8.94	1.21	0.987	0.990
4/12/83	0.88	55.50	50.70	8.99	1.96	1.072	1.062
5/01/83	0.85	70.31	55.03	7.29	1.68	0.962	0.944

*ILR are the optimal values for HEC-1.

The values of m and C_1 are functionally related within RORB and to a certain extent changes in their values can have similar effects on the calculated hydrograph. Hence, it is quite likely that the calibrated values of m and C_1 will be significantly correlated due to their functional interactions and effects on the calculated hydrograph. For the 30 events calibrated, a correlation coefficient of -0.849 was found between m and C_1. Thus, the relationship between m and C_1 must be considered when analyzing the modeling uncertainty using any of the reliability analysis methods.

Laurenson and Mein (1985) pointed out that varying m generally has much less of an effect on the calculated hydrograph than does varying C_1. While calibrating RORB, it was observed that the optimal region of the objective function is quite flat over m given the optimal value of C_1 for each m (recall ILR and CLR are already fixed at their "optimal" values). Furthermore, the magnitude and timing of the calibrated peak discharge remain nearly constant for wide ranges of m. Therefore, it was decided to fix m at its "best" value and account for the uncertainty of m in C_1 and, to a lesser extent, in λ_{mr}. By summing the optimal objective function value for each value of m over all the events, the overall "best" value of m was found to be 0.90. Hence, C_1 for m equal to 0.90 is given in Table C.7. If the linear regression equation relating the calibrated values of m and C_1 were used to predict C_1, it would explain 71 percent of the variance in C_1. By fixing m at 0.90, the variance of C_1 is reduced 63.7 percent. Therefore, the simplification of fixing m at 0.90 is quite adequate to account for the relationship between m and C_1.

Table C.8 displays the quality of the hydrologic fits provided when calibrating RORB with m fixed at 0.90. As expected, the hydrologic fit quality is generally not adversely affected. The calibrated peaks generally are within ten percent of the measured peaks in terms of magnitude and timing, and the coefficient of model efficiency remains generally greater than 95 percent. Thus, RORB with m fixed at 0.90 is a reasonable model of the Vermilion River watershed.

C.6 Real-Time Flood Forecasting Scheme

The calibration results discussed in section C.5 revealed that given the proper ("optimal") parameter values for a given event both HEC-1 and RORB are able to accurately simulate that event on the Vermilion River watershed. However, as shown in Tables C.6 and C.7, the optimal parameter values often vary considerably from event to event. This parameter variation is caused by the transfer of data uncertainties (especially rainfall spatial and temporal variation not measured by the rain gage network) and model structure uncertainties to the parameters via the calibration process. Hence, the deterministic HEC-1 and RORB models produce stochastic forecasts and predictions due to the parameter uncertainties which have been amplified by the calibration process. The parameter variation also makes the selection of the "best" parameter values for real-time forecasting and/or general watershed simulation quite difficult, and it makes the reliability of such forecasts or simulations suspect.

Table C.8. Quality of Hydrologic Fit for RORB with m Fixed at 0.90

Date	Percent Error Q_p	Percent Error t_p	EFF (%)
12/24/65	0.	-4.00	96.0
12/11/67	0.86	0.	97.2
2/01/68	9.39	-8.33	97.4
6/24/68	9.19	10.00	96.1
4/18/70	-2.05	-14.81	98.5
9/21/70	-11.00	-13.33	94.3
11/12/72	-8.11	-3.57	97.3
3/09/73	-2.64	0.	96.1
3/31/73	-2.61	-12.00	98.0
4/20/73	4.48	-8.92	98.3
6/03/73	-6.07	-9.38	97.7
5/21/74	--	--	--
6/05/74	-1.77	-3.57	95.0
6/21/74	-12.95	-3.45	95.3
2/16/76	6.81	-4.34	97.9
2/20/76	-1.77	-5.00	95.4
3/03/76	13.01	-3.57	95.0
4/23/76	-4.05	-6.25	96.4
9/30/77	-1.92	-4.54	98.3
7/12/78	2.83	-6.25	98.4
4/11/79	4.71	-11.54	90.0
8/18/79	-4.65	-4.88	96.3
6/01/80	--	--	--
6/07/80	8.86	23.53	88.7
4/13/81	26.31	12.50	79.6
5/09/81	-11.09	-3.33	91.6
5/13/81	7.03	3.85	97.7
6/24/81	0.89	0.	95.2
8/14/81	6.21	-4.76	97.5
4/01/83	1.05	-3.70	98.2
4/12/83	-5.87	-4.00	98.0
5/01/83	5.90	7.14	98.1

The analysis of hydrologic modeling uncertainties is a function of the specific modeling scheme used and its objective. Hence, in the following paragraphs, a modeling scheme for real-time flood forecasting for the Vermilion River at Pontiac using either HEC-1 or RORB is described. The scheme makes use of the considerable calibration information available.

C.6.1 Best Estimate of the Initial Loss

Typically in hydrology, the term "initial losses" refers to interception and depression storage which must be satisfied before the initiation of runoff. In HEC-1 and RORB, the initial loss also includes the high infiltration loss which occurs at the beginning of a storm. The magnitude of this loss is a function of the storm's antecedent conditions. The continuing loss rate approximates the asymptotic equilibrium infiltration capacity which is nearly a constant for a given soil regardless of antecedent conditions (Horton, 1939). The various hydrograph parameters, TC and S_R for HEC-1 and C_1 and m for RORB, are considered to be constants based on the geomorphology of a given watershed. Hence, theoretically the continuing loss rate and the hydrograph parameters for each model should have one constant, best value for all events, but due to uncertainties they do not. The initial loss should vary not only due to uncertainties, but also due to antecedent conditions.

The initial loss does indeed display the largest variation of any of the parameters for either model. However, a significant portion of this variance can be accounted for by the relation between initial loss and antecedent conditions. The primary reasons for the reduction of infiltration capacity during a storm are (Horton, 1939, and ASCE, 1949):

1) occupation of some soil voids by soil water,
2) swelling of colloids and closing of soil-cracks and sun checks,
3) inwashing of fine materials to the surface-pores in the soil, and
4) rain-packing, i.e., the compaction of the soil surface due to raindrop impact.

Thus, the initial infiltration capacity and, hence, the initial loss are functions of the soil surface and soil moisture conditions at the beginning of the storm. Furthermore, the soil surface condition is related to the soil moisture because soil-cracking and sun checks are a product of a dry soil, while high soil moisture may be indicative of recent rainstorms which led to inwashing and rain-packing. Hence, the initial loss is highly related to the antecedent soil moisture.

Several indices have been proposed to reflect antecedent soil moisture including (Musgrave and Holtan, 1964):

1) antecedent precipitation indices,
2) indices based upon the status of baseflow in the area, and
3) indices derived by soil moisture accounting.

For this study, the baseflow at the beginning of each storm was readily available and was chosen to be representative of the antecedent soil

moisture. Figure C.11 displays a logarithmic plot of the optimal initial loss in inches versus the baseflow at the beginning of the rainfall event, Q_B, in cfs. A linear regression of the logarithms of initial loss and baseflow yields the following expression

$$IL = b_1 Q_B^{-0.599} \qquad (C.10)$$

with b_1 equal to 16.13 for IL in inches and 409.7 for IL in mm. A correlation coefficient of 0.877 describes the relation between the measured initial loss and that calculated using Eq. C.10. Furthermore, Eq. C.10 explains 72.2 percent of the variance in the measured initial loss values. Figure C.11 shows Eq. C.10 and its corresponding one standard deviation (of the logarithms) confidence bounds.

It should be noted that those events which include recession flow from a previous storm show much higher variance in the initial loss relative to Eq. C.10. This is not surprising because for such events the streamflow is not as accurate a measure of the soil moisture as is a long established near constant baseflow. Nevertheless, considering the high quality of the statistical and visual evidence over the entire range of baseflows, it seems reasonable to use Eq. C.10 to determine the best estimate of initial loss for any event to be forecast.

C.6.2 Best Estimates of the Continuing Loss Rate and Unit Hydrograph Parameters

Theoretically, the continuing loss rate and the unit hydrograph parameters are functions of the watershed geomorphology and soil types and as such should remain nearly constant for all events given a relatively unchanging watershed. However, due to natural, data, and model structure uncertainties transferred to the model parameters as well as the inherent uncertainties in the model parameters themselves, the optimal model parameters display considerable variation as shown in Tables C.6 and C.7. The effects of each of the parameters on the model output is nonlinear, hence, merely averaging the parameter values will not provide the parameter best estimate for use in forecasting over all events. Instead, the parameter best estimates for TC, S_R, and CL of HEC-1 and C_1 and CLR of RORB must be found via simultaneous calibration of the parameters over all the events (32 for HEC-1; 30 for RORB).

The overall parameter calibration scheme used involved one parameter at a time quadratic interpolation. In this approach, the objective function is minimized via quadratic interpolation over one parameter with the other parameters held constant. The locally optimized parameter is then fixed at its optimal value, and minimization over the next parameter is performed. The scheme cycles through the parameters until sufficient convergence in the objective function and the parameters is obtained.

Several different objective functions were examined:

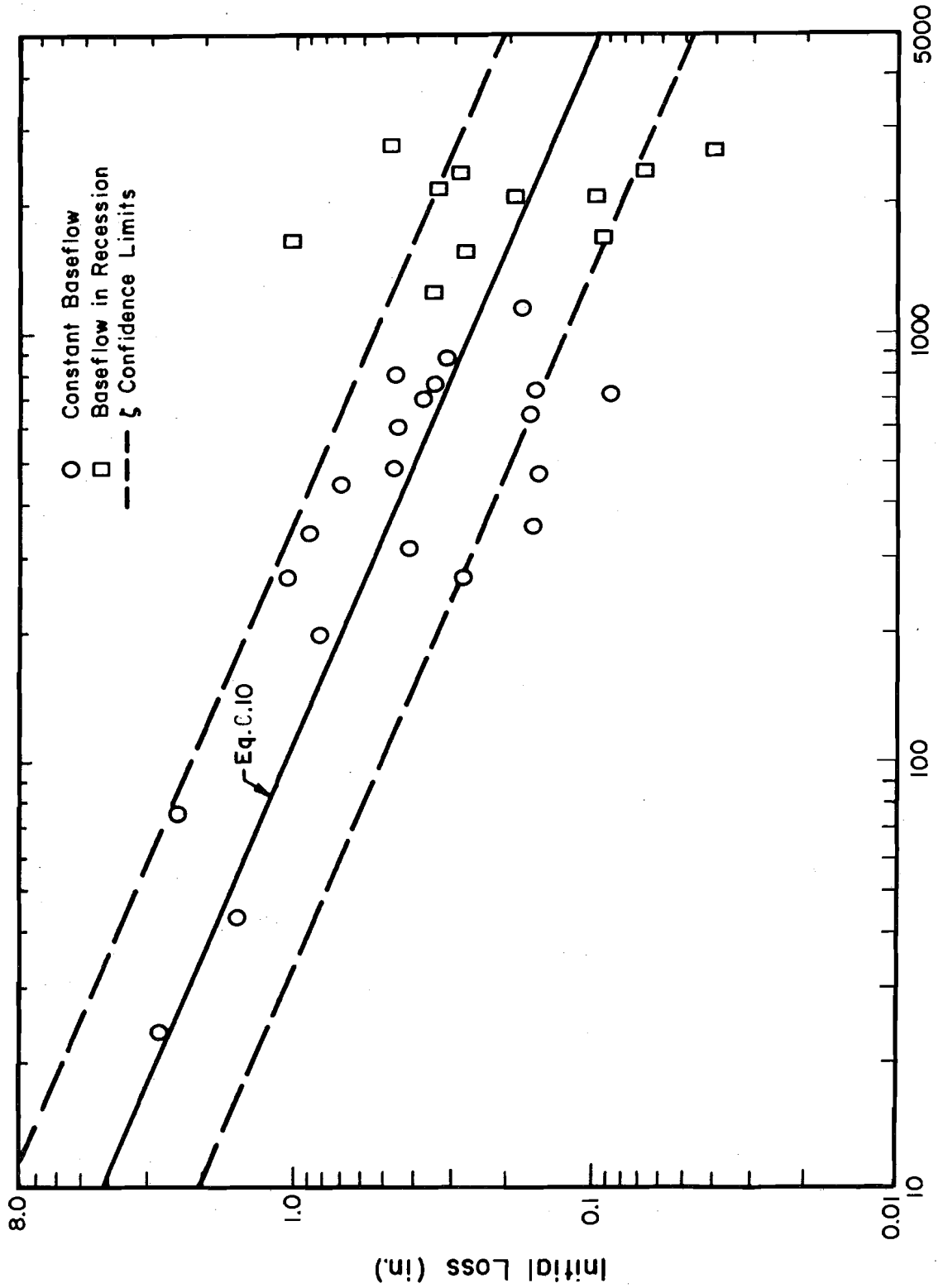

Figure C.11. Relation between baseflow and initial loss

1. A simple sum of the individual event calibration objective functions as calculated via Eqs. 5.6 and 5.7. This approach was used to fix m in RORB, but it is biased toward larger events which have larger event objective functions.

2. A sum of the fraction of the deviations of the event calibration objective function, i.e.,

$$\sum_j \left[(f_j(\theta^I) - f_j(\theta_j^*)) \; / \; f_j(\theta_j^*) \right] \qquad (C.11)$$

where $f_j(\cdot)$ = the calibration objective function (given by Eqs. C.6 and 5.7) for event j with parameters $\cdot$,

θ^I = the vector of model parameters for iteration I, and

θ_j^* = the vector of optimal parameters for event j.

3. A sum of the fraction of the deviations from the minimum sum of squares difference, i.e.,

$$\sum_j \left[(h_j(\theta^I) - h_j(\theta_j^*)) \; / \; h_j(\theta_j^*) \right] \qquad (C.12)$$

where $h_j(\cdot)$ = the unweighted sum of squares difference between the measured and simulated (using parameters $\cdot$) hydrographs for event j.

During the overall calibration iterations, the value of initial loss was fixed at that calculated from Eq. C.10. In this way, the parameter best estimates would be derived corresponding to the conditions of the real-time flood forecasting scheme.

When performing the overall calibration for HEC-1, some difficulty was encountered with regard to the optimal value of the storage coefficient, S_R. The value of S_R moved outside the range of optimal S_R values for the individual events far above the mean value and even above the unusually large value (59.37) for the June 1, 1980 event. Such large S_R values flatten and lengthen the recession limb and decrease the peak of the simulated hydrograph. The overall calibration scheme derives such a hydrograph because the use of Eq. C.10 to estimate the initial loss and of a single continuing loss rate for all events often leads to simulated runoff volumes far in excess of the measured runoff volume, and only by using an unrealistically high S_R value can the peak magnitude be held near the true value. The resulting overestimates in the recession limb comparing high S_R to low S_R do not have as large an effect on the individual event sum of squares difference (both weighted by Eq. C.7 or unweighted) as the overestimates in the peak region comparing low S_R to high S_R. Hence, the overall calibration results lead to a somewhat generic simulated hydrograph

shape which is the best overall hydrograph shape mathematically, but not a particularly realistic or representative hydrograph for any of the events encountered.

Similar results were not encountered when performing overall calibration for RORB. In RORB, the nonlinearity exponent, m, performs essentially the same function (expressing the release from storage) as does S_R in HEC-1. The value of m was fixed at 0.9 before the overall calibration was performed. Hence, a similar generic hydrograph shape was not obtained when overall calibration of RORB was performed. It was decided to fix S_R at its mean value of 27.71 hr and optimize only TC and CL over all events to circumvent HEC-1's unrealistic hydrograph shape problem.

The results of the overall calibration for both HEC-1 and RORB are summarized in Table C.9. The overall best estimates are different from the parameter mean values, but the improvement in the objective function obtained by using the best estimates versus the mean value is insignificant (two to three percent). The reason for this is a combination of two factors: the aforementioned large overestimation of runoff volume for many events and the wide variety of events in the calibration data set. The event variety undoubtedly kept the tradeoff between events best modeled with parameters close to the mean values versus those close to the best estimates nearly equal. In fact, the iteration results obtained by the optimization procedure indicate a flat objective function surface in the vicinity of the optimal solution. Given these findings, it was decided that using the

Table C.9 Overall Calibration Results

(a) HEC-1

Parameters	TC (hr)	S_R (hr)	CL (in./hr)	Obj. Func. Type	Obj. Func. Value
Mean	38.02	27.71	0.0876	2	282.81
Optimal	44.76	27.71	0.0813	2	275.07

(b) RORB

Parameters	C_1	m	CLR (mm/hr)	Obj. Func. Type	Obj. Func. Value
Mean	65.44	0.90	2.065	1	1285.4
Optimal	70.50	0.90	1.802	1	1259.2
Mean	65.44	0.90	2.065	2	141.80
Optimal	69.50	0.90	1.760	2	138.59

parameter mean values in the real-time flood forecasting scheme would be preferred to using the parameter best estimates because the mean values greatly simplify the application of reliability analysis procedures for consideration of modeling uncertainties without greatly sacrificing the validity of the model. Furthermore, the use of the parameter mean values in rainfall-runoff modeling is not uncommon in hydrology (e.g., see Loague and Freeze, 1985).

For general modeling cases, using the mean values of the parameters obtained from individual event calibration is only recommended when similarly large and diverse event calibration data sets are available. For cases with smaller or more homogeneous event calibration data sets, overall calibration of parameters is recommended to determine the parameter best estimates.

C.6.3 Model Correction Factor Relationship

The model correction factor, λ_m, describes the amount by which the model using optimal parameters underpredicts or overpredicts the measured peak flow in the form of a ratio between the measured and predicted peak flows. As such, the correction factor accounts for remaining errors and uncertainties in the modeling process (including model structure uncertainty) which due to the modeling scheme cannot be accounted for elsewhere and yet still lead to error and uncertainty in the peak flow estimate.

Troutman (1983) and others have noted that due to uncertainties (especially in the precipitation data), hydrologic models tend to overpredict large events and underpredict small events. The results of the extensive calibration work conducted in this study concur with Troutman's conclusions. Figures C.12 and C.13 display the relationship between λ_m and the predicted peak discharge, Q_p for HEC-1 and RORB, respectively (Note: values of λ_m greater than unity indicated underprediction while those less than unity indicate overprediction). It is believed that the calibration data set is sufficiently large and varied such that a mathematical relation between $\hat{Q}_p$ and λ_m may be derived.

Both linear and logarithmic relationships between $\hat{Q}_p$ and λ_m yield nearly equivalent correlation coefficients and reductions of variance in λ_m. However, when these expressions are extended beyond the range of available data, the linear relationship leads to a rapid tradeoff between increases in Q_p and decreases in λ_m such that the maximum adjusted peak discharge $Q_p^*(=E[\lambda_m]Q_p)$ is 11,970 cfs (Q_p = 21,810 cfs) and 10,650 (Q_p = 18,600 cfs) for HEC-1 and RORB, respectively. This is a very unrealistic situation. For the logarithmic relationship, a maximum adjusted peak also occurs, but in this case it is well above 100,000 cfs and corresponds to Q_p far greater. Hence, the logarithmic relationship provides reasonable results for the range of events encountered when forecasting. Of course, for any forecast event outside the range of the events used to derive the logarithmic relations, the calculated $E[\lambda_m]$ will be less reliable. Nevertheless, the logarithmic relations offer a reasonable extrapolation for the purpose of demonstrating the incorporation of reliability analysis in a real-time flood

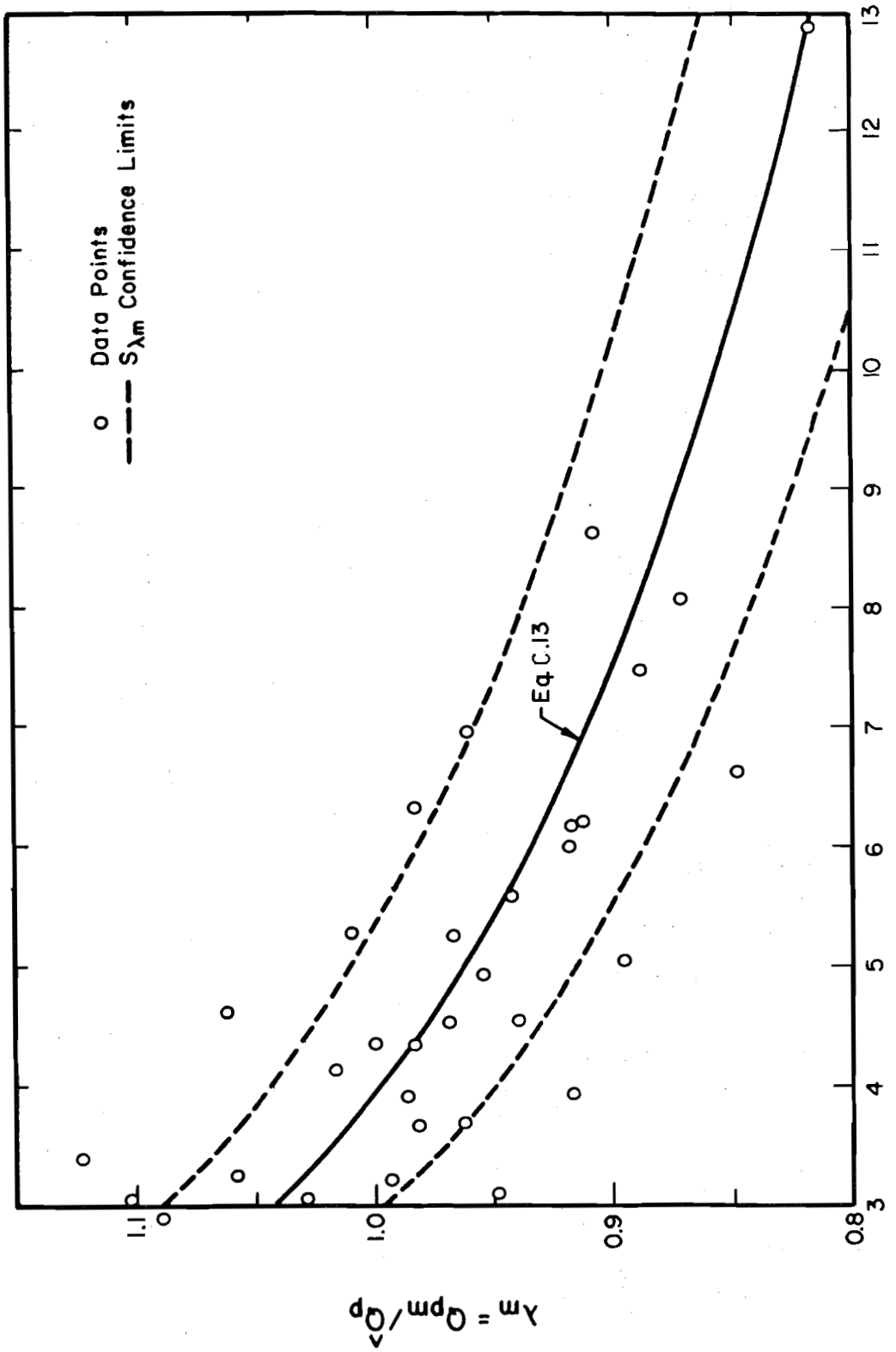

Figure C.12. Relation between $\hat{Q}_p$ and λ_{mh} for HEC-1

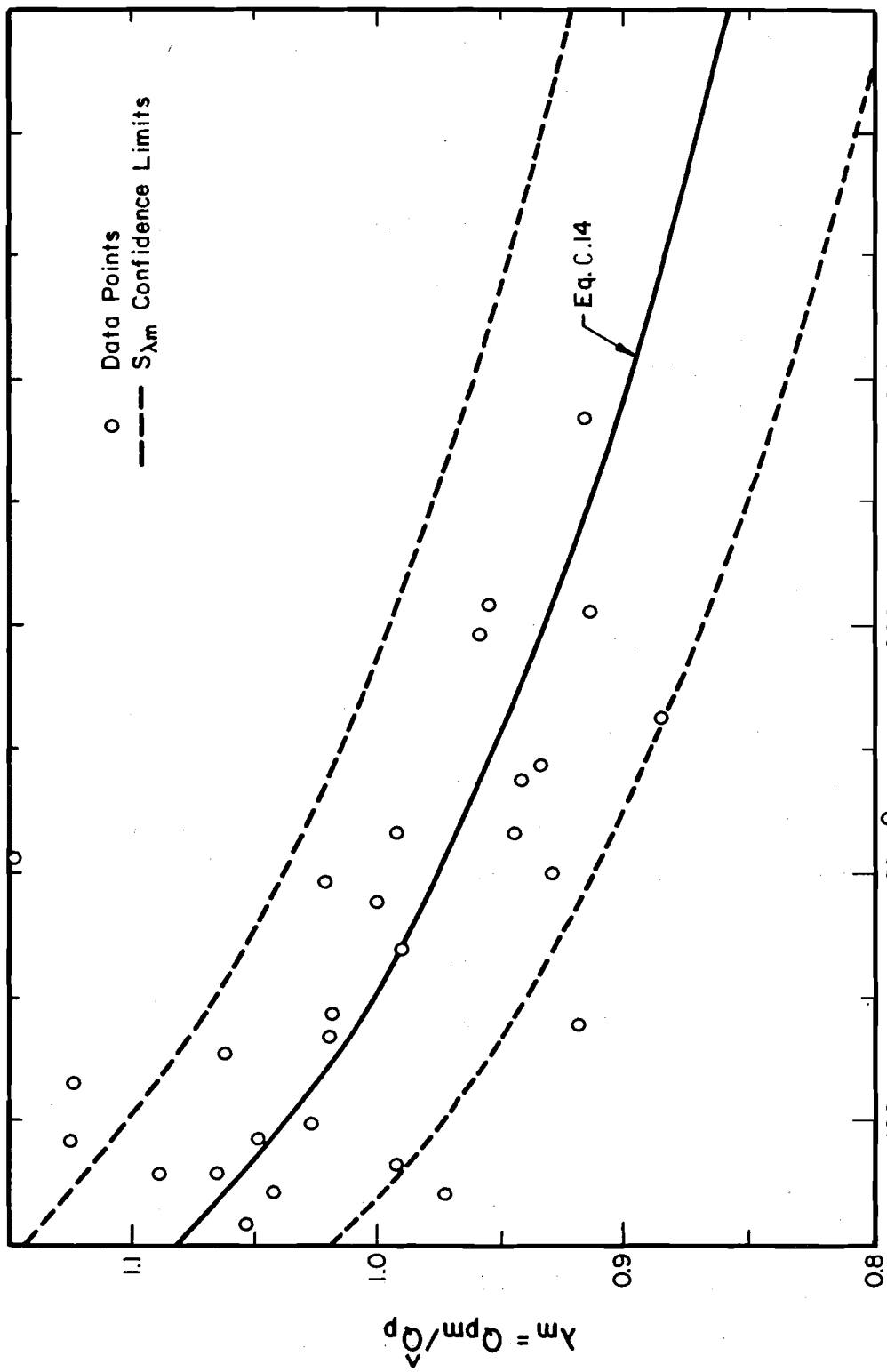

Figure C.13. Relation between $\hat{Q}_p$ and λ_{mr} for RORB

forecasting scheme. Furthermore, use of the logarithmic relations certainly provide a better estimate of the true flood peaks than does ignoring the tendency of the hydrologic models to overpredict large events.

The logarithmic relation between λ_{mh} and $\hat{Q}_{pH}$ for HEC-1 is

$$E[\lambda_{mh}] = 2.275 - 0.154 \ln \hat{Q}_{pH} \qquad (C.13)$$

where $\hat{Q}_{pH}$ = the predicted peak discharge estimated by HEC-1 in cfs, and

λ_{mh} = the model correction factor for HEC-1.

This equation has a correlation coefficient of 0.762 and it explains 56.6 percent of the variance in the measured λ_{mh}. The logarithmic relation between λ_{mr} and $\hat{Q}_{pR}$ for RORB is

$$E[\lambda_{mr}] = 1.737 - 0.152 \ln \hat{Q}_{pR} \qquad (C.14)$$

where $\hat{Q}_{pR}$ = the predicted peak discharge estimated by RORB and in m^3/s, and

λ_{mr} = the model correction factor for RORB.

This equation has a correlation coefficient of 0.599 and it explains 34.8 percent of the variance in the measured λ_{mr}. Figures C.12 and C.13 show plots of Eqs. C.13 and C.14, respectively, as well as their respective one standard deviation confidence bounds. Based on this evidence, the use of Eqs. C.13 and C.14 to estimate the values of λ_m for adjusting the predicted peak discharges from HEC-1 and RORB, respectively, is an improvement relative to assuming the λ_m values are totally random.

C.6.4 Summary of the Real-Time Flood Forecasting Schemes

For HEC-1, the adjusted flood peak prediction $\hat{Q}^*_{pH}$, is given by

$$\hat{Q}^*_{pH} = E[\lambda_{mh}]\ f_H(\overline{TC},\ \overline{S_R},\ E[IL],\ \overline{CL}) \qquad (C.15)$$

where $E[\lambda_{mh}]$ = the expected value of the model correction factor for HEC-1 given by Eq. C.13,

$f_H(\cdot)$ = function representing the HEC-1 model,

$\overline{TC}$ = the mean value of the time of concentration, 38.02 hr,

$\overline{S_R}$ = the mean value of the watershed storage factor, 27.71 hr,

E[IL] = the expected value of the initial loss given by Eq. C.10, and

$\overline{CL}$ = the mean value of the continuing loss rate, 0.0876 in./hr.

For RORB, the adjusted flood peak prediction, $\hat{Q}^*_{pR}$, is given by

$$\hat{Q}^*_{pH} = E[\lambda_{mr}]\ f_R(\overline{C_1},\ m^*,\ E[ILR],\ \overline{CLR}) \qquad (C.16)$$

where $E[\lambda_{mr}]$ = the expected value of the model correction factor for RORB given by Eq. C.14,

$f_R(\cdot)$ = function representing the RORB model,

$\overline{C_1}$ = the mean value of watershed delay time factor, 65.44,

m^* = the "best" estimate of the watershed nonlinearity exponent, fixed at 0.90,

E[ILR] = the expected value of the initial loss given by Eq. C.10, and

$\overline{CLR}$ = the mean value of the continuing loss rate, 2.065 mm/hr.

It should be noted that the functions $f_H(\cdot)$ and $f_R(\cdot)$ in Eqs. C.15 and C.16, respectively, could be considered to include the relationship between Q_p and λ_m defined by Eqs. C.13 and C.14. This view redefines the model functions to include the model's tendency to overpredict large events and underpredict smaller events, leaving λ_m to describe the random variation about Eqs. C.13 and C.14. However, the purpose of λ_m is to express the model structure inadequacies (errors and uncertainty), and hence, it is probably best to keep the model's tendencies to overpredict and underpredict separate from the model function.

C.7 Statistical Analysis

With the exception of m^* for RORB, all the parameters in Eqs. C.15 and C.16 are subject to a considerable amount of variation and uncertainty as can be seen in Tables C.6 and C.7 and Figs. C.11, C.12, and C.13. In this section, the appropriate statistics will be derived from the individual event calibration data to allow the various reliability analysis techniques to be combined with the real-time flood forecasting schemes. These appropriate statistics include estimates of the basic variable (i.e., the parameters of Eqs. C.15 and C.16) means, variances, and probability distributions.

C.7.1 Assumptions in the Statistical Analysis of Basic Variable Uncertainty

C.7.1.1 Sample Representativeness

The primary assumption in the following statistical analysis is that the results of the individual event calibration comprise a representative

sample of the large events likely to occur on the Vermilion River watershed for which real-time flood forecasts would be needed. The question of sample representativeness has two facets: Does the sample contain a sufficient variety of events, and does it contain a sufficient number of events to justify estimating basic variable statistics and, especially, distributions?

The sample contains a large rainstorm, June 1, 1980 (5.55 in.), which resulted in a serious flood; another large convective rainstorm, July 12, 1978 (3.00 in.), which due to the watershed being very dry, resulted in a very low peak discharge (2940 cfs); and a wide variety storm rainfall depths, watershed soil moisture conditions, and resulting peak discharges in between. Furthermore, the data set contains events from each season of the year and nearly every month of the year with the majority of the events in the heavy rainfall prone spring months (April-June). Also, a variety of rainstorm types from intense, localized convective thunderstorms to longer term steady rainstorms are included. Hence, it is likely that the common assumption of statistical hydrology that the events sampled are representative of the events to be forecast in the future has been satisfied.

With regard to the size of the sample, the U.S. Water Resources Council (1981) recommends that stream gaging records be at least ten years long before use of flood frequency analysis is warranted. Ang and Tang (1975, p. 236) stated that if sample size is large (for instance, greater than 20), the sample variance is a good estimator of the population variance. Therefore, from a practical hydrologic viewpoint, the sample sizes of 32 events for HEC-1 and 30 events for RORB are adequate for the statistical analysis.

Another key factor tied in with sample representativeness is sample homogeneity, i.e., is the entire sample of events a subset of the same population of events and, hence, a product of a unique physical rainfall-runoff process. Seasonal variation in watershed vegetation and soil conditions, in storm types, etc., is the most common reason to suspect the events result from different physical processes and, hence, represent different populations. Tables C.10 and C.11 display the effects of seasonal variations on the mean values, $\bar{x}_i$, and standard deviations, σ_i, of the parameters of HEC-1 and RORB, respectively.

With the exception of the initial loss and the continuing loss rate, the mean values of the various parameters remain nearly constant for all seasons. For the summer events, dry watershed conditions may have contributed to the high mean values of the initial loss and the continuing loss rate. This contribution in the initial loss is partially accounted for in Eq. C.10. Considering the general agreement of the mean values over the seasons, it is reasonable to establish the flood warning schemes based on the overall mean parameter values and to assume that at least on the first moment level the events are from the same population.

Table C.10. Effect of Seasonal Variations on the Basic Variables of HEC-1

Period		TC (hr)	S_R (hr)	IL (in.)	CL (in./hr)	λ_{mh}	TP (hr)	CP
All 32 Events	$\bar{x}_i$	38.02	28.70	0.554	0.088	0.9674	33.64	0.650
	σ_i	8.94	6.98	0.647	0.061	0.0717	6.72	0.088
Summer Storms (June-August) 10 Events	$\bar{x}_i$	36.00	30.40	0.928	0.126	0.9479	31.92	0.623
	σ_i	10.72	11.91	0.984	0.086	0.0814	8.06	0.136
Spring Storms (March-May) 14 Events	$\bar{x}_i$	36.71	27.10	0.349	0.069	0.9672	32.54	0.655
	σ_i	7.67	3.07	0.227	0.037	0.0729	5.65	0.057
Fall & Winter 8 Events	$\bar{x}_i$	42.84	29.38	0.445	0.073	0.9922	37.73	0.676
	σ_i	7.82	2.51	0.466	0.037	0.0560	5.57	0.049

Table C.11. Effect of Seasonal Variations on the Basic Variables of RORB

Period		m	C_1	C_1(m=0.90)	ILR (mm)	CLR (mm/hr)	λ_{mr}
All 30 Events	$\bar{x}_i$	0.900	67.04	65.44	14.45	2.065	0.9963
	σ_i	0.078	19.30	11.62	16.90	1.385	0.0779
Summer Storms (June-August) 9 Events	$\bar{x}_i$	0.918	64.31	67.94	25.73	2.760	0.9907
	σ_i	0.097	22.02	16.33	25.51	2.133	0.0802
Spring Storms (March-May) 13 Events	$\bar{x}_i$	0.889	67.94	62.45	8.58	1.735	0.9867
	σ_i	0.076	21.46	7.54	5.91	0.831	0.0897
Fall & Winter 8 Events	$\bar{x}_i$	0.898	68.68	67.48	11.31	1.818	1.0097
	σ_i	0.062	13.65	11.32	11.84	0.816	0.0645

The seasonal variation has a much more significant effect on the parameter standard deviations. The summer events tend to be mainly intense, localized convective thunderstorms. Hence, large parameter standard deviations are to be expected for these storms with high temporal and spatial variability. Events throughout the rest of the year tend to be more spatially uniform, steady rainstorms. Such events should display much smaller parameter standard deviations than the summer events. This is indeed the case for the events sampled here. Nevertheless, the reliability analysis techniques will make use of the statistics of the entire set of events because the sample really is not large enough to derive separate statistics for summer events and the error introduced to the analysis by using a slightly non-homogeneous sample is not large enough to negate the goals of this research.

C.7.1.2 Parameter Independence

While methods exist for handling basic variable correlation in first-order second moment and Monte Carlo analyses, these analyses are much less complicated when dealing with uncorrelated basic variables. The simplified expressions for these analyses with independent basic variables are given in Chapter 3. In the following paragraphs, the independence of the basic variables is examined.

From a strictly theoretical viewpoint, all of the model parameters for HEC-1 and RORB are functionally independent with the exception of C_1 and m in RORB whose interdependence has already been accounted for. Even the initial loss and continuing loss rate are theoretically independent because the continuing loss rate is a function of the soil type alone while the initial loss is a function of the soil type and, perhaps to a greater extent, the antecedent soil conditions. The model correction factor is correlated to the predicted peak discharge, $\hat{Q}_p$, which in turn is a function of the model parameters. Hence, some correlation between the model correction factor and the model parameters is expected. However, after accounting for the relationship between $\hat{Q}_p$ and λ_m via Eqs. C.13 and C.14, the correlation between the model parameters and the data residuals (measured λ_m minus λ_m estimated from the appropriate equation) is likely to be insignificant.

While theoretically the interrelations between the model parameters and between the model parameters and the data residuals of the model correction factor should be insignificant, the calibration process has long been known to impose artificial correlation between parameters which serve similar functions. Tables C.12 and C.13 display the estimated correlation coefficients between the basic variables for the real-time flood forecasting schemes using HEC-1 and RORB, respectively. In the reliability analysis, the basic variables are not the measured values of the IL and λ_m, but rather the data residuals of their values about the appropriate estimation equation (Eq. C.10 for IL and Eqs. C.13 and C.14 for λ_m). Hence, the correlation of the other basic variables with the data residuals of IL, res(IL), and of λ_m, res(λ_m), are also given in Tables C.12 and C.13.

Table C.12. Correlation Between Basic Variables for HEC-1

Basic Variable	Correlation Coefficient						
	TC	S_R	IL	CL	λ_{mh}	res(IL)	res(λ_{mh})
TC	---	-0.203	-0.018	-0.246	-0.589	-0.299	-0.379
R	-0.203	---	-0.148	0.258	-0.428	-0.355	0.088
IL	-0.018	-0.148	---	0.580	-0.135	---	---
CL	-0.246	0.258	0.580	---	-0.454	0.418	-0.322
λ_{mh}	-0.589	-0.428	0.135	-0.454	---	---	---
res(IL)	-0.299	-0.355	---	0.418	---	---	-0.339
res(λ_{mh})	-0.379	0.088	---	-0.322	---	-0.339	---

Table C.13. Correlation Between Basic Variables for RORB

Basic Variable	Correlation Coefficient					
	C_1	ILR	CLR	λ_{mr}	res(IL)	res(λ_{mr})
C_1	---	0.213	0.324	0.376	-0.035	0.616
ILR	0.213	---	0.557	0.080	---	---
CLR	0.324	0.557	---	-0.155	0.396	-0.045
λ_{mr}	0.376	0.080	-0.155	---	---	---
res(ILR)	-0.035	---	0.396	---	---	-0.133
res(λ_{mr})	0.616	---	-0.045	---	-0.133	---

Yevjevich (1971) discussed several tests for the significance of sample correlation coefficients. One of the simplest and most powerful tests views the relation between the sample correlation coefficient, r, and the population correlation coefficient, ρ, by using a transformation to a third variable Z. The standardized value of Z may be assumed to be approximately normal (i.e., follows the standard normal distribution) for t in the neighborhood of zero so that (Yevjevich, 1971, p. 238)

$$t = \frac{\sqrt{N_s - 3}}{2} \ln \left[\frac{1+r}{1-r} \cdot \frac{1-\rho}{1+\rho} \right] \qquad (C.17)$$

where N_s = the sample size.

Reorganizing Eq. C.17 to define bounds on r in terms of ρ and t

$$r_B = \frac{(1+\rho)\ \exp\ (2t/(N_s-3)^{1/2}) - (1-\rho)}{(1+\rho)\ \exp\ (2t/(N_s-3)^{1/2}) + (1-\rho)} \qquad (C.18)$$

by setting $t = 1.96$ and $\rho = 0$, the 95 percent confidence bound on r being not significantly different from 0 (independent variables case) is obtained. for HEC-1's 32 events $r_{95} = \pm 0.349$, while for RORB's 30 events $r_{95} = \pm 0.360$.

Based on the results of Eq. C.18, it is safe to assume that seven of ten basic variable interrelations for HEC-1 are statistically as well as functionally independent. The correlation coefficients between TC and res(λ_{mh}) and S_R and res(IL) only slightly exceed the 95 percent confidence bound, and so it is probably reasonable to assume these basic variables are independent from a practical viewpoint. The correlation coefficient between CL and res(IL) is slightly more significant, but this correlation only accounts for approximately 16 percent of the variance in either variable. Hence, from a practical viewpoint, it is reasonable to assume these variables are independent. It is also reassuring to note that, as expected, the significant correlation between λ_{mh} and TC, S_R, and CL becomes insignificant for the data residuals of λ_{mh}.

For RORB, it is safe to assume that four of the six basic variable interrelations are statistically as well as functionally independent. The correlation coefficient between CLR and res(ILR) is only slightly outside the 95 percent confidence bounds, and so from a practical viewpoint these basic variables may be considered independent. The relatively high correlation coefficient between C_l and res(λ_{mr}) was not expected. The relation between λ_{mr} and $\hat{Q}_p$ is not as strong for RORB as for HEC-1. Hence, it is possible that the relation between C_l and λ_{mr} is not properly expressed within the relation between λ_{mr} and $\hat{Q}_p$. Furthermore, by removing the influence of $\hat{Q}_p$ on λ_{mr}, the influence of other factors (such as C_l) on the res(λ_{mr}) is magnified in terms of a correlation coefficient because the residual variance is less than that for the measured parameter. Thus, in terms of the total variance of measured λ_{mr} values, C_l affects a small, insignificant portion, but C_l affects a much more significant portion of the reduced variance of res(λ_{mr}). Therefore, it seems likely that ignoring this correlation and assuming C_l and res(λ_{mr}) are independent will not adversely effect the reliability analysis from a practical viewpoint.

C.7.2 HEC-1 Basic Variable Statistics

C.7.2.1 Initial Loss, IL

As discussed in section C.6, a strong relation exists between the logarithms of the initial loss and baseflow (streamflow) at the beginning of the event. One of the basic assumptions of any linear regression analysis is that the residuals of the regression equation are independent, normal variables. Hence, it was felt the data residuals of initial loss might be lognormally distributed about Eq. C.10. Two well known statistical tests--the skewness test of normality (Salas et al., 1980, p. 92) and the

Kolmogorov-Smirnov (K-S) test (Law and Kelton, 1982, p. 199) -- were used to test the hypothesis that the res(IL) are lognormally distributed.

The skewness test of normality is based on the fact that the skewness coefficient for a normal variable is zero. Hence, this is a test to determine if the sample skewness of a variable is significantly different from zero, if not the hypothesis that the variable is normally distributed cannot be rejected at the specified significance level. For the logarithms of res(IL), the skewness coefficient, γ, is 0.0276. Thus, based on the skewness test, the hypothesis that res(IL) is lognormally distributed cannot be rejected at very high significance levels (e.g., at the 10 percent significance level for a sample size of 32 the bound on γ is ± 0.646).

The K-S test examines the correctness of the assumed distribution by determining the largest deviation between an empirical cumulative distribution function derived from the data and the theoretical cumulative distribution function for the assumed distribution. In this study, an adjusted, more powerful Kolmogorov-Smirnov statistic (maximum distance) is used. Developed by Stephens (1974), it accounts for the fact that the sample mean and standard deviation are used instead of the population values. For this adjusted K-S test, the hypothesis that res(IL) is lognormally distributed cannot be rejected at approximately the four percent significance level.

Considering the high significance of the skewness test and the practical advantage of the lognormal distribution, the initial loss is considered lognormally distributed with

$$E[\ell n(IL)] = 2.7806 - 0.599\ \ell n\ Q_B \qquad (C.19)$$

$$\zeta_{IL} = [\mathrm{Var}\ (\ell n(IL))]^{1/2} = 0.7184^*$$

For the MVFOSM method, only the mean and variance of IL are required. Hence, for this method

$$E[IL] = 16.13\ Q_B^{-0.599}\ \text{(in.)} \qquad (C.20)$$

$$S_{IL} = 0.3411^*\ \text{in.}$$

---

*NOTE: These values are the conditional standard deviations calculated considering the regression analysis for the mean as described in Ang and Tang (1975, p. 288).

C.7.2.2 Continuing Loss Rate, CL

Figure C.14 displays a histogram of the optimal CL values for HEC-1 in one-third standard deviation intervals. Based on visual inspection, it seems reasonable to assume that CL is lognormally distributed. The skewness of the logarithms of CL is 0.0932. Hence, based on the skewness test, the hypothesis that CL is lognormally distributed cannot be rejected at significance levels far above ten percent. The adjusted K-S test indicates that the hypothesis that CL is lognormally distributed cannot be rejected at the 15 percent significance level. Therefore, the continuing loss is considered lognormally distributed with

$$E[\ell n(CL)] = -2.644$$

$$\zeta_{CL} = 0.6447$$

For the MVFOSM method, the mean and standard deviation are

$E[CL] = 0.0876$ in./hr

$S_{CL} = 0.0611$ in./hr

C.7.2.3 Time of Concentration, TC

Figure C.15 displays a histogram of the optimal TC values for HEC-1 in one-half standard deviation intervals. Based on visual inspection, the distribution of TC might be reasonably assumed to be normal or lognormal. Upon examining the hypothesis that TC is normally distributed, the skewness of the TC values was found to be 0.671. Hence, based on the skewness test, the hypothesis that TC is normally distributed cannot be rejected at approximately the nine percent significance level. The adjusted K-S test indicates that the hypothesis that TC is normally distributed cannot be rejected at approximately the eight percent significance level.

Therefore, it is reasonable to consider the time of concentration as normally distributed with

$$E[TC] = 38.02 \text{ hr}$$

$$S_{TC} = 8.94 \text{ hr}$$

These statistics are used in the MVFOSM analysis.

It should be pointed out that the hypothesis that TC is lognormally distributed cannot be rejected by both the skewness and adjusted K-S tests at much higher significance levels. Nevertheless, the estimated normal distribution was used in this study for simplicity.

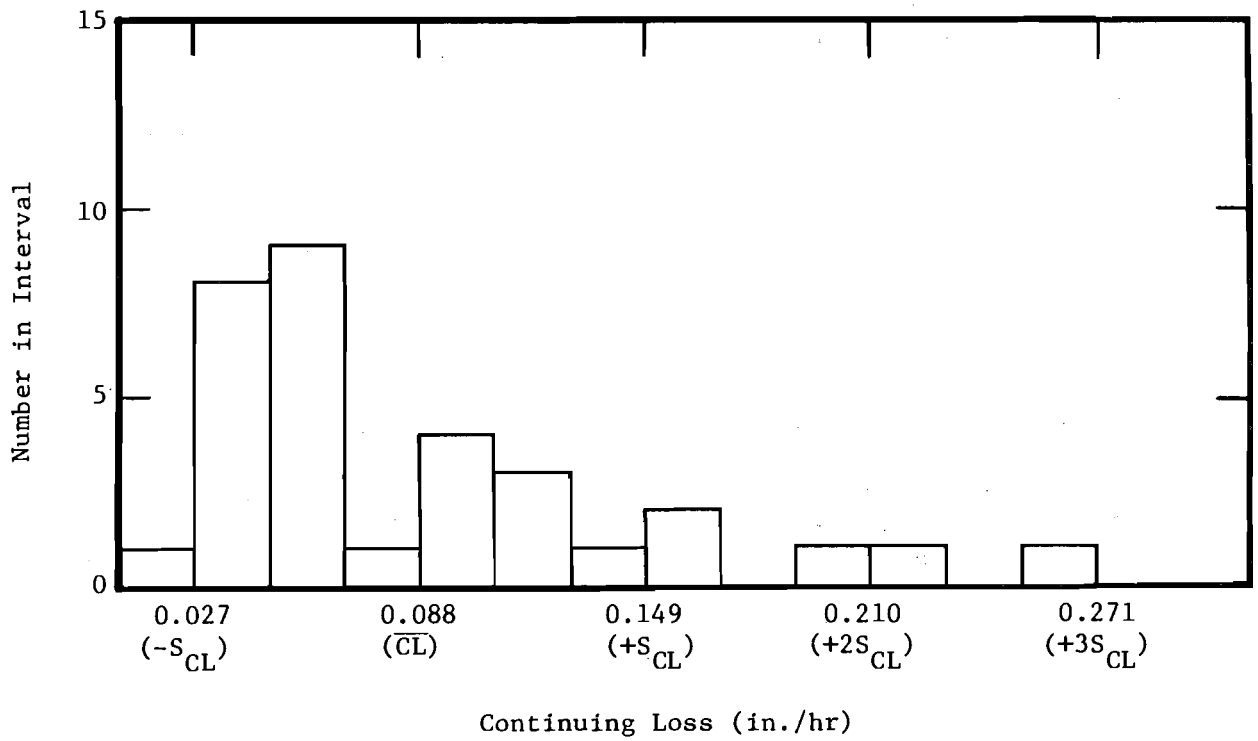

Figure C.14. Histogram of optimal CL values for HEC-1

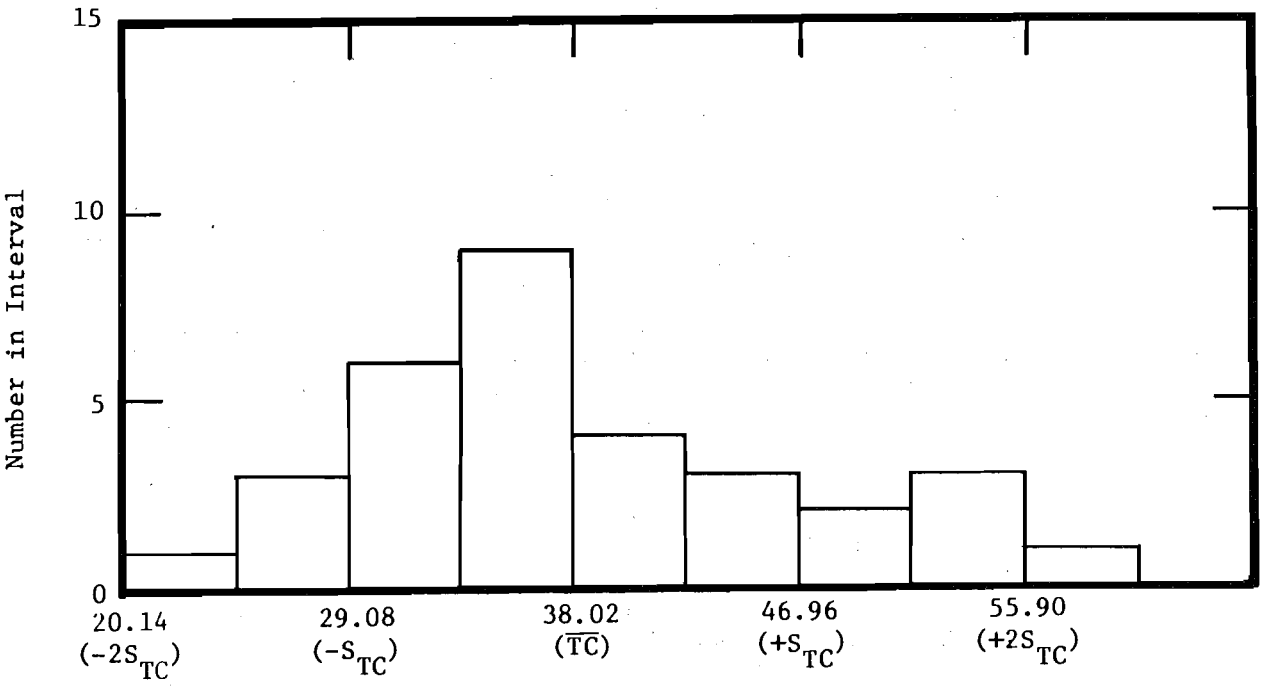

Figure C.15. Histogram of optimal TC values

C.7.2.4 Watershed Storage Factor, S_R

If the unusually high S_R value for the June 1, 1980 storm is temporarily ignored, the mean and standard deviation of the remaining 31 values are

$$E[S_R] = 27.71 \text{ hr}$$

$$S_{S_R} = 4.176 \text{ hr}$$

Figure C.16 displays a histogram of the optimal S_R values for HEC-1 in one standard deviation intervals (based on the statistics of the 31 event sample). Based on visual inspection, it seems that the assuming S_R to be normally distributed is reasonable. The skewness coefficient of the 31 S_R values is 0.696. Hence, based on the skewness test, the hypothesis that S_R is normally distributed cannot be rejected at approximately the nine percent significance level. The adjusted K-S test indicates that the hypothesis that S_R is normally distributed cannot be rejected at the 15 percent significance level.

When the entire 32 event sample is considered, both the skewness test and adjusted K-S test indicate that the hypothesis of S_R being normally distributed can be rejected with a less than one percent chance that the true distribution is being rejected. If S_R was truly normally distributed as described by the 31 event sample, it is possible that the 32nd event drawn randomly from the normally distributed population could be seven standard deviations from the mean. The adjusted K-S test was performed on the 32 event data set assuming the normal distribution estimated from the 31 event data set. This test indicated the hypothesis that S_R is normally distributed cannot be rejected at the 15 percent significance level.

Therefore, it is reasonable to assume that the storage coefficient is normally distributed with mean and standard deviation given above. These statistics are used in the MVFOSM analysis.

This assumed distribution and statistics slightly underestimate the parameter variance measured for the entire data set, and so the HEC-1 forecast reliability may be slightly overpredicted. Nevertheless, the amount of this overprediction should not greatly alter the general conclusions of this research.

C.7.2.5 Model Correction Factor, λ_{mh}

As noted previously, the residuals of a linear regression equation should be independent, normal variables. Hence, a normal distribution for res(λ_{mh}) was estimated and tested. The skewness coefficient for res(λ_{mh}) of HEC-1 was found to be 0.163. Hence, based on the skewness test, the hypothesis that res(λ_{mh}) is normally distributed cannot be rejected at significance levels in excess of ten percent. The adjusted K-S test indicates that the hypothesis that res(λ_{mh}) is normally distributed cannot be rejected at the 15 percent significance level.

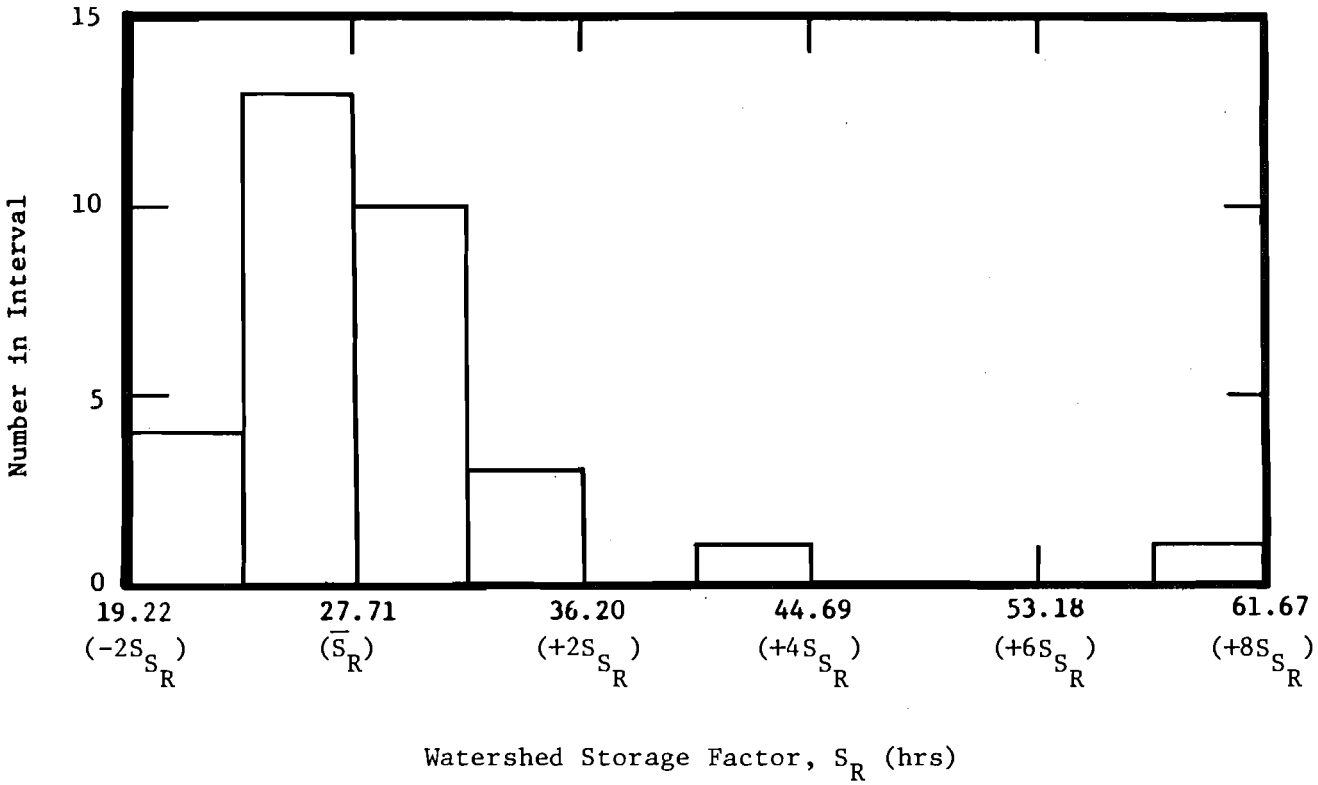

Figure C.16. Histogram of optimal S_R values

Therefore, the model correction factor for HEC-1 is considered normally distributed with

$$E[\lambda_{mh}] = 2.275 - 0.154 \ln \hat{Q}_p \qquad (C.21)$$

$$S_{\lambda_{mh}} = 0.0472$$

These statistics are used in the MVFOSM analysis.

C.7.3 RORB Basic Variable Statistics

C.7.3.1 Initial Loss, ILR

The same initial loss relation is used for HEC-1 and RORB with only a change in dimensions from in. to mm. Therefore, in RORB, the initial loss is considered to be lognormally distributed with

$$E[\ln(ILR)] = 6.015 - 0.599 \ln(Q_B) \qquad (C.22)$$

$$\zeta_{ILR} = 0.7184$$

For the MVFOSM method, the mean and standard deviation are

$$E[ILR] = 409.7\ Q_B^{-0.599} (mm) \qquad (C.23)$$

$$S_{ILR} = 8.702 \text{ mm}$$

C.7.3.2 Continuing Loss Rate, CLR

Figure C.17 displays a histogram of the optimal CLR values for RORB in one-third standard deviation intervals. Based on visual inspection, CLR is assumed to be lognormally distributed. The skewness of the logarithms of CLR is 0.370. Hence, based on the skewness test, the hypothesis that CLR is lognormally distributed cannot be rejected at the ten percent significance level (bound equal to 0.662 for a sample size of 30). The adjusted K-S test indicates that the hypothesis that CLR is lognormally distributed cannot be rejected at the 15 percent significance level. Therefore, the continuing loss rate for RORB is considered lognormally distributed with

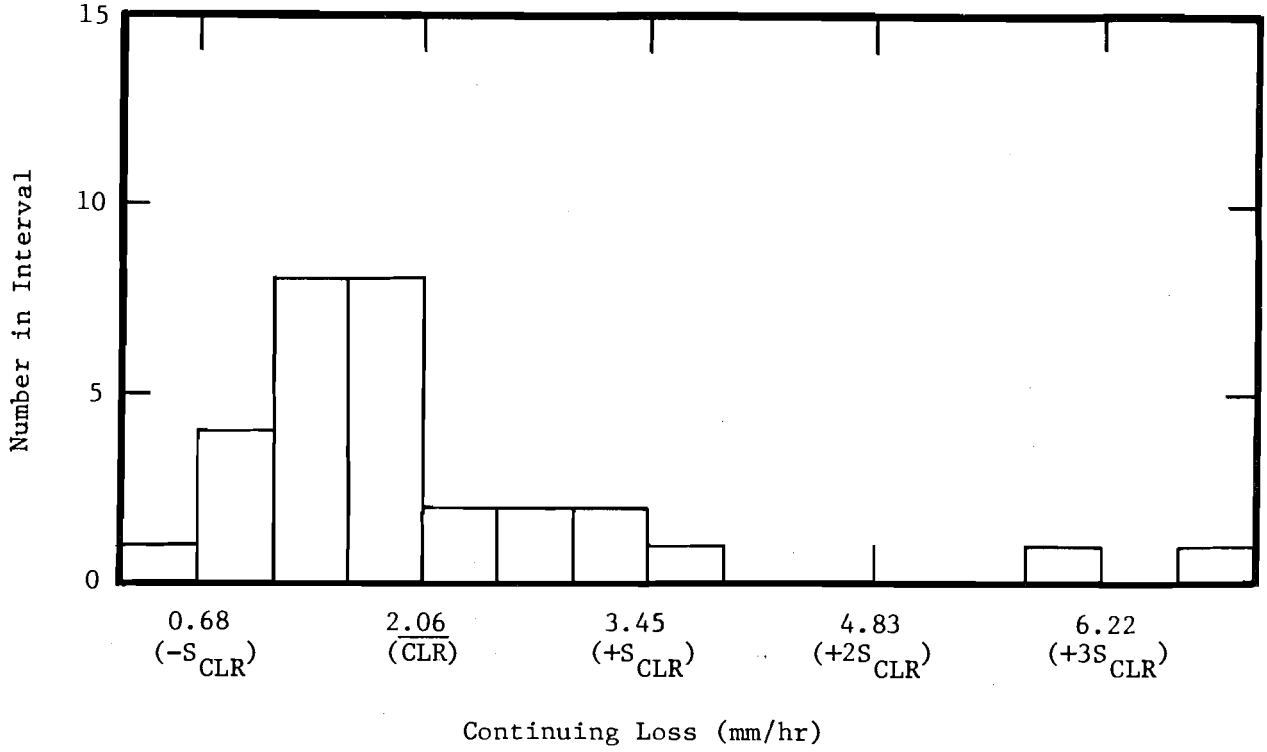

Figure C.17. Histogram of optimal CLR values for RORB

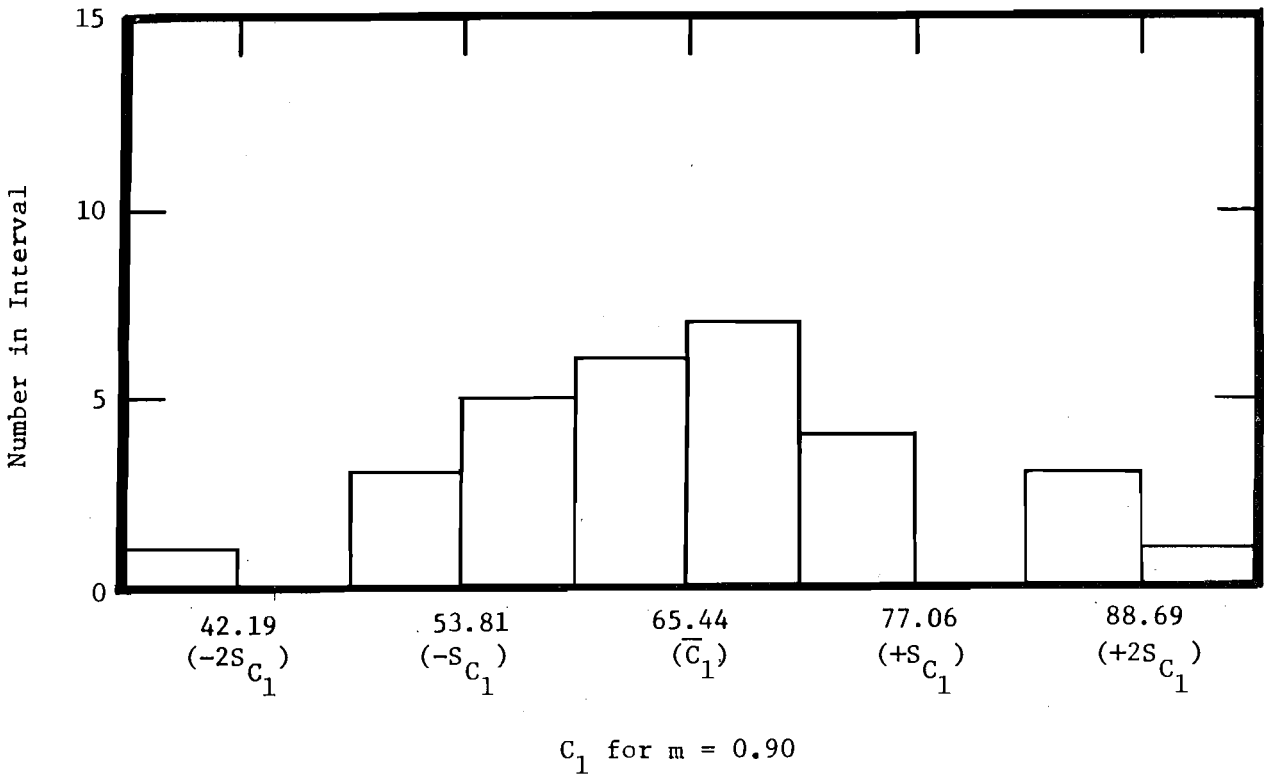

Figure C.18. Histogram of optimal C_1(m = 0.90) values

$$E[\ell n(CLR)] = 0.5636$$

$$\zeta_{CLR} = 0.5565$$

For the MVFOSM method, the mean and standard deviation are

$$E[CLR] = 2.065 \text{ mm/hr}$$

$$S_{CLR} = 1.385 \text{ mm/hr}$$

C.7.3.3 Watershed Delay Time Factor, C_1

Figure C.18 displays a histogram of the optimal C_1 values for RORB in one-half standard deviation intervals. Based on visual inspection, C_1 is assumed to be normally distributed. The skewness coefficient for C_1 was found to be 0.380. Hence, based on the skewness test, the hypothesis that C_1 is normally distributed cannot be rejected at the ten percent significance level. The adjusted K-S test indicates that the hypothesis that C_1 is normally distributed cannot be rejected at the 15 percent significance level.

Therefore, the watershed time delay factor is considered normally distributed with

$$E[C_1] = 65.44$$

$$S_{C_1} = 11.62$$

These statistics are also used in the MVFOSM analysis.

C.7.3.4 Model Correction Factor, λ_{mr}

A normal distribution for res(λ_{mr}) was estimated and tested. The skewness coefficient for res(λ_{mr}) of RORB was found to be 0.011. Based on the skewness test, the hypothesis that res(λ_{mr}) is normally distributed cannot be rejected at significance levels far greater than ten percent. The adjusted K-S test indicates that the hypothesis that res(λ_{mr}) is normally distributed cannot be rejected at the five percent significance level.

Therefore, the model correction factor for RORB is considered normally distributed with

$$E[\lambda_{mr}] = 1.737 - 0.152 \ell n \hat{Q}_p \qquad (C.24)$$

$$S_{\lambda_{mr}} = 0.0635$$

These statistics are also used in the MVFOSM analysis.

C.8 Application of Reliability Analysis Methods

The Monte Carlo and MVFOSM reliability analysis methods were applied to the reliability of the real-time flood forecasting schemes as described in Chapter 2. However, as described in section 2.1 one percent increase in parameter values is used in HEC-1's automatic calibration scheme, hence, such a $\Delta\theta_j$ is likely to lead to a reasonable change in the system performance function for evaluating the partial derivatives.

The AFOSM method calculations followed the standard iteration procedure shown schematically in Fig. B.1 using an IBM PC-AT with math co-processor chip. In using this procedure, no initial estimate of β was made.

C.8.1 Calculation of the Partial Derivatives

For real-time flood forecasting within a flood warning and preparedness system, it is desired to know the reliability of the peak discharge estimate. Hence, the R-L system performance function is

$$Z = Q_F - \lambda_m Q(\theta) \tag{C.25}$$

where Q_F = the peak discharge (flood level) whose probability of occurring due to the current storm is sought,

$Q_p(\theta)$ = the peak discharge estimated by the hydrologic model in question, and

θ = the vector of model parameters.

While the ℓn(R/L) system performance function is

$$Z = \ell n \left[\frac{Q_F}{\lambda_m Q_p(\theta)} \right] \tag{C.26}$$

As recommended in Chapter 2, the partial derivatives for the model parameters are estimated by taking a forward difference

$$\frac{\partial Z}{\partial \theta_j} = \frac{Z(\theta_j + \Delta\theta_j, \theta) - Z(\theta)}{\Delta\theta_j} \tag{C.27}$$

The change in Z also includes the change in λ_m as $\hat{Q}_p$ changes due to the change in θ_j. Furthermore, during iteration i+1, the value of λ_m used in determining the partial derivatives is

$$\lambda_{m(i+1)} = a + b \ln \hat{Q}_p - \alpha_i \beta_i S_{\lambda_m} \quad (C.28)$$

where a,b = the appropriate regression coefficients,

α_i = the variance weight for λ_m from iteration i, and

β_i = the reliability index for iteration i(i=1, β_i=0).

In this forward difference scheme, the $\Delta\theta_j$ was chosen to be one percent of parameter value. A one percent increase in parameter values is used in HEC-1's automatic calibration scheme, hence, such a $\Delta\theta_j$ is likely to lead to a reasonable change in the system performance function for evaluating the partial derivatives.

The partial derivatives for λ_m can be evaluated analytically and they are for Z=R-L and Z=ln(R/L), respectively.

$$\frac{\partial Z}{\partial \lambda_m} = -\hat{Q}_p \quad (C.29)$$

$$\frac{\partial Z}{\partial \lambda_m} = -\frac{1}{\lambda_m} \quad (C.30)$$

C.8.2 Termination Criteria

The majority of the cases studied in this research converge as for the ideal case. However, for several cases, such ideal convergence was not obtained and the value of β^* (the value of β for $\underline{x}^*$) must be approximated.

One of the key assumptions of the AFOSM method is that the system performance function is continuous and differentiable or at least locally differentiable. Due to the use of block hyetograph data and the initial loss-continuing loss rate approach, the system performance function is discontinuous. These discontinuities lead to two significant convergence problems.

For the case when the relationship between the initial loss and the precipitation up to and including time period i, P_i, is

$$P_i - bCL < IL < P_i \quad (C.31)$$

where b = 2 for RORB and is related to the difference between IL and P_i for HEC-1.

The value of IL between these bonds is irrelevant in the calculation of the rainfall excess. When the iteration scheme moves to such a point, $\partial Z/\partial IL$ equals zero which is generally a drastic change from its previous non-zero value and this leads to problems with iteration convergence. This is more of a problem with HEC-1, which uses a single hyetograph, than for RORB, which uses multiple hyetographs (two in this case study). Generally, these problems can be circumvented by making IL equal to P_1. Hence, $\partial Z/\partial IL$ will have a non-zero value and the iterations will continue toward convergence.

The iteration scheme also has problems with iterations which go back and forth from one side of a discontinuity to the other and, hence, cannot converge in the basic variables. Generally, for such cases, the value of β has converged to the second decimal place. Hence, a very good approximation of β^* may be obtained.

As discussed in section 2.1.3, the iterations diverged for extreme probability cases ($\beta > 2.5$). The difference in β values for Z near zero (less than three percent of the target flood level) was typically on the order of 0.2 to 0.4. The iteration whose β value was closest to zero was chosen as a reasonable estimate of the true β^*. In this study, the β values so approximated were generally on the order of 2.5-4.5. The corresponding exceedance probabilities are on the order of 0.006-0.00004. Hence, from a practical viewpoint, such approximations of β^* do not greatly change the estimated flood risk for the event in question.

C.9 Storm Events for Verification

Storm events for verification were chosen from the data from the summer of 1955 through November 1965 using the guidelines for selecting calibration events described in section C.4.4 with the exception of the requirement of total runoff volumes greater than 10 mm (0.4 in.) because storm runoff volumes are difficult to estimate from daily discharge data (recall hourly discharge values are not available before November 1965). The daily discharge data also leads to slight differences in the population from which the calibration and verification data sets are sampled. In the calibration data set for single events, the instantaneous discharge at the beginning of the event is used to determine the direct runoff peak discharge and to define the relation which predicts the initial loss. For the verification data set, the baseflow from the storm date or the previous day is used. Hence, the estimated initial loss and direct runoff peak discharge are slightly different than they would be if the instantaneous flows were available.

For cases where event separation must be performed, the divergence between the calibration and verification data sets becomes more pronounced. For the calibration events, separation was performed by assuming the recession of the first event is parallel to the recession of the final event. For the verification events, separation was performed by using HEC-1 or RORB to simulate the first event and matching the daily average direct runoff volumes and the magnitude and timing of peak discharge as best as possible or by using the recession curve from a similar event in the calibration data set. Hence, the estimated initial loss and direct runoff

peak discharge may be considerably different than if estimated from continuous data. Nevertheless, these events provide an interesting test for the real-time flood forecasting schemes.

Strictly speaking, the verification data set is not from the same population as the calibration data set, and so the assumptions of the reliability analysis techniques and the verification process are violated. Nevertheless, the effects of the violations on the results of the reliability analysis and the forecasting scheme verification are insignificant from a practical viewpoint.

Table C.14 lists the storm events and their significant direct runoff characteristics (including the discharge level corresponding to the total runoff flood discharge of 10880 cfs, Q_F) used to verify the real-time flood forecasting schemes. Of the 23 events between the summer of 1955 and

Table C.14. Storms for Verification

Date	Precipitation		Q_B (cfs)	Q_p (cfs)	t_p (hr.)	Q_F (cfs)
	Fairbury (in.)	Piper City (in.)				
6/21/56	1.05	3.31	234.	2956.	50.	10646.
4/17/57	2.97	2.16	462.	4448.	52.	10418.
4/24/57	3.29	3.47	2400.*	9020.	100.	9930.
7/13/57	2.16	2.24	106.	3334.	30.	10774.
7/22/57	3.23	1.30	315.	3055.	30.	10565.
6/09/58	2.14	3.57	332.	5558.	46.	10548.
6/12/58	1.25	1.97	2900.*	6630.	34.	9800.
7/14/58	4.12	3.09	474.*	8480.	36.	10690.
4/26/59	2.08	2.56	275.	5545.	40.	10605.
9/23/61	2.83	2.14	80.	3500.	66.	10800.
5/10/62	1.07	1.46	1250.*	5580.	26.	10220.
4/05/65	1.40	1.25	778.	4622.	36.	10102.
4/08/65	1.20	0.85	2380.*	3440.	34.	9680.
4/23/65	1.79	2.74	568.	4552.	44.	10312.
5/04/65	2.23	2.55	640.	7700.	32.	10240.
6/16/73	3.05	1.60	468.	6685.	30.	10412.
5/12/70	3.55[1]	4.77	1940.*	9790.	46.	10420.
12/02/82[2]	4.40	--	800.	12300.	34.	10080.

*Flow at the beginning of this storm is in recession from a previous event.

[1]Only accumulated totals were available at Fairbury. Temporal distribution weighted as for Piper City.

[2]Piper City raingage malfunctioned, so Fairbury record is used for the entire watershed. The streamgage also malfunctioned in early part of the event so t_p is only approximate.

November 1965, which had total runoff peak discharges greater than 3000 cfs, 15 met the selection criteria (5 were eliminated due to snowmelt, 2 due to separation problems, and 1 due to missing data). The June 16, 1973 event was not included in the calibration data set because a second storm event occurred shortly after the hydrograph recession began making event separation infeasible, however, it may be included in the verification data set. For the May 12, 1970 and December 2, 1982 events, either the stream-gage and/or one of the raingages malfunctioned, but because both of these events resulted in serious flooding they were included in the verification data set. Hence, these events were examined to see how the real-time flood forecasting schemes would perform for actual floods (albeit using even less reliable input data).

APPENDIX D. LIST OF SYMBOLS

$\bar{a}$ = the correction factor relating the difference between the true and measured point rainfall due to wind effects

C_i = $\partial g/\partial x_i$ = the partial derivative of the system performance function with respect to basic variable i

CL = the continuing loss rate in in./hr, a parameter of HEC-1

CLR = the continuing loss rate in mm/hr, a parameter of RORB

C_l = the watershed delay time factor, a parameter of RORB

E = the average absolute sampling error in areal storm rainfall due to gage network inadequacy

E_a = the average absolute sampling error in areal one-minute rainfall due to gage network inadequacy

e_a = a random variable describing the uncertainty associated in determining $\bar{a}$

EFF = the coefficient of model fit efficiency

G = the gaging ratio = the number of square miles per rain gage

$g(\cdot)$ = the functional description of the system performance function

$h_M(\cdot)$ = a function which represents the selected hydrologic model's estimate of the hydrologic information in question

IL = the initial loss in in., a parameter of HEC-1

ILR = the initial loss in mm, a parameter of RORB

K_H = the soil saturated hydraulic conductivity

L = the load placed on the system (in this study the peak discharge forecast by a hydrologic model)

m = the storage nonlinearity exponent parameter in RORB

N = the number of rain gages on the watershed

n = the total number of hydrograph ordinates calculated

p = the number of basic variables for the system

P_E = the hydrologic target level exceedance probability

P_e = the estimated, based on point measurements, precipitation depth over the entire watershed

P_t = the true precipitation depth over the entire watershed

P_x = the true precipitation at point x

P_{xm} = the measured precipitation at point x

Q_B = the baseflow (streamflow) at the beginning of the rainfall event

Q_{ci} = the calculated direct runoff discharge at time i

QF_p = the direct runoff discharge level corresponding to the total runoff flood discharge of 10880 cfs

Q_{mi} = the measured direct runoff discharge at time i

$\overline{Q_m}$ = the average measured direct runoff discharge for a given event

Q_p = the measured direct runoff peak discharge

$\hat{Q}_p$ = the forecast (or predicted) direct runoff peak discharge produced by the hydrologic model using the expected values (best estimates) of the parameters and input data

$\hat{Q}_p^*$ = $\lambda_m \hat{Q}_p$ = the adjusted direct runoff peak discharge forecast (or prediction) produced by the hydrologic model accounting for the model correction factor, λ_m

Q_{pc} = the direct runoff peak discharge for the calibrated hydrograph

R = the system's resistance capacity (in the study the hydrologic target level)

r = the sample correlation coefficient

R_a = the true one-minute precipitation rate over the entire watershed

R_{ae} = the estimated, based on point measurements, one-minute precipitation rate over the entire watershed

R_ℓ = the system reliability

R_s = the system risk (probability of system failure)

S_R = the watershed storage factor in hours, a parameter of HEC-1

TC = the watershed time of concentration in hours, a parameter of HEC-1

T_H = the hydrologic target level whose exceedance probability is sought

t_p = the measured time to peak direct runoff from the beginning of the event

Δt = the computational time interval used in hydrologic modeling

$\underline{x}$ = the vector of the basic variables of the system includes data, model parameters, and model correction factor

$\bar{x}_i$ = the mean value of basic variable i

$\bar{x}_i^N$ = the mean value of the transformed normal basic variable i

x_i^* = the value of basic variable i at the failure surface

Δx_i = a small change in the value of x_i used to numerically evaluate partial derivatives

Z = the system performance function

α_i = the total forecast variance linearization factor for basic variable i

β = the reliability index for the system

β_F = the reliability index corresponding to the difference between the forecast peak discharge and the flood level

β_M = the reliability index corresponding to the difference between the measured and forecast peak discharges

ζ = the standard deviation of the logarithms for a lognormally distributed variable

λ_M = the model correction factor which expresses the relationship between the model's optimal performance and the true value of the hydrologic information to be estimated (in this study = Q_p/Q_{pc})

λ_{mh} = the model correction factor for HEC-1

λ_{mr} = the model correction factor for RORB

ρ = the population correction coefficient

σ_a = the coefficient of variation of the error in precipitation measurements due to wind effects

σ_i = the standard deviation of basic variable i

σ_i^N = the standard deviation of the transformed normal basic variable i

σ_p = the standard deviation of the precipitation input

σ_z = the standard deviation of the system performance function

$\Phi(\cdot)$ = the standard normal integral

REFERENCES

Abadie, J., and Carpentier, J., "Generalization of the Wolfe Reduced Gradient Method to the Case of Nonlinear Constraints," in Optimization, edited by R. Fletcher, Academic Press, London, 1969.

American Society of Civil Engineers, "Hydrology Handbook," ASCE Manual No. 28, New York, 1949.

Ang, A. H.-S., and Tang, W. H., Probability Concepts in Engineering Planning and Design Vol. I: Basic Principles, John Wiley & Sons Inc., New York, 1975.

Ang, A. H.-S., and Tang, W. H., Probability Concepts in Engineering Planning and Design Vol. II: Decision, Risk, and Reliability, John Wiley & Sons Inc., New York, 1984.

Askew, A. J., "Use of Catchment Models for Flood Forecasting in Central America," Logistics and Benefits of Using Mathematical Models of Hydrologic and Water Resource Systems, edited by A. J. Askew, F. Greco, and J. Kindler, Pergamon Press, New York, pp. 99-106, 1981.

Bailey, R. A., and Dobson, C., "Forecasting for Floods in the River Severn Catchment," Journal of the Institution of Water Engineers and Scientists, Vol. 35, No. 2, pp. 168-178, March 1981.

Barnes, H. H., Jr., "Roughness Characteristics of Natural Channels," USGS Water-Supply Paper 1849, U.S. Geological Survey, Washington, DC, 1967.

Barge, B. L., Humphries, R. G., Mak, S. J., and Kuhnke, W. K., "Rainfall Measurements by Weather Radar: Applications to Hydrology," Water Resources Research, Vol. 15., No. 6, pp. 1380-1386, December 1979.

Bel'chikov, V. A., "Model of the Formation of Rain Floods in the Rioni River Basin and Its Use for Short-Range Forecasts," Soviet Hydrology: Selected Papers, Vol. 14, No. 1, pp. 40-44, 1975.

Bel'chikov, V. A., "Forecast of the Flash Flood Hydrograph on the Ingoda River," Soviet Hydrology: Selected Papers, Vol. 16, No. 1, pp. 21-25, 1977.

Bergstrom, S., "Operational Hydrologic Forecasting by Conceptual Models in Sweden," Logistics and Benefits of Using Mathematical Models of Hydrologic and Water Resource Systems, edited by A. J. Askew, F. Greco, and J. Kindler, Pergamon Press, New York, pp. 61-74, 1981.

Bidwell, V. J., "The Design of a Flood Forecasting Procedure for the Klang River at Kuala Lumpur," Journal of Hydrology (New Zealand), Vol. 18, No. 1, pp. 29-35, 1979.

Boyer, M. C., "Streamflow Measurement," Handbook of Applied Hydrology, edited by V. T. Chow, McGraw-Hill, New York, 1964.

Bras, R. L., and Rodriguez-Iturbe, I., "Rainfall Network Design for Runoff Prediction," Water Resources Research, Vol. 12, No. 6, pp. 1197-1208, December 1976.

Burges, S. J., "Analysis of Uncertainty in Flood Plain Mapping," Water Resources Bulletin, Vol. 15, No. 1, pp. 227-243, February 1979.

Burnash, R.J.C., and Ferral, R. L., "An Operational System for Computer Preparation of Short-Term River Forecasts on the North Coast of California," Symposium on Use of Analog and Digital Computers in Hydrology, Tucson, Arizona, December 1968, IAHS Publication No. 80, Vol. 1, pp. 300-306, 1968.

Burnash, R.J.C., Ferral, R. L., and McGuire, R. A., A Generalized Streamflow Simulation System: Conceptual Modeling for Digital Computers, U.S. Department of Commerce, National Weather Service/State of California, Department of Water Resources, Sacramento, California, 1973.

Carter, R. W., and Anderson, I. E., "Accuracy of Current Meter Measurements," Journal of the Hydraulics Division, ASCE, Vol. 89, No. HY4, pp. 105-115, July 1963.

Cheng, S.-T., "Overtopping Risk Evaluation for an Existing Dam," Ph.D. Thesis, Department of Civil Engineering, University of Illinois at Urbana-Champaign, 1982.

Chow, V. T., "Statistical and Probability Analysis of Hydrologic Data," Handbook of Applied Hydrology, edited by V. T. Chow, McGraw-Hill, New York, 1964.

Chow, V. T., "Hydrologic Modeling," The Seventh John R. Freeman Memorial Lecture, Boston Society of Civil Engineers, February 17, 1972.

Chowdhury, M.S.K., and Bell, F. C., "New Routing Model for Continuous Runoff Simulation," Journal of the Hydraulics Division, ASCE, Vol. 106, No. HY4, pp. 489-500, April 1980.

CIRIA, "Rationalization of Safety and Serviceability Factors in Structural Codes," Report 63, London, 1977.

Clark, C. O., "Storage and the Unit Hydrograph," Transactions, American Society of Civil Engineers, Vol. 110, pp. 1419-1488, 1945.

Clarke, R. T., "A Review of Some Mathematical Models Used in Hydrology, with Observations on Their Calibration and Use," Journal of Hydrology, Vol. 19, No. 1, pp. 1-20, 1973.

Cornell, C. A., "Bounds on the Reliability of Structural Systems," Journal of the Structural Division, ASCE, Vol. 93, No. ST1, pp. 171-200, February 1967.

Cornell, C. A., "First-Order Analysis of Model and Parameter Uncertainty," Proceedings, International Symposium on Uncertainties in Hydrologic and Water Resources Systems, Vol. 2, Tucson, Arizona, pp. 1245-1272, December 1972.

Crawford, N. H., and Linsley, R. K., "Digital Simulation in Hydrology: Stanford Watershed Model IV," Stanford University, Department of Civil Engineering Technical Report 39, 1966.

Davis, D. R., and Nnaji, S., "The Information Needed to Evaluate the Worth of Uncertain Information, Predictions and Forecasts," Journal of Applied Meteorology, Vol. 21, pp. 461-470, April 1982.

Dawdy, D. R., "Considerations Involved in Evaluating Mathematical Modeling of Urban Hydrologic Systems," USGS Water Supply Paper 1591-D, U.S. Geological Survey, Washington, D.C., 1969.

Dawdy, D. R., and Bergmann, J. M., "Effect of Rainfall Variability on Streamflow Simulation," Water Resources Research, Vol. 5, No. 5, pp. 958-966, October 1969.

Dawdy, D. R., and O'Donnell, T., "Mathematical Models of Catchment Behavior," Journal of the Hydraulics Division, ASCE, Vol. 91, No. HY4, pp. 123-137, July 1965.

Dawdy, D. R., Lichty, R. W., and Bergmann, J. M., "A Rainfall-Runoff Simulation Model for Estimation of Flood Peaks from Small Drainage Basins," USGS Professional Paper 506-B, U.S. Geological Survey, Washington, D.C., 1972.

Day, H. J., "Flood Warning Benefit Evaluation - Susquehanna River Basin (Urban Residences)," ESSA Technical Memorandum WBTM Hydro 10, Silver Spring, Maryland: National Weather Service, Office of Hydrology, March 1970.

Day, H. J., and Lee, K. K., "Flood Damage Reduction Potential of River Forecast Services in the Connecticut River Basin," NOAA Technical Memorandum NWS HYDRO-28, Silver Spring, Maryland: National Weather Service, Office of Hydrology, February 1976.

Eyre, W. S., and Crees, M. A., "Real-Time Application of the Isolated Event Rainfall-Run-Off Model," Journal of the Institution of Water Engineers and Scientists, Vol. 38, No. 1, pp. 70-78, February 1984.

Federal Insurance Administration, Flood Insurance Study, City of Pontiac, Illinois, Livingston County, U.S. Department of Housing and Urban Development, June 1979.

Ford, D. T., Morris, E. C., and Feldman, A. D., "Corps of Engineers' Experience with Automatic Calibration of Precipitation-Runoff Model," Water and Related Land Resources Systems, edited by Y. Haimes and J. Kindler, Pergamon Press, New York, 1980.

Fread, D. L., "Numerical Properties of Implicit Four-Point Finite Difference Equations of Unsteady Flow," NOAA Technical Memorandum NWS HYDRO-18, Silver Spring, Maryland: National Weather Service, Office of Hydrology, 1974.

Fread, D. L., "Computation of Stage-Discharge Relationships Affected by Unsteady Flow," Water Resources Bulletin, Vol. 11, No. 2, pp. 213-228, April 1975.

Garen, D. C., and Burges, S. J., "Approximate Error Bounds for Simulated Hydrographs," Journal of the Hydraulics Division, ASCE, Vol. 107, No. HY11, pp. 1519-1534, November 1981.

Georgakakos, K. P., "A Generalized Stochastic Hydrometeorological Model for Flood and Flash-Flood Forecasting 1. Formulation," Water Resources Research, Vol. 22, No. 13, pp. 2083-2095, December 1986.

Georgakakos, K. P., "A Generalized Stochastic Hydrometeorological Model for Flood and Flash-Flood Forecasting 2. Case Studies," Water Resources Research, Vol. 22, No. 13, pp. 2096-2106, December 1986.

Georgakakos, K. P., and Bras, R. L., "Real-Time, Statistically Linearized, Adaptive Flood Routing," Water Resources Research, Vol. 18, No. 3, pp. 513-524, June 1982.

Goring, D. G., "Flood Routing by a Linear Systems Analysis Technique," Journal of Hydrology, Vol. 69, No. 1, pp. 59-76, February 1984.

Hamon, W. R., "Estimating Potential Evapotranspiration," B.S. Thesis, Department of Civil and Sanitary Engineering, Massachusetts Institute of Technology, 1960.

Hamon, W. R., "Estimating Potential Evapotranspiration," Journal of the Hydraulics Division, ASCE, Vol. 87, No. HY3, pp. 107-120, May 1961.

Hasofer, A. M., "Reliability Index and Failure Probability," Journal of Structural Mechanics, Vol. 3, No. 1, pp. 25-27, 1974.

Hasofer, A. M., and Lind, N. C., "Exact and Invariant Second-Moment Code Format," Journal of the Engineering Mechanics Division, ASCE, Vol. 100, No. EM1, pp. 111-121, February 1974.

Heatherwick, G., "Development of a Flood Forecasting System for the Latrobe River at Yallourn," Proceedings, WMO/UNESCO Symposium on Hydrological Forecasting, Queensland, Australia, 1967, WMO Technical Note No. 92, pp. 110-132, 1969.

Heatherwick, G., and Quinnell, A. L., "Optimizing Benefits to Urban Residents of a Total Flood Warning System for the Brisbane Valley," Preprints of Papers, Hydrology Symposium, Sydney, Australia, pp. 61-66, 1976.

Hershfield, D. M., "Rainfall Frequency Atlas of the United States for Durations from 30 Minutes to 24 Hours and Return Periods from 1-100 Years," U.S. Weather Bureau Technical Paper No. 40, Washington, DC, 1961.

Hershfield, D. M., and Engman, E. T., "Short Duration Rainfall Relationships," Urban Stormwater Hydraulics and Hydrology, edited by B. C. Yen, Water Resources Publications, Littleton, Colorado, pp. 1-10, 1982.

Hillier, F. S., and Lieberman, G. J., Introduction to Operations Research, Holden-Day, Inc., San Francisco, 1980.

Horton, R. E., "Accuracy of Areal Rainfall Estimates," Monthly Weather Review, Vol. 51, pp. 348-353, July 1923.

Horton, R. E., "Drainage Basin Characteristics," Transactions, American Geophysical Union, Vol. 13, pp. 350-361, 1932.

Horton, R. E., "Analysis of Runoff-Plat Experiments with Varying Infiltration-Capacity," Transactions, American Geophysical Union, Vol. 20, pp. 693-711, 1939.

Huff, F. A., "Spatial Distribution of Rainfall Rates," Water Resources Research, Vol. 6, No. 1, pp. 254-260, February 1970.

Huff, F. A., and Neill, J. C., "Rainfall Relations on Small Areas in Illinois," Illinois State Water Survey Bulletin 44, 1957.

Huff, F. A., and Schickedanz, P. T., "Space-Time Uncertainties in Precipitation Measurement," Proceedings, International Symposium on Uncertainties in Hydrologic and Water Resources Systems, Vol. 1, Tucson, Arizona, pp. 395-409, December 1972.

Hughes, L. A., and Longsdorf, L. L., "Guidelines for Flash Flood and Small Tributary Flood Prediction," NOAA Technical Memorandum NWS CR-58 (Revised), March, 1978.

Ibbitt, R. P., "Effects of Random Data Errors on the Parameter Values for a Conceptual Model," Water Resources Research, Vol. 8, No. 1, pp. 70-78, February 1972.

International Organization for Standardization, Measurement of Liquid Flow in Open Channels, ISO Standards Handbook 16, Geneva, Switzerland, 1983.

Iwasaki, T., "Flood Forecasting in the River Kitakami," Proceedings, International Hydrology Symposium, Fort Collins, Colorado, Vol. 1, pp. 103-112, 1967.

Jackson, D. R., and Aron, G., "Parameter Estimation in Hydrology: The State of the Art," Water Resources Bulletin, Vol. 7, No. 3, pp. 457-472, June 1971.

Jackson, T. J., and Schmugge, T. J., "Passive Microwave Remote Sensing of Soil Moisture," Advances in Hydroscience, Vol. 14, edited by B. C. Yen, Academic Press, New York, pp. 123-159, 1986.

Jamieson, D. G., Wilkinson, J. C., and Ibbitt, R. P., "Hydrologic Forecasting with Sequential Deterministic and Stochastic Stages," Proceedings, International Symposium on Uncertainties in Hydrologic and Water Resources Systems, Vol. 1, Tucson, Arizona, pp. 177-187, December 1972.

Jones, D.M.A., "Variability of Evapotranspiration in Illinois," Illinois State Water Survey Circular 89, 1966.

Kadoya, M., and Hayase, Y., "Long Term Runoff Analysis by a Conceptual Physical Model," Floods and Droughts, edited by E. F. Schulz, V. A. Koelzer, and K. Makmood, Water Resources Publications, Fort Collins, Colorado, pp. 200-212, 1973.

Kitanidis, P. K., and Bras, R. L., "Adaptive Filtering Through Detection of Isolated Transient Errors in Rainfall-Runoff Models," Water Resources Research, Vol. 16, No. 4, pp. 740-748, August 1980a.

Kitanidis, P. K., and Bras, R. L., "Real-Time Forecasting With a Conceptual Hydrologic Model 1. Analysis of Uncertainty," Water Resources Research, Vol. 16, No. 6, pp. 1025-1033, December 1980b.

Kitanidis, P. K., and Bras, R. L., "Real-Time Forecasting With a Conceptual Hydrologic Model 2. Applications and Results," Water Resources Research, Vol. 16, No. 6, pp. 1034-1044, December 1980c.

Kooman, D., Vrijling, J. K., Maldir, T., and Quelirij, L. de, "Probabilistic Approach to Determine Loads and Safety Factors," Symposium on Foundation Aspects of Coastal Structures, Delft, 1978.

Krzysztofowicz, R., and Davis, D. R., "A Methodology for Evaluation of Flood Forecast-Response Systems 1. Analysis and Concepts," Water Resources Research, Vol. 19, No. 6, pp. 1423-1429, December 1983.

Krzysztofowicz, R., and Davis, D. R., "A Methodology for Evaluation of Flood Forecast-Response Systems 2. Theory," Water Resources Research, Vol. 19, No. 6, pp. 1431-1440, December 1983.

Krzysztofowicz, R., and Davis, D. R., "A Methodology for Evaluation of Flood Forecast-Response Systems 3. Case Studies," Water Resources Research, Vol. 19, No. 6, pp. 1441-1454, December 1983.

Kumaraswamy, E.R.P., "Flood Warning Through a Hydrological-Cum-Mathematical Model and VHF Telemetry," Proceedings, IAHR Symposium on River Mechanics, Bangkok, Thailand, Vol. II, pp. 397-407, January, 1973.

Lambert, A. O., "The River Dee Regulation Scheme: Operational Experience of On-Line Hydrological Simulation," Logistics and Benefits of Using Mathematical Models of Hydrologic and Water Resource Systems, edited by A. J. Askew, F. Greco, and J. Kindler, Pergamon Press, New York, pp. 75-98, 1981.

Larimore, W. E., and Mehra, R. K., "The Problem of Overfitting Data," Byte, Vol. 10, No. 10, pp. 167-180, October 1985.

Larson, L. W., and Peck, E. L., "Accuracy of Precipitation Measurements for Hydrologic Modeling," Water Resources Research, Vol. 10, No. 4, pp. 857-863, August 1974.

Lasdon, L. S., Waren, A. D., and Ratner, M. W., GRG-2 User's Guide, University of Texas at Austin, February 1982.

Laurenson, E. M., Personal Communication, Victoria, Australia, 1986.

Laurenson, E. M., and Mein, R. G., "RORB-Version 3 Runoff Routing Program User Manual," Department of Civil Engineering, Monash University, Victoria, Australia, March 1985.

Laurenson, E. M., and O'Donnell, T., "Data Error Effects in Unit Hydrograph Derivation," Journal of the Hydraulics Division, ASCE, Vol. 95, No. HY6, pp. 1899-1917, November 1969.

Law, A. M., and Kelton, W. D., Simulation Modeling and Analysis, McGraw-Hill, New York, 1982.

Laws, J. O., and Parsons, D. A., "The Relation of Raindrop - Size to Intensity," Transactions, American Geophysical Union, Vol. 24, Pt. II, pp. 452-460, 1943.

Light, P., and Shands, A. L., "The Reliability of Areal Rainfall Determination," Thunderstorm Rainfall, Hydrometeorological Report 5, U.S. Weather Bureau, U.S. Army Corps of Engineers, 1947.

Linsley, R. K., "Flood Estimates: How Good Are They," Water Resources Research, Vol. 22, No. 9, pp. 159S-164S, August 1986.

Linsley, R. K., and Kohler, M. A., "Variations in Storm Rainfall Over Small Areas," Transactions, American Geophysical Union, Vol. 32, No. 2, pp. 245-250, April 1951.

Linsley, R. K., Kohler, M. A., Paulhus, J. L. H., Hydrology for Engineers, McGraw-Hill, New York, 1975.

Loague, K. M., and Freeze, R. A., "A Comparison of Rainfall-Runoff Modeling Techniques on Small Upland Catchments," Water Resources Research, Vol. 21, No. 2, pp. 229-248, February 1985.

Maddox, R. A. and Chappell, C. F., "Flash Flood Defenses," Water Spectrum, Vol. 11, No. 2, pp. 1-8, Spring 1979.

Mayer, H., Du Sicherheit der Bauwerk (The Safety of Structures), Springer-Verlag, Berlin, 1926.

McBean, E. A., Penel, J., and Siu, K.-L., "Uncertainty Analysis of a Delineated Floodplain," Canadian Journal of Civil Engineers, Vol. 11, pp. 387-395, 1984.

McGuinness, J. L., "Accuracy of Estimating Watershed Mean Rainfall," Journal of Geophysical Research, Vol. 68, No. 16, pp. 4763-4767, August 15, 1963.

McLean, D. G., and Anderson, M. D., "Hydraulic and Morphological Process on the Peace River Near Fort Vermilion, Report SWE 80-2, Alberta Research Council, Transportation and Surface Water Engineering Department, Edmonton, Alberta, 1980.

Mein, R. G., and Brown, B. M., "Sensitivity of Optimized Parameters in Watershed Models," Water Resources Research, Vol. 14, No. 4, pp. 299-303, April 1978.

Mein, R. G., Laurenson, E. M., and McMahon, T. A., "Simple Nonlinear Model for Flood Estimation," Journal of the Hydraulics Division, ASCE, Vol. 100, No. HY11, pp. 1507-1518, November 1974.

Melching, C. S., and Wenzel, H. G., "Calibration Procedure and Improvements in MULTSED," Report No. 38, Hydraulic Engineering Series, Department of Civil Engineering, University of Illinois at Urbana-Champaign, July, 1985.

Melching, C. S., and Yen, B. C., "Slope Influence on Storm Sewer Risk," Stochastic and Risk Analysis in Hydraulic Engineering, edited by B. C. Yen, Water Resources Publications, Littleton, Colorado, pp. 79-89, 1986.

Melching, C. S., Wenzel, H. G., Jr., and Yen, B. C., "Application of System Reliability Analysis to Flood Forecasting," presented at the International Symposium on Flood Frequency and Risk Analysis, May 14-17, 1986, Baton Rouge, Louisiana.

Mimikou, M., "Floodflow-Forecasting During Dam Construction," International Water Power and Dam Construction, Vol. 36, No. 5, pp. 15-17, May 1984.

Mogil, H. M., Monro, J. C., and Groper, H. S., "NWS's Flash Flood Warning and Disaster Preparedness Programs," Bulletin of the American Meteorological Society, Vol. 59, No. 6, pp. 690-699, June 1978.

Mol, A., Ligteringen, H., and Paape, A., "Risk Analysis in Breakwater Design," Proceedings, Conference on Breakwaters-Design Construction, London, May 4-6, 1983, Thomas Telford Ltd., London, pp. 81-86, also Delft Hydraulics Laboratory Publication No. 301, 1983.

Morgan, D. L., and Lourence, F. J., "Comparison Between Rain Gage and Lysimeter Measurements," Water Resources Research, Vol. 5, No. 3, pp. 724-728, June 1969.

Muller, C. C., and Kidder, E. H., "Rain Gage Catch Variation Due to Airflow Disturbances Around a Standard Rain Gage," Water Resources Research, Vol. 8, No. 4, pp. 1077-1082, August 1972.

Musgrave, G. W., and Holtan, H. N., "Infiltration," Handbook of Applied Hydrology, edited by V. T. Chow, McGraw-Hill, New York, 1964.

Nash, J. E., and Sutcliffe, J. V., "River Flow Forecasting Through Conceptual Models, 1. A Discussion of Principles," Journal of Hydrology, Vol. 10, pp. 282-290, 1970.

Natale, L., and Todini, E., "A Stable Estimator for Linear Models 1. Theoretical Development and Monte Carlo Experiments," Water Resources Research, Vol. 12, No. 4, pp. 667-671, August 1976.

Natale, L., and Todini, E., "A Stable Estimator for Linear Models 2. Real World Hydrologic Applications," Water Resources Research, Vol. 12, No. 4, pp. 672-676, August 1976.

National Science Foundation, A Report on Flood Hazard Mitigation, National Science Foundation, Washington, D.C., 1980.

National Weather Service, "The Disastrous Southern California and Central Arizona Floods, Flash Floods, and Mudslides of February 1980," National Disaster Survey Report NWS-81-1, March 1981.

Nnaji, S., Linvill, D. F., and Robbins, K. D., "Use of Digitized Radar and Microcomputers to Forecast Local Floods and Irrigation Needs, "Research Report No. 113, Water Resources Research Institute, Clemson University, June 1983.

NOAA, "National Weather Service River Forecast System Forecast Procedures," NOAA Technical Memorandum NWS HYDRO-14, Silver Spring, Maryland: National Weather Service, Office of Hydrology, December 1972.

Nordenson, T., "The Application of Conceptual Catchment Models to River Forecasting," Proceedings, WMO/UNESCO Symposium on Hydrologic Forecasting, Queensland, Australia, 1967, WMO Technical Note No. 92, pp. 181-192, 1969.

Oegema, B. W., and McBean, E. A., "Uncertainties in Flood Plain Mapping," presented at the International Symposium on Flood Frequency and Risk Analysis, May 14-17, 1986, Baton Rouge, Louisiana.

Owen, H. J., Wendell, M., Jorgenson, J., and Hughes, M., Reducing Flood Insurance Claims Through Flood Warning and Preparedness, Flood Loss Reduction Associates, Palo Alto, California, April 1983.

Packer, M. R., "Analysis of Streamflow Forecasting Uncertainty," Proceedings, International Symposium on Uncertainties in Hydrologic and Water Resources Systems, Vol. 1, Tucson, Arizona, pp. 115-121, December 1972.

Parsons, D. A., "Calibration of a Weather Bureau Tipping-Bucket Rain Gage," Monthly Weather Review, Vol. 69, p. 205, July 1941.

Peck, E. L., "Catchment Modeling and Initial Parameter Estimation for the National Weather Service River Forecast System," NOAA Technical Memorandum NWS HYDRO-31, Silver Spring, Maryland: National Weather Service, Office of Hydrology, June 1976.

Permut, A. R., Permut, A. A., and Permut, R. M., "Early Flood Warning System, U.S. Patent No. 4153881, Official Gazette of the United States Patent Office, Vol. 982, No. 2, p. 744, May 8, 1979.

Phanartzis, C. A., and Kisiel, C. C., "Uncertainties in Point and Areal Sampling of Precipitation and Their Importance in Hydrologic Computations," Proceedings, International Symposium on Uncertainties in Hydrologic and Water Resources Systems, Vol. 1, Tucson, Arizona, pp. 341-357, December 1972.

Pilgrim, D. H., Cordery, I., and Boyd, M. J., "Australian Development in Flood Hydrograph Modeling," Rainfall-Runoff Relationships, edited by V. P. Singh, Water Resources Publications, Littleton, Colorado, pp. 37-48, 1982.

Plate, E. J., "Reliability Analysis in Hydraulic Design," Stochastic and Risk Analysis in Hydraulic Engineering, edited by B. C. Yen, Water Resources Publications, Littleton, Colorado, pp. 37-47, 1986.

Rackwitz, R., "Practical Probabilistic Approach to Design," Bulletin 112, Comite European du Beton, Paris, France, 1976.

Rackwitz, R., and Fiessler, B., "Non-normal Vectors in Structural Reliability," SFB 96 Report 29, Technical University of Munich, pp. 1-22, 1978.

Rajendran, R., Mein, R. D., and Laurenson, E. M., "A Spatial Model for the Prediction of Losses on Small Rural Catchments," Australian Water Resources Council Technical Paper No. 75, Australian Government Publishing Service, Canberra, 1982.

Ramser, C. E., "Flow of Water in Drainage Channels," U.S. Department of Agriculture, Technical Bulletin No. 129, November 1929.

Rao, S. S., Optimization: Theory and Applications, John Wiley & Sons, New York, 1979.

Rawls, W. J., Brakensick, D. L., and Miller, N., "Green-Ampt Infiltration Parameters from Soils Data," Journal of Hydraulic Engineering, ASCE, Vol. 109, No. 1, pp. 62-70, January 1983.

Renard, K. G., The Hydrology of Semiarid Rangeland Watersheds, ARS 41-162 (USDA - Agricultural Research Service, 1970).

Rockwood, D. M., "Application of Streamflow Synthesis and Reservoir Regulation - 'SSARR' - Program to the Lower Mekong River," Symposium on Use of Analog and Digital Computers in Hydrology, Tucson, Arizona, December 1968, IAHS Publication No. 80, Vol. 1, pp. 329-344, 1968.

Salas, J. D., Delleur, J. W., Yevjevich, V., and Lane, W. L., Applied Modeling of Hydrologic Time Series, Water Resources Publications, Littleton, Colorado, 1980.

Salomonson, V. V., Ambaruch, R., Rango, A., and Ormsby, J. P., "Remote Sensing Requirements as Suggested by Watershed Model Sensitivity Analysis," Proceedings, Tenth International Symposium on Remote Sensing of Environment, Ann Arbor, Michigan, Vol. 2, pp. 1273-1284, October 1975.

Sandgren, E., and Ragsdell, K. M., "The Utility of Nonlinear Programming Algorithms: A Comparative Study - Part I," Journal of Mechanical Design, ASME, Vol. 102, No. 3, pp. 540-546, July 1980a.

Sandgren, E., and Ragsdell, K. M., "The Utility of Nonlinear Programming Algorithms: A Comparative Study - Part II," Journal of Mechanical Design, ASME, Vol. 102, No. 3, pp. 547-551, July 1980b.

Sangsit, S., "Basinwide Flood Forecasting System for the Lower Mekong Basin," Proceedings, IAHR Symposium on River Mechanics, Bangkok, Thailand, Vol. II, pp. 431-442, January, 1973.

Sargent, R. J., "Haddington Flood Warning Scheme," Journal of the Institution of Water Engineers and Scientists, Vol. 38, No. 2, pp. 108-118, April 1984.

Schermerhorn, V. P. and Kuehl, D. W., "Operational Streamflow Forecasting with the SSARR Model," Symposium on Use of Analog and Digital Computers in Hydrology, Tucson, Arizona, December 1968, IAHS Publication No. 80, Vol. 1, pp. 317-328, 1968.

Schilling, W., "Effect of Spatial Rainfall Distribution on Sewer Flows," Water Science and Technology, Vol. 16, No. 8/9, pp. 177-188, 1984.

Schilling, W., and Fuchs, L., "Errors in Stormwater Modeling - A Quantitative Assessment," Journal of Hydraulic Engineering, Vol. 112, No. 2, pp. 111-123, February 1986.

Scobey, F. C., "Flow of Water in Irrigation and Similar Canals," U.S. Department of Agriculture, Technical Bulletin No. 652, February 1939.

Sevruk, B., "Inaccuracy of Precipitation Measurement - A Serious Problem of Water Resources Instrumentation," Proceedings, 2nd World Congress, International Water Resources Association, New Delhi, Vol. 3, pp. 429-440, 1975.

Shinozuka, M., "Basic Analysis of Structural Safety," Journal of Structural Engineering, ASCE, Vol. 109, No. 3, pp. 721-740, March 1983.

Singh, K. P., "Derivation and Regionalization of Unit Hydrograph Parameters for Illinois (Dam Safety Program)," Illinois State Water Survey Contract Report No. 258, June 1981.

Singh, V. P., "Sensitivity of Some Runoff Models to Errors in Rainfall Excess," Journal of Hydrology, Vol. 33, pp. 301-318, 1977.

Sittner, W. T., "Determination of Flood Forecast Effectiveness by the Use of Mean Forecast Lead Time," NOAA Technical Memorandum NWS HYDRO-36, Silver Spring, Maryland: National Weather Service, Office of Hydrology, August 1977.

Smith, R. S., DeTurk, E. E., Bauer, F. C., and Smith, L. H., "Ford County Soils," Soil Report 54, Agricultural Experiment Station, University of Illinois at Urbana-Champaign, April 1933.

Sniedovich, M., and Davis, D. R., "Evaluation of Flood Forecasting-Response Systems," Journal of the Water Resources Planning and Management Division, ASCE, Vol. 103, No. WR1, pp. 83-97, May 1977.

Snyder, F. F., "Synthetic Unit Graphs," Transactions, American Geophysical Union, Vol. 19, pp. 447-454, 1938.

Sorooshian, S., Gupta, V. K., and Fulton, J. L., "Parameter Estimation of Conceptual Rainfall-Runoff Models Assuming Autocorrelated Streamflow Data Errors - A Case Study," Statistical Analysis of Rainfall and Runoff, edited by V. P. Singh, Water Resources Publications, Littleton, Colorado, pp. 491-504, 1982.

Stalmann, V., "Radio Control of Water Level Gauges in Watercourses Endangered by High Water Levels," Symposium on Hydrometry, Koblenz, West Germany, IAHS Publication No. 99, Vol. II, pp. 730-736, September 1970.

Stephens, M. A., "EDF Statistics for Goodness of Fit and Some Comparisons," Journal of the American Statistical Association, Vol. 69, No. 347, pp. 730-737, 1974.

Su, H.-L., "Statistical Approach to Structural Design," Proceedings, Institution of Civil Engineers, London, Vol. 13, pp. 353-362, 1959.

Sullivan, D. L., Personal Communication, Pontiac, Illinois, March 1986.

Tang, W. H., and Yen, B. C., "Hydrologic and Hydraulic Design Under Uncertainties," Proceedings, International Symposium on Uncertainties in Hydrologic and Water Resources Systems, Vol. 2, Tucson, Arizona, pp. 868-882, December 1972.

Thurman, J. L., and Roberts, R. T., "Hydrologic Data for Experimental Agricultural Watersheds in the United States, 1977," U.S. Department of Agriculture, Agricultural Research Service, Miscellaneous Publication Number 1454, 1987.

Troutman, B. M., "The Effect of Input Errors in Using Precipitation-Runoff Models for Runoff Prediction," Statistical Analysis of Rainfall and Runoff, edited by V. P. Singh, Water Resources Publications, Littleton, Colorado, pp. 305-314, 1982a.

Troutman, B. M., "An Analysis of Input Errors in Precipitation-Runoff Models Using Regression with Errors in the Independent Variable," Water Resources Research, Vol. 18, No. 4, pp. 947-964, August 1982b.

Troutman, B. M., "Runoff Prediction Errors and Bias in Parameter Estimation Induced by Spatial Variability of Precipitation," Water Resources Research, Vol. 19, No. 3, pp. 791-810, June 1983.

Tung, Y.-K., "Uncertainty of National Weather Service Rainfall Frequency Atlas," Journal of Hydraulic Engineering, ASCE, Vol. 113, No. 2, pp. 179-189, February 1987.

Tung, Y.-K., and Mays, L. W., "Risk Analysis for Hydraulic Design," Journal of the Hydraulics Division, ASCE, Vol. 106, No. HY5, pp. 893-913, May 1980.

Tung, Y.-K., and Mays, L. W., "Risk Models for Flood Levee Design," Water Resources Research, Vol. 17, No. 4, pp. 833-841, August 1981.

U.S. Army Corps of Engineers, Draft Detailed Project Report for Section 205 Flood Control Project, Vermilion River, Pontiac, Illinois, with Draft Environmental Assessment, Rock Island District, October 1984.

U.S. Army Corps of Engineers, Feasibility Study for Vermilion River Basin, Illinois, Rock Island District, April 1986.

U.S. Army Corps of Engineers, HEC-1 Flood Hydrograph Package: User's Manual, The Hydrologic Engineering Center, Davis, California, January 1985.

U.S. Water Resources Council, "Guidelines for Determining Flood Flow Frequency," Hydrology Committee Bulletin No. 17B, September 1981.

U.S. Water Resources Council, Estimated Flood Damages: Appendix B, Nationwide Analysis Report, Washington, D.C., 1977.

Vogel, J. L., Personal Communication, Champaign, Illinois, February 1986.

Vogel, J. L., and Changnon, S. A., Jr., "Selected Results from Studies of Illinois Dense Raingage Network Data," Urban Stormwater Hydraulics and Hydrology, edited by B. C. Yen, Water Resources Publications, Littleton, Colorado, pp. 1-20, 1982.

Vrijling, J. K., "Design of Concrete Structures: Probability Design Method," Cement, Vol. 34, No. 11, pp. 721-728, 1982.

Wang, S. H., Yao, J.T.P., and Chen, W. F., "Reliability of Antenna Structures," Recent Advances in Engineering Mechanics and Their Impact on Civil Engineering Practice, edited by W. F. Chen and A.D.M. Lewis, Vol. II, West Lafayette, Indiana, pp. 855-858, 1983.

Wascher, H. L., Smith, R. S., and Odell, R. T., "Livingston County Soils," Soil Report 72, Agricultural Experiment Station, University of Illinois at Urbana-Champaign, August 1949.

White, G. F., Flood Hazard in the United States: A Research Assessment, Institute of Behavioral Science, University of Colorado, Boulder, 1975.

Wilson, C. B., Valdes, J. B., and Rodriguez-Iturbe, I., "On the Influence of the Spatial Distribution of Rainfall on Storm Runoff," Water Resources Research, Vol. 15, No. 2, pp. 321-328, April 1979.

Wood, E. F., "An Analysis of the Effects of Parameter Uncertainty in Deterministic Hydrologic Models," Water Resources Research, Vol. 12, No. 5, pp. 925-932, October 1976.

Wood, E. F., "Filtering of Partitioned Large Scale Hydrologic Systems," Hydrological Sciences Bulletin, Vol. 26, No. 1, pp. 33-46, March 1981.

World Meteorological Organization, "Manual on Stream Gaging, Volume I: Fieldwork," Operational Hydrology Report No. 13, WMO Technical Note No. 819, 1984.

Yeh, W. W.-G., "Parameter Estimation in Rainfall-Runoff Modeling, Statistical Analysis of Rainfall and Runoff, edited by V. P. Singh, Water Resources Publications, Littleton, Colorado, pp. 481-490, 1982.

Yeh, W. W.-G., Becker, L., and Sohn, R. L., "Information Requirements for Improving Hydropower," Journal of the Water Resources Planning and Management Division, ASCE, Vol. 104, No. WR1, pp. 139-156, November 1978.

Yen, B. C., "Research on Watershed Hydrology at the University of Illinois," Global Water: Science and Engineering - The Ven Te Chow Memorial Volume, Journal of Hydrology, Vol. 68, pp. 3-17, 1984.

Yen, B. C., "Reliability of Hydraulic Structures Possessing Random Loading and Resistance," Engineering Reliability and Risk in Water Resources, edited by L. Duckstein and E. Plate, NATO ASI Series, E. M. Nijhoff, Dordrecht, The Netherlands, pp. 95-113, 1987.

Yen, B. C., and Tang, W. H., "Reliability of Flood Warning," Stochastic Processes in Water Resources Engineering, Proceedings of the 2nd International Symposium on Stochastic Hydraulics, Lund, Sweden, 1976, Water Resources Publications, Littleton, Colorado, pp. 333-347, 1977.

Yen, B. C., Cheng, S.-T., and Melching, C. S., "First Order Reliability Analysis," Stochastic and Risk Analysis in Hydraulic Engineering, edited by B. C. Yen, Water Resources Publications, Littleton, Colorado, pp. 1-36, 1986.

Yen, B. C., Cheng, S.-T., and Tang, W. H., "Reliability of Hydraulic Design of Culverts," Proceedings, International Conference on Water Resources Development, IAHR Asian Pacific Division Second Congress, Vol. 2, Taipei, Taiwan, pp. 991-1001, May 1980.

Yen, B. C., Wenzel, H. G., Jr., Mays, L. W., and Tang, W., H., "Advanced Methodologies for Design of Storm Sewer Systems," Research Report No. 112, Water Resources Center, University of Illinois in Urbana-Champaign, August 1976.

Yevjevich, V., Probability and Statistics in Hydrology, Water Resources Publications, Littleton, Colorado, 1971.

Zebrun, G., "Livingston County Surface Water Resources," Illinois Department of Conservation, Division of Fisheries, March 1969.